Polymer Synthesis by (Dual) *N*-Heterocyclic Carbene/Lewis Acid Catalysis

Von der Fakultät Chemie der Universität Stuttgart

zur Erlangung der Würde eines

Doktors der Naturwissenschaften (Dr. rer. nat.)

genehmigte Abhandlung

vorgelegt von

Hagen Jürgen Altmann

aus Aalen

Hauptberichter:	Prof. Dr. Michael R. Buchmeiser
1. Mitberichter:	Prof. Dr. Sabine Laschat
2. Mitberichter:	Prof. Dr. Sabine Ludwigs

Tag der mündlichen Prüfung: 19.10.2021

Institut für Polymerchemie der Universität Stuttgart

2021

DANK

1 Declaration of Authorship

Eigenständigkeitserklärung

Hiermit erkläre ich die vorliegende Arbeit, mit dem Titel „Polymer Synthesis by (Dual) *N*-Heterocyclic Carbene/Lewis Acid Catalysis", selbst angefertigt zu haben, fremde Quellen und Werke und daraus entnommene Teile sind gekennzeichnet.

Declaration of Independence

Herewith I declare to have made the present work, with the title "Polymer Synthesis by (Dual) *N*-Heterocyclic Carbene/Lewis Acid Catalysis", myself, foreign sources and works and parts taken from them are marked.

Publications resulting from this thesis

Parts of this dissertation are already published. I wish to refer to these publications throughout all this thesis. These patents and publications are listed in the below summary.

Protected *N*-heterocyclic carbenes as latent organocatalysts for the low-temperature curing of anhydride-hardened epoxy resins, Hagen J. Altmann, Stefan Naumann, Michael R. Buchmeiser, *Eur. Polym. J.*, **2017**, *95*, 766-774.

Catalysts for the synthesis of oxazolidinones, WO 2020/025805 A1, Carsten Koopmans, Elena Frick-Delaittre, Aurel Wolf, Christoph Guertler, Hagen J. Altmann, Stefan Naumann, Michael R. Buchmeiser.

Synthesis of Linear Poly(oxazolidin-2-one)s by Cooperative Catalysis Based on *N*-Heterocyclic Carbenes and Simple Lewis Acids, Hagen J. Altmann, Manuel Clauss, Simon König, Elena

Frick-Delaittre, Carsten Koopmans, Aurel Wolf, Christoph Guertler, Stefan Naumann, Michael R. Buchmeiser, *Macromolecules*, **2019**, *52*, *2*, 487-494.

Dual Catalysis with an *N*-Heterocyclic Carbene and a Lewis Acid: Thermally Latent Pre-Catalysts for the Polymerization of Azepan-2-one, Hagen J. Altmann, Mark Steinmann, Iris Elser, Mathis J. Benedikter, Stefan Naumann, Michael R. Buchmeiser, *ACS Marco Lett.*, **2020**, *58*, *22*, 3219-3226.

A Spirocyclic Parabanic Acid Masked *N*-Heterocyclic Carbene as Thermally Latent Pre-Catalyst for Polyamide 6 Synthesis and Epoxide Curing, Hagen J. Altmann, Wolfgang Frey, Michael R. Buchmeiser, *Macromol. Rapid Commun.*, **2020**, *41*, *20*, 2000338.

Latent catalyst systems and processes for the production of polyamides (patent pending), Hagen J. Altmann, Mathis J. Benedikter, Iris Elser, Stefan Naumann, Michael R. Buchmeiser.

Synthesis of dihydroxy telechelic oligomers of β-butyrolactone catalyzed by titanium (IV)-alkoxides and their use as macrodiols in polyurethane chemistry, Hagen J. Altmann, Martin R. Machat, Aurel Wolf, Christoph Gürtler, Dongren Wang, Michael R. Buchmeiser, *J. Polym. Chem.*, **2021**, 1-8.

Datum/date: _____

Name/name: Hagen Jürgen Altmann

Unterschrift/signature: _____

2 Index

3 Units, Abbreviations and NHC Nomenclature

3.1 International System of Units[1]

quantity name	unit name	unit symbol	defining equation
time	second	s	$\Delta\nu_{Cs}$=9192631770 s^{-1}
length	meter	m	c=299792458 m s^{-1}
mass	kilogram	kg	h=6.62607015·10^{-34} kg m^2 s^{-1}
electric current	ampere	A	e=1.602176634·10^{-19} As
thermodynamic temperature	kelvin	K	k_B=1.380649·10^{-23} kg m^2 s^{-2} K^{-1}
amount of substance	mole	mol	N_A=6.02214076·10^{23} mol^{-1}
luminous intensity	candela	cd	K_{cd}=683 cd sr s^3 kg^{-1} m^{-2}

3.2 Metric Prefixes

Name	Symbol	Power	Name	Symbol	Power
yotta	Y	10^{24}	deci	d	10^{-1}
zetta	Z	10^{21}	centi	c	10^{-2}
exa	E	10^{18}	milli	m	10^{-3}
penta	P	10^{15}	micro	μ	10^{-6}
tera	T	10^{12}	nano	n	10^{-9}
giga	G	10^9	pico	p	10^{-12}
mega	M	10^6	femto	f	10^{-15}
kilo	k	10^3	atto		10^{-18}
hecto	h	10^2	zepto		10^{-21}
deca	da	10^1	yokto		10^{-24}
-	-	10^0			

3.3   Abbreviations

5u-Me-CO$_2$	1,3-dimethylimidazolium-2-carboxylate
Ac	acetyl
AcOH	ethanoic acid
Ad	adamantyl
Ar	aryl/aromatic substituent
BBL	4-methyloxetan-2-one
BDO	1,4-butandiol
BnOH	phenylmethanol
BPL	oxetan-2-one
br	broad signal
CAAC	cyclic alkyl aminocarbene
AEO	azepan-2-one/ε-caprolactam
AEO-Ac	1-acetylazepan-2-one
Cy	cyclohexyl
d	day(s)
d	doublet
δ	chemical shift in ppm
dd	doublet of doublets
dt	doublet of triplets
Đ$_M$	polydispersity index
DCE	1,2-dichlorethane
CH$_2$Cl$_2$	dichlormethane

DFT	density functional theory
Dipp	2,6-bis(prop-2-yl)phenyl
Dmac	*N*,*N*-dimethylacetamide
DME	1,2-dimethoxyethane
DMF	*N*,*N*-dimethylformamide
DMSO	dimethyl sulfoxide
DSC	differential scanning calorimetry
dt	doublet of triplets
EA	ethyl acetate
EDO	1,2-ethanediol
eq.	equivalents
Et	ethyl
et al.	et alii
EtOH	ethanol
FT-IR	Fourier transformed infrared
GC-MS	gas chromatography paired with mass spectrometry
GPC	gel permeation chromatography
h	hour(s)
$H_{12}MDI$	1,1-bis(4-isocyanato cyclohexyl) methane
HDI	1,6-diisocyanatohexane
HOMO	highest occupied molecular orbital
HRMS	high resolution mass spectrometry
IPDI	5-isocyanato-1-(isocyanatomethyl)-1,3,3-trimethylcyclohexane

iPr	2-propyl/isopropyl
iPrOH	2-propanol/isopropanol
IR	infrared
IUPAC	International Union of Pure and Applied Chemistry
KHMDS	potassium bis(trimethylsilyl)amide
LA	Lewis acid
LASER/Laser	light amplification by stimulated emission of radiation
LUMO	lowest unoccupied molecular orbital
m/z	mass to charge ratio
MALDI-ToF-MS	matrix-assisted laser desorption/ionization-time of flight-mass spectrometry
MDI	1,1-bis(4-isocyanatophenyl) methane
Me	methyl
MeCN	acetonitrile
MeOH	methanol
Mes	2,4,6-trimethylphenyl
min	minute(s)
M_n	number-average molecular weights
M_w	weight-average molecular weights
NHC	*N*-heterocyclic carbene
NHC-CO_2	CO_2-protected *N*-heterocyclic carbene
NHO	*N*-heterocyclic olefin
NMR	nuclear magnetic resonance (spectroscopy)
OTf	trifluoromethane sulfonate

p	conversion
PDI	polydispersity index
Ph	phenyl
ppm	parts per million
Pr	propyl
PU	polyurethane
q	quartet
RIM	reaction injection molding
RTM	reaction transfer molding
rt	room temperature
s	second(s)
s	singlet
SEC	size exclusion chromatography
t	time
t	triplet
tt	triplet of triplets
tBu	2-methylpropyl/tertbutyl
TDI	2,4-diisocyanato-1-methylbenzene
TEP	Tolmans electronic parameter
THF	tetrahydrofuran
TMS	trimethylsilyl
X_n	degree of polymerization

3.4 Terminology of *N*-Heterocyclic Carbenes

The chemical manipulations discussed herein are often initiated or catalyzed by *N*-heterocyclic carbenes (NHCs). Hence, the systematic of naming used herein is explained in the following.
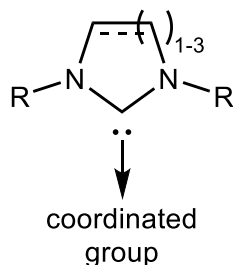
Scheme 1: General structure of (latent) *N*-heterocyclic carbenes.

A-B-C

A: Ring size, five-, six- and seven-membered rings. In case of 5-membered rings "u" indicates an unsaturated imidazole ring, "s" a saturated imidazoline ring.

B: Side groups bound to the intracyclic nitrogen atoms (R in Scheme 1). As this nomenclature only names symmetrical substituted NHCs both side groups have the same structure.

C: Coordinated group. The carbene might be protected by molecules e. g. $MgCl_2$, CO_2 or exist as imidazolium salt or others. No mentioned coordination group indicates the free carbene.

Examples:

5u-Me-CO$_2$ 1,3-dimethylimidazolium-2-carboxylate

5s-Cy   1,3-dicyclohexylimidazolidin-2-ylidene

7-Mes-HBr   1,3-bis(2,4,6-trimethylphenyl)-1,3-diazepanium bromide

4 Zusammenfassung

In dieser Arbeit werden fünf Themenschwerpunkte aus dem Forschungsfeld der Polymersynthese behandelt. Zu Beginn werden die Gebiete eingeführt durch einen Überblick der Literatur. Vorab werden Grundlagen der Polymerchemie und, weil sie im weiteren Verlauf der Arbeit eine außerordentliche Rolle spielen, *N*-heterozyklische Carbene (NHCs) eingeführt. Anschließend werden die fünf Themenschwerpunkte, nämlich (I) latente, anhydridgehärtete Epoxidharze, (II) lineare Polyoxazolidin-2-one, (III) latente Polyamide-6-systeme, (IV) Erweiterung der Schutzgruppen latenter *N*-heterozyklischer Carbene und (V) niedermolekulare, dihydroxytelechelische Poly(4-methyloxetan-2-on)e sowie die dazu durchgeführten Arbeiten im Detail beschrieben.

Im Schwerpunkt latente, anhydridgehärtete Epoxidharze wurde ein bekanntes Konzept aufgegriffen und erweitert. Der Einsatz von latenten *N*-heterozyklischen Carbenen als Initiator der Quervernetzungsreaktion von Diepoxiden und Anhydriden wurde bereits 2014 beschrieben.[2] Im Gegensatz zu den verschiedenen von Buchmeiser *et al.* untersuchten Carbenen wurde in der vorliegenden Arbeit der Fokus auf 1,3-Dimethylimidazolium-2-carboxylat (**5u-Me-CO$_2$**) gelegt, da dieser Initiator sich durch seine effiziente Synthese auszeichnet.[3] Um die, im Vergleich zu den Carbenen aus vorangegangenen Studien, geringere Reaktivität auszugleichen wurde eine Vielzahl von verschiedenen, substituierten Anhydriden und Diepoxiden untersucht.[4] Die aus DSC-Experimenten erhaltenen Maxima der Energiefreisetzung (T_{max}) während der Reaktionen im ersten Heizzyklus wurden herangezogen um die Reaktivitäten zu vergleichen. Ausgewählte Systeme wurden am Rheometer auf ihr Fließverhalten und ihr Härtungsprofil untersucht.

Lineare Polyoxazolidin-2-one wurden durch kooperative Katalyse von *N*-heterozyklischen Carbenen und Lewissäuren hergestellt.[5] Der atomökonomischste Syntheseweg führt über die Polyaddition von Diisocyanaten und Diepoxiden. Um thermoplastische Polymere zu erhalten ist die Vermeidung von Nebenreaktionen und -produkten essenziell, besonders die Trimerisierung der Diisocyanate zu Isocyanuraten. Die kooperative Katalyse mit Lewissäuren und -basen, hohe Temperaturen und der Einsatz geeigneter Lösemittel (beispielsweise Sulfolan oder 1,3-Dimethylimidazolidin-2-on) erlauben die Herstellung von ausschließlich linearen Polyoxazolidin-2-onen. Die Regioisomerie der Oxazolidin-2-on-Wiederholungseinheiten wurde anhand von monofunktionalen Vergleichssubstanzen und ^{13}C NMR-Daten untersucht. Für die hergestellten Polymere ergab sich eine überwiegende Substitution an der Ringposition 5. Nach einigen vergleichenden Experimenten wurde auch hier aufgrund der Robustheit und der einfachen Synthese überwiegend **5u-Me-CO₂** als Katalysator eingesetzt obwohl die Latenz, bei Temperaturen von 200°C, eine unwesentliche Rolle spielte. Sowohl mit LiCl als auch mit $MgCl_2$ wurden gut Ergebnisse bezüglich der Abwesenheit von Trimeren erzielt. LiCl lieferte etwas zuverlässiger lineare, isocyanauratfreie Polymere. Wesentlich für die erfolgreiche Synthese war auch die Reaktionsführung bei der die Monomere kontinuierlich der Katalysatorenlösung zugeführt wurden. Es konnten Polymere mit Molekulargewichten bis zu 50000 g/mol isoliert werden.

Eine weiter Einsatzmöglichkeit von **5u-Me-CO₂** und dessen latenten Eigenschaften ergab sich bei der anionischen ringöffnenden Polymerisation (AROP) von Azepan-2-on zu Polyamid 6.[6] Auch zu diesem Themenschwerpunkt gab es bereits Vorarbeiten von Buchmeiser *et al.*, wiederum wurden darin die verschiedenen *N*-heterozyklischen Carbene und deren unterschiedliche Auswirkungen auf die Polymerisation beschrieben.[7-9] Der in der vorliegenden

Arbeit eingesetzte **5u-Me-CO₂** lieferte unter vergleichbaren Bedingungen nur geringe Ausbeuten. Die Reaktion, die ohne Lösemittel in der Monomerschmelze bei etwa 160 bis 200°C durchgeführt wird, konnte durch kooperative Katalyse mit zusätzlichen Aktivatoren (Acetylazepan-2-on) und Lewissäuren (MgCl₂) zu quantitativen Umsätzen geführt werden. Besonders zu erwähnen ist dabei, dass weder die alleinige Zugabe von Lewissäuren noch die alleinige Zugabe von Aktivatoren zum Monomer/NHC-Gemisch einen vollständigen Umsatz ermöglichen. Das Zusammenwirken der beiden Substanzen konnte mittels NMR-Spektroskopie nachvollzogen werden. Die Solidifikationszeiten von wenigen Minuten werden hauptsächlich vom molaren Verhältnis des Monomers zu NHC, Lewissäure und Aktivator sowie der Temperatur beeinflusst. Dasselbe molare Verhältnis beeinflusst auch das Molekulargewicht der Produkte. Zu den wichtigsten Ergebnissen dieses Abschnitts gehört die Möglichkeit latente 1-Komponentenmischung herstellen zu können. Dazu werden **5u-Me-CO₂**, Aktivatoren und Lewissäuren in der Monomerschmelze (~80°C) gelöst ohne, dass die Polymerisation ausgelöst wird. Die erhaltene Mischung kann mehrere Tage im geschmolzenen und daher flüssigen Zustand oder über Monate abgekühlt auf Umgebungstemperatur, als Feststoff gelagert werden, jeweils ohne Verlust der Reaktivität. Da die Reaktion über einen anionischen Mechanismus verläuft ist der Eintrag von Luftfeuchtigkeit zu vermeiden weil dadurch die anionischen Spezies gequencht werden. Nichtsdestotrotz konnten auch unter Umgebungsatmosphäre hohe Ausbeuten mit erhöhter Solidifikationszeit beobachtet werden.

5u-Me-CO₂ konnte mit zwei Äquivalenten Cyclohexylisocyanat unter Freisetzung von CO_2 in 1,3-Dicyclohexyl-6,9-dimethyl-1,3,6,9-tetraazaspiro[4.4]non-7-ene-2,4-dion (**5u-Me-(OCN-Cy)₂**) überführt werden.[10] Die Struktur des spirocyclischen Parabansäurederivats konnte mittel Einkristall-Röntgenstrukturanalyse, NMR und HRMS gelöst werden. **5u-Me-(OCN-Cy)₂** wurde

als latenter Initiator für anhydridgehärtete Epoxidharze und zur Polyamid 6-Synthese eingesetzt. Eine mit **5u-Me-CO₂** vergleichbare Reaktivität wurde beobachtet. Im Gegensatz zur Freisetzung des Carbens aus **5u-Me-CO₂** wird bei der Freisetzung aus **5u-Me-(OCN-Cy)₂** kein Gas freigesetzt, was für potentielle Anwendung, wie Harzspritzgießen (engl. (thermoplastic-)resin transfer molding (T-)RTM)), von Vorteil sein dürfte. Die gebildeten zwei Äquivalente Isocyanat werden vermutlich entweder durch Einbau in das Makromolekül oder Additionsreaktionen abgefangen.

Der fünfte Themenschwerpunkt befasst sich mit der Darstellung von niedermolekularen, dihydroxytelechelischen Poly(4-methyloxetan-2-on)en aus 4-Methyloxetan-2-on und aliphatischen Diolen.[11] Die besondere Reaktivität von viergliedrigen Lactonen verhindert eine klassische, anionisch ringöffnende Polymerisation. Daher wurden verschiedene Titan(IV)alkoxide als Katalysatoren eingesetzt die einem Koordination-Insertion-Mechanismus folgen. Die Reaktionen konnten bei Temperaturen zwischen 60 und 100°C ohne Lösemittel erfolgreich durchgeführt werden. Die Struktur der Produkte wurde mittels NMR, IR, Titration und MALDI-ToF-MS bestimmt. Über das Verhältnis von Diol zu Lacton konnte die Kettenlänge gesteuert werden, welche über GPC-Messungen erhalten wurden. Durch Reaktionsoptimierung konnten Nebenreaktionen, wie die Initiierung des Kettenwachstums ausgelöst durch Alkoxidliganden der Titankatalysatoren, minimiert werden, sodass im Produkt nur etwa 0.1 wt.-% Titan enthalten war. Dies wirkte sich auch positiv auf die Molekulargewichte der als Qualitätskontrolle synthetisierten Polyurethane aus. Hierzu wurden die dihydroxytelechelischen Oligomere mit 1,1-Bis(4-isocyanatophenyl)methylen (MDI) in THF umgesetzt. Für die bei Raumtemperatur ablaufende Reaktion wurde kein zusätzlicher Katalysator benutzt. Die

Polyurethane wurden über NMR und IR identifiziert und die Molekulargewichte mittels GPC bestimmt. Es ergaben sich Polymerisationsgrade von bis zu 44 (~50000 g/mol).

Die praktischen Herangehensweisen, Daten und Spektren, Chemikalienherkunft und Messmethoden sind im Experimentalteil zusammengefasst. Abschließend sind Anfragen zum Nachdruck, ein Lebenslauf und die genutzten Quellen aufgeführt.

5 Abstract

In this thesis five main topics from the field of polymer synthesis are discussed and introduced by a literature overview. Beforehand, basic principles of polymer chemistry and, because of their extraordinary role in further course of this thesis, *N*-heterocyclic carbenes (NHCs) are introduced. After the introduction, the five main topics, i.e. (I) latent, anhydride-hardened epoxide resins, (II) linear polyoxazolidin-2-ones, (III) latent polyamide 6 systems, (IV) extension of protective groups of latent *N*-heterocyclic carbenes and (V) low molecular weight poly(4-methyloxetan-2-one)s and the related work are discussed in detail.

For the topic latent, anhydride-hardened epoxide resins a well-known concept was taken up and extended. The usage of latent *N*-heterocyclic carbenes as initiators for the crosslinking reaction of diepoxides and anhydrides was already described in 2014.[2] In contrast to the various *N*-heterocyclic carbenes investigated by Buchmeiser *et al.* the present work focuses on 1,3-dimethylimidazolium-2-carboxylate (**5u-Me-CO$_2$**), since this initiator is characterized by its efficient synthesis.[3] To compensate for the reduced reactivity a wide range of different, substituted anhydrides and epoxides was investigated.[4] The maximum of energy release (T_{max}), obtained from the first cycle of DSC experiments, during the reaction were used to compare the reactivities. Selected systems were measured on the rheometer to investigate their flow behavior and curing profile.

Linear polyoxazolidin-2-ones were synthesized by cooperative catalysis of *N*-heterocyclic carbenes and Lewis acids.[5] The most atom-economic synthesis route proceeds via the polyaddition of diisocyanates and diepoxides. Cooperative catalysis using Lewis acids and bases, elevated temperatures and the use of suitable solvents (like sulfolane or 1,3-

dimethylimidazolidin-2-one) allow for the synthesis of exclusively linear polyoxazolidin-2-ones. The regio-constitution of the oxazolidin-2-one repeat units was examined on the basis of monofunctional reference substances and ^{13}C NMR data. The synthesized polymers were predominantly substituted at the 5-position of the ring. After a brief catalyst screening **5u-Me-CO₂** was almost exclusively used although latency played a minor role at temperatures of 200°C. Good results in terms of trimer avoidance were achieved with LiCl as well as MgCl₂. However, LiCl delivered slightly more reliably linear, isocyanate-free polymers. The reaction control, in which the monomers were continuously added to the catalyst solution, was also essential for the successful synthesis. Polymers with molecular weights up to 50000 g/mol were isolated.

A further opportunity to use **5u-Me-CO₂** and its latent properties arose with the anionic ring-opening polymerization (AROP) of azepan-2-one to polyamide 6.[6] Preliminary work from Buchmeiser *et al.* was available, describing the impact of various *N*-heterocyclic carbenes on the polymerization.[7-9] **5u-Me-CO₂**, used in the present work, delivered only moderate yields under comparable circumstances. The reaction, which was conducted without solvent in the molten monomer at around 160 to 200°C, reached quantitative yields by cooperative catalysis with additional activators (acetlyazepan-2-one) and Lewis acids (MgCl₂). It should be particularly mentioned that neither the sole addition of Lewis acids nor the sole addition of activators to the monomer/NHC mixture allowed for quantitative conversion. The interaction of both substances was reconstructed by NMR spectroscopy. The solidification times of a few minutes were found to be mainly influenced by the molar ratio of the monomer to NHC, Lewis acid and activator as well as the temperature. The same molecular ratio influences the molecular weights of the products. One of the most important results of this section is the possibility to produce latent 1-component mixtures. For this purpose, **5u-Me-CO₂**, activators and Lewis acids were dissolved in

a monomer melt (~80°C) without initiating the polymerization. The obtained mixtures were stored for several days in the molten and thus liquid state and several months at ambient temperatures as solids, without loss of activity. As the reaction proceeds via an anionic mechanism the entry of air humidity must be avoided, otherwise the anionic species is quenched. Still, high yields were achieved under ambient atmosphere, although solidification times were increased.

5u-Me-CO₂ was converted to 1,3-dicyclohexyl-6,9-dimethyl-1,3,6,9-tetraazaspiro[4.4]non-7-ene-2,4-dione (**5u-Me-(OCN-Cy)₂**) by the addition of two equivalents of cyclohexyl isocyanate and under release of CO_2.[10] The structure of the spirocyclic parabanic acid derivative was solved by X-ray structure analysis, NMR and HRMS. **5u-Me-(OCN-Cy)₂** was applied as latent initiator for anhydride-hardened epoxide resins and for polyamide 6 synthesis. A reactive behavior comparable to that of **5u-Me-CO₂** was observed. In contrast to **5u-Me-CO₂**, no gas is released on the liberation of the free carbene from **5u-Me-(OCN-Cy)₂**, which is an important advantage for potential applications like (thermoplastic)resin transfer molding ((T-)RTM). The two equivalents of isocyanate formed upon carbene liberation are probably captured by trimerization or addition reactions.

The fifth main topic deals with the synthesis of low molecular weight, dihydroxy telechelic poly(4-methyloxetan-2-one)s from 4-methyloxetan-2-one and aliphatic diols. The exceptional reactivity of four-membered lactones disables classical, anionic ring-opening polymerization. Instead, various titanium(IV) alkoxides were used as catalysts. The reactions were performed solvent-free at elevated temperatures between 60 and 100°C. The product structure was determined by NMR, IR, titration and MALDI-ToF-MS. The ratio of diol to lactone allows for control of the chain length, determined by GPC. Side reactions like the initiation of chain-growth

21

by the alkoxide ligands of the titanium catalysts, was suppressed by reaction optimization, thus a product with less than 0.1 wt.-% Ti was obtained. Further, the low titanium content was positively affecting the molecular weights of the derived polyurethanes which were used as quality probe for end-group fidelity. For this purpose, the dihydroxy telechelic oligomers were converted with 1,1-bis(4-isocyanatophenyl)methylene (MDI) in THF. No additional catalyst was used for this polyaddition reaction, proceeding at room temperature. The polyurethanes were characterized by NMR and IR and their molecular weights were determined by GPC. Degrees of polymerization up to 44 (~50000 g/mol) were found.

The practical approaches, data and spectra, chemical suppliers and measurement details are summarized in the experimental section. Finally reprint requests, a curriculum vitae, and references are listed.

6   Introduction

6.1   General

Several different polymerizations types will be discussed in the course of this thesis. Therefore, a brief overview summarizes the basic, important and related types. Further, most chapters are related to carbenes and their reactivity as initiator or catalyst. Thus, a fundamental introductory section is dedicated to these remarkable molecules. The five following sections provide a detailed introduction to the tasks addressed by this work and the literature thereof.

6.2   Carbenes

6.2.1   General and IUPAC Definition

An introduction to carbenes in general and to *N*-heterocyclic carbenes (NHCs) in particular is given here as wide parts of the thesis deal with NHCs. Electronic structure and properties of different kinds of NHCs are discussed and compared as well as basic mechanisms as initiator or catalyst in chemical transformations by means of selected examples.

The IUPAC describes carbenes as:

"The electrically neutral species H_2C: and its derivatives, in which the carbon is covalently bonded to two univalent groups of any kind or a divalent group and bears two nonbonding electrons, which may be spin-paired (singlet state) or spin-non-paired (triplet state)."[12]

Further, carbenes are described by various books and publications and it is common to describe them as neutral, divalent carbon atom bearing an electron sextet.[13-15]

Ernst Otto Fischer (*1918-[†]2007) is known, aside from the isolation of carbenes, for his work on sandwich complexes. He was awarded the Chemistry Nobel Prize in 1973 together with Geoffrey Wilkinson "for their pioneering work, performed independently, on the chemistry of the organometallic, so called sandwich compounds."[16-19]

The first isolation of a metal-carbene complex is attributed to A. Maasböl and Ernst O. Fischer, published in 1964.[16] Conversion of $W(CO)_6$ with phenyl lithium or methyl lithium and subsequent protonation and addition of a methyl group allowed the isolation of $W(CO)_5(=C(OCH_3)CH_3)$, although the final structure was not conclusively clarified at that time. Methylation of the carbonyl ligands via Meerwein salts is used as alternative route.[20] Fischer is the namesake for the carbene-metal complexes that bear a heteroatom adjacent to the carbenoid carbon.

Another type of carbene-metal complex is named after Richard Royce Schrock who published these results in 1974. From a reaction of $Ta[CH_2C(CH)_3]_3Cl_2$ and two equivalents of 2,2-dimethyl propane lithium $Ta[CH_2C(CH)_3]_3[CHC(CH_3)_3]$ was isolated.[21]

Richard Royce Schrock (*1945) developed and investigated organometallic metathesis catalysts and, specifically, their behavior in ROMP. Together with Yves Chauvin and Robert Howard Grubbs he was awarded the Chemistry Nobel Prize in 2005 "for the development of the metathesis method in organic synthesis."[21-25]

Both, Fischer and Schrock carbenes have the metal carbon double bond in common. However, quite some dividing lines must be drawn. Whereas Fischer carbenes are substituted by heteroatoms, bear a negatively polarized and usually low oxidation state central atom, Schrock carbenes are not heteroatom substituted, the central metal is usually in high oxidation states and positive polarized. Further, Schrock carbenes appear as triplet carbenes, unlike Fischer carbenes which are in singlet state.[26-27] The orbital situation is visually described in Scheme 2.
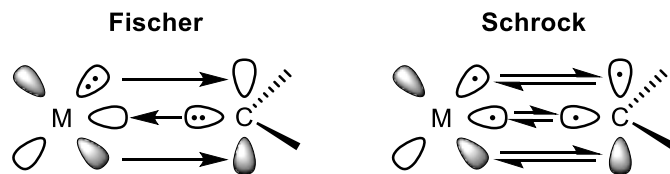
Scheme 2: Orbitals of singlet Fischer and triplet Schrock carbenes in comparison.

6.2.2 *N*-Heterocyclic Carbenes

Interestingly, researching free carbenes, not bound to a metal has a long history starting in the 19th century.[28-30] Carbon dioxide (+IV) and carbon monoxide (+II) were known along with methane (-IV) hence the existence of methylene (-II) and derivatives was quite plausible. Higher homologous of carbon like tin and lead are very stable in oxidation state +II.

Hans-Werner Wanzlick (*1917-[†]1988) studied in Berlin, his doctoral supervisor was Helmuth Scheibler (*1882-[†]1966). Among other things, both were researching on divalent carbon.[28-29]

NHCs are carbenes bearing one or more nitrogen atoms covalently bound to the carbene carbon atom, both located in a cyclic structure. The development of *N*-heterocyclic carbenes (NHCs) took off when Wanzlick, in 1960, isolated the product of a subsequent reaction of a carbene.[31-33] Although no stable, free carbene was isolated from heating 1,3-diphenyl-2-trichloromethylimidazolidine in solution, the carbene dimer and 1,3-dimethylimidazolidin-2-one, the addition product of an oxygen atom to a carbene, were identified (Scheme 3).[34]
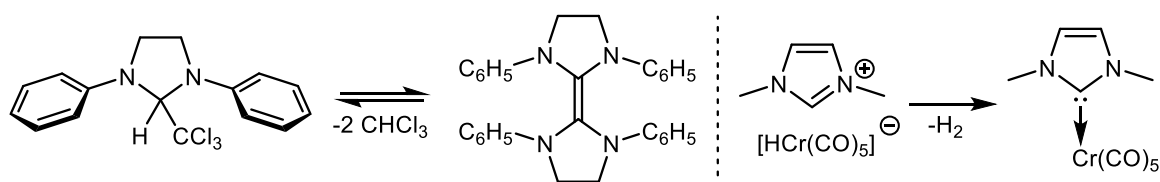
Scheme 3: At 150°C chloroform was released from 1,3-diphenyl-2-trichloromethyl imidazolidine and the dimer of 1,3-diphenyl imidazolidine was isolated (left); Chromium NHC complex formation (right).[31, 34-35]

The molecular weight determined for 1,3-diphenylimidazol-2-ylidene were higher than expected; thus, the scientists speculated about an equilibrium between the monomeric and

dimeric form, the so called Wanzlick-equilibrium. This hypothesis was controversially discussed in the following years until 2000 when experiments confirmed the equilibrium between tetraamines and carbenes for some examples.[32-33, 36-43]

1,3-Dimethylimidazol-2-ylidene pentacarbonyl chromium, the first NHC metal complex, was synthesized and isolated by Öfele in 1968 by heating 1,3-dimethylimidazolium hydrogen pentacarbonyl chromate (-I) under hydrogen formation (Scheme 3, right).[35] Both Wanzlick and Öfele were pioneers in the field of *N*-hetercyclic carbenes and their metal complexes.[44-49] However, attempts to isolate free, uncoordinated NHCs did not succeed.

Anthony Joseph Arduengo III (*1952) received his PhD from Georgia Institute of Technology and is well known for the first successful isolation of an *N*-heterocyclic carbene and the structural elucidation.[28, 50-52]

In 1991, Arduengo published the crystal structure of 1,3-diadamantylimidazol-2-ylidene isolated from the reaction 1,3-dimethylimidazolium chloride and sodium hydride in THF with catalytic amounts of DMSO (Scheme 4).[50]
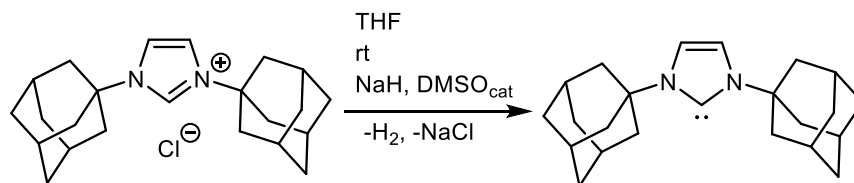
Scheme 4: Synthesis of the first isolated *N*-heterocyclic carbene (NHC).[50]

The remarkable stability of this free N-heterocyclic carbene (NHC) under inert gas conditions was underlined by the observation of the decomposition-free melting point of 240-241°C. On the one hand, the stability of this carbene was attributed to the kinetic stabilization by the sterically demanding adamantly groups adjacent to the nitrogen atoms. On the other hand, electron density is donated into the empty $p\pi$-orbital of the carbenoid carbon (C_2) by the nitrogen atoms and the NHC backbone in a π-framework. Further, the electronegative nitrogen atoms reduce the electron density along the σ-bonds and thus the nucleophilicity of the double occupied, non-

binding sp^2-orbital at C_2.[50] Note, that in case of an imidazoline-2-ylidene an aromatic situation prevails due to the six electrons in the π-system (Scheme 5, grey).
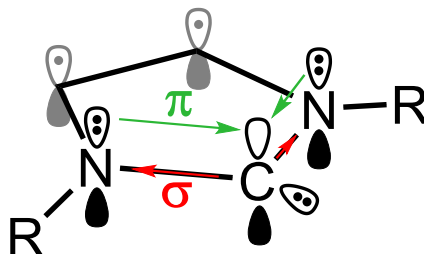

Scheme 5: Quantitative electronic behavior of five-membered NHCs. The σ-interactions, caused by the electronegativity of the nitrogen atoms, reduce the electron density at the carbon atom C_2 (red). The double occupied p-orbitals on the nitrogen atoms provide electron density to the empty carbene carbon p-orbital by forming a π-system (green); in the case of unsaturated carbenes this effect is enhanced (grey).[30]

Accordingly, the major differences between the isolable 1,3-diadamantylimidazoline-2-ylidene and the 1,3-diphenylimidazolidine-2-ylidene, only existing in the monomer/dimer equilibrium, are the unsaturated backbone and the higher steric demand of the residues adjacent to the nitrogen atoms of the latter. Subsequent publications pointed out that NHCs with sufficient electronic stabilization can be isolated without kinetic stabilization by sterically demanding substituents on the nitrogen atom.[51, 53-54] Several scientists contributed to the investigation of the dimerization behavior of NHCs.[13, 39-42, 55-58] Initial considerations, that unsaturation of the backbone (C_4 and C_5) is a prerequisite for the isolation of free carbenes, were proven wrong, although (unlike for imidazole scaffolds) bulky groups like 2,4,6-trimethylphenyl were required for the isolation of carbenes with saturated backbones.[59-60] The electronic configuration of NHCs contributes as a very pronounced factor to their stability. Scheme 6 shows the four possible configurations. $^1A_1$ (p_π^2) is of high energy thus it can be neglected. $^1A_1$ (σ^2) is the typically assumed state of NHCs with both electrons paired in the sp^2-orbital. $^1B_1$ ($\sigma^1\pi^1$) is a single state with on electron in the sp^2-orbital and one electron in the p_π-orbital, their spin is antiparallel. $^3B_1$ ($\sigma^1\pi^1$) is a triplet state again with one electron in the sp^2-orbital and one electron

in the p_π-orbital, but here the electrons have parallel spins. The sp^2-orbital represents the highest occupied molecular orbital (HOMO), the p_π-orbital represents the lowest unoccupied molecular orbital (LUMO). The energy gap between HOMO and LUMO is ΔE_{dim}, the required energy to promote one electron from the HOMO sp^2-orbital to the LUMO p_π-orbital. The additional stabilization (lowering of the energy level) of $^1A_1$ (σ^2), which is gained by the electronegativity of the nitrogen atoms or their σ-electron density withdrawing effect, respectively, is called E_{S-T}.

[13, 56, 60-62]

$$^1\mathbf{A_1}\ (\sigma^2) \qquad ^3\mathbf{B_1}\ (\sigma^1 p_\pi^1) \qquad ^1\mathbf{B_1}\ (\sigma^1 p_\pi^1) \qquad ^1\mathbf{A_1}\ (p_\pi^2)$$
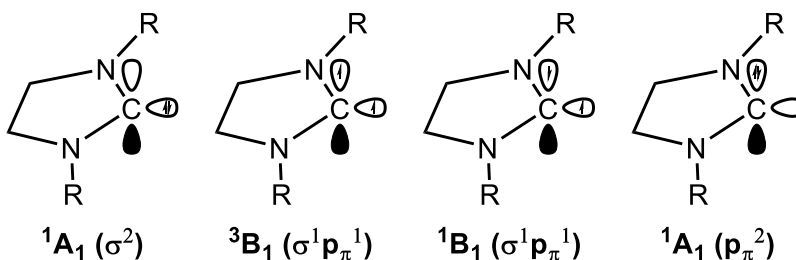
Scheme 6: Four electronic configurations of *N*-heterocyclic carbenes.[60] Although the backbone is drawn as saturated imidazolin-2-ylidene it is still valid for unsaturated imidazol-2-ylidenes and benzannulated derivatives.

Cavallo *et al.* published a study based on density-functional theory (DFT) to rationalize the dimerization tendency of NHCs.[62] Dimerization energies E_{dim} were calculated according to equation 1.

$$E_{dim} = (A \cdot NHC_{steric}) + (B \cdot NHC_{electronic}) + C \qquad (1)$$

For the molecular descriptors NHC_{steric} the buried volume ($\%V_{bur}$) and for $NHC_{electronic}$ singlet-triplet splitting E_{S-T} is used. A, B and C are empirically fitted parameters.[60, 62] The investigated imidazoles, imiazolines and benzannulated imidazoles and the various nitrogen substituents are shown in Scheme 7.
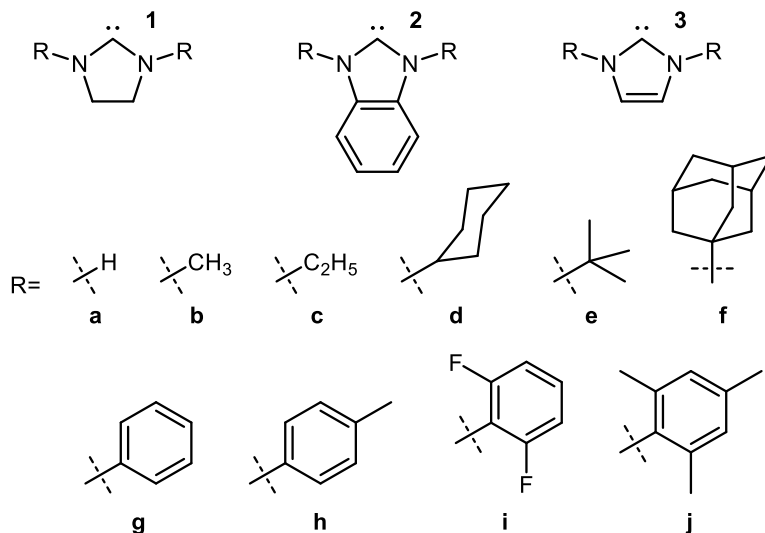
Scheme 7: Carbene structures investigated by Cavallo *et al.* in terms of dimerization.[62] A basic skeleton (**1**, **2** or **3**) always combines with one type of residue R (**a**, **b**, **c**, **d**, **e**, **f**, **g**, **h**, **i** or **j**) on the nitrogen atoms, accordingly only symmetric NHCs were investigated.

A plot of the dimerization energy ΔE_{dim}^{Fit} versus the ΔE_{dim}^{DFT} (reference) show quite similar behavior (R^2=0.93; Scheme 8). NHCs known to dimerize are displayed as red spares, yellow triangles display NHCs that are in equilibrium with the corresponding dimer. Green rhombus NHCs are stable, free carbenes and NHCs with unclear experimental behavior are depicted as colorless circles. A trend from negative to positive energies is visible. At negative energies, the dimers of NHCs can be found while at positive energies the stable, free carbenes and in the middle (just below zero) NHCs in the equilibrium between dimer and carbene are located. Among the stable, free carbenes are most of the imidazole-based structures and none of them dimerize. In turn many of the imidazoline-based structures can be found at higher energies either known or supposed to exist as dimers. Scheme 8 reproduces several results of Wanzlick and Arduengo.[31, 34, 50-51, 59-60, 62] 1,3-diphenylimidazoline-2-ylidene (**1g** in Scheme 8) is a dimer as isolated by Wanzlick while 1,3-diadamantylimidazol-2-ylidene (**3f**) as well as 1,3-bis(2,4,6-trimethylphenyl)imidazoline-2-ylidene (**1j**) are shown as stable carbenes. Neglecting those molecules bearing only hydrogen as nitrogen substituent, the tendency to dimerize is lowest for

imidazole derivatives, medium (dimer/carbene equilibrium) for benzimidazoles and highest for imidazolines.[38, 41, 43, 57, 62]
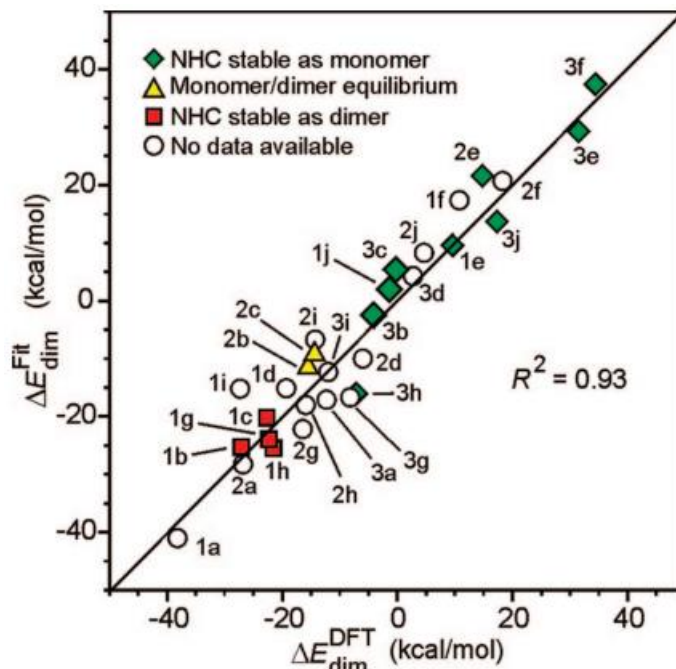
Scheme 8: Numbers and letters within the plot area correspond to those in Scheme 7 and stand for different NHCs. Reprinted with permission from (*Organometallics*, **2008**, *27*, *12*, 2679-2681). Copyright (2008) American Chemical Society.[62]

Nowadays *N*-heterocyclic carbenes of many shapes are known and well characterized (Scheme 9).[13, 32-33, 63] Aside from five-membered saturated imidazoline (**5s-R**) and unsaturated imidazole (**5u-R**) derivatives, six- (**6-R**) and seven- (**7-R**) membered NHCs are well known.[64-70] Six-membered NHCs, e.g., 1,3-dimethyltetrahydropyrimidin-2-ylidene, were not found to dimerize.[70-72] In addition, carbenes with ring sizes of four atoms were isolated.[73] Further, carbenes are not limited to structures bearing two nitrogen atoms in the ring. Carbenes with one (cyclic alkyl amino carbene; **CAAC**), three (**triazole**) and even four (**tetrazole**) nitrogen atoms were isolated.[74-77] Alder *et al.* examined that acyclic carbenoid systems are possible (**acyclic**).[78] Substitution of one nitrogen atom by sulfur leads to thiazol-2-ylidenes while

substitution of the two nitrogen atoms of a triazol-2-ylidene by phosphorus leads to 2,4-diphosphazol-2-ylidenes (*P*-heterocyclic carbene (PHC) **diphosphazole**).[79-80]

5u-R **5s-R** **6-R** **7-R**

CAAC **triazole** **tetrazole** **acyclic**

oxazol **diphosphazole**
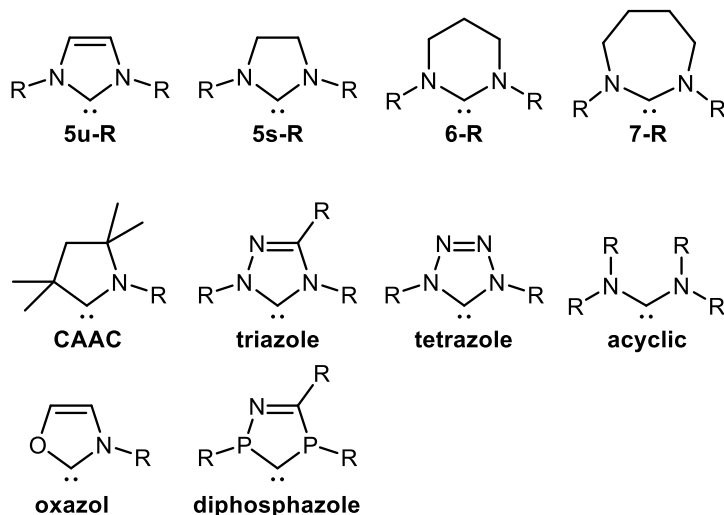
Scheme 9: Various structural motives of *N*-heterocyclic carbenes. Various backbone substitutions, including benzannulation, exist and for CAACs the methyl groups can be substituted.

6.2.3 Carbenes in Catalysis

The electron sextet, basicity and nucleophilicity of *N*-heterocyclic carbenes make them an interesting class of substances for applications in catalysis and coordination chemistry.[71-72, 81-84] Well-known examples are NHC metal complex-mediated reactions for carbon-carbon bond formation. Single bond formation is achieved by cross-coupling reactions based on nickel or palladium complexes among others with NHC ligands.[85-87] Further, carbon-carbon double bond formation is catalyzed by ruthenium-based Grubbs and Grubbs-Hoveyda catalysts of the second generation, both bearing NHCs, and group IV oxo and imido alkylidene NHC complexes (Scheme 10).[88-97] Both, the cross-coupling and olefin metathesis chemistry were awarded with the Nobel prize and NHCs contributed and still contribute to their development.[98-99]
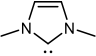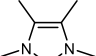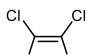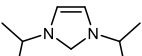
31
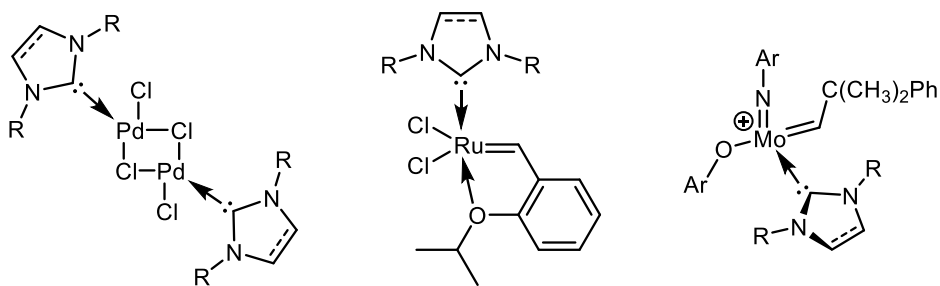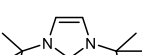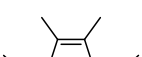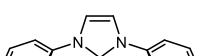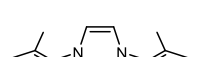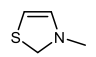
Scheme 10: Cross-coupling catalyst (left), Grubbs-Hoveyda second generation catalyst (middle) and molybdenum NHC alkylidene catalyst (right).[97, 100-101]

However, NHCs contribute not only as ligands in organometallic chemistry. A remarkable Brønsted basicity is an inherent property of NHCs.[63, 102] Thus, numerous scientists spent efforts in quantifying this basicity on the pK_a scale. Magill and Yates calculated pK_a values of imidazolium in the gas phase and in aqueous environment.[103] Three reactions were investigated. First, deprotonation of one of the nitrogen atoms, second, deprotonation of C_2 as well as deprotonation of C_4 and C_5, respectively. For most NHCs NH deprotonation (reaction 1) is neglectable since both nitrogen atoms are usually substituted by organic residues. However, it turned out that deprotonation of one of the heteroatom-bound protons proceeds at the lowest pK_a values. Followed by the deprotonation of C_2 (reaction 2) and finally deprotonation of the backbone C_4/C_5 (reaction 3, leading to abnormal NHCs) take place at the highest pK_a values. For the deprotonation of C_2 (reaction 2), pK_a values from 24.3 to 25.8 (aqueous phase) and for backbone deprotonation (reaction 3) pK_a values from 32.2 to 34.7 (aqueous phase) were found. This fits an ex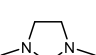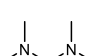perimental study where for the deprotonation of C_2 a pK_a of 23.8 was found for imidazole.[104] Further, the authors found values for 1,3-dimethylimidazolium (23.0), 1,3-dimethylbenzimidazolium (21.6) and 1,3-bis(1-phenylethyl)benzimidazole (21.2) for C_2. Yates *et al.* further published a study concerning calculated pK_a values of twelve different NHCs in DMSO or acetonitrile, respectively (Table 1).[105] Irrespective of the solvent, some trends and tendencies can be observed. The following discussion is based on the averaged, relative values in

DMSO. The influence of residues adjacent to nitrogen is visible in entries 1 (Me, 21.3), 4 (iPr, 22.3) and 5 (tBu, 22.8), pK_a increases with increasing positive inductive effect.

Table 1: Structures and pK_a values in DMSO and acetonitrile, respectively.[105]

entry	structure	pK_a (DMSO)	pK_a (acetonitrile)
1		21.3	32.2
2		23.9	34.7
3		16.4	27.2
4		22.3	33.1
5		22.8	33.7
6		24.7	35.6
7		16.3	27.2
8		17.0	28.0
9		22.5	33.4
10		27.3	38.2
11		28.1	38.9
12		14.6	25.5

A comparison of entries 1 to 3 as well as entries 4 and 6 highlights the impact of the backbone substitution. Methyl group substitution increases the pK_a values by 2.6 (entries 1 and 2) and 2.4 (entries 4 and 6), respectively. In contrast, substitution by chloride decreases the pK_a by 4.9. By

comparison of entries 1, 4 and 5 with 7 and 8 it appears that aromatic substituents at the nitrogen atoms decrease the pK_a. This effect is about as strong as the substitution with chloride in the backbone. Entries 1 and 9 allow to contrast the basicity of saturated (22.5) and unsaturated (21.3) *N*-heterocyclic carbenes. Further, a ring expansion to tetrahydropyrimidine (six membered) in entry 10 gives the highest pK_a values (27.3) in this study for cyclic substances. Interestingly, acyclic carbenes exploit even higher values of 28.1 (entry 11). On the contrary, the lowest pK_a (14.6) was found for the methylthiazol-2-ylidene.

Cheng *et al.* investigated the pK_a values of ten 1-methyl-3-organyl imidazolium compounds in DMSO.[106] No substantial differences were found for methyl, ethyl, n-butyl and n-octyl (pK_a=22.0 to 22.1) moieties adjacent to the nitrogen atom. In contrast, the pK_a values increased for the substitution of a linear side group by one (pK_a=22.6) or two (23.2) tertbutyl group. An even stronger influence was found for methyl-substituents in the imidazole backbone (pK_a=23.4). In addition, a minor impact of the counter ion was observed. O'Donoghue *et al.* published a study in which pK_a values of imidazolium, imidazolinium and tetrahydropyrimidinium salts in aqueous media were investigated.[107] However, a comparable tendency as in the aforementioned references was found. The highest pK_a values were found for tetrahydropyrimidine, followed by alkyl substituted imidazolium salts, followed by aryl substituted imidazolinium salts and lowest for aryl substituted imidazolium salts. A generalized illustration is shown in Scheme 11.[102, 107] Further NHC structures were investigated by Ji *et al.* and Harper *et al* (vide infra).[108-110]
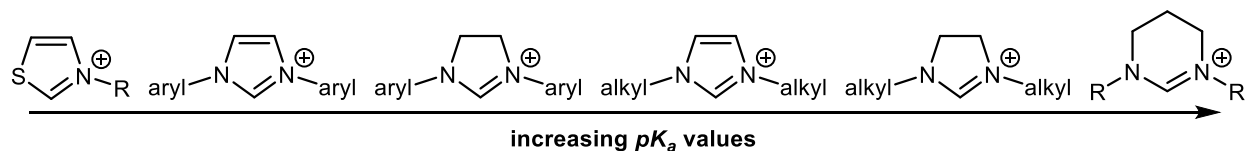
Scheme 11: Generalized structures of NHCs aligned according to increasing pK_a values.

The synthesis of polyurethane (PU) is one example for the utilization of the basicity of *N*-heterocyclic carbenes in polymer chemistry. Publications by Buchmeiser *et al.* and Destarac *et al.* show how NHCs can be applied to prepare crosslinked and linear polyurethanes, respectively.[111-113] Mechanistically it was pointed out that an activation of the diol monomer is achieved by reducing the bond strength between oxygen and hydrogen (or complete deprotonation) caused by proton attraction by the basic carbenoid carbon (Scheme 12). Imidazol-2-ylidenes appear most suitable to promote the carbamate formation. The application of NHCs as catalysts for the polyurethane synthesis in a polyaddition reaction of diols and diisocyanates is all the more interesting as it is known that NHCs can also be used as catalyst to trimerize isocyanates to isocyanurates.[114-118] Further, dimerization of isocyanates was observed in some cases.[113] The tendency to dimerize or trimerize isocyanates depends on the NHC applied as well as on the substrate.[118]
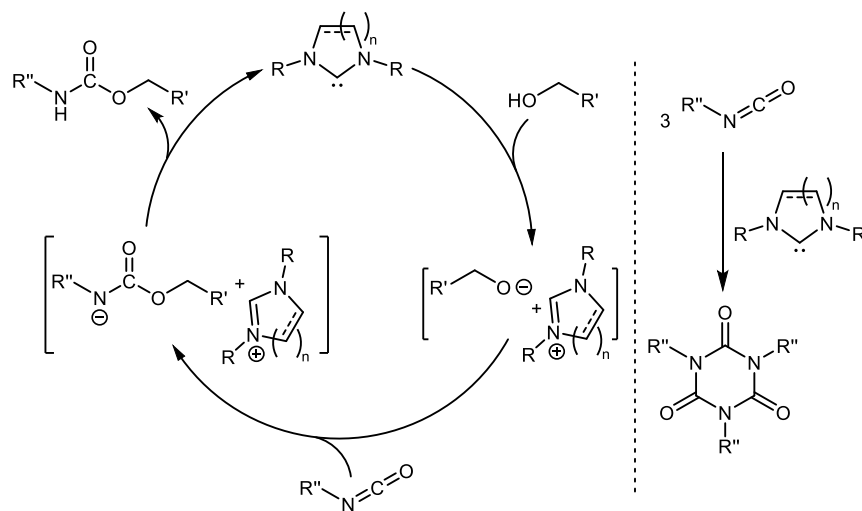
Scheme 12: NHC mediated carbamate bond formation (left). The alcohol-NHC adduct might possibly be an imidazolium alcoholate. Trimerization of isocyanate to isocyanurates catalyzed by NHCs (right).

The basicity of NHCs is exploited in further reactions like the amidation of esters, the ring-opening polymerization of lactones initiated by alcohols and in the ring-opening polymerization of lactams.[7, 119-120]

Many publications concerning the organocatalytic properties of NHCs, however, do not deal with their basicity but their nucleophilicity. Prominent examples are the benzoin condensation, Stetter reaction, homoenolate formation, 1,2-addition reactions, the trimerization of isocyanates and ring-expansions.[117-118, 121-131] The Tolman electronic parameter (TEP) is a measure to quantify the electron donating property of *N*-heterocyclic carbenes, although not the only one.[63, 132-133] Originally, the TEP was developed for phosphines. Its measurand is the IR wavenumber (cm^{-1}) of CO ligands in complexes of the ligand to be analyzed (L) and nickel tricarbonyl $[Ni(L)(CO)_3]$. Electron donation from (L) to the metal causes a shift of electron density from the metal to the anti-binding π^* orbitals of the CO ligands. Thus, stronger electron donation properties of (L) lead to lower stretching frequencies. Due to the toxicity of nickel carbonyl complexes alternative iridium and rhodium complexes were developed as well as methods to convert the values obtained from iridium ($[IrCl(CO)_2(L)]$) and rhodium ($[RhCl(CO)_2(L)]$) complexes to those values obtained from nickel complexes ($[Ni(CO)_3(L)]$) with high accuracy.[63, 133-139] Scheme 13 summarizes some NHCs and phosphines and their TEP values. Phosphines, triazolylidenes and thiazolylidenes are relatively electron-poor compared to imidazolylidenes and imidazolinylidenes. Within the latter two there is rather a small range of variation of the TEP value (from $2052.4\,cm^{-1}$ to $2049.5\,cm^{-1}$; $\Delta TEP=2.9\,cm^{-1}$). Most electron-rich are the tetrahydropyrimidine- and diazepinylidenes as well as CAACs. However, only a small selection of the known NHCs (and phosphines) is shown here and the impact of the backbone substitution, and nitrogen substituents (or other side groups) and eventually their substitution on Tolmans electronic parameter must not be neglected. Thus, it is interesting to note the difference between the two CAACs depicted (Scheme 13). The variation in the substitution of the side group (on C_2 and C_4) from hydrogen to prop-2-yl and methyl, respectively lowers the TEP value from

2048.5 cm^{-1} to 2042.2 cm^{-1} (ΔTEP=6.3 cm^{-1}) and is considerably high in contrast to the above mentioned variation within the imidazol(in)ylidenes.[63, 133]
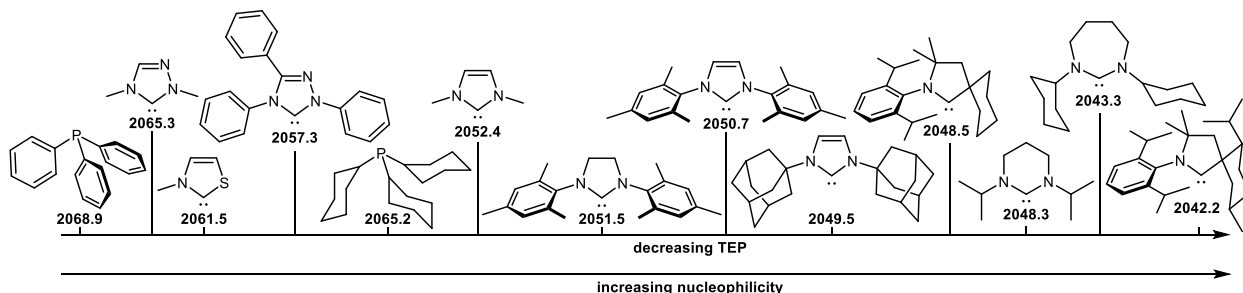
Scheme 13: Selected examples of *N*-heterocyclic carbenes and phosphines and the corresponding Tolman electronic parameters.[63]

Benefit from the nucleophilicity of NHCs towards catalysis can be obtained, for example, by polybenzoin condensation.[116, 130, 140] This step-growth polymerization is based on the benzoin condensation, a reaction that was conducted in the presence of strong bases and thiazolium or imidazolium salts, respectively before the isolation of a free carbene. However, it was found that the active species is a carbene and the reactions proceeds via the Breslow intermediate (Scheme 14).[115, 117, 141-145]
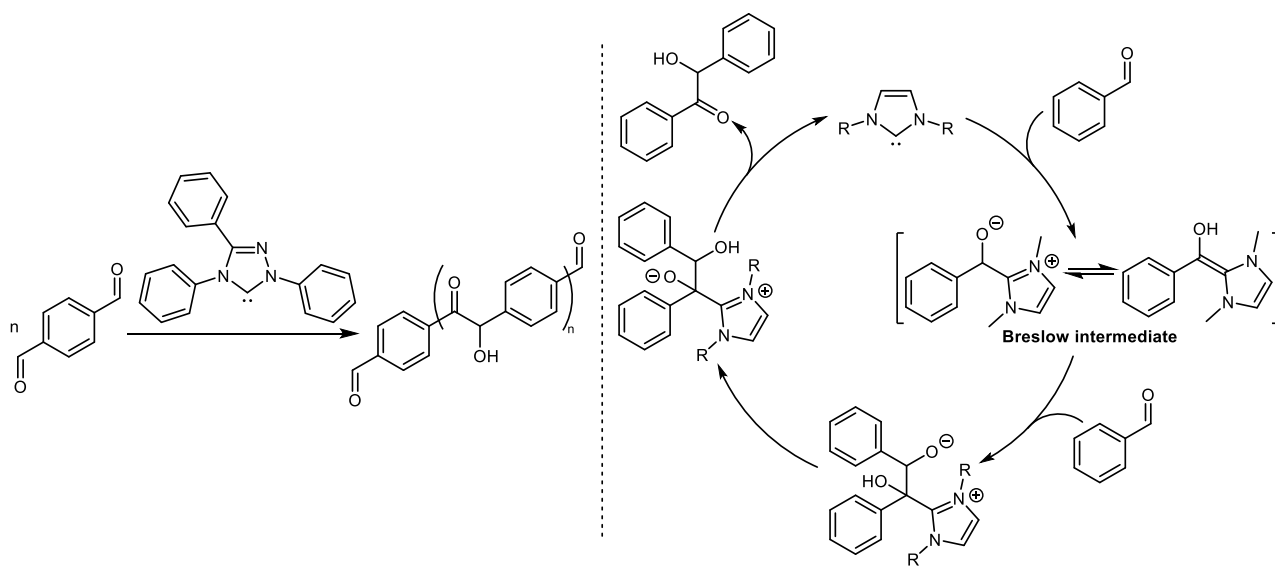
Scheme 14: Polycondensation reaction of benzene-1,4-dicarbaldehyde to poly(benzene-1,4-dicarbaldehyde) catalyzed by *N*-heterocyclic carbenes (left). Catalytic cycle of the benzoin condensation with Breslow intermediate.[130, 140-145]

6.2.4 Latent *N*-heterocyclic Carbenes

The benefits of *N*-heterocyclic carbenes come along with drawbacks concerning their stability towards air and moisture. Formation of imidazolin-2-one derivatives as an oxidation product of free NHCs and ambient oxygen were described by Wanzlick *et al.*, however, studies by Denk *et al.* drew a different picture.[31, 34, 48-49, 146] It was observed that both 1,3-ditertbutylimidazol-2-ylidene (**5u-tBu**) and 1,3-ditertbutylimidazoline-2-ylidene (**5s-tBu**) are inert towards oxygen and other oxidizing agents like CuO, Cu$_2$O and HgO. The different behavior found by Wanzlick *et al.* is probably due to the formation of the dimer whereas the singlet-triplet splitting of **5u-tBu** and **5s-tBu** is too high to form dimers (Scheme 15). In contrast, decomposition was observed when water was added to the carbenes.
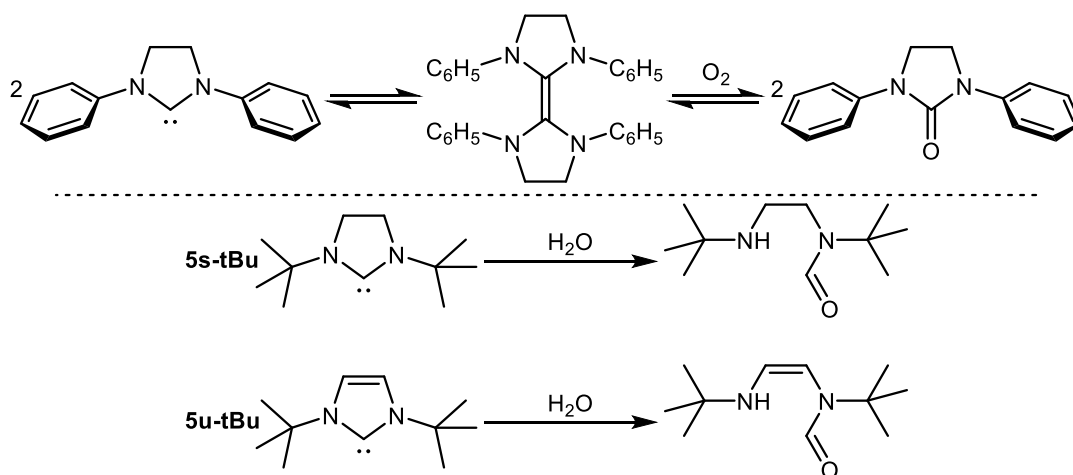
Scheme 15: Reaction presumably observed by Wanzlick *et al.* (top).[31, 34, 48-49] Decomposition reactions of NHCs in the presence of water (bottom).[146]

1,3-Bis(2,4,6-trimethylphenyl)-4,5-dichloro imidazol-2-ylidene (**5u$_{Cl}$-Mes**) is one of the rare examples stable under ambient conditions.[54]

Nonetheless, in recent years the number of metal complexes using *N*-heterocyclic carbenes as ligands and their usage in catalysis reached a remarkable level.[147-149] Air- and moisture-stable alkylidene complexes of ruthenium and NHCs (Grubbs catalysts) allow for ring-opening

metathesis polymerization (ROMP) under ambient conditions, metathesis reactions in water and column chromatography of the organometallic compounds.[150-154] The stability of this NHC metal complexes, however, does not reflect the stability of free carbenes. In addition, metal complexes can often be synthesized *in situ* from a metal precursor, an **NHC-HX** precursor and a base strong enough to bind the proton from the carbenoid center. However, strong bases are necessary and it should be noticed that many substrates are sensitive to strong bases or initiate side reactions.[155]

Adducts of NHCs and CO_2 (NHC-carboxylate, **NHC-CO$_2$**) proved to be useful in the synthesis of palladium NHC complexes, which were applied *in situ* in a Suzuki-Miyaura cross-coupling reaction.[156] In addition examples for rhodium, iridium, ruthenium and further NHC metal complexes synthesized from **NHC-CO$_2$** are known.[134, 157] This is all the more interesting as it was possible to transfer this technique to polymer-supported *N*-heterocyclic carbene carboxylates introduced to the crosslinked ROMP polymer by copolymerization.[158]

The concept of blocking the reactive carbenoid carbons was also used to produce latent *N*-heterocyclic carbenes. Here, both electrons of the sp^2 orbital are coordinated to electron-deficient moieties but can again be released upon exposition to external stimuli.[102, 155, 159-160] The bond between NHC and electrophile can be of covalent or coordinative nature depending on the electrophile. Scheme 16 depicts a selection of strategies to protect the carbene comprising betaines like **NHC-CO$_2$** and **NHC-CS$_2$**, hydrogen carbonates like **NHC-H$_2$CO$_3$**, sp^3 hybridized C_2 carbon atoms like **NHC-HOR'**, **NHC-HCCl$_3$** and **NHC-ArX$_m$** as well as coordinative, non-covalent bonds like **NHC-MX$_n$**.
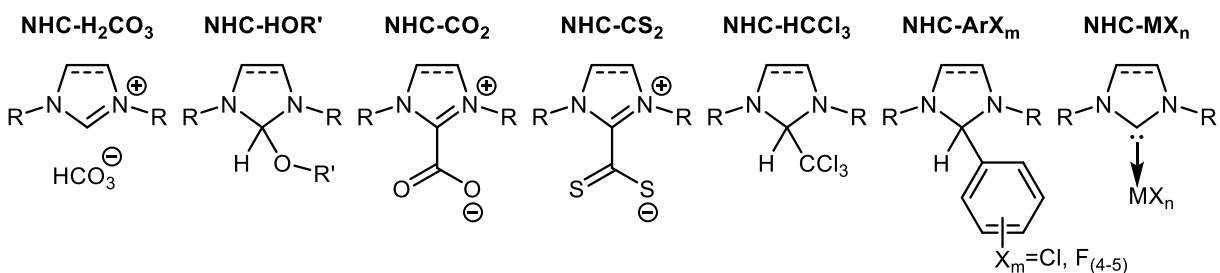
Scheme 16: Structures of blocked *N*-heterocyclic carbenes with various protecting groups. Although only imidazole(in) derivatives are depicted many strategies can be applied for triazole, benzannulated, tetrahydropyrimidine and diazepan derivatives.[155]

NHC-H₂CO₃ precursors, upon increased temperature, release the carbene and carbonic acid, which decomposes to H_2O and CO_2.[102, 161-163] Their synthesis is quite comfortable as an anion metathesis from e.g. imidazolium halides with alkali metal hydrogen carbonate leading to the desired molecule without the necessity to form a free and thus reactive or sensitive carbene as intermediate. An ambivalent characteristic is the release of water that limits the use of **NHC-H₂CO₃** to non-water-sensitive reactions but at the same time these precursors provide a certain stability towards ambient humidity and long-term storability. The sp^3-hybridized precursors allow for a comfortable liberation or isolation of the free carbene since the released small molecule, the former protective group, might be evaporated and removed from the reaction at elevated temperatures and/or reduced pressure.[31, 34, 48-49, 74-75, 164-166] Further, the release of an alcohol might be used beneficially e.g., in ring-opening polymerizations.[167] **NHC-MXₙ** and may have a dual impact on catalyzed reactions. The carbene, on the one hand, affects the reactions as Lewis or Brønsted base while the metal compound MX_n, on the other hand, acts as Lewis acid. This was observed for both, AROP of lactones and step-growth polymerization of polyurethanes.[111-112, 120, 159, 167-169] The released Lewis acids often increase the electrophilicity and facilitate the attack of the NHC or another nucleophile activated by the NHC. The synthesis of silver halide NHC complexes (**NHC-AgX**) is, like the synthesis of **NHC-H₂CO₃**, accomplished from of the **NHC-HX** salt. Two equivalents of **NHC-HX** mixed with one

equivalent Ag_2O produce two equivalents of the organometal compounds and one equivalent of H_2O. **NHC-AgX** complexes are widely used to transmetallize NHCs to complexes in chemical environments not tolerating free carbenes but also found application as catalysts.[81, 170-177] Among the protected NHCs, the carboxylates are probably the best investigated class, whereas the isoelectronic and structurally related **NHC-CS₂** precursors are less researched, mainly due to the stability of the adduct, making them less interesting in latent catalysis. Another drawback is the released, toxic CS_2.[178-179] Further, CS_2 is liquid at ambient temperatures whereas gaseous CO_2 is easily removed from the reaction mixture. Noteworthy, the mixed form, **NHC-COS** was isolated, the structure resolved by single crystal X-ray structure analysis, compared to **NHC-CO₂** and **NHC-CS₂** and the catalytic activity tested for transesterification and benzoin condensation.[180] A closer look at the structure of NHC carboxylates shows a zwitterionic charge separation where the positive charge is distributed between N-C-N (or the aromatic imidazole moiety) and the negative charge is distributed between O-C-O. Both carbons are covalently bound to each other although the electron density distribution is shaped comparable to NHC metal complexes, where most of the electron density is located at the electron-deficient center. Further, the CO_2 moiety is twisted relative to the plane of the heterocycle. This torsion angle Θ can be determined by X-ray structure analysis or quantum mechanically calculated.

An outstanding issue for the latency of **NHC-CO₂** catalysts and initiators is the stability of the adduct of NHC and CO_2. Mixtures of 1,3-diisopropyl-4,5-dimethylimidazol-2-ylidene (**5u$_{Me}$-iPr**) and 1,3-bis(2,4,6-trimethylphenyl)imiazolium-2-carboxylate (**5u-Mes-CO₂**) or 1,3-di(2,6-diisopropylphenyl)imidazolium-2-carboxylate (**5u-Dipp-CO₂**) result in **5u$_{Me}$-iPr-CO₂** and **5u-Mes** or **5u-Dipp**, respectively (Scheme 17).[114] The reaction of **5u-Mes** or **5u-Dipp** with **5u$_{Me}$-iPr-CO₂** does not result in **5u-Mes-CO₂** or **5u-Dipp-CO₂**. In addition, the reaction of **5u-Mes**

and **5u-Dipp-CO₂** leads to **5u-Mes-CO₂** and **5u-Dipp**, again the back reaction was not observed. Thus the authors concluded the following order of stability **5u$_{Me}$-iPr-CO₂>5u-Mes-CO₂>5u-Dipp-CO₂**.[181]
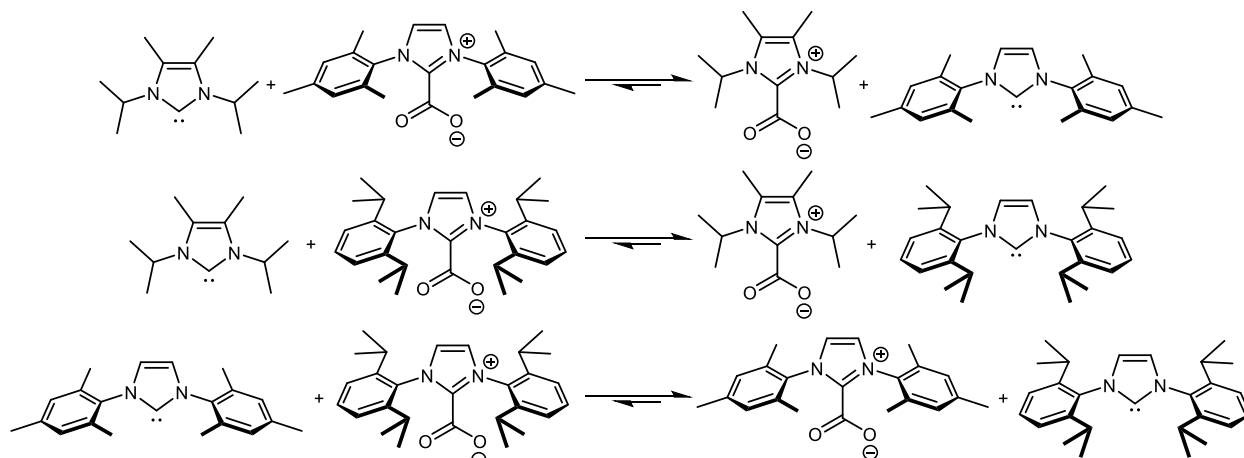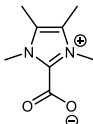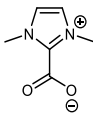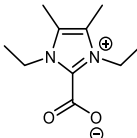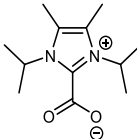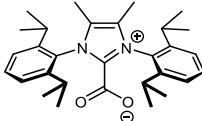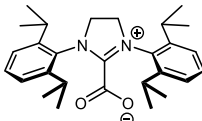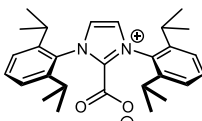
Scheme 17: Reactions of NHCs with NHC-CO₂.[114, 181]

With respect to the application of latent *N*-heterocyclic carbenes in catalysis it was found that the CO_2 and carbene release is facilitated for higher torsion angles Θ.[178, 182] It was argued that the π conjugation is disturbed for larger angles which in turn weakens the C-C bond. Louie *et al.* correlated the **NHC-CO₂** decarboxylation temperatures received from thermogravimetrical analysis measurements (TGA) and torsion angles from X-ray structure analysis (Table 2).[182] Comparison of entries 1 and 2 shows a remarkable strong influence of backbone methyl group substitution. An increase in torsion angle of about 7° results in a decrease of the decarboxylation temperature by 20°C. Further, the same backbone alkylation in entry 5 compared to 7 leads to a difference of 41° in torsion angle and a decreased decarboxylation temperature from 136 to 108°C. Consequently, the steric demand of the nitrogen substituents is not the only factor affecting the decarboxylation temperature. This is exemplified if entries 6 and 7 are compared where the saturation state of the backbone results in a 30° difference in torsion angle and 12°C in decarboxylation temperature. Nonetheless, steric properties of the nitrogen substituents have got

an important effect underlined by the steadily increasing steric bulk in entries 1, 3 and 4 resulting in increasing torsion angles and decreasing carboxylation temperatures while maintaining the backbone substitution.

Table 2: Decarboxylation temperatures determined by TGA and torsion angles determined by single crystal X-ray analysis of various **NHC-CO$_2$**.[182]

entry	NHC-CO$_2$	decarboxylation temperature [°C]	torsion angle Θ [°]
1		182	22.4
2		162	29.0
3		144	47.5
4		139	69.0
5		136	46.7
6		120	58.0
7		108	88.1

In solution, the stability of the **NHC-CO$_2$** adduct is influenced additionally by the solvent. **5u-Me-CO$_2$** was found to be stable in both, pure water and anhydrous MeCN.[183] However,

solutions of **5u-Me-CO₂** in MeCN upon the addition of water exhibit quantitative formation of the 1,3-dimethylimidazolium salt as observed by NMR. The observation was investigated more in depth for MeCN, MeOH and 1,4-dioxane. For all three solvents, the rate of decomposition decreased with increasing amounts of water. Further, it was found that decarboxylation was faster for less polar solvents. The order of decomposition rate is thus reduced from dioxane over MeCN to MeOH. DFT calculations showed shorter C_2-CO_2 bond lengths with simultaneously increasing dipole moments and increasing dissociation bond lengths for more polar solvents.

The pK_a value of the **NHC-HX** salts was compared to the stability of carbene CO_2 adducts by means of DFT.[108] A linear correlation was found i.e., increasing stability (ΔG) of the adduct occurs with higher basicity of the NHCs (Scheme 18).
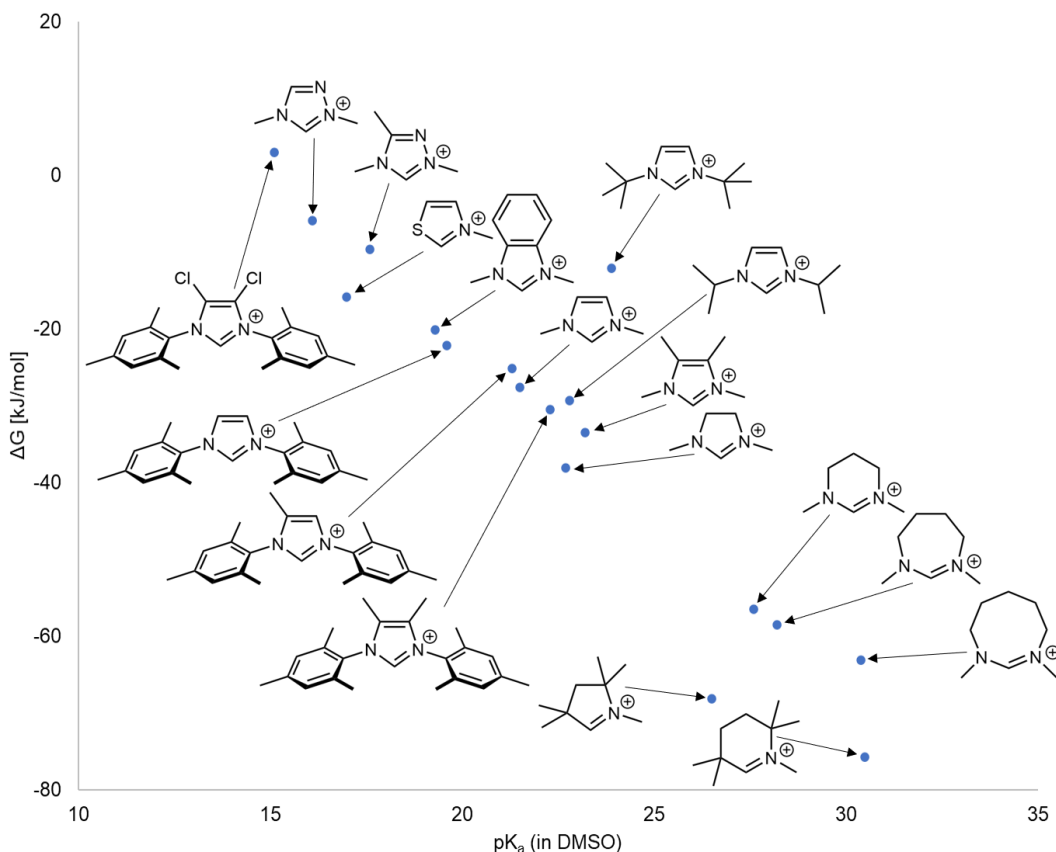
Scheme 18: Selected examples of NHC precursors from publications of Ji *et al.* Plotted *ΔG* of the **NHC-CO₂** adduct vs. *pKa* of the NHC-H⁺ salt.[108-109]

44

The study included 90 NHC carboxylates based on triazoles, imidazolines and imidazoles. However, a follow up publication was enhanced to more than 400 structures including imidazoles, benzimidazoles, triazoles, imidazolines, tetrahydropyrimidines, diamidocarbenes, diazepanes, thiazoles, cyclic alkyl amino carbenes, 1,3-diazocyclo octan and mesoionic carbenes.[109] Again, good linear correlation of the pK_a and the stability of the CO_2 carbene adduct was found. Nonetheless, perfluorinated or tertbutyl side groups deviate partially from this behavior.

Increasing interest in latent NHCs fostered the development of various synthetic methods for NHCs and the respective carboxylates.[184] A solvent-free one-pot procedure was established by Rogers *et al.* in 2003 (Scheme 19).[3] The authors heated a mixture of dimethyl carbonate and 1-methylimidazole to from 1,3-dimethylimidazolium-2-carboxylate (**5u-Me-CO₂**) which precipitated from the mixture. **5u-Me-CO₂** can be synthesized, isolated, purified and stored at ambient conditions.
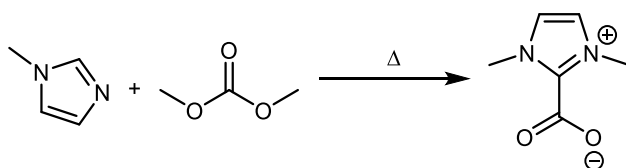
Scheme 19: Synthesis of **5u-Me-CO₂** according to Rogers *et al.*[3]

The concept of converting *N*-alkyl or *N*-aryl imidazoles with dimethyl carbonate was extended for the synthesis of unsymmetric NHC carboxylates.[185-187] Competitive carboxylation of the C_4 or C_5 of the imidazole ring and C_2 was found for temperatures above 95°C whereas above 120°C only substitution in 4 or 5 position was observed.[157, 181] Pure C_2 substituted product was found for temperatures below 95°C. The proposed mechanism starts with the methylation of the unsubstituted imidazole nitrogen. The 1,3-dimethylimidazolium cation is deprotonated by the methyl carbonate anion to form 1,3-dimethylimdazol-2-ylidene and instable methyl hydrogen

carbonate, which decomposes to methanol and CO_2, which is in turn coordinated by the formed carbene to result in 1,3-dimethylimidazolium-2-carboxylate.

A convincing possibility to form **NHC-CO₂** is via deprotonation of the **NHC-HX** and subsequent addition of CO_2. This method is widely applied and allows converting many free NHCs to the respective carboxylate. Further, this method also allows for preparing carboxylates of saturated and unsaturated five membered NHCs with and without backbone substitution as well as six and seven membered.[188-189] However, the formation of free carbenes requires careful synthetic handling of both, the strong bases necessary to deprotonate the imidazolium salts and the free carbene intermediates. Tommasi and Sorrentino published a route applying 1,3-dialkylimidazolium chlorides and Na_2CO_3 under an atmosphere of 500000 Pa CO_2 thereby avoiding the formation of a free carbene intermediate.[190]

Noteworthy, NHC adducts with carbodiimide were reported (**NHC-C(NR)₂**) representing isoelectronic structures to NHC carboxylates.[191] Comparable to **NHC-CO₂** they were proven to exhibit a betaine structure. A torsion angle of 85.6° was found for **5u_Me-iPr-C(NiPr)₂** whereas for **5u_Me-iPr-CO₂** an angle of 69.0° was observed.[182] The different torsion angles can be attributed to the varying steric demand of the electrophiles. The authors list the steric shielding of the four isopropyl groups as the reason for chemical inertness.

Underappreciated and comparably early, isocyanate and isothiocyanate protected NHCs were synthesized. However, these early representatives were prepared from bis(1,3-diorganyl imidazoline-2-ylidene)s and isocyanates and/or isothiocyanates (Scheme 20) more than 20 years before the first *N*-heterocyclic carbene was isolated and barely recognized as latent catalysts.[45, 50, 192-194] Winberg and Coffman converted bis(1,3-diethylimidazolin-2-ylidene) with two

equivalents of phenyl isothiocyanate and isolated the betaine phenyl(1,3-diethylimiazolinium-2-thionyl)amide. After subsequent reaction with iodomethane, the methyl group was found to be bound to the sulfur atom, thus it seemed natural that the highest electron density is located on the sulfur. In contrast, protonation upon treatment with $HClO_4$ occurs at the nitrogen and conversion with ethyl isocyanate or methyl isothiocyanate produced the spirocycles 1-ethyl-3-phenyl-6,9-dimethyl-1,3,6,9-tetraazaspiro[4.4]nonan-2-on-4-thione or 1-methyl-3-phenyl-6,9-dimethyl-1,3,6,9-tetrazaspiro[4.4]nonan-2,4-dithione, respectively, and a thiocarbonyl moiety was observed whereas the nitrogen is part the five ring atoms.[195] Spirocycles of comparable constitution were also synthesized from phenyl(1,3-diethylimidazolinium-2-thionyl)amide by incorporation of but-1-en-3-one, prop-2-ennitrile and methyl prop-2-enoate. Interestingly, the non-substituted CH_2 group is bound to the nitrogen.[192]
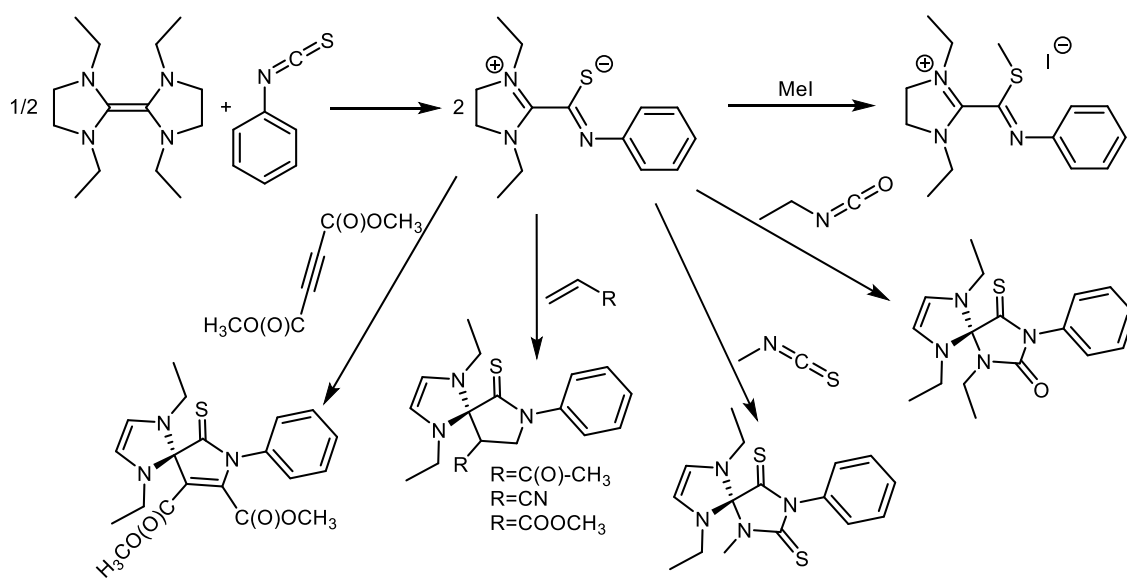
Scheme 20: Formation of phenyl(1,3-diethylimiazolinium-2-thionyl)amide and subsequent conversion with iodomethane or ethyl isocyanate or methyl isothiocyanate.[192]

Bis(1,3-diphenylimidazoline-2-ylidene) and its reactions with isocyanates and thioisocyanates were investigated in a study published by Regitz and Hocker.[194] Conversion in the ratio of 1 to 4 resulted in the formation of spirocycles for isocyanates and isothiocyanates. This finding was

almost independent of the substitution of the applied iso(thio)cyanate. However, the formation of betaines was described exclusively for deactivated isothiocyanates (-Ph-NO$_2$ group for example) when converted with the bis(diphenylimidazoline-2-ylidene)s in a ratio 2:1. Methyl benzthiazolium salts as well as 3,4,5-trimethylthiazolium were found to give the 1-thio-4,6,8-triaazaspirocycles when converted with iso(thio)cyanates.[196] In contrast, reactions starting from 1,3-dimethylimidazolium with either methyl isocyanate or phenyl isocyanate resulted in the formation of 1,3-diazetidine-2,4-diones or 1,3,5-triazan-2,4,6-triones. Betaines of NHCs and isocyanates were usually not isolated.[181]

For the sake of completeness, the successful syntheses of spirocycles with an imidazol(in)e moiety with higher homologous like isoselenocyanates as well as reactions with other hetero cumulenes like α-(thio)carbonyl and CS$_2$ and the formation of 1,3-diphenylimidazolin-2-carboxylate as a hydrolysis product of aforementioned molecules must be mentioned.[181, 195, 197-198]

With respect to synthetic applications, the reversibility of the NHC isothiocyanate adduct formation was investigated by Norris and Bielawski for 1,3-bis(2,2-dimethylpropyl)benzimidazole-2-ylidene and phenyl isothiocyanate by means of NMR in toluene-d8 (Scheme 21, top).[199] An equimolar mixture of the products on the left and on the right side was found after 20 h at 120°C. The actual goal of the study, to synthesize a reversible, conjugated polymer, was fulfilled by adjusting the temperature and the ratio of the monomers. The polymer synthesis is depicted in Scheme 21, (middle). Bielawski *et al.* also published on a study in which 1,3-bis(2,4,6-trimethylphenyl)imidazole-2-ylidene, protected by adduct formation with phenyl isothiocyanate, was applied as organo catalyst for the trimerization of phenyl isocyanate and the anionic ring-opening polymerization of lactide (Scheme 21, bottom).[200]

Different substitutions of the protective phenyl isothiocyanate derivative allowed to adjust the catalyst activation temperature significantly. The strongest activation temperature decrease was observed for the π electron donating 4-methoxyphenyl isothiocyanate.
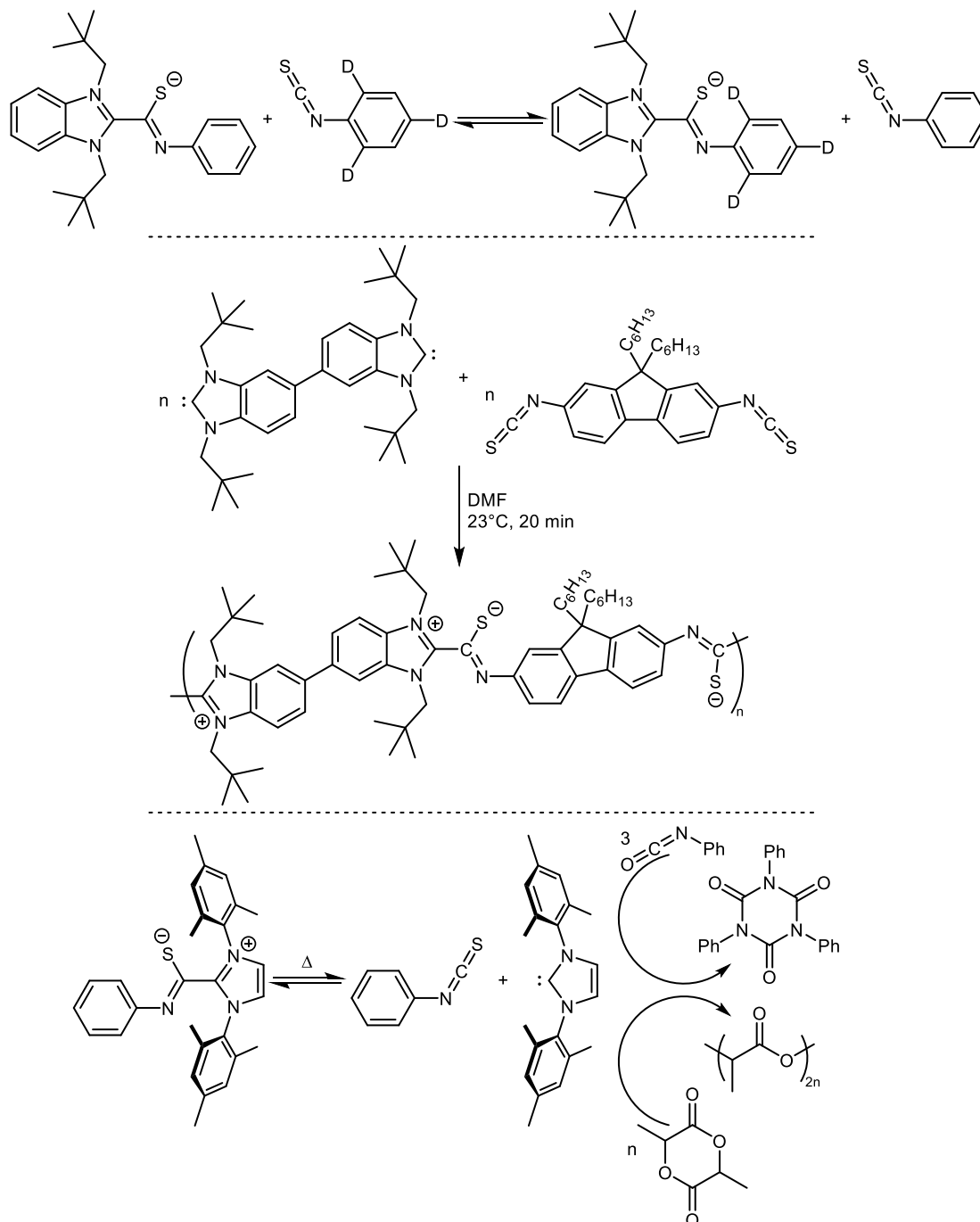
Scheme 21: Equilibrium with deuterated and non-deuterated phenyl isothiocyanate (top). Polymerization of a dicarbene and a diisothiocyanante (middle). Latent NHC organo catalyst and applications (bottom).[199-200]

Katritzky *et al* reported the syntheses and investigation of various CS$_2$- and (double)isothiocyanate-protected NHCs.[201-202] The behavior of the benzimidazole based spirocycles towards increased temperatures was investigated by NMR experiments (Scheme 22). A first decomposition step, releasing the NHC isothiocyanate adduct and non-bound isothiocyanate was found at 70°C. Upon cooling, the sample below 70°C the initial spirocycle was re-formed. Heating the mixtures above 80°C led to the formation of two equivalents of isothiocyanate and the free carbene. It was claimed that this behavior could be exploited to generate "on demand" catalysts.[202]
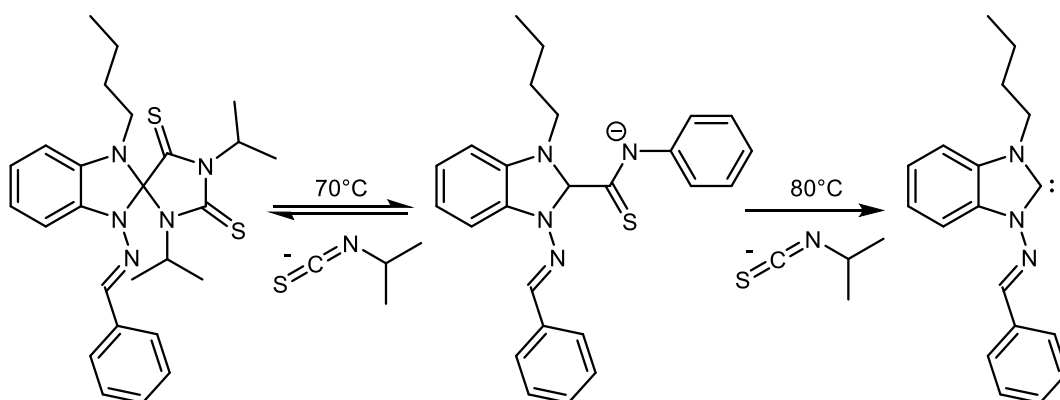
Scheme 22: Stepwise liberation of a free carbene from a double isothiocyanate protected NHC.[202]

Whereas betaines of NHCs and isothiocyanates are often isolated only a few examples of isolated isocyanate adducts are known. Even if substoichiometric amounts of isocyanate are added to the NHC, formation of the 1,3,6,9-tetraaza spirocycle seems to be preferred. Moieties with electron-withdrawing properties adjacent to the isocyanate stabilize the betaine structure. [181, 195] However, spirocycles from either imidazolines or triazoles or thiazoles or benzimidazole or benzthiazoles and two equivalents isocyanates are well known and their syntheses and structures are described accurately in the literature.[194, 196-197, 203-208]

6.3 Anhydride-Hardened Epoxide Resins

Epoxide resins are curable materials based on oxirane derivatives.[209] The polymerizable mixtures are often called thermosets.[210] Usually, the monomers bear two or more oxiranyl groups, however, reactive thinners with only one oxirane moiety can be used additionally.[211] After the curing reaction, duroplastic, crosslinked materials are formed. Epoxide resins find application in various areas like coatings, windmill blades, microelectronics, ships, architectures, automotive and aerospace parts, adhesives and matrices for fiber matrix composites.[209, 212-214] Characterizing properties are high electrical resistance, adhesion to many materials, low curing shrinkage, heat resistance and mechanical capacities to withstand stress. All those properties can be tuned according to need. The degree of crosslinking has significant impact on the material properties.[214-215] Higher crosslinking results in material with higher T_g and higher chemical resistance. Lower crosslinking content leads to greater elongation before break and improved toughness as well as reduced shrinkage during curing.[215] The different resin types for different applications are, among other characteristics, distinguished by the curing agents. Aromatic and aliphatic primary amines react in a ring-opening fashion with the oxirane moieties (Scheme 23). Each primary amine undergoes two of these reactions commonly followed by a proton transfer. Crosslinking is usually caused by the application of di- and polyfunctional amines. The curing reaction of an amine with epoxides is depicted in Scheme 23.[209, 216] In principle, both, the substituted and the unsubstituted position of the terminal three-membered ring are accessible for the attack. In the following, reaction schemes are drawn showing the attack at the sterically less crowded, unsubstituted carbon atom.
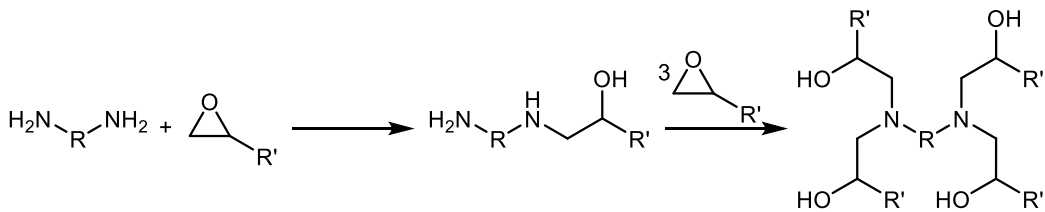
Scheme 23: Reaction of a primary diamine with four epoxides.

Another group of curing agents comprises benzylsulfonium, benzylpyridinium, benzylammonium and phosphonium salts.[209, 217-223] The mode of action of these activators generally increases electrophilicity of the oxirane moiety by coordination or even covalent bond formation (Meerwein-like) between the oxirane oxygen and the cationic moiety. Thus, the neighboring carbon atoms of the oxirane oxygen become accessible for nucleophilic ring-opening attacks by other oxiranes. In some cases, these initiators are latent and become activated by external stimuli like heat or UV light. The third group of curing agents includes imidazole base or tertiary amines. Both are often used as accelerators in conjunction with other curing agents, however, this is not necessarily the case.[209, 224-225] For use as accelerator, both imidazole and tertiary amines can be used in conjunction with (primary) amines or with the fourth group of curing agents namely anhydrides, more precisely cyclic anhydrides.[209, 214, 226] For anhydrides also hydroxyl curing agents can be applied as accelerator.[226-230]

The initiation of anhydride-hardened epoxide resins is often described by starting from the epoxide-immanent sp^3 carbon-bound secondary hydroxyl groups. These hydroxyl groups result from reactions of the oxirane moieties with primary alcohols (mostly phenol derivatives). One famous example is 2,2-di-4,4'(oxiranylmethoxyphenyl)propane commonly known as bisphenol-A-digylcidyl ether (BADGE) (Scheme 24 (top)). BADGE is synthesized from 2,2-di-4,4'(hydroxyphenyl)propane and 2-(chlormethyl)oxirane and is one of the most important monomers in epoxide resin chemistry ("workhorse").[212, 231] Remarkably, the initial addition

reaction of 2-(chlormethyl)oxirane to 4,4'(hydroxyphenyl)propane proceeds under oxirane ring-opening and proton transfer while the ring-closing and condensation products are formed in the downstream reaction under the impact of NaOH. Further, the pK_a of phenolic alcohols in DMSO is around 18-19 for unsubstituted derivatives or small aliphatic substitutions on the aromatic ring. The pK_a of propan-2-ol is 30 (in DMSO).[232-233] Weak phenolic acids react with the oxirane moieties in an addition reaction whereas the non-acidic secondary alcohols coexist with epoxides (or react very slowly) even at elevated temperatures.[234] However, in the presence of e.g. tertiary amines, secondary hydroxyl groups undergo anhydride-hardened epoxide curing reactions probably due to the activation of the anhydride.[227, 230] It should further be noted that the addition of one equivalent 2,2-di-4,4'(hydroxyphenyl)propane to two equivalents 2,2-di-4,4'(oxiranylmethoxyphenyl)propane does not necessarily correspond to the exact structure as depicted in Scheme 24 (top). On the contrary a mixture of BADGE and addition products of various chain length must be expected (Scheme 24, bottom).[235] Therefore, the epoxide equivalent weight is an important measure and refers to the mass of the resin that contains one mole of oxirane moieties.[210, 226] In other words one mole oxiranyl groups has a certain molecular weight that is described by the epoxide equivalent weight. However, this measure is not only used for BADGE and other diepoxides that are prepolymerized but also for epoxide resins like bio-based epoxidized fatty acid triglycerides and novolaks. Novolaks are synthesized from phenol and substoichiometric methanal and subsequently converted with 2-(chlormethyl)oxirane to give oligomers with a single-digit number of repeat units each bearing an oxirane unit (Scheme 25).[236-237]
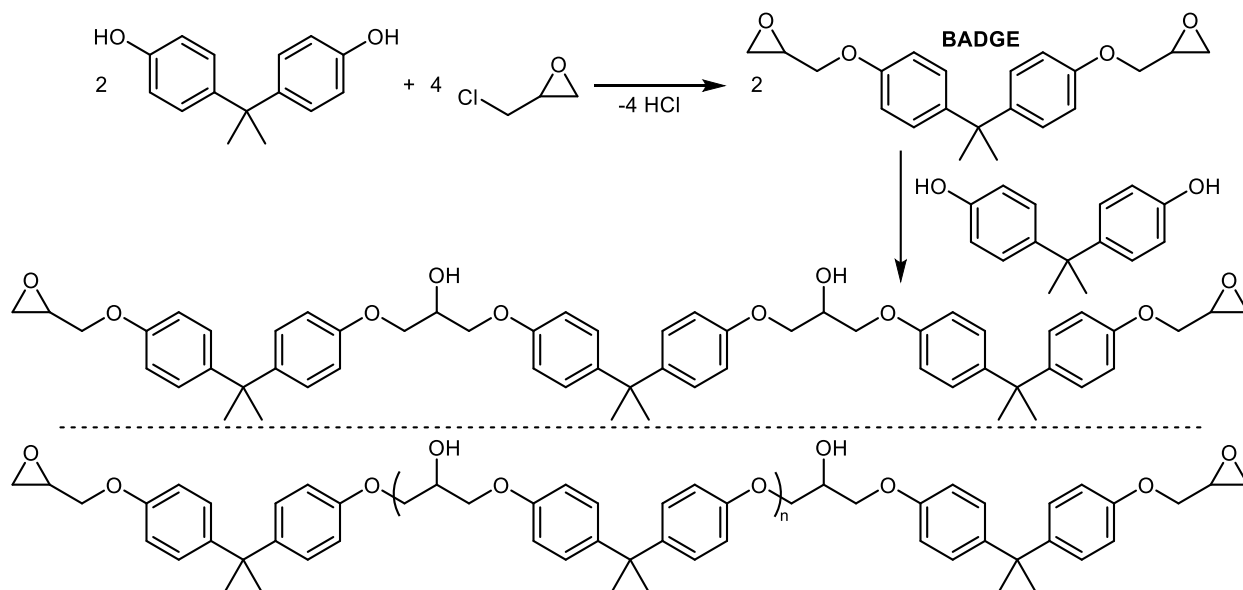
Scheme 24: Synthesis of BADGE and formation of a "prepolymer" (top). Polymeric structure resulting from BADGE and 2,2-di-4,4'(hydroxyphenyl)propane (bottom).
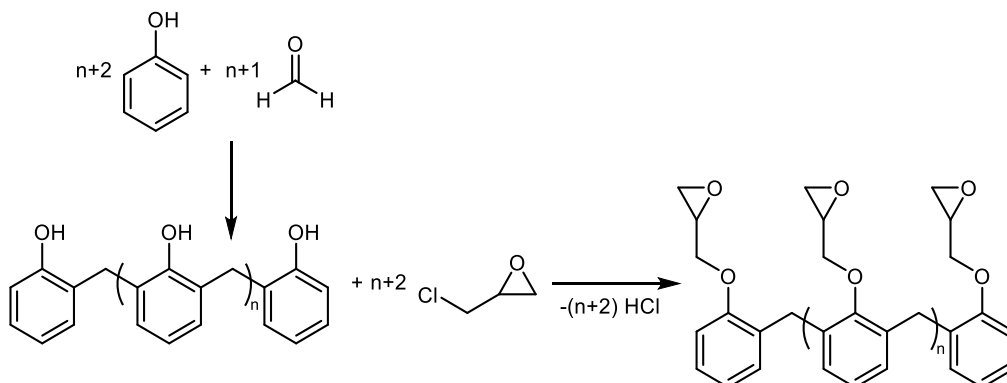
Scheme 25: Synthesis from phenol and methanal and the structure of novolak.

If alcohols are present in the anhydride-hardened curing reaction of epoxides two reaction pathways occur. Both are initiated by a nucleophilic attack of an alcohol on the carbonyl carbon of an anhydride and subsequent ring-opening under carboxylic acid formation (Scheme 26, top). Two pathways are possible from the carboxylic acid (Scheme 26). On the one hand, reactions with an oxirane moiety is possible. The ring is opened and an ester bond is formed as well as an alcohol representing the new end-group (Scheme 26, right). Subsequent alternating incorporation of anhydrides and epoxides leads to the formation of a polyester. On the other hand, the formed carboxylic acid protonates an epoxide which in turn leads to an increased electrophilicity of the

carbon atoms in the three-membered ring adjacent to the protonated oxygen.[227, 230, 234, 238] Thus, a nucleophilic attack of another oxirane moiety at one of these carbon atoms initiates the formation of a polyether (Scheme 26, left). In anhydride-hardened epoxide curing reactions containing hydroxyl groups a certain amount of polyether will form under the catalytic influence of the carboxylic acids as depicted in the reaction pathway in Scheme 26 (left).[234]
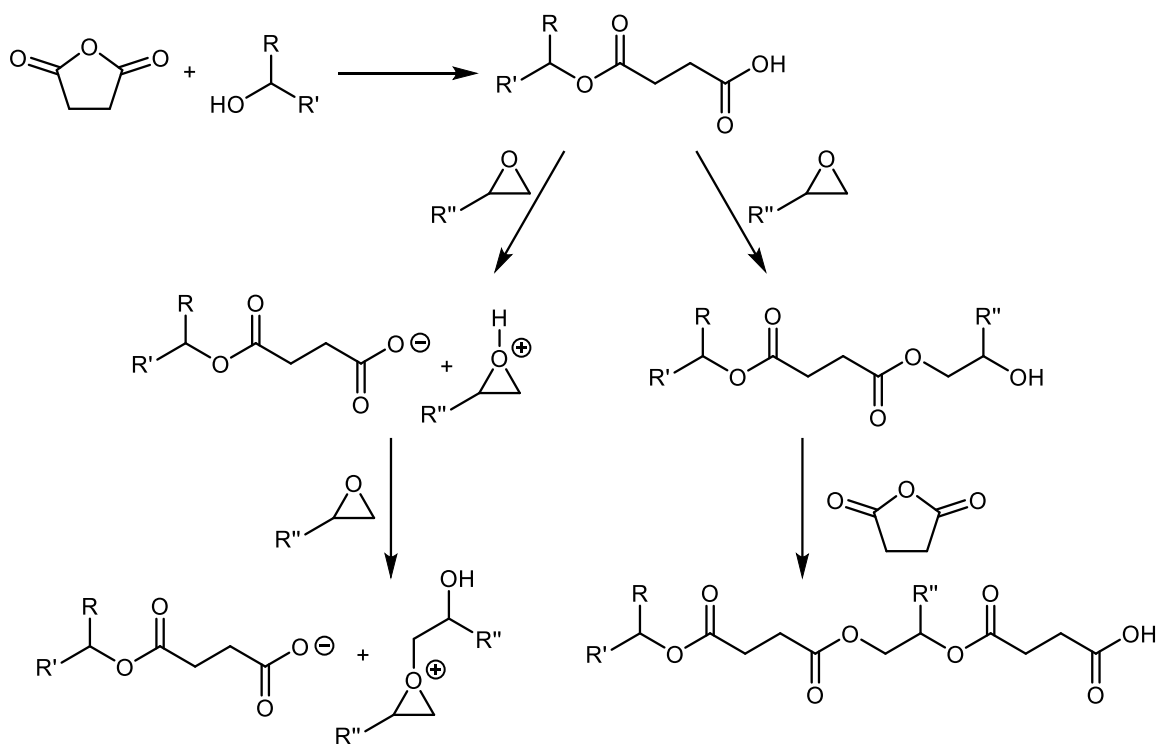
Scheme 26: Two reaction pathways for reactions in the presence of alcohols. Polyester formation on the right an polyether formation on the left.[227, 230, 234]

Tertiary amine curing agents are widely used in anhydride-hardened epoxide curing reactions.[209] In a model study it was shown that in the benzyldimethylamine-catalyzed reaction of 2-(phenoxymethyl)oxirane with benzoic acid anhydride or ethanoic acid anhydride the tertiary amine binds covalently and irreversibly to a carbon atom of the former oxirane ring (Scheme 27).[239] The resulting betaine consists of a quaternary ammonium and an alkoxide function. The alkoxide in turn attacks the carbonyl carbon of the acid anhydride to form an ester and releases a

carboxylate which is not bond to the former molecule due to the acyclic structure. This carboxylate then reacts with an oxirane in a ring-opening fashion, resulting in formation of an ester and an alkoxide within the same molecule. A diester is produced by subsequent esterification with an anhydride. The reaction cycle is restarted hereafter by the released carboxylate. 1-Phenoxy propane-2,3-dibenzoate or 1-phenoxy propane-2,3-diethanoate, respectively, were recognized as the main products of the amine catalyzed reaction. Low concentrations of tertiary amine resulted in 99% of the diester, higher concentrations produced a slightly increased amount of byproducts within the single-digit percentage range.[239]
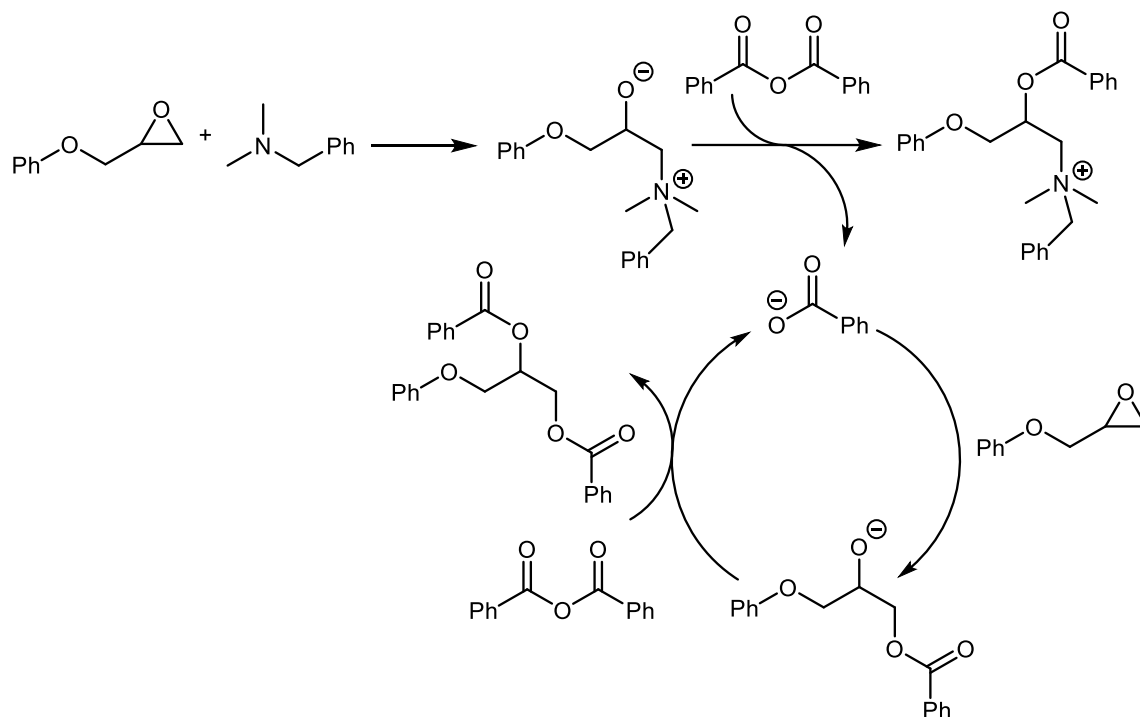
Scheme 27: Proposed mechanism of benzoic anhydride and 2-(phenoxymethyl)oxirane polymerization initiated by a tertiary amine as a model for epoxide resins.[239]

Conversely, other authors claim that the initial step is a nucleophilic attack of the tertiary amine at the carbonyl carbon of an anhydride and subsequent formation of a betaine comprising a quaternary ammonium and a carboxylate group (Scheme 28).[240] The formed carboxylate group in turn attacks an oxirane moiety leading to an alkoxide after ring-opening. Here, again, two

reaction paths are conceivable, i.e. either the incorporation of another anhydride, or another epoxide, depending on the ratio of oxirane moieties to anhydrides.[229, 239] Equimolar amounts result in the concomitant consumption of both reaction partners and esters are formed instead of ethers. Further, epoxide homopolymerization is more pronounced if non-terminal epoxides like cyclohexene oxide and vinylcyclohexene oxide are used. 75-80% of the epoxide moieties undergo reactions with anhydrides and form ester bonds whereas the remaining 20-25% undergo epoxide homopolymerization and form polyethers.[240]
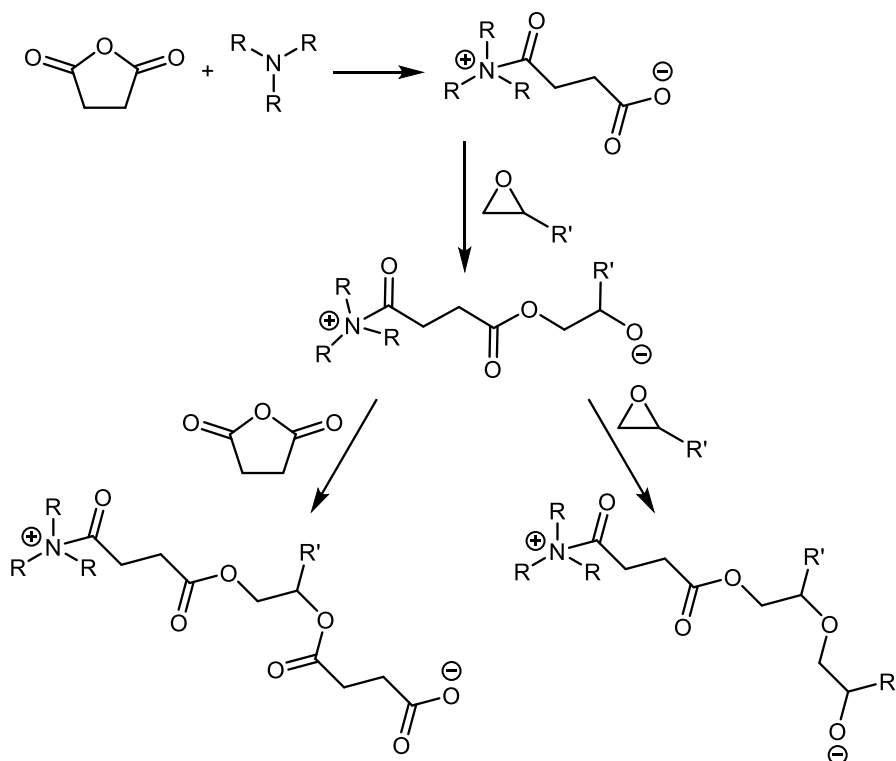
Scheme 28: Reaction path of an anhydride-hardened epoxide resin accelerated by a tertiary amine. After the incorporation of an oxirane moiety two reaction paths are accessible.[210, 227, 239]

An initiation by oxirane ring-opening is also proposed if imidazoles are applied as accelerators (Scheme 29).[238, 241] Burchard *et al.* analyzed the reaction mechanism of imidazole-driven polymerizations using MALDI-ToF-MS and found that a homopolyester is formed from the reaction of 2-(phenoxymethyl)oxirane and 2-benzofuran-1,3-dione.[238] Mass spectroscopic

analysis showed formation of both, carboxylic acid-terminated polymers with 2-benzofuran-1,3-dione on the last incorporated molecule as well as alcohol-terminated polymers in which 2-(phenoxymethyl)oxirane was incorporated last. The hydroxyl groups drawn in red in Scheme 29 were postulated but not observed by MALDI-ToF-MS. Usually these mass spectra contain a proton or an alkali metal cation (Li^+, Na^+), which is necessary for the analyte to fly and which is added during sample preparation. Here, however, due to the cationic end-group of the polyester no alkali metal cation was observed. Thus, the initiating imidazoles are chemically bound after initiation, underlining the C-N bond stability.[238]
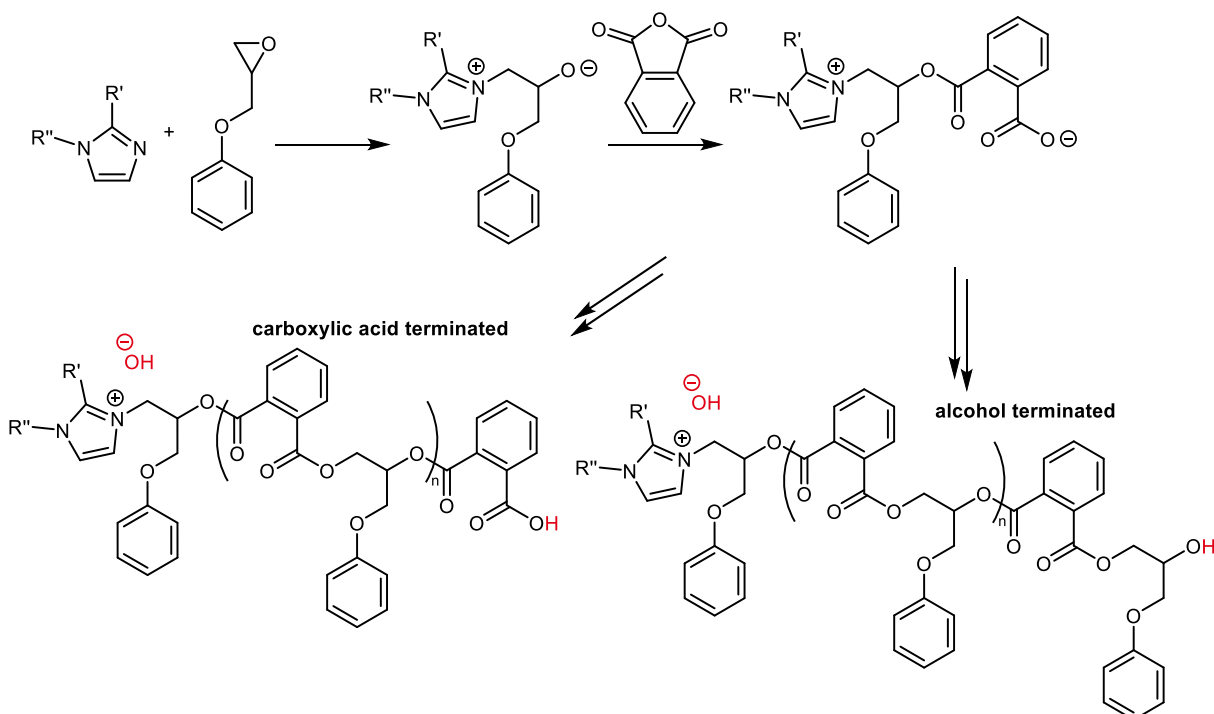
Scheme 29: Polyester synthesis from 2-(phenoxymethyl)oxirane and 2-benzofuran-1,3-dione. After the workup carboxylic acid (bottom, left) as well as alcohol (bottom, right) terminated end-groups were found by MALDI-ToF-MS.[238]

More recently, Buchmeiser *et al.* published on the curing of anhydride-hardened epoxide resins accelerated by NHCs.[2, 242] The proposed polymerization mechanism is initiated by the nucleophilic attack of the carbene at the carbonyl carbon of the anhydride under formation of a betaine consisting of a NHC+ moiety and a carboxylate.[2] It was argued that only moderate

reactivity between e.g. 1,3-diprop-2-ylimidazol-2-ylidene and methyloxirane (epoxide homopolymerization, 3 d, 50°C) was found in previous publications and therefore the initiation at an oxirane moiety is less likely than at the anhydride. In addition, the NHC initiated ring-opening of epoxides strongly depends on the carbene structure whereas for the anhydride-hardened epoxide systems many carbenes show equally satisfying curing behavior.[2, 243-244] Further, the assumption was made that the carbene is released again after a nucleophilic attack of an intermediary formed alkoxide at the carbonyl carbon bound to the NHC^+ moiety. If so, there is a certain probability for the released carbene to attack another anhydride.[2]
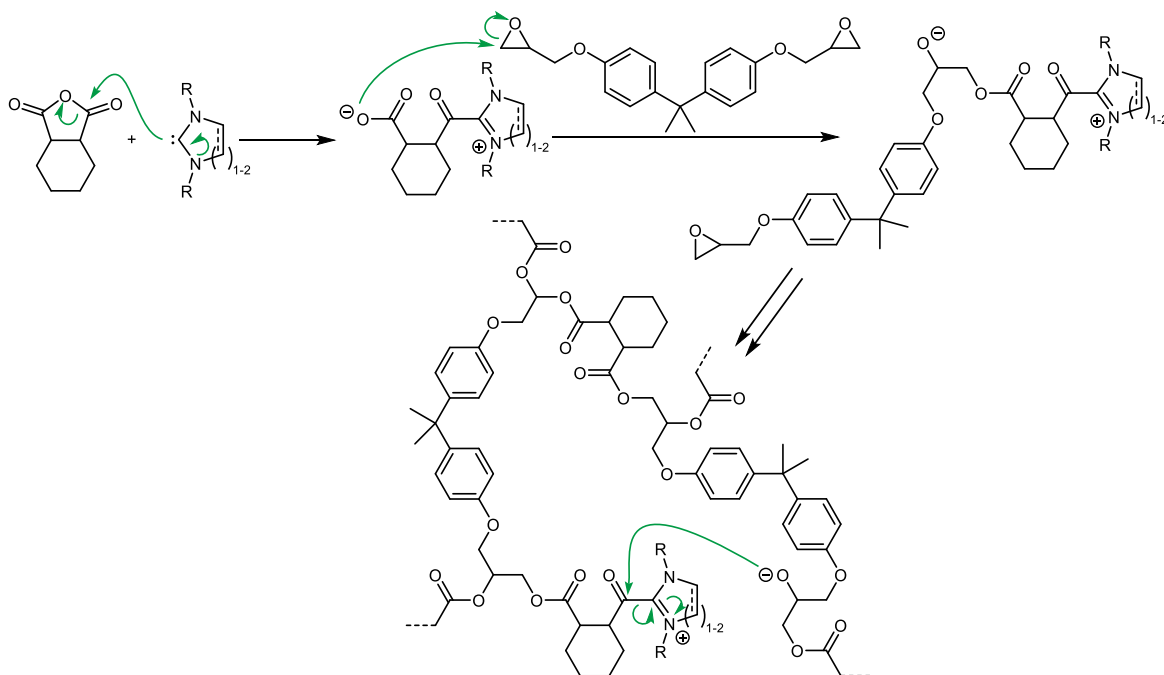
Scheme 30: Proposed mechanism of the anhydride-hardened epoxide curing accelerated by a NHC and the release of the latter while polymerization.[2]

Buchmeiser *et al.* applied CO_2, $MgCl_2$, $ZnCl_2$ and $SnCl_2$, protected saturated and unsaturated five- as well as six-membered NHCs. Before initiation, the protection group had to be removed by heating to release the free carbene. In addition, the mixtures of anhydride, epoxide and protected carbene were found to be stable for days and even weeks at ambient conditions. By DSC the released energies during curing were determined directly after compounding and one,

two, three and four weeks after compounding. Only in one case after four weeks less than half of the initial heat tinting was observed. If 2-benzofuran-1,3-dione was used as hardener for BADGE, solidification times for various NHCs were between three and seven minutes, whereas for hexahydro-2-benzofuran-1,4-dione solidification times of four to ten minutes were observed. The T_{max} value was defined as the temperature of maximum negative heat flow in DSC measurements of one equivalent of carbene precursor, 100 equivalents of BADGE and 200 equivalents of anhydrides at a heat rate of 5 K/min. Lewis acid protected carbenes were found to display the highest T_{max} values, ranging between 169°C for **5s-Mes-ZnCl₂** over 172°C for **6-Mes-ZnCl₂** to 175°C for **5s-Mes-MgCl₂**. However, **5s-Mes-SnCl₂** with a T_{max} of 155°C is situated in-between the unsaturated five-membered NHCs **5u-Cy-CO₂** (158°C) and **5u-tBu-CO₂** and **5u-Ad-CO₂** (both 154°C). The lowest T_{max} values were found for CO_2-protected tetrahydropyrimidines comprising **6-Cy-CO₂** (146°C), **6-2,6-(OMe)Ph-CO₂** and **6-Mes-CO₂** (both 150°C). An exception is represented by **6-Me-CO₂** with an increased T_{max} of 162°C, which is explained by the decreased steric pressure caused by small methyl groups compared to the sterically demanding nitrogen substituents in other tetrahydropyrimidines. The authors concluded that deprotection of the carbene and reactivity of the carbene determine the curing rate. The observed increased reactivity of CO_2 compared to Lewis acid protected carbenes was attributed to the evaporation of the gas, thus precluding the back reaction to the protected carbene. Most active **6-Cy-CO₂** was further used to prepare glass fiber composites.[242] Resins made from hexahydro-2-benzofuran-1,3-dione and BADGE were prehomogenized with the carbene precursor. The mixture was processed by vacuum assisted resin infusion (VARI process) and subsequent curing at temperatures from 85 to 165°C. Pot times of more than two weeks were observed.

The chemical structure of the monomers together with the type of curing agent strongly influence the properties of the thermosets.[209] Already introduced novolak epoxides cause a high crosslinking density and thus desirable resistance against thermal, chemical and solvent impact.[245-246] Cycloaliphatic epoxides are based on the structure of cyclohexene oxide, bear one or more of these groups and contribute to thermal and UV stability as well as weatherability.[247-248] Biobased resins can consist of cycloaliphatic epoxides (e.g. limonene dioxide) or of epoxidized triglycerides of unsaturated fatty acids. The latter bear three, four, five, six and more epoxide groups leading to high crosslinking densities for demanding applications but remain low in price as the epoxidation is executed by hydrogen peroxide.[218, 221, 236, 241, 249-250] The curing of tetrafunctional epoxides results in high crosslinking density and high thermal stability as well as chemical resistance, UV blocking and high modulus.[250-251] Fillers like surface-modified silicon dioxide nanoparticles, aluminum oxide nanoparticles or carbon nanotubes improve the mechanical properties.[212-213, 252-253] The water (and other fluids) uptake ability might be adjusted by the choice of monomer and curing program.[211, 245]

6.4 Polyoxazolidin-2-ones

Polyoxazolidin-2-ones are characterized by a five-membered ring comprising a carbamate group within the polymer main chain (Scheme 31). Due to the structural similarity some authors see them as subgroup of the polyurethanes.[254] However, their adjustable properties, including chemical inertness, high glass transition temperature, high temperature stability, electrical as well as mechanical behavior, enabled by a huge pool of available monomers, render them unique with a broad range of possible applications.[254-264]

polyoxazolidin-2-one   **polyurethane**
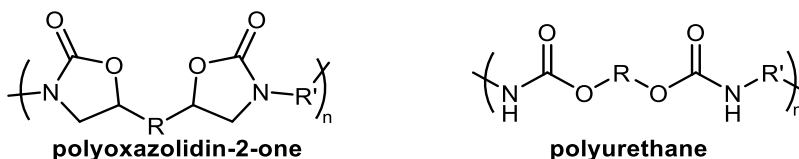
Scheme 31: Generalized polymer structures of polyoxazolidin-2-ones (left) and polyurethanes (right). They have the carbamate group in common.

Low molecular weight cyclic carbamates serve as auxiliaries in stereoselective synthesis. They can be prepared from amino acids by reduction and cyclization (Scheme 32). Benzyl-substituted oxazolidin-2-ones synthesized from phenylalanine are very common. These auxiliaries are named after David Evans.[265-267]
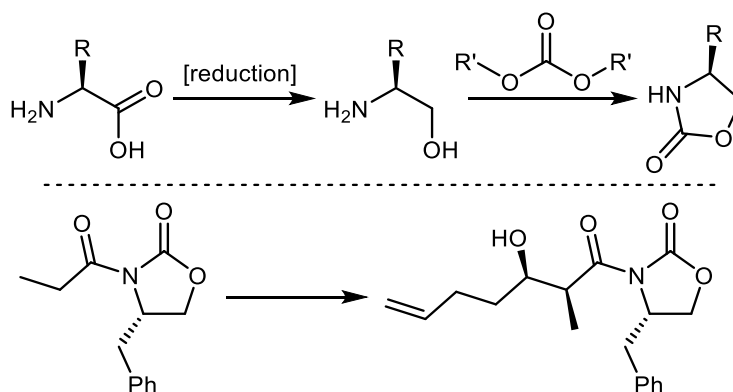
Scheme 32: Synthesis of the auxiliary molecules from amino acids (top). Usage of the auxiliary to gain stereocontrol (bottom).[265-267]

Concerning polyoxazolidin-2-ones a major challenge is their synthesis.[254] Various approaches, starting from different monomers, are known. Most common is the synthesis from diepoxides and diisocyanates. This polyaddition proceeds under formal oxirane ring expansion at elevated temperatures (typically 150 to 200°C). However, some effort was spent to avoid isocyanates not only due to their toxic properties but also due to their reactivity. Several isocyanate-free synthesis procedures have been reported.

Diamines and cyclic dicarbonates were polymerized in a ring-opening fashion resulting in a polyurethane with ketone side groups (Scheme 33).[254, 268-270] A subsequent ring-closing reaction leads to a polyoxazolidin-2-one with tertiary hydroxyl groups in the polymer backbone, which in turn can be removed by dehydration leading to a methylidene group in the polymer backbone.[254]
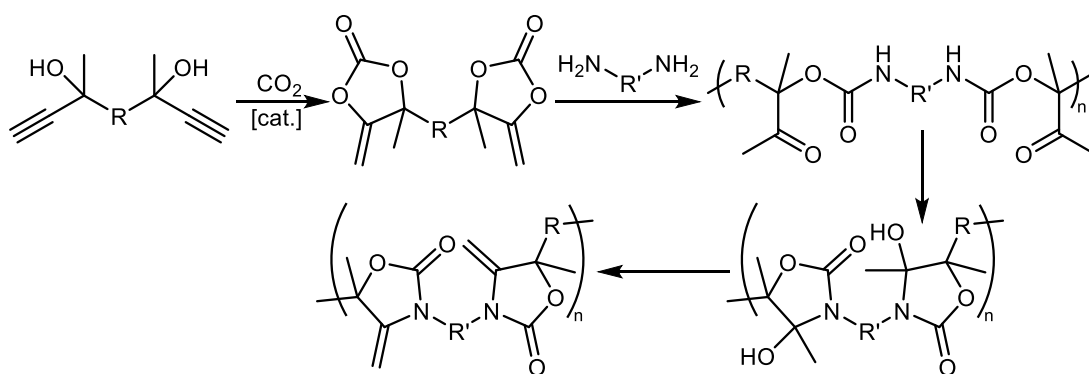
Scheme 33: Polyoxazolidin-2-one synthesis from cyclic dicarbonates and diamines.[254, 268-270]

A copper-catalyzed four-component reaction comprising CO_2, aldehydes, alkynes and amines (or the respective ammonium salts) resulted in oxazolidin-2-ones.[271] The reaction proceeds at 75°C overnight in ethanol. Usage of dialkynes and diamines led to the respective polyoxazolidin-2-ones (Scheme 34, top).[272-273] Again, temperatures as low as 75 to 80°C are sufficient to execute the manipulations. In addition two reaction mechanisms were proposed (Scheme 34, bottom). Both start from the amine, however the sequence of substrate addition remains unclear.
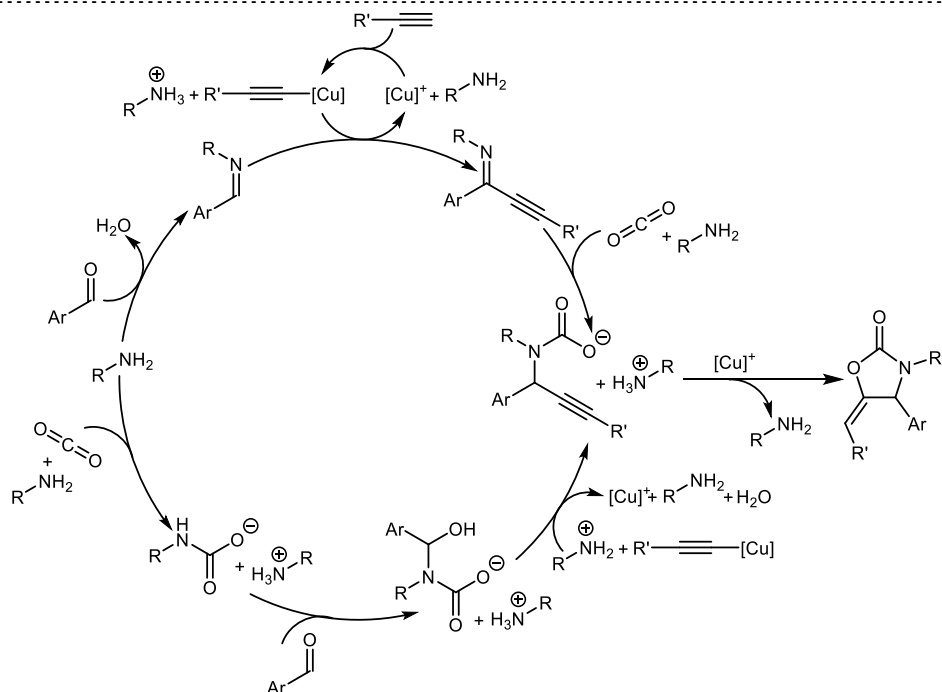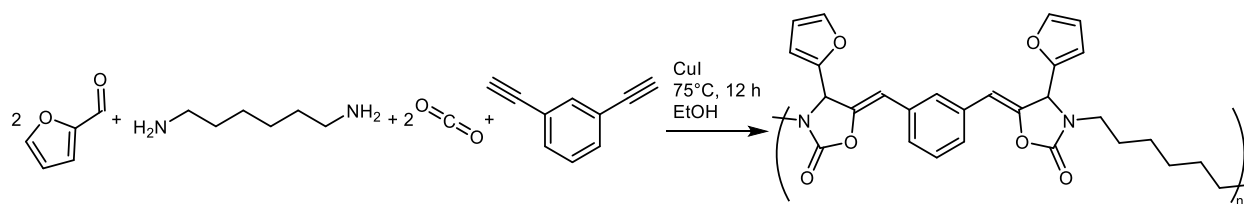
Scheme 34: Four component polyoxazolidin-2-one synthesis catalyzed by CuI (top). Proposed mechanism (bottom).[273]

Dicarbamates and diepoxides can be used as starting material for polyoxazolidin-2-one synthesis (Scheme 35).[255, 274-275] The reactions are catalyzed by a base, for example by tertiary amines or quaternary ammonium salts. Even though the avoidance of isocyanates has advantages, the most atom-economic formation of carbamates comprises isocyanates. A major advantage of applying carbamates as starting material are the low reaction temperatures (25 to 140°C, mostly 90°C) at which the reaction proceeds at least for monofunctional substrates.[275] Further, the carbamate approach allowed for monofunctional substrates to work without any solvent and a reaction time of 2 h. For difunctional substrates the polymerization was executed in solution (DMF) and the reaction times at 90 to 100°C were expanded to 5 to 32 h.[274]
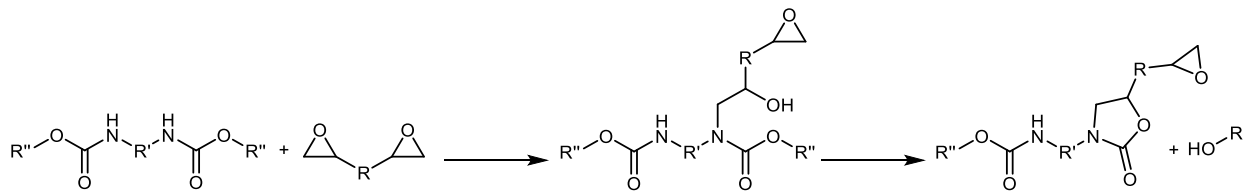
Scheme 35: Reaction pathways for the polycondensation reaction of dicarbamates and diepoxides which, under release of an alcohol, react to a polyoxazolidin-2-one.

A related approach, despite starting from diisocyanates, is catalyzed by alkoxides (Scheme 36).[276] Noteworthy, the diisocyanate (2,4-diisocyanato-1-methylbenzene, TDI) was added to the diepoxide (BADGE) and the alkoxide (lithium n-butoxide) dissolved in 1,2-dichlorobenzene at 180°C over a period of 60 min. For initial experiments with monofunctional epoxides and isocyanates it was found that yields increase if the isocyanate was added portionwise. Dileone also investigated the reaction between the alkoxide and the epoxide as well as the reaction between epoxide and isocyanate. In both cases no reaction was observed.[276]
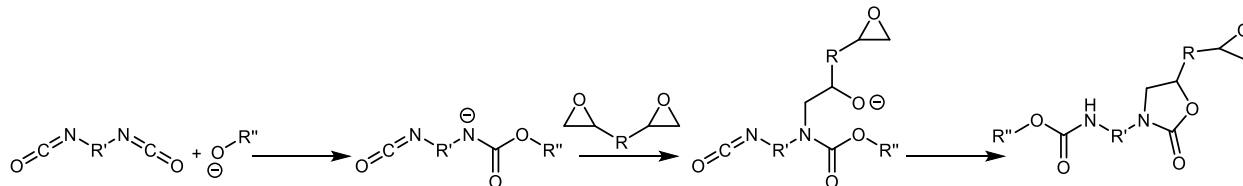
Scheme 36: The alkoxide attacks the isocyanate, the formed carbamate anion in turn attacks the oxirane moiety under ring-opening resulting in an alkoxide end-group, which subsequently releases the initial alkoxide under oxazolidin-2-one formation.

The polyaddition of diepoxides and diisocyanates is the most common and most atom-economic approach to synthesize polyoxazolidin-2-ones. Both, diepoxides and diisocyanates are commercially available with many varying molecule cores in-between the two functional groups. The consequence of changing from 1,1-bis(4-isocyanatophenyl)methane (MDI) to TDI is an increase in T_g from 170 to 195°C and a decrease in tensile strength from 66 to 55 MPa, respectively.[276] Therefore, most of the developments focus on the investigation of catalyst

systems, the preparation of prepolymers and reaction setups (solvents, temperature, monomer ratio and addition).[277]

The employed catalysts comprise several types and classes.[277] Among others, ammonium salts like tetramethylammonium iodide, hexadecyltrimethylammonium bromide and chloride, tetraethylammonium bromide and iodide, ethyltriprop-2-ylammonium iodide; tertiary amines like triethylamine, 2,4,6-tris(dimethylaminomethyl)phenol; phosphonium halides like tetraphenyl phosphonium bromide; Lewis acids like LiF, LiCl, LiBr, LiI, KI, $MgCl_2$, MgI_2 $AlCl_3$ and complexes thereof with hexamethylphosphor amide, *N*-methylpyrrolidone, diethyl ether, THF and triphenylphosphine oxide; alkoxides like lithium n-butoxide; nitril-based catalysts like 1-cyano-2-ethyl-4-methylimidazole and cyanoacetamides as well as triphenyl antimony iodine and more have been employed.[255-256, 261, 263, 276-287]

Mechanisms were proposed for many of these catalysts and initiators. An initial nucleophilic attack at the oxirane moiety under ring-opening and alkoxide formation is frequently published, e.g. for catalysts like phosphonium and ammonium halides as well as for Lewis acids and tertiary amines (Scheme 37, top).[277, 280, 283, 286-288] The alkoxide attacks the carbon atom of an isocyanate moiety. This mechanism was excluded for alkoxides as no reaction took place in the sole presence of epoxide and alkoxide.[276] Other authors proposed the formation of isocyanurates as the initial step (Scheme 37, middle).[278, 287] The isocyanurate ring-opening nucleophile can be a halide but also other available nucleophiles and must not necessarily be anionic, but is depicted as anionic X in Scheme 37. For example, it is conceivable that the oxirane moiety attacks and opens the six-membered ring. The negative charge subsequently located at the nitrogen atom attacks the oxirane ring under opening the O-CH$_2$ bond ("leaving group") and formation of an N-

CH$_2$ bond. In Scheme 37, bottom the reaction shown represents the generalized version of the reaction in Scheme 36 clarifying the mechanism.[276]
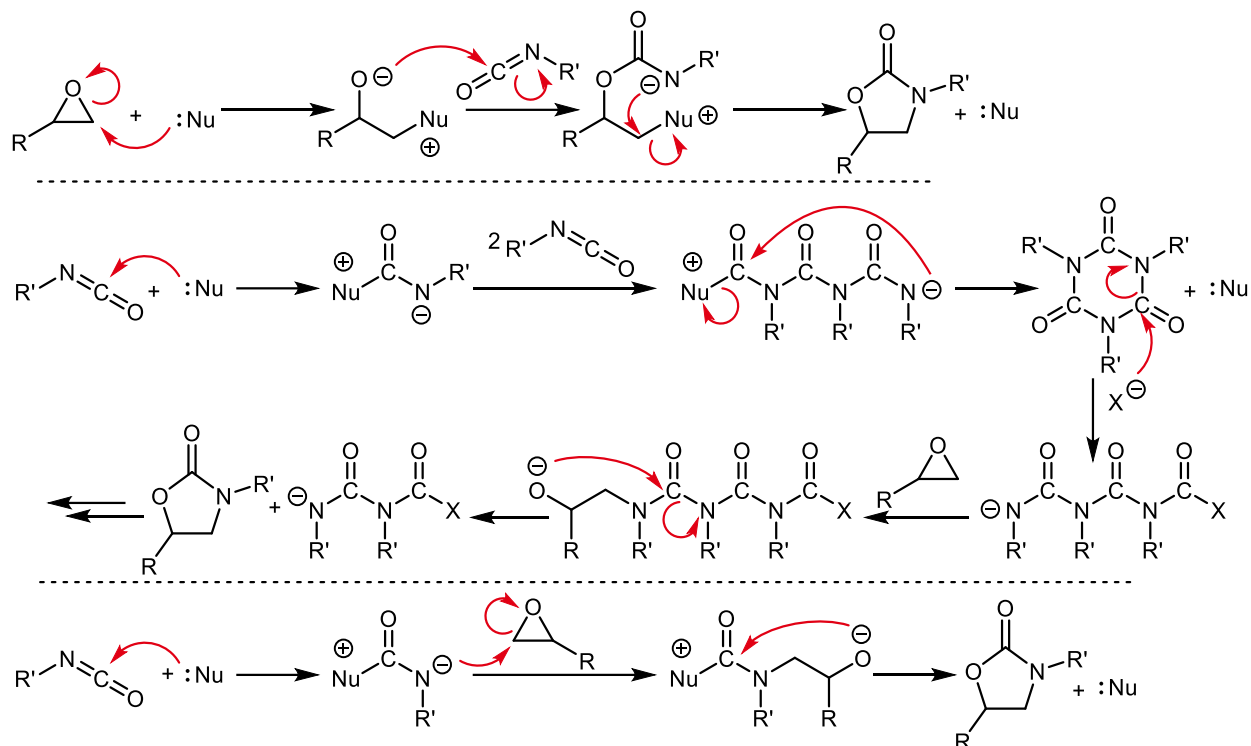
Scheme 37: Selected proposed mechanisms of the oxazolidin-2-one formation from the cited literature.[288]

Good experimental arguments for all mechanisms were found.[288] In a given reaction system, there is no necessity to assume only one mechanism. Two or more reaction pathways are conceivable simultaneously (or in case of isocyanurate ring-opening subsequently) for most cases. Competitive formation of oxazolidin-2-ones (Scheme 37, top and bottom) and isocyanurates (Scheme 37, middle) are not mutually exclusive, nor is a subsequent ring-opening of the latter and transformation to oxazolidin-2ones in the presence of epoxides excluded.[264] For example, isocyanate and oxirane moieties disappear simultaneously when oxazolidin-2-one formation is catalyzed by AlCl$_3$·triphenylphosphine oxide.[277] On the contrary, other experiments showed disappearance of the isocyanates after several minutes while the full intensity of the oxazolidin-2-one carbonyl vibration was only observed after hours, implying an

isocyanurate ring-opening.[264] This underlines the strong dependence of the mechanism on the reaction conditions and the catalyst type.[255, 288]

The production of polyoxazolidin-2-one thermosets must be mentioned here for completeness but are not discussed further because this work focuses on thermoplastic materials and defects, crosslinking and side reactions (discussed in the following) do not hamper or even improve the thermosets.[256, 263]

Two major side reactions were observed in polyoxazolidin-2-one chemistry using diisocyanates and diepoxides as monomer. First, epoxide homopolymerization and second, as mentioned above, isocyanate homopolymerization, typically leading to trimers and dimers of isocyanates (Scheme 38).[277, 281-282]
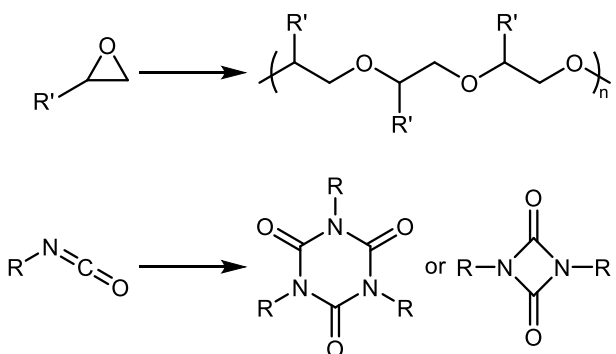
Scheme 38: Homopolymerization of oxiranes (top) and isocyanates (bottom).

The occurrence of side reactions depends on the catalyst, solvent and temperature as well as the monomers and their ratio.[261, 277, 289] The trimerization of diisocyanates results in trisisocyanates with an isocyanurate core structure. Trifunctional groups in polyaddition reactions force the formation of crosslinked polymers.[261] It therefore does not matter whether a monomeric diisocyanate or a polymeric diisocyanate or poly-α-epoxide-ω-isocyanate undergoes the trimerization. A mixture of phenyl isocyanate and 2-(phenoxymethyl)oxirane in the presence of N(CH$_3$)$_4$I in DMF formed the desired oxazolidinone at temperatures of 140 to 160°C.[278] From

the same mixture at lower temperatures (56.1°C) the isocyanurate (trimer) was produced as major product. Most interesting, the polyoxazolidin-2-one is formed in 17% yield if 1 equivalent of trimer is heated to 140-160°C with 3 equivalents 2-(phenoxymethyl)oxirane in the presence of the catalyst in DMF, underlining the principial reversibility of the trimerization.
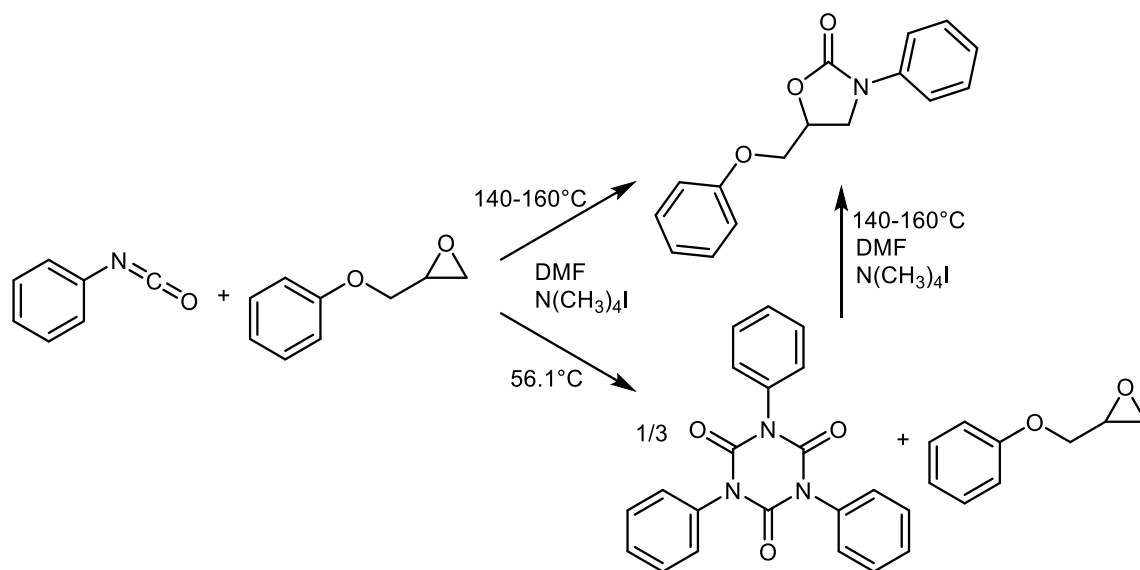
Scheme 39: Synthesis of oxazolidinone from isocyanate and from isocyanurate.[278]

Structure analysis of polyoxazolidin-2-ones was achieved by IR spetroscopy. Typically, the carbonyl vibration of an oxazolidin-2-one can be found around 1735 to 1750 cm^{-1}, while isocyanurates cause signals around 1690 to 1710 cm^{-1} (aliphatic and aromatic, respectively).[261, 285]

Whitmore and Herweh produced polyoxazolidin-2-one from diepoxides and aliphatic and aromatic isocyanates under reflux conditions in DMF applying LiCl as catalyst.[285] Molecular weights between 1000 and 5000 g/mol were found. Aromatic diisocyanates resulted in lower molecular weights compared to aliphatic diisocyanates. Formamidine end-groups were found by NMR and IR. The authors affiliated these end-groups to the incorporation of the solvent, DMF. The formamidine moieties were found more frequently in polymers synthesized from aromatic

diisocyanates and prohibit chain-growth. In addition, Braun and Weinert identified issues with other solvents like hexamethylphosphoramide, ethanoic anhydride, bis(2-methoxyethyl) ether and 3-methylpyridine.[279] The remarkable approach to circumvent solvent-induced side reactions was the synthesis and application as reaction solvent of low melting oxazolidin-2-one solvents, namely 3-phenyl-3-methyloxazolidin-2-one (mp. 80°C) and 3,4-diphenyloxazolidin-2-one (mp. 130°C). Although, due to insolubility of LiCl, the catalyst had to be changed to tetramethylammonium iodide, the produced polymers displayed higher thermal stability than polymers synthesized in DMF. Concluding, isocyanates are very reactive towards many functional groups including several common solvents.[289]

In a more recent approach Azechi and Endo used LiBr as catalyst and NMP as solvent for the polyoxazolidin-2-one synthesis.[290] The applied 9,9-diglycidyl fluorene was polymerized with MDI at temperatures between 100 and 180°C (Scheme 40, top). A magnification of the carbonyl area of the recorded IR spectra of these polymers was presented. Two major peaks were observed, one at 1710 cm^{-1} caused by the isocyanurate and a second at 1750 cm^{-1}, caused by the oxazolidin-2-one moieties. Different polymerization temperatures resulted in different relative ratios of these peaks. Equally pronounced intensities were found at low temperatures of 100 to 120°C, decreasing intensities of the isocyanurate were observed for reactions at higher temperatures of 160 and 180°C. Thus, the oxazolidin-2-one content increased whereas trimer content decreased at higher temperatures. Further, with increasing temperature, narrower molecular weight distributions were found, however, accompanied by decreasing molecular weights (120°C: M_n=4100 g/mol, Đ=8.5; 180°C: M_n=2700 g/mol, Đ=2.0). Wolf *et al.* used tetraphenylphosphonium bromide as catalyst and 1,2-dicholobenzene as solvent for the polymerization.[283] TDI was polymerized with various diglycidyl ethers of bisphenols (Scheme

40). Increasing T_g values from 156 to 211°C were observed with increasing steric demand of the diepoxide core. Noteworthy, the molecular weights were determined in two different ways. One included the low molecular weight fractions >500 g/mol while the other included fractions >2000 g/mol. The differences in the molecular weights between the measuring methods were about a factor of two. The low molecular weight fractions were assigned to cyclic oligomers of polyoxazolidin-2-one. The lowest number-average molecular weights were found for BFDGE (M_n=11000 g/mol), all other diepoxides resulted in comparable molecular weights between 16000 and 18000 g/mol (all values without parts below 2000 g/mol). Weight-average molecular weights (M_w) (and as a consequence also the molecular weight dispersities) increase with the steric demand of the diepoxide core (31000 to 85000 g/mol). Luinstra *et al.* used tetrabutylammonium chlorides, bromides and iodides as catalysts in reactions without solvent to convert 2-(2-methylphenoxymethyl)oxirane (monofunctional) or BADGE (difunctional) with MDI in the ratio of 3 to 1 at 170°C.[264] Quantitative consumption of the isocyanate within 30 s, the rapid (1 min) formation of oxazolidin-2-one and isocyanurate as well as the increase of signal intensity of oxazolidin-2-one relative to the signal intensity of isocyanurate over 3 h was reported. The conversion rate of isocyanurates to oxazolidin-2-ones decreased from chloride to bromide to iodide. Due to the excess of epoxide monomer, oxirane terminated prepolymers were formed.
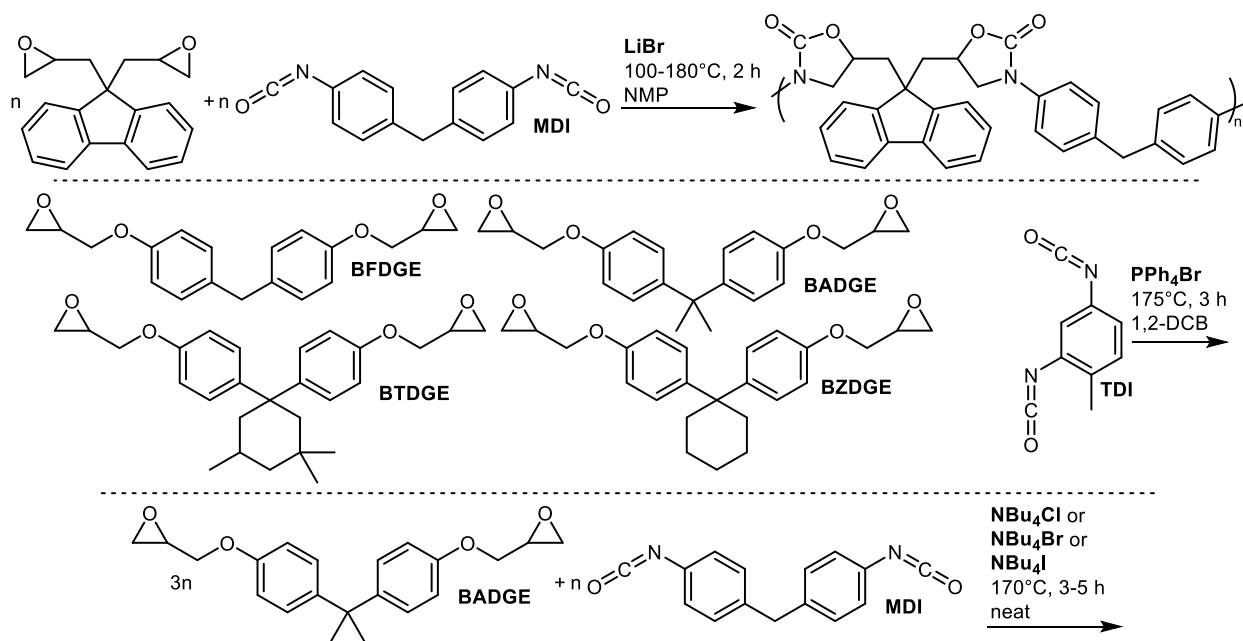
Scheme 40: Three different polyoxazolidin-2-one synthesis approaches.[264, 283, 290]

In a study using monofunctional phenyl isocyanate and 2-(phenoxymethyl)oxirane as model compounds to investigate the reactivity of various $AlCl_3$ complexes, two oxazolidin-2-one regioisomers were observed by HPLC (Scheme 41).[277] The ratio of four (4-Oxa) to five (5-Oxa) substituted oxazolidin-2-one rings was strongly influenced by the catalyst, the temperature and the solvent. An $AlCl_3$ complex with a triphenylphosphine oxide ligand in 1,2-dichlorobenzene at 80°C led to a ratio of 4-Oxa : 5-Oxa of 17 : 100. Temperature decrease to 60°C resulted in a 4-Oxa : 5-Oxa ratio of 2.5 : 100. On the contrary, a temperature increase to 140°C gave a ratio of 20 : 100. The same aluminum complex at 80°C in benzene produced a ratio of 4-Oxa : 5-Oxa of 2 : 100. In the very same study, no isocyanurate formation was observed for the $AlCl_3$ complexes of triphenylphosphine oxide and hexamethylphosphoramide. The low reaction temperatures, compared to the above described procedures, are also noteworthy. Further, no reactivity at was found for LiCl in boiling benzene and the productivity of ligand-free or THF coordinated $AlCl_3$

was below the one of other complexes. The authors attributed this to the low solubility of the catalysts.
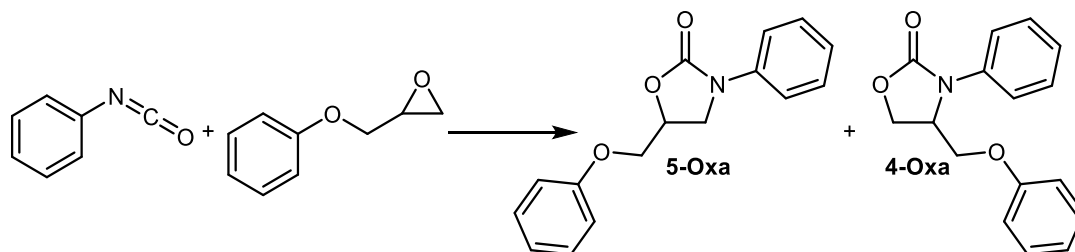
Scheme 41: Formation of the regioisomers 5- phenoxymethyl-3-phenyloxazolidin-2-one (5-Oxa) and 4-phenoxymethyl-3-phenyloxazolidin-2-one (4-Oxa).

6.5 Polyamide 6 Synthesis

Many polyamides like polyamide 6.6 (PA6.6), polyamide 6.10 (PA6.10), poly(para-phenylene terephthalamide) are accessible by polycondensation reactions from amino acids (AB monomer) or diamines and dicarboxylic acids (AA/BB monomer).[292] The aliphatic polymer derivatives of the AA/BB monomers are named by the number of carbons in the chain of the monomers starting with the diamine (e.g. 1,6-diamino hexane and octanedioic acid result in PA6.8). Other polyamides are produced by ring-opening polymerizations of lactams. For example, polyamide 6 (PA6) is a semicrystalline, thermoplastic macromolecular material with applications as fiber and engineering plastic, which is synthesized from azepan-2-one (AEO).[291, 293] The number of carbon atoms within the ring are namesake for this polyamide class.

Paul Schlack (*1897-†1987) discovered that azepan-2-one was polymerizable to PA6 and developed the production of fibers from the material. [291]

6.5.1 Hydrolytic Ring-Opening Polymerization of Polyamide 6

The majority of the world consumption of PA6 is produced by hydrolytic ring-opening polymerization.[291] At temperatures above the melting point of PA6 (~220°C), azepan-2-one and water react to 6-aminohexanoic acid as initial step of the polymerization (Scheme 42). Step-growth (condensation) and step-wise addition take place simultaneously.[294] Reaction times for the hydrolytic polymerization commonly range between 4 and 24 h.[291]
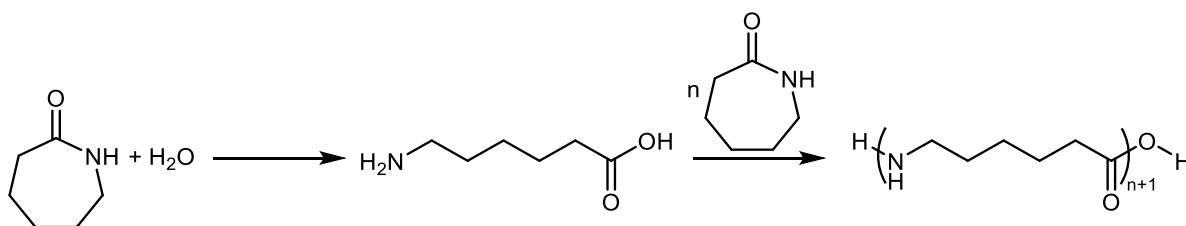
Scheme 42: Hydrolytic synthesis of PA6.[293]

6.5.2 Cationic Ring-Opening Polymerization of Polyamide 6

The cationically driven polymerization of azepan-2-one is conducted under anhydrous conditions using non-anhydride forming acids.[293, 295] Additionally, salts of these acids formed with amines or amides can be used as well as Lewis acids.[294] By protonation (or coordination of a Lewis acid) of the amide nitrogen, the electrophilicity of the carbonyl carbon is increased. Thus, a nucleophilic attack by the lone pair of the nitrogen of a neutral monomer is facilitated, followed by ring opening (Scheme 43). However, the mechanism of the cationic polymerization of azepan-2-one is complex and ambiguous for different catalysts.[294-295] Due to insufficient conversion and molecular weights, cationic polymerization of azepan-2-one is uncommon.[291] Unlike anionic ring-opening polymerization of lactams, cationic ring-opening polymerization allows to convert monomers with substitutions on the nitrogen of the monomer.[294]
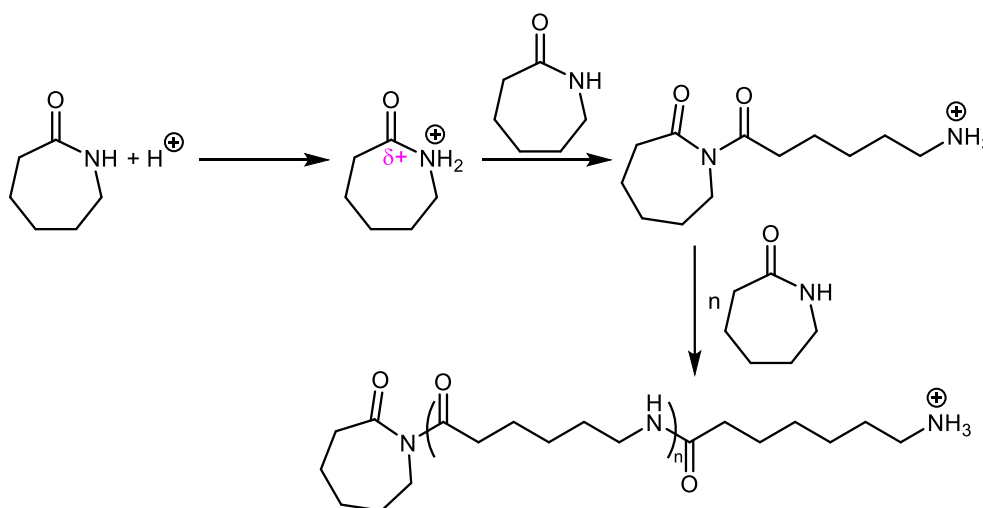
Scheme 43: Cationic synthesis of PA6.[293]

6.5.3 Anionic Ring-Opening Polymerization of Polyamide 6

Anionic polymerization of azepan-2-one proceeds via the deprotonated monomer often added as sodium azepan-2-onate (Na-AEO, compare also Scheme 46, bottom) or magnesium bromide azepan-2-onate (MgBr-AEO).[296-297] However, *in situ* preparation of the anions by addition of

sodium hydride or Grignard compounds is also common.[298-300] Further bases applied for anionic ROP are carbonates, amides and alkali metal as well as alkaline earth metal hydroxides.[291] A nucleophile attack of the lactamate on the carbonyl carbon of a neutral monomer is the initial step of the anionic polymerization. However, this initial step proceeds slowly compared to the chain growth.[301] Anionic ROP (AROP) of azepan-2-one is divided into reactions that proceed above the melting point of PA6 (~220°C) and reactions that proceed in a temperature range between the melting point of azepan-2-one (~70°C) and the melting point of PA6. For the latter method, temperatures from 130 to 200°C are common.[291, 297, 302] Despite the slow initiation, AROP of is among hydrolytic, cationic and anionic the fastest polymerization method for azepan-2-one. Quantitative yields were described for processing times of minutes and below.[292, 294]
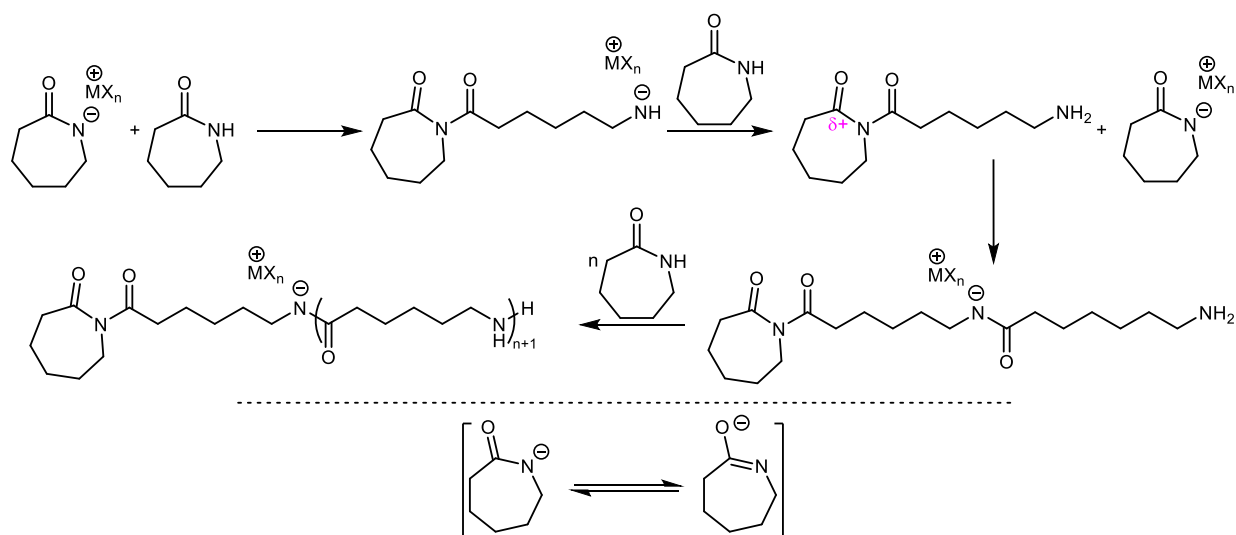
Scheme 44: Anionic synthesis of PA6 (top) and the two possible structures of the azepan-2-onate.[293]

Anionic, cationic and hydrolytic polymerizations of azepan-2-one suffer from side reactions.[293] However, only polymerization details of the anionic PA6 (also known as cast PA6) formation are discussed here.

The mechanism for the AROP of azepan-2-one is shown in Scheme 45.[301] The cyclic monomer is attacked by the nucleophilic lactamate and ring-opening results in an amide anion (Scheme 45, **A**). This reaction is actually an equilibrium reaction and proceeds slowly. The amide anion deprotonates the next monomer to regenerate the lactamate (**B**). Despite the structural relationship, the nucleophilic attack **C** at the cyclic moiety of the previously formed dimer differs from the initial nucleophilic attack **A**. The initial step **A** is a nucleophilic attack on an amide. Step **C** is a nucleophilic attack on an imide. The electron-withdrawing properties of the additional carbonyl group adjacent to the nitrogen increase the electrophilicity of the carbonyl carbon within the ring. Thus, the nucleophilic attack is eased in step **C** compared to step **A** and proceeds faster.[291, 293, 301] The initial step **A** was identified as rate-determining step.[291]
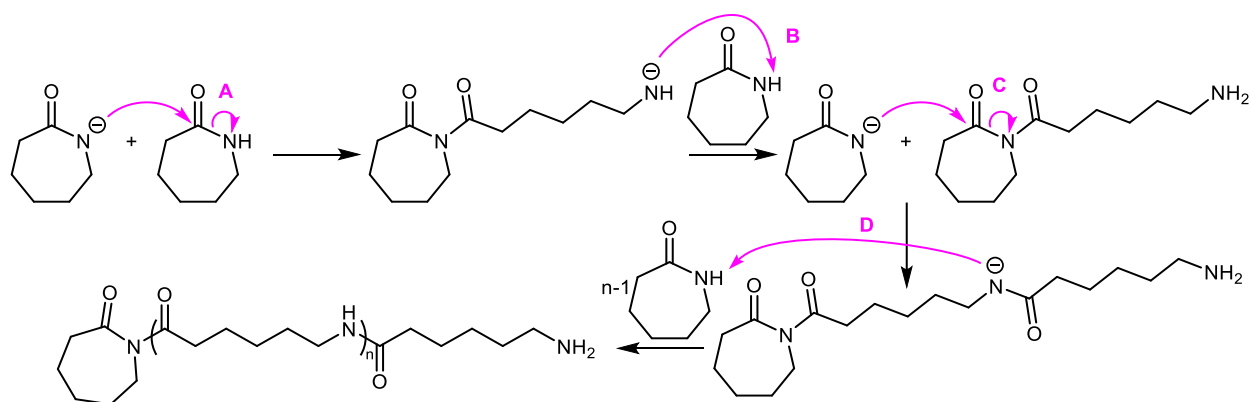
Scheme 45: Mechanism of the anionic ring-opening polymerization of azepan-2-one.[301]

A comparison of the basicity of the aminic anion and the amidic anion is interesting. The pK_a value of AEO is 27.2 (in DMSO) and the pK_a values of NH_3 and pyrrole are 41 and 44, respectively (both in DMSO).[303-304] Although no data were found for primary amines in DMSO, the values of ammonia and a secondary amine (assuming a primary amine to be in between) are a valid hint to suggest that the basicity of the initially formed aminic anion is greater than that of the cyclic amide or the amidic anion.[291] Thus, proton transfer (Scheme 45, step **B**) and formation of a further cyclic nucleophile is favored. Bordwell and Fried compared the pK_a values

of cyclic compounds and their open-chain analogues.[305] Among these substances is *N*-ethylpropanamide with a pK_a of 26.5 as an open-chain derivative and pyrrolidine-2-on and piperidin-2-on with pK_a values of 24.2 and 26.6, respectively, as a cyclic derivative. Other authors found pK_a values of 24.8 for the five-membered lactam, 26.7 for the six-membered lactam and, as cited above, 27.2 for the seven-membered lactam.[303] The similarity of the values for linear and cyclic amides found in the literature and the different structure of the polymer, that might also affect the pK_a, result in the assumption that the proton transfer in step **D** and thus the formation of cyclic nucleophiles is as pronounced as its backreaction (formation of the lactam). However, electrophilicity of the chain-end imide and the released ring strain drive the reaction towards the polymer despite comparable small differences in basicity of lactams and amides. Overall, the proton transfers in step **B** and **D** do not hamper the reaction and proceed fast.[291, 303]

As mentioned above, the initiation step of the PA6 synthesis (Scheme 45, step **A**) is slow while the proton transfer as well as the chain growth are fast (steps **B**, **C** and **D**).[291, 303] To accelerate the initial step, the addition of activators to the reaction mixture is common. Electron-withdrawing properties must increase the electrophilicity of the carbonyl carbon to ease the nucleophilic attack. Therefore, it is common to substitute the nitrogen atom of the monomer with, e.g. carbonyl groups and dope the monomer with the electron-deficient molecules.[292, 297, 300, 306] The structure of activators often mimics the imide structure formed by the attack of the lactamate anion and subsequent ring-opening. Commonly applied activators are based on aromatic and aliphatic (di-)isocyanates or acylated azepan-2-one (Scheme 46). The use of activators allows to fully polymerize azepan-2-one in an anionic fashion within single digit minutes.[292, 294] Type and concentration of the applied activator strongly influence the reaction. Polymerization initiated by Na-AEO were found to be 'very fast' and 'fast' (reaction time below

one minute and between one and two minutes, respectively), when initiators like *N*-cyclohexyl-2-oxoazepane carboxamide (CI-AEO) or the adduct of hexane-1,6-diisocyanate and two equivalents of AEO (HDI-AEO$_2$) were used. 'Slow' (two or more minutes) reactions were found if acetyl azepan-2-one (AEO-Ac) or 1,3,5-tripheyl-2,4,6-trion-1,3,5-triazin (trimer of phenyl isocyanate, an isocyanaurate) served as activators.[294] Further known activators are based on addition or condensation products of azepan-2-one and 1,1-bis (4-isocyanato cyclohexyl) methane (H$_{12}$MDI), 5-isocyanato-1-(isocyanatomethyl)-1,3,3-trimethylcyclohexane (IPDI), phenyl isocyanate, 2,4-diisocyanato-1-methylbenzene (TDI), benzoic acid and propanoic acid. (Cyclic) esters, carbamates and (di-)isocyanate are also added in order to form the activating substances *in situ*.[294, 302, 307-308] Special activator precursors are based on urea (e.g. diphenyl urea), carbodiimides (e.g. *N*,*N*'-dicyclohexylmethane diimine) and methanal derivatives (e.g. bis(2-oxoazepane)methanone).[294]
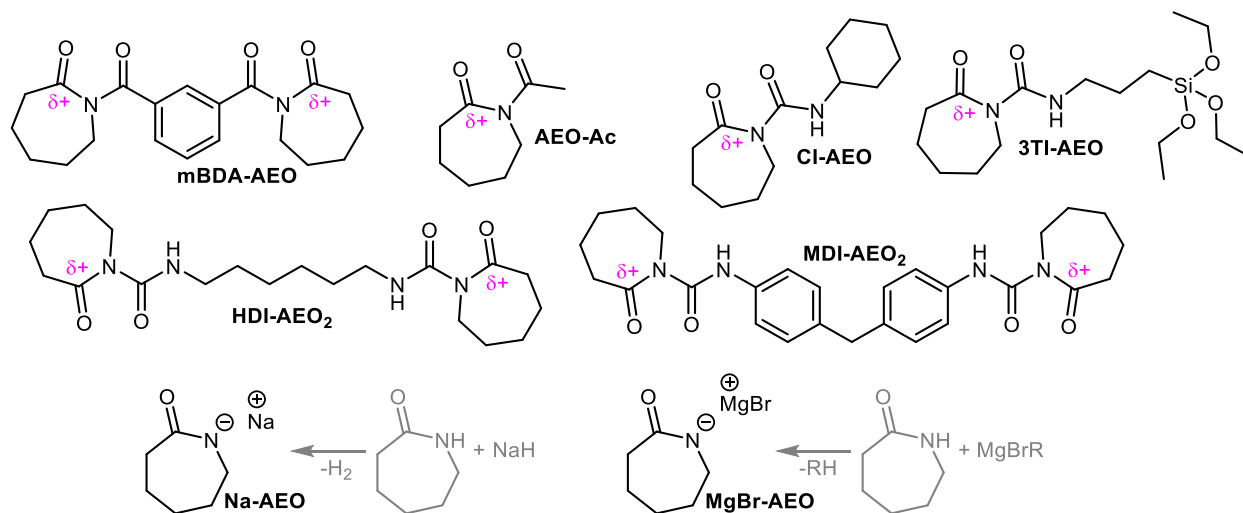
Scheme 46: Various activators (top and middle) and initiators (bottom) commonly used in polyamide 6 synthesis.[294, 300]

Although, activators are most commonly built from azepan-2-one with a carbonyl moiety adjacent to the nitrogen, the end group functionalities of the resulting polymers differ. Isocyanate-based activators form urea end groups whereas acyl-based activators form amide end

79

groups.[294] Also within the group of carbamoyl lactams (isocyanate azepan-2-one addition adducts) differences in the end-groups were found.[309] A series of carbamoyl lactams comprising n-butyl-, benzyl-, 4-methoxy phenyl, phenyl, 4-nitrile phenyl and 4-nitro phenyl isocyanates were applied as activators. Decreasing acidity (order as given above) of the resulting end-group resulted in increased initial reaction velocity. This was attributed to the lower amount of lactamate anions quenched by the end-groups of lower acidity.[293, 309] All the more, the discussion on acidity and basicity can be intensified comparing systems with activators and systems without activators. Whereas amides and urea derivatives are found for systems with activator, stronger basic amines can be found, too. In addition, the influence of steric hindrance of the acyl substituents adjacent to the nitrogen was investigated.[293, 310-311] Bulky tertbutyl groups show decreased initial reaction rates compared to methyl and n-propyl groups. However, methyl and n-propyl isocyanate adducts do not differ much. The application of activators, especially such bearing carbonyl groups adjacent to the amide nitrogen atom of azepan-2-one, resulted in the publication of modified or specified reaction mechanisms.

The 'lactamolytic' mechanism (Scheme 47, top) is based on Na-AEO or MgX-AEO initiators and acyl- or isocyanate-based activators.[291, 294] The cation (Na^+ or $[MgBr]^+$) is coordinated by the imide structure of the activator. As a result, the electrophilicity of the carbonyl carbon of the activator (or growing chain end) and the concentration of (unshielded) free lactamate is increased.[294, 312-313] Both accelerate the polymerization reaction. Unlike the 'lactamolytic' mechanism in the 'coordinative-ion' mechanism, the azepan-2-onate anion participates in the complexation of the cation as ion pair (Scheme 47, bottom).[314-315] The attacking nucleophile is not necessarily the coordinating lactamate. However, aside from free or paired ions, both mechanisms are similar and bear inaccuracies with respect to side reactions.[294]
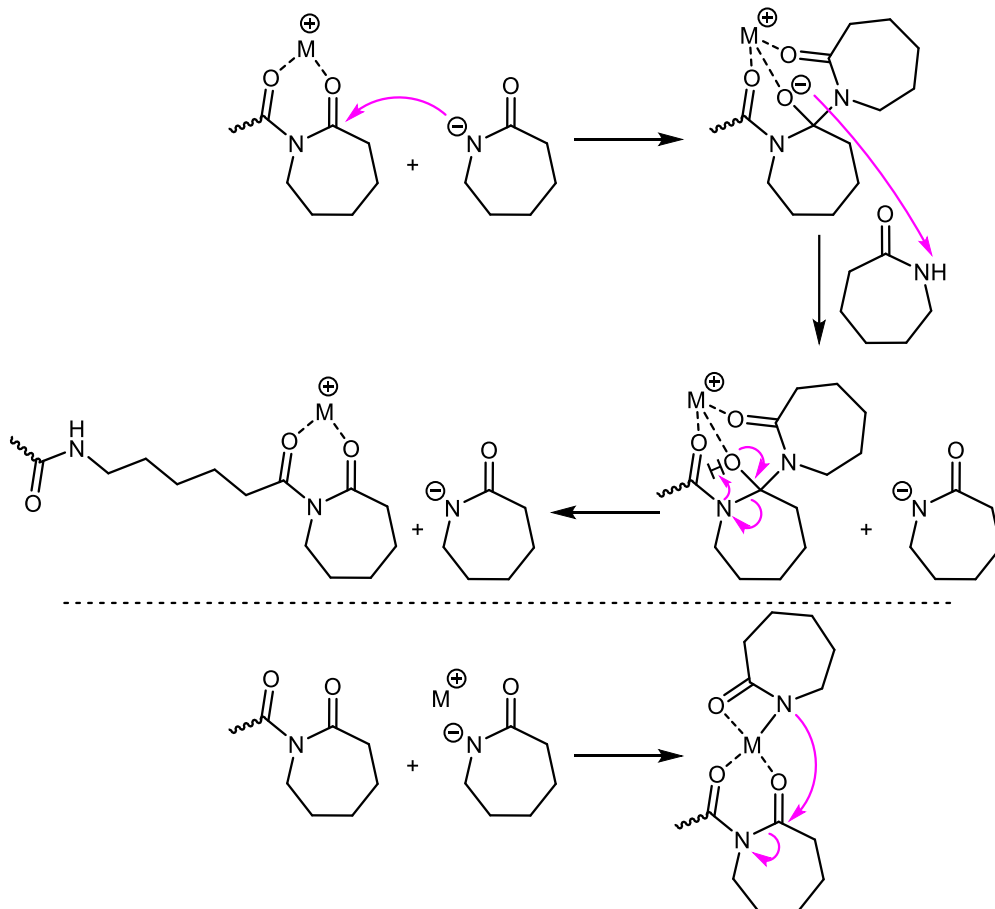
Scheme 47: The 'lactamolytic' mechanism (top) and the 'ion-coordinative' mechanism (bottom).[291, 294, 312-315]

The strongly basic conditions, increased polymerization temperatures and reaction times as well as the high reactivity of the substances applied for the polymerization of PA6 cause various side reactions.[294] The large number of side reactions e.g. transacylation, transamidation, Claisen-type condensations, undergone by imide groups in strong alkaline conditions, or the further consequences of the acidity of the α-carbonyl C-H bonds and the impact on monomer consumption and degree of polymerization are discussed in several reviews and publications.[291, 293-294, 300, 316-318]

6.5.4 *N*-Heterocyclic Carbenes in Polyamide 6 Synthesis

Aside from Na-AEO and MgBr-AEO NHCs were applied in the synthesis of cast polyamide 6. In a patent from 2006, the carbenes **5u-Ad**, **5u-Cy** and **5s-Ad** were applied to polymerize AEO.[319] Reactions at 200°C (and higher) for 40 min (and longer) resulted in 84% (M_n=37 kg/mol, AEO:NHC=30:1), 11% (M_n=48 kg/mol, AEO:NHC=160:1) and 8% (M_n=55 kg/mol, AEO:NHC=114:1) conversion of the monomer, respectively. However, the different reaction conditions and ratios of AEO : NHC allowed no meaningful comparison of the reaction system. A publication by Buchmeiser *et al.* investigated the application of latent NHCs, protected by CO_2, $MgCl_2$ and $ZnCl_2$, for the polymerization of azepan-2-one.[7] At 180°C many of the applied precursors produced polymers in up to 85% yield within 45 min. The metal salt protected derivatives **5s-Mes-MgCl₂** and **5s-Mes-ZnCl₂**, however, showed no reactivity under the mentioned reaction conditions using an AEO : NHC ratio of 140 : 1. For some CO_2-protected precursors no or low reactivity was found e.g. for the seven-membered **7-Mes-CO₂**, the six-membered rings with aromatic substituents on nitrogen (**6-Mes-CO₂** and **6-Dipp-CO₂**) as well as for the five-membered carbene precursors with cyclohexyl (**5u-Cy-CO₂**) and 2-propyl groups (**5u-iPr-CO₂**) adjacent to nitrogen. On the contrary, 1,3-ditertbutyl substituted five-membered ring based NHCs produced polymer. Yield of 62% and 41% were found for the saturated **5s-tBu-CO₂** and unsaturated **5u-tBu-CO₂**, respectively. The viscosity average molecular weights were determined to be 180 kg/mol and 170 kg/mol, respectively. Further, six-membered rings with aliphatic side groups showed even higher activities. Initiators with 2-propyl substituents on nitrogen (**6-iPr-CO₂**) produced polyamide 6 in 69% yield with a molecular weight of 140 kg/mol (ratio NHC:AEO 1:110). With 4-heptyl groups (**6-Hept-CO₂**) a polymer in 78% yield with a molecular weight of 240 kg/mol (ratio NHC:AEO 1:120) and with cyclohexyl groups (**6-Cy-**

CO₂) a polymer in 85% yield with a molecular weight of 280 k/mol were found. Ratios of NHC to AEO of 1 : 300 were investigated for **6-Cy-CO₂** and **6-iPr-CO₂**. Yields of 76 and 35% as well as molecular weights of 420 and 250 kg/mol were observed. Although yields decreased, the average molecular weights increased with decreasing initiator loading. This finding goes along with the assumption that each equivalent of initiator initiates the growth of one polymer chain. The authors argue that the yield is strongly correlated with the pK_a of the carbenes (or the respective NHC-H⁺ salt) although arguably not the only important factor. The following order of basicity was proposed **6-Cy-CO₂** ≈ **6-Hept-CO₂** ≈ **6-iPr-CO₂** >> **5s-tBu-CO₂** > **5u-tBu-CO₂** > **5u-Cy-CO₂** ≈ **5u-iPr**, in accordance with the literature.[108-109] The observed trend for basicity does not explain why **5u-tBu-CO₂** (pK_a 23.9) produces polymer whereas **6-Mes-CO₂** (pK_a 24.2), **6-Dipp-CO₂** (pK_a 24.5) and **7-Mes-CO₂** (pK_a 24.5) resulted in low or no yield.[7, 109] In a further study Buchmeiser *et al.* investigated the polymerization of azacyclotridecan-2-one and its copolymerization with AEO, both initiated by latent NHCs.[8] For the homopolymerization of azacyclotridecan-2-one various carbene precursors were investigated. Insightful overlaps of the activity towards polymerization of AEO were found. For example, Lewis acid ($MgCl_2$, $ZnCl_2$ and $SnCl_2$) complexes of **5s-Mes** produced no polyamide 12 (PA12) at 180°C within 45 min at a ratio of NHC to monomer of 1 to 100. No polymer formation was observed for six- and seven-membered NHC carboxylates with aromatic nitrogen substituents. Reactions with **5-Cy-CO₂** and **5-iPr-CO₂** resulted in low yields of 23 and <5%, respectively. Again, high yields (96 and 71%) were found for polymerizations applying **5s-tBu-CO₂** and **5u-tBu-CO₂**. In addition, six-membered NHC-CO₂ bearing aliphatic side groups readily produced PA12. Remarkably, **6-Cy-CO₂** produced quantitative yields not only in the ratio of 1 : 100 (NHC to monomer) but also in the ratio of 1 : 300. Even at a ratio of 1 : 500 77% yield were reached. If high yields were

obtained from reactions with a NHC : monomer ratio of 1 : 100, the resulting number-average molecular weights were between 6.7 kg/mol and 8.5 kg/mol. For a NHC : monomer ratio of 1 : 300 molecular weights up to 13.9 kg/mol were isolated. Further, the polymerization behavior was investigated by rheological measurements. For this purpose, **5s-tBu-CO₂** : monomer in the ratio of 1 : 100 was applied at 170 and 180°C, respectively. As expected, at higher temperatures the viscosity increased faster. An induction time with constantly low viscosities was observed at both temperatures.[8]
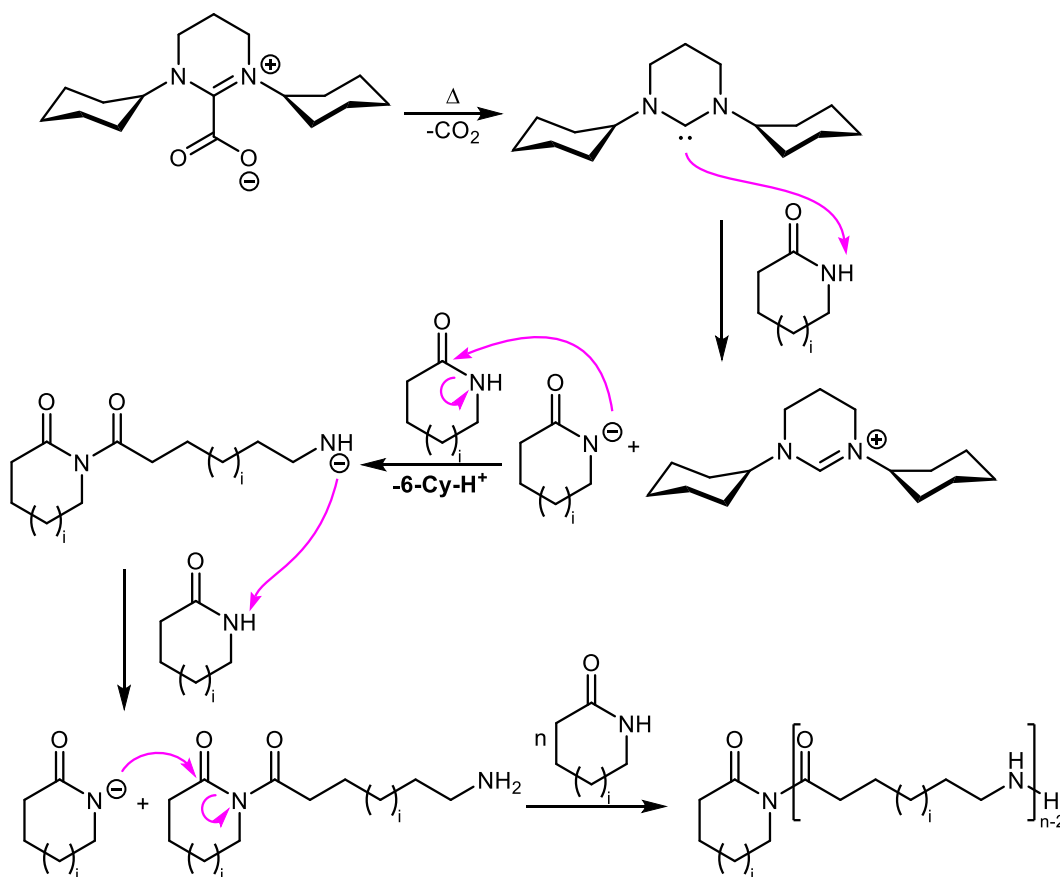
Scheme 48: Polyamide synthesis initiated by an NHC and the liberation of the NHC from its CO_2 adduct.

In a more practical approach Buchmeiser *et al.* investigated the fiber production by copolymerization of the aforementioned seven- and thirteen-membered lactams for *in situ* melt spinning.[9] **6-Cy-CO₂** and **6-Me-CO₂** were applied as initiators in high loadings of up to

5 wt.-%. The fibers, produced at 180-190°C, contained one third to almost half of oligomers (M_n<1000 g/mol) which, as suggested by the authors, serve as softeners. Both NHC carboxylates were investigated towards their temperature stability or in other words their room temperature latency. By proton NMR a release (or initiation) temperature of 100°C was found. Special care was spent to work under water free conditions, especially, if copolymers were synthesized as azepan-2-one is very hygroscopic and anionic polymerizations are sensitive towards proton sources.[318, 320-321]

6.6 4-Methyloxetan-2-one

6.6.1 General

Polyesters formally produced by the ring-opening polymerization (ROP) of (substituted) four membered cyclic esters, so called β-lactones (oxetan-2-ones), represent a common class of biopolymers.[322] Equivalent structures as produced by ROP are accessible via polycondensation of 3-hydroxy alkyl acids. Polyesters can be found in many microorganisms and the most common derivative is formally made up of 4-methyloxetan-2-one.[323] Natural occurring polyesters can be divided into high (10000 to 1000000 repeat units) and low (~200 repeat units) molecular weight fractions. In biological systems, the latter are often associated covalently and non-covalently to other macromolecules and fulfill various functions.[324-327] The higher molecular weight polymers possess a low solubility resulting in no increase of osmotic pressure within the cells and are therefore ideal to serve as carbon and energy storage.[327] Various research groups investigated the intracellular metabolism of poly(4-methyloxetan-2-one) in different organisms.[328-330] It was found to be an intermediate storage of acetyl-SCoA before entering the citric acid cycle (Scheme 49).

Biodegradability is a property of many poly(oxetan-2-one)s. Remarkably, depolymerization proceeds more rapidly under anaerobic than under aerobic conditions. Naturally occurring poly(4-methyloxetan-2-one)s are linear, chiral and isotactic polyesters.[322, 324] However, synthetic poly(4-methyloxetan-2-one)s with different degrees of tacticity or copolymers thereof where also found to be biodegradable.[331] Despite the higher molecular weight, degradation of the natural, isotactic (R)-poly(4-methyloxetan-2-one) occurs much faster (factor of ~10) compared to synthetic, syndiotactic and atactic polymers.[332-333] Copolymers containing different ratios of 4-methyloxetan-2-one and oxepan-2-one or 4-methyloxetan-2-one and oxan-2-one,

respectively were investigated for their degradation properties. In both cases, a higher 4-methyloxetan-2-one content resulted in an increased degradation velocity.

HO

HO''' ''''OH

HO OH

glucose

O

SCoA

citric acid cycle

ketothiolase

synthease

O O

SCoA

$NAPH+H^+$

reductase

$NADP^+$

O O

OH

$NAPH+H^+$

dehydrogenase

$NADP^+$

OH O

OH O

SCoA

synthease

OH O

OH

depolymerase H O O OH n

HSCoA
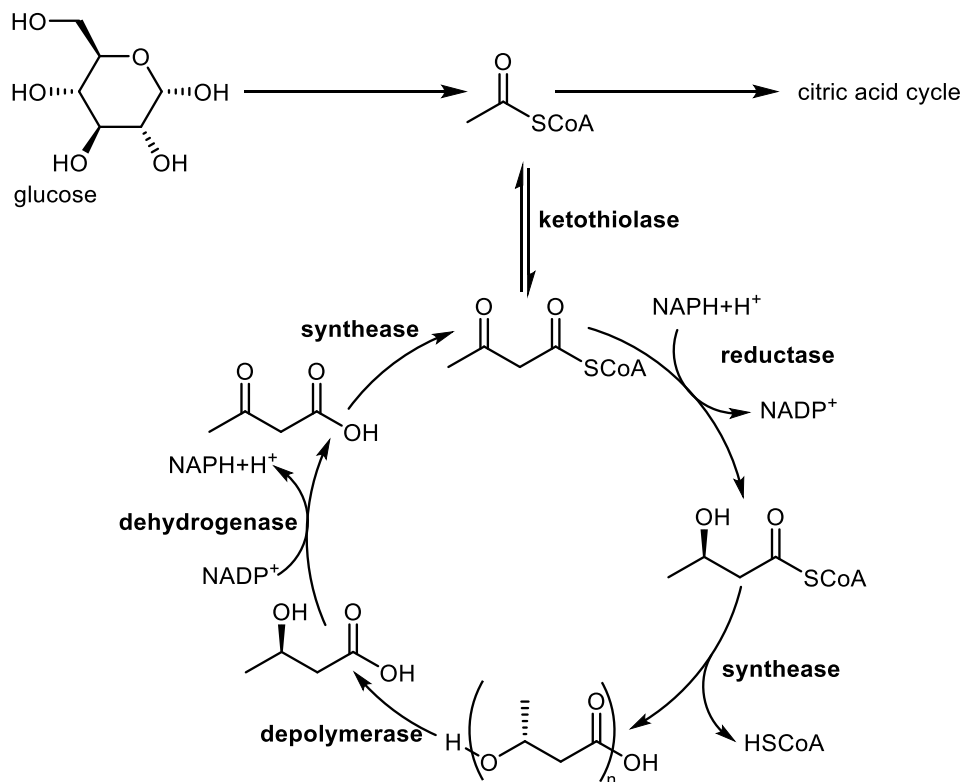
Scheme 49: Metabolic pathway of poly(4-methyloxetan-2-one).[322]

Degradation, however, seems to be correlated with the thermal and mechanical properties.[334] These polyesters are thermoplastic and therefore purposed to have a certain potential to substitute polyolefins (poly(propene) in particular) in areas like packaging, in order to reduce environmental harm caused by plastics, and in the broad field of bio-medical applications.[335-336] Isotactic poly(4-methyloxetan-2-one) and isotactic poly(propene) (PP) have comparable melting areas (~170-190°C vs. ~170-200°C) and glass transition temperatures (5°C vs. 0°C).[337] The material properties in turn strongly depend on tacticity. Naturally occurring, isotactic poly(4-methyloxetan-2-one) is highly crystalline and brittle.[334, 338] A crystallinity of 67% (±5) was found for the isotactic material whereas the atactic polymer is an amorphous material, which does not possess any crystallinity and has a glass transition temperature of -1°C. Unlike

poly(propene) (decomposition starting around 300°C), the proximity of the melting point of isotactic poly(4-methyloxetan-2-one) and its decomposition temperature of around 250°C complicate industrial processing.[339-343] Therefore, several research groups investigated the application of plasticizers and blends of iso- and atactic polymers.[334, 338] Other approaches were the synthesis of macromolecules with tailored tacticities or copolymers by ring-opening polymerization.[331, 335, 344] These efforts resulted in decreased melting points, sometimes below 50°C.[344]

ROP offers an attractive avenue to polyesters. Adding to biocompatibility, biodegradability and the mechanical properties of poly(4-methyloxetan-2-one), the four-membered cyclic monomers are accessible via an atom economic (waste consuming) synthesis.[345] Methyloxirane is catalytically carbonylated by ring expansion with carbon monoxide. Tetracarbonyl cobaltate is commonly used in carbonylation reactions.[345-346] For example Coates *et al.* published a study where [(salophen)Al(THF)$_2$][Co(CO)$_4$] was applied to produced various β-lactones in bulk reactions.[345]
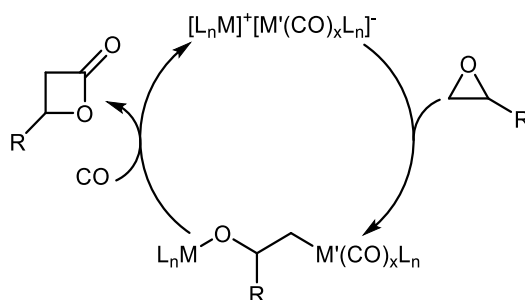
Scheme 50: Generalized catalytic cycle of the production of β-lactams.[345]

The polymerization of four-membered lactones follows three different mechanisms. Anionic ring-opening polymerization (AROP), insertion polymerization or a cationic mechanism (activated monomer mechanism, active chain-end mechanism).[347] The ring-opening polymerization of 4-methyloxetan-2-one is a favored reaction path since a ring strain of -59,2 kJ

is released per mole.[335] Therefore, four-membered lactones bear a special reactivity among lactones, which will be introduced along with the three different mechanisms. Generally, the ROP of 4-methyloxetan-2-one proceeds via two fundamentally different paths. Either by cleavage of the O-acyl bond (Scheme 51, pathway A) as known for the most of the lactones or by O-alkyl cleavage (Scheme 51, pathway B). [301]
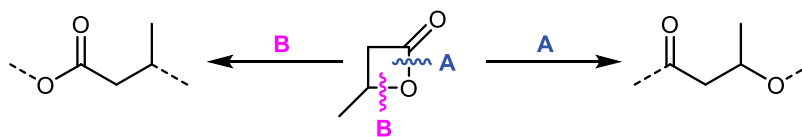
Scheme 51: Two observed ring-opening modes for 4-methyloxetan-2-one.[301]

6.6.2 Cationic Ring-Opening Polymerization of 4-Methyloxetan-2-one

Among the catalysts and initiators used for the cationic polymerization of four-membered lactones are carboxylic acids, mineral acids (H_2SO_4, $HOSO_2CF_3$), Lewis acids ($Zn(C_6F_5)_2$, $Et_2O \cdot BF_3$), triethyloxonium hexafluorophosphate and methyl trifluoromethanesulfonate, often in conjunction with alcohols.[348-352] However, three reaction pathways are discussed for the cationic polymerizations of four-membered lactones.[350] The initial step of the 'activated monomer' mechanism is the protonation (or alkylation) of the ring oxygen followed by a nucleophilic attack at the alkyl group connected to the oxygen and ring-opening (Scheme 52, top). In turn, the 'active chain-end' mechanism starts with the protonation (or alkylation) of the carbonyl oxygen followed by the attack of the next monomer unit and an opening of the ring (Scheme 52, middle). The activated monomer mechanism is commonly accepted for many lactones although it is often described with the electron-withdrawing moiety at the carbonyl oxygen and the nucleophilic attack at the carbonyl carbon (bottom).[295, 353-355]
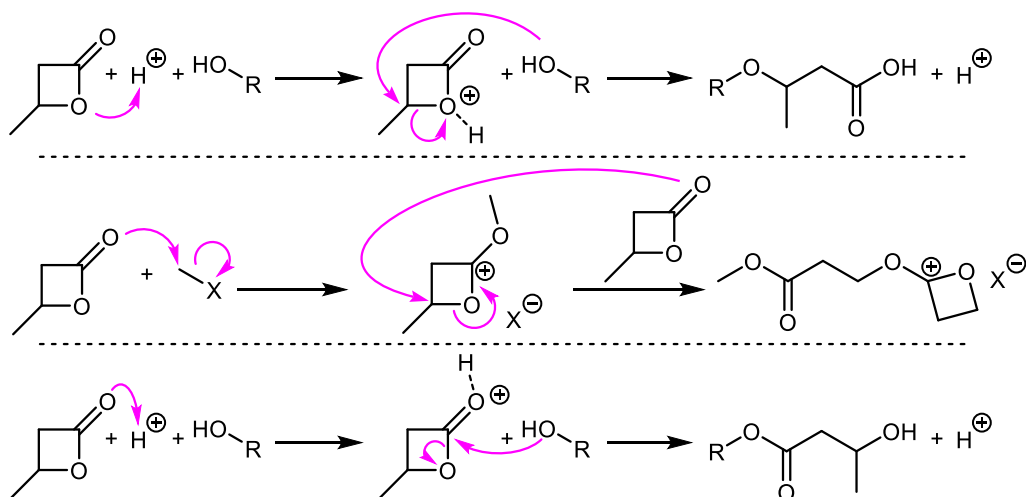
Scheme 52: Top: 'Activated monomer' mechanism initiated by an electrophilic attack at the ring oxygen. Middle: 'Active chain-end' mechanism initiated by an electrophilic attack at the carbonyl oxygen.[301, 350, 354-355]

Approaches following Scheme 52, bottom, were described by Pohl *et al.* and Couffin *et al*. Both used trifuoromethanesulfonic acid (HOTf) in conjunction with primary alcohols as initiators to polymerize 4-methyloxetan-2-one in either toluene or benzene.[354-355] Pohl *et al.* reached degrees of polymerization up to 54 and suggested a living polymerization from NMR data and thus alcoholate end-groups and O-acyl cleavage. Technically interesting, HOTf was replaced by nafion (a perfluorinated polyolefin with sulfonic acid groups), which can be removed from the reaction mixture.[355] Couffin *et al.* reported number-average molecular weights up to 8090 g/mol (DP of 94) and underlined hydroxyl end-group fidelity by block-copolymerization with oxepan-2-one, chain extending onto the poly(4-methyloxetan-2-one).

6.6.3 Anionic Ring-Opening Polymerization of 4-Methyloxetan-2-one

The nucleophilic attack of an anion at 4-methyloxetan-2-one and other four-membered lactones takes place at the carbonyl carbon or at the carbon atom on the other side of the ester group (Scheme 53).[301] Which mechanism prevails depends on the solvent polarity, the counter ion (nature and size) as well as on the presence of complexing agents (crown ethers and cryptands) and the propagating chain end (carboxylate or alcoholate).[356-357]
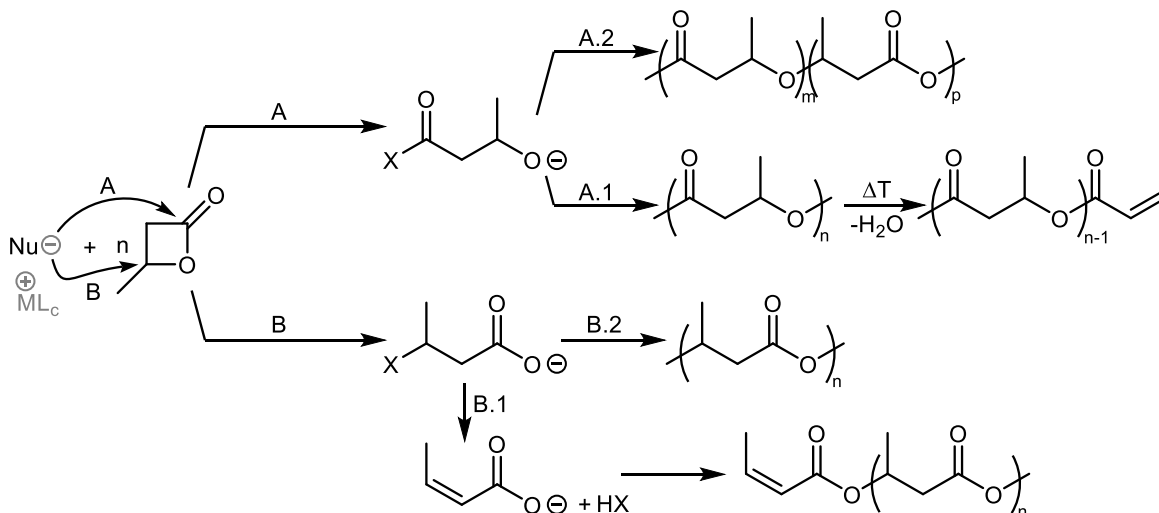
Scheme 53: The different pathways of anionic polymerization of four-membered lactones including some side and downstream reactions.[301, 356, 358-360]

The initiator Nu in Scheme 53 can be neutral or ionic (grey). In case, anionic initiators are used the counterion (M) and its ligand(s) (L_c) affect the reaction. For example, crown ethers or cryptant serve as ligand and enable "living" reactions. [361-364] Increasing solvent polarity favors formation of ionic compounds that are necessary to undergo crotonate formation (B.1). Crotonate formation is commonly observed in the polymerization of four-membered lactones often forming the initiating carboxylate (and more often described than B.2).[356, 358, 364-366] Following pathway A (O-acyl cleavage) and A.2, the active chain-end can change from alkoxide to carboxylate by changing from O-acyl scission to O-alkyl scission. The other way around leads to the formation of anhydrides, which is principially not excluded, but, if a change in reaction pathway was observed over time an increased concentration of carboxylates, serving as active chain-end, was found.[358-359, 367-368] Finally, A.1 leads to alkoxide end-groups, which were rarely observed as only product of an anionic polymerization.[368] For example, the reaction of potassium methanolate and 4-methyloxetan-2-one in conjunction with crown ethers forms methylbut-2-enoate and complexed potassium cations with hydroxyl counterions.[365] Even if an alkoxide is

formed, elimination, driven by the formation of a conjugated system, and thus formation of dead chain ends make it a challenge to produce hydroxyl end-groups.[301]

6.6.4 Coordination Insertion Polymerization

Both, O-acyl and O-alkyl scission were also observed for coordination insertion polymerization.[301] Aluminum alkoxides, lanthanum alkoxides, yttrium alkoxides and zinc alkoxides were found to undergo O-acyl cleavage (Scheme 54, A).[331, 335, 369-370] O-alkyl scission was observed for aluminum chlorides (B).[369]
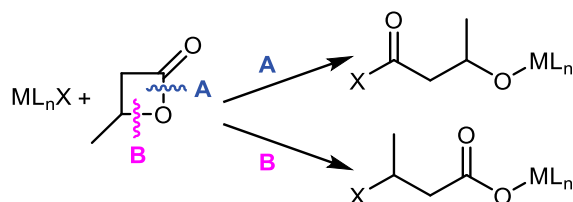
Scheme 54: O-Acyl and O-alkyl bond scission observed for metal insertion polymerizations.[301, 369]

Several studies investigated the ring-opening polymerization mechanism of yttrium alkoxides.[371-373] It is commonly accepted that the monomer initially coordinates via the carbonyl oxygen to the metal center thereby increasing the electrophilicity of the carbonyl carbon before electron density is shifted from the alkoxide oxygen to the carbonyl carbon and a covalent bond is formed (Scheme 55, right). Further on, a bond from the former carbonyl oxygen to the metal center and coordination of the latter to the ring oxygen is established. Finally, the carbonyl is restored and the new yttrium alkoxide is formed under O-acyl scission. All in all, O-acyl ring-opening and monomer insertion into the central metal alkoxide oxygen bond was claimed. A very similar mechanism was also proposed for zinc alkoxides (Scheme 55, left).[340] Both Zn and Y complexes proved active in the polymerization of 4-methyloxetan-2-one and produced molecular weights of >100000 g/mol while the polydispersities remained below 2.[340, 374]

Scheme 55: Exemplary metal insertion mechanism.[340, 371-373]
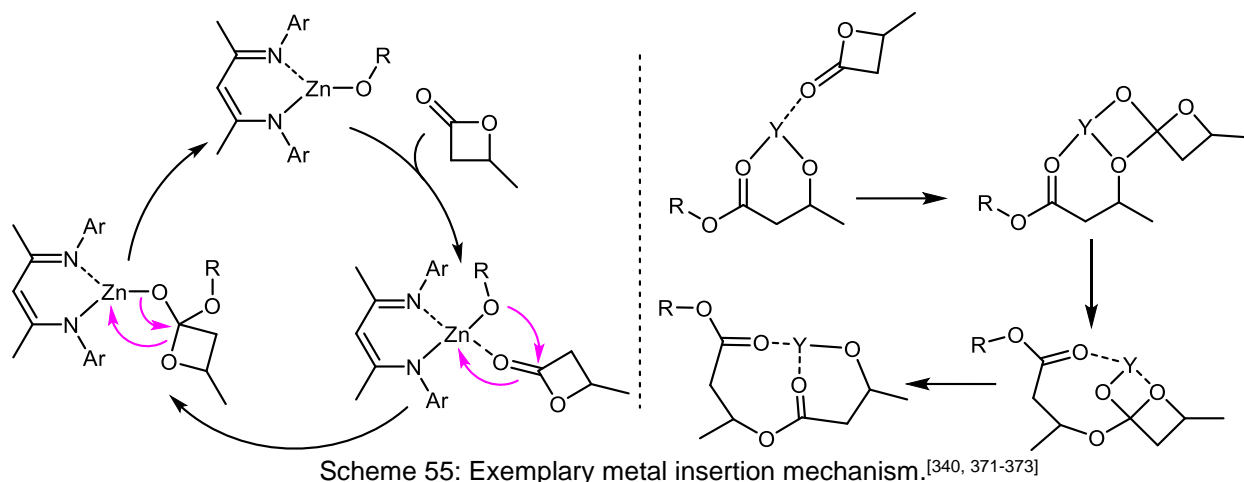
Titanium complexes are also widely used for the polymerization of lactones.[375-380] The ligand setup for these catalysts can simply consist of alkoxides or, more sophisticated, of tri- and tetravalent ligands. Del Hierro *et al.* synthesized several titanium dialkoxide di-2-propanolate complexes and used them to polymerize oxepan-2-one in CH_2Cl_2 (Scheme 56). For oxepan-2-one, O-acyl scission was observed. Upon addition of fresh monomer to the active polymer chain a propagation reaction and further increase of molecular weight was observed.[379]
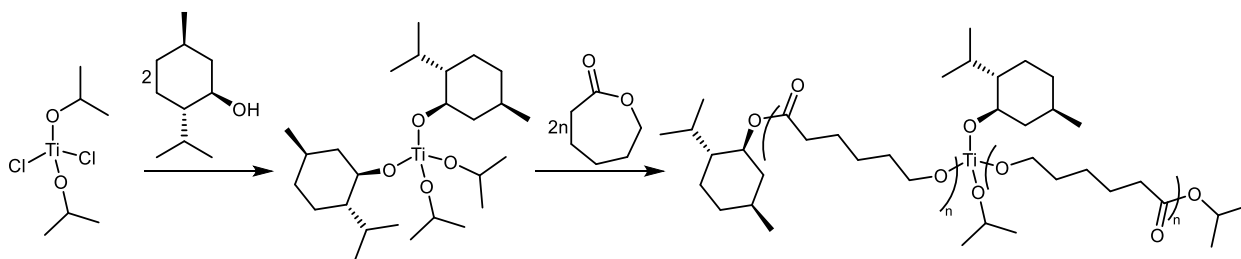
Scheme 56: Synthesis of a titanium complex and subsequent application in the polymerization of oxepan-2-one.[379]

6.6.5   α,ω-Dihydroxy Telechelic Macroesters and Polyurethanes Thereof

Couffin *et al.* extended their approach of using trifluoromethansufonic acid initiators in benzene to dihydroxy initiators resulting in a α,ω-dihydroxy telechelic poly(4-methyloxetan-2-one) and proved the end-group fidelity by the synthesis of a block-copolymer with five blocks, a molecular weight of 29000 g/mol and a polydispersity of 1.33.[354]

In a remarkable study, Davidson *et al.* published the preparation of an air-stabile metal organic framework built up from Ti(OiPr)$_4$ and excess 1,4-butandiol.[381] The resulting material was applied in the ring-opening polymerization of oxepan-2-one and 1,4-dioxol-2,5-dione and produced polymers with molecular weights of 22000 g/mol ($Đ_M$=1.24) and 34000 g/mol ($Đ_M$=1.76), respectively, in ≥90% yield. These polymers were found to be α,ω-dihydroxy telechelic leading to the description of the Ti ligands in the framework as chain extenders.

Kricheldorf *et al.* reported on dialkyl tin (di-)alkoxides and oxides in conjunction with diols in the synthesis of macrodiols based on 4-methyloxetan-2-one, 1,4-dioxol-2,5-dione and oxepan-2-one.[382-385] Increasing molecular weights were found for increasing monomer to initiator ratios. In the following the same group described an approach using dioctyl tin as catalyst to synthesize macrodiols from 1,4-butandiol and oxepan-2-one.[386] The molecular weights depended on the monomer to diol feed ratio. The same authors also describe methods to synthesize tri- and tetrafunctionalized polyesters.

Copolymers of 4-methyloxetan-2-one and oxepan-2-one were polymerized to α,ω-dihydroxy telechelic macrodiols based on ethanediol or 1,4-butanediol. Dioctyltin was applied as catalyst at 110°C for 4 days.[344] The actual amount of 4-methyloxetan-2-one incorporated into the polymer was lower than in the monomer feed. Further, the molecular weights (9000 g/mol for oxepan-2-one, 7000 g/mol for 70:30 oxepan-2-one:4-methyloxetan-2-one) and the crystallinity decreased with increasing 4-methyloxetan-2-one ratio. Subsequently, the macrodiols were converted with a six-fold excess of MDI, mixed with dibutyl tin dilaurate before a five-fold excess of 1,4-butandiol in DMAc was added. Once the reaction was finished, thermoplastic polyurethane was found. GPC investigations revealed a molecular weight of 22000 g/mol for sole oxepan-2-one-based prepolymers and a M_n of 20000 g/mol for a prepolymer based on 70:30 oxepan-2-one:4-

methyloxetan-2-one. Interestingly, melting points were reduced about 10°C (~30 to 40°C) compared to the respective polyester (~40 to 60°C) while melting enthalpies were reduced about 40 J/g (polyesters ~50 to 80 J/g, polyurethanes ~10 to 40 J/g). Within the respective polymer class the lowest melting points and enthalpies were found for the highest 4-methyloxetan-2-one content.

Brzeska *et al.* published a series of studies on the properties of polyurethanes based on diols and triols of macroesters of 4-methyloxetan-2-one and oxepan-2-one as soft segments.[387-389] The diols based on 4-methyloxetan-2-one were synthesized by anionic ring-opening using 3-hydroxybutyric acid sodium salt whereby the sodium was complexed with 18-crown-6. Finally, the hydroxy end-groups were introduced by converting the polymers with 2-bromethanol or 2-iodethanol.

7 Results and Discussion

7.1 Anhydride-hardened Epoxide Resins

The basics of this work were elaborated by Buchmeiser *et al.*[2, 155, 159, 242] The authors reported on various Lewis acid and CO_2-protected NHCs as latent initiators for the curing of anhydride-hardened epoxide resins. The resins were prepare from BADGE and hexahydro-2-benzofuran-1,3-dione (A1) (Scheme 57) or 2-benzofuran-1,3-dione.

The aim of this project was the formulation of an anhydride-hardened epoxide resin meeting the following requirements:

- a viscosity low enough to spray the resin ($[\eta]$<500 mPa·s is required)

- a latent resin formulation at room temperature

- air- and moisture stability of the initiator and the formulation

- fast curing/polymerization reaction at moderate temperatures (80-140°C)

- favorable in price of chemicals and starting materials

- simple synthesis

Most of the results of this topic are published: H. J. Altmann, S. Naumann, M. R. Buchmeiser, Protected *N*-heterocyclic carbenes as latent organocatalysts for the low-temperature curing of anhydride-hardened epoxy resins, *Eur. Polym. J.* **2017**, *95*, 766-774.[4]

This work focused on the application of a specific NHC-CO_2 - 1,3-dimethylimidazolium-2-carboxylate (**5u-Me-CO₂**). This precursor is favorable due to its convenient synthesis, the stability towards air and moisture and the low-priced starting materials.[3] Consequently, the reaction system had to be optimized for the application of **5u-Me-CO₂**. On the one hand a broad

spectrum of diepoxides and (di-)anhydrides was investigated. On the other hand, suitable precursor loadings had to be found with respect to the specific reactivity of **5u-Me-CO₂**. Thus, a mixture of BADGE and A1 was chosen as a benchmark system to compare the behavior of **5u-Me-CO₂** to other initiators (compare Table 3).

Mixing BADGE and A1 in a molar ratio 1 : 2 results in a homogeneous, colorless and clear solution. The mixtures of BAGDE, A1 and NHC precursor were homogenized at 40°C until a clear solution was achieved (typically 30 min). Although the starting materials were stored and mixed inside the glove box, homogenization and sample preparation for DSC was executed under ambient atmosphere.
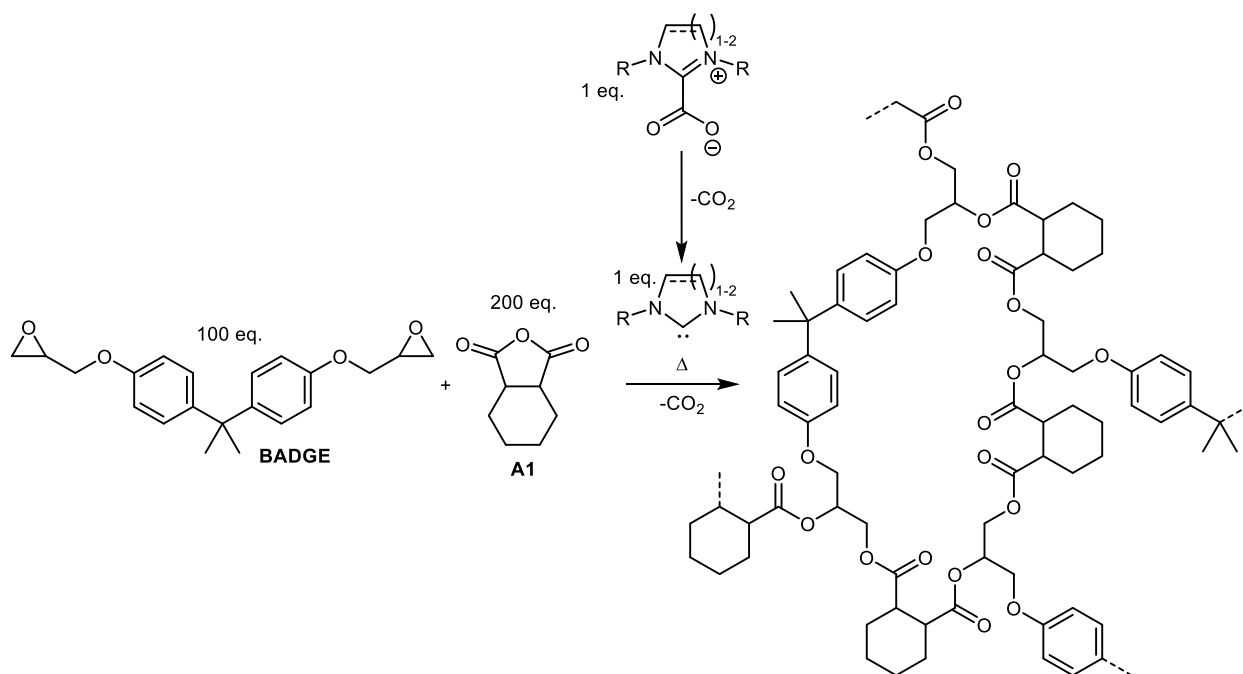
Scheme 57: Curing reaction of BADGE and A1 catalyzed by a NHC depicted as carboxylate precursor as executed for the experiments summarized in Table 3.

The prepared mixtures were submitted to DSC and heated with 10 K/min. Typically, energy is released while the epoxide resin is cured and the energy release is measured by DSC. The temperature at the maximum of exothermic energy release in the first heat cycle is called T_{max}

and given in °C. T_{max} is used as measure to compare the activity of various carbenes towards the anhydride-hardened epoxide resin taking in account both, the carbene release, depending on the carbene structure and the protective group, and the reactivity of the free carbene, depending on the carbene structure. Initially, for the benchmark experiments in Table 3 a comparison to literature is reasonable. T_{max} of 146°C was found by Buchmeiser *et al.* for the curing reaction catalyzed by **6-Cy-CO₂** whereas within this work a value of 148°C was observed (entry 7).[2] A similarly small difference was measured for **6-Me-CO₂** (entry 3). A T_{max} of 162°C was reported while a value decreased by only 3°C was found here. Even more consistent values were found for **6-Mes-CO₂** where in both studies a T_{max} value of 150°C was observed (entry 5). However, values for **6-Mes-ZnCl₂** differ slightly by 8°C from 172 to 180°C (entry 1). The following discussion relies on the values measured in the course of this work. Resin curing with **5u-Me-CO₂** led to a T_{max} value of 163°C (entry 2). This is very close to the decarboxylation temperature of 162°C for **5u-Me-CO₂** found by Louie *et al.*[182] However, this proximity must not be overrated, as comparison of dissolved NHC carboxylates to with those in solid state is not viable.[183] If **5u-Me-CO₂** is compared to the other CO_2-protected imidazolium derivate **5u-Mes-CO₂** (entry 8) showing a T_{max} of 147°C, the small nitrogen substituents of **5u-Me-CO₂** probably strongly contribute to the increased T_{max} by reduction of steric pressure onto the CO_2 moiety and thus higher stability.[182] In addition, the lower pK_a value of **5u-Mes-HX** (19.6) compared to **5u-Me-HX** (21.5) comes along with a decreased CO_2 adduct stability.[108-109] The lower stability of the NHC-CO_2 adduct **5u-Mes-CO₂** eases the release of the free carbene at lower temperature compared to **5u-Me-CO₂**. In order to discuss the reactivity of the free carbenes the Tolman electronic parameter (TEP) is a useful starting point. **5u-Mes-CO₂** showed a TEP of 2050.7 cm^{-1} and thus a higher nucleophilicity than **5u-Me-CO₂** displaying a TEP of 2052.4 cm^{-1}.[63] Higher

TEP values can result in higher reactivities, however, it is difficult to pinpoint reactivities to only one factor or cause in epoxide curing.[142-145, 390] Although backbone-saturated **5s-Mes-HX** displays a pK_a value of 20.8 and is therefore situated between the two previously discussed NHCs, the observed T_{max} value was identical to the T_{max} of the unsaturated derivative **5u-Mes-CO₂** (entry 9). This is in contrast to the aforementioned impact of nucleophilicity judged from the respective TEP values (2051.5 cm^{-1} for **5s-Mes-CO₂**). Both, pK_a and TEP should place the T_{max} of **5s-Mes-CO₂** in-between **5u-Mes-CO₂** and **5u-Me-CO₂**. Seemingly, pK_a and TEP values are only valuable to the discussion to a certain extend. Denning and Falvey studied the solvent polarity-depending decarboxylation behavior of **5u-Me-CO₂** and found increased NHC-CO₂ adduct stability in solvents of higher polarity.[183] An extension of this study to other NHCs could enlighten the differences between various NHCs in epoxide/anhydride media. The entries 1, 4 and 5 in Table 3 show latent derivatives of **6-Mes** with different protecting groups. The T_{max} values range from 150°C for the carboxylate to 180°C for the ZnCl₂ protected derivative. A T_{max} of 156°C was observed for **6-Mes-AgBr**. Despite different adduct stabilities with the different protecting groups, gaseous CO₂ leaving the reaction mixture is not accessible for the reformation of the adducts whereas the metal salts remain within the epoxide/anhydride mixture.[2] Further, Buchmeiser *et al.* postulated the possibility of non-innocent behavior of the released Lewis acids such as Lewis acid coordination to the carbonyl oxygen, thereby increasing the electrophilicity of the carbonyl carbon and the accessibility for a nucleophilic attack. The influence of the Lewis acid within the reaction mixture will be discussed below. However, aiming at lower T_{max} values, NHC carboxylates are more promising candidates. Interestingly, **6-Mes-CO₂** and **6-Dipp-CO₂** show the same T_{max} of 150°C although a higher steric pressure and therefore lower T_{max} was expected for **6-Dipp-CO₂**. Conversely, the pK_a values for **6-Mes-H⁺** and **6-Dipp-H⁺** are almost

the same (24.2 for entry 5 vs. 24.5 for entry 6).[109] **7-Mes-CO₂** with a pK_a value of 24.5 shows a stark decrease of T_{max} to 132°C and is by far the most active initiator investigated (entry 10). The highest pK_a value of 27.6 was found for **6-Me-HX**.[109] Although **6-Cy-HX** was not included in the study by Ji *et al.* a similar pK_a is expected since **6-iPr-HX** and **6-tBu-HX** display values of 27.5 and 29.4, respectively.

In conclusion, among the five-membered ring-based NHCs saturation does not seem to be decisive for reactivity (Table 3, entries 8 and 9). Methyl substituents at the nitrogen seem to decrease reactivity (Table 3, entries 2 and 3) more by their reduced steric demand than by their aliphatic character. This is underlined by **6-Cy-CO₂** which shows a T_{max} value of 148°C which is within the typical range, for five- and six-membered carbenes, protected by CO_2 and bearing cyclic substituents on the nitrogen. Sterically demanding side-groups are a common feature of the more active initiators (Table 3, entries 5 to 10). Lewis acid-based protecting groups resulted in increased T_{max} values compared to CO_2 (Table 3, entries 1 and 4). This is in agreement with observations by Buchmeiser *et al.*[2]

Table 3: T_{max} values determined by DSC from 30 to 250°C (5 K/min). Mixtures of BADGE:A1:NHC-precursor (ratio 100:200:1) were investigated to compare the reactivity of different initiators.

entry	name	structure	T_{max} [°C]
1	**6-Mes-ZnCl₂**		180
2	**5u-Me-CO₂**		163
3	**6-Me-CO₂**		159
4	**6-Mes-AgBr**		156
5	**6-Mes-CO₂**		150
6	**6-Dipp-CO₂**		150
7	**6-Cy-CO₂**		148
8	**5u-Mes-CO₂**		147
9	**5s-Mes-CO₂**		147
10	**7-Mes-CO₂**		132

T_{max} is the maximum of the exothermic peak during curing reaction in DSC first cycle.

Several examples, taken from Table 3, namely **5u-Me-CO₂** (red curve), **6-Dipp-CO₂** (black), **6-Cy-CO₂** (blue) and **7-Mes-CO₂** (green) are displayed in Scheme 58 to demonstrate typical curing profiles as determined by DSC (Table 3, entries 2, 6, 7 and 10).
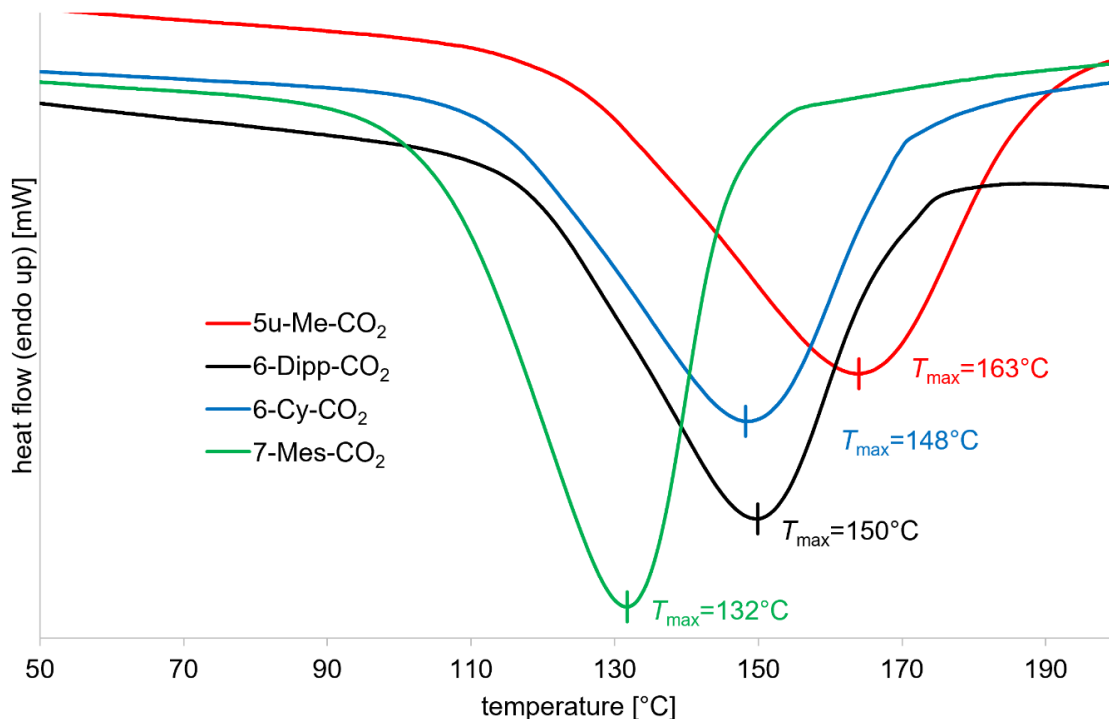
Scheme 58: Typical DSC thermograms of anhydride-hardened epoxide resins consisting of BADGE, A1 and a carbene precursor (ratio 100:200:1).

Variation of the NHC precursor loading is an evident measure to improve the reactivity of a given epoxide resin system. Suitable precursor loadings for **5u-Me-CO₂** were determined and compared to those of other initiators. An overview is summarized in Table 4. Increased precursor loadings decreased the T_{max} values in all curing reactions investigated. Whereas loadings of eight equivalents result in a reduction of T_{max} of up to 38°C (for **6-Mes-AgBr**) compared to 1 equivalent loading; the T_{max} reduction by increasing the catalyst loading from eight to 15 equivalents lowers T_{max} only in the single digit range. This indicates a certain limit of improvement that can be achieved by addition of higher amounts of initiator. Noteworthy, the differences between **6-Mes-CO₂** and **6-Mes-AgBr** have vanished for loadings of eight

equivalents whereas the distance to the T_{max} of **6-Mes-ZnCl₂** remains constant. For the application of **5u-Me-CO₂** an initiator loading of 8 equivalents was chosen. This increase is possible due to the straightforward synthesis and inexpensive starting material for **5u-Me-CO₂**. Especially when compared to the effort that must be spent for the synthesis of the other NHCs.

Table 4: T_{max} [°C] values of different carbene precursors of 1, 8 and 15 equivalents loading relatively to 100 equivalents of BADGE and 200 equivalents A1 determined by DSC with a heat rate of 5 K/min.

loading	5u-Me-CO₂	6-Cy-CO₂	6-Mes-CO₂	6-Mes-AgBr	6-Mes-ZnCl₂
1	163	148	150	156	180
8	125	120	117[a]	118[a]	152[a]
15	120	111[a]	110[a]	-	-

[a] inhomogeneous mixtures were used.

As mentioned above, epoxide anhydride curing experiments in conjunction with various Lewis acids were carried out. 10 equivalents of metal salts were added to the mixtures of 100 equivalents BADGE, 200 equivalents A1 and 8 equivalents **5u-Me-CO₂** precursor, homogenized, if possible, and submitted to DSC. Again, T_{max} was chosen to evaluate the reactivity. Since the enhanced polarization of the monomer caused by the coordination of Lewis acids to almost any ring-opening reaction can be enhanced by Lewis acid addition, which encouraged the investigation of Lewis acids in conjunction with anhydrides.[2, 391-392] However, the expected decrease of T_{max} was not observe for the investigated mixtures. On the contrary, T_{max} values were increased if Lewis acids were added. The effect is limited to 3 to 6°C for all fully inorganic Lewis acids, underlined by entry 1 in Table 5 compared to the entries 2 to 5. Furthermore, entries 6 and 7, employing B(Ph)₃ and Sn(OAc)₂ as Lewis acids show T_{max} values increased by 17°C compared to the reaction without any Lewis acid (entry 1). B(Ph)₃ and Sn(OAc)₂ were chosen due to their organic ligands, which were expected to lead to an increased solubility in the resin. Neither full solubility nor higher reactivity was observed. Especially in the

case of B(Ph)$_3$, the reduced reactivity may partially be attributed to borate complex formation with the active anionic growing center. Additionally, for all Lewis acids an adduct with the released NHC can be postulated. Examples of Lewis acid-protected NHCs were shown in the introduction and in the literature as well as in this chapter.[2, 111-112] Due to the counterproductive influence of the Lewis acids the experiments were not pursued any further.

Table 5: T_{max} values of epoxide curing reactions with BADGE:A1:**5u-Me-CO₂**:Lewis acid (ratio: 100:200:8:10) determined by DSC with a heat rate of 5 K/min.

entry	Lewis acid	T_{max} [°C]
1	-	125
2	MgCl$_2$	131
3	GaBr$_3$	129[a]
4	AlCl$_3$	129[a]
5	ZnCl$_2$	128[a]
6	B(Ph)$_3$	142[a]
7	Sn(OAc)$_2$	142[a]

[a] inhomogeneous mixtures were used.

Instead, a broader range of diepoxides and (di-)anhydrides was investigated for their curing behavior. The selected monomers are depicted in Scheme 59. All diepoxides were liquid at room temperature (the D.E.R. 332 standard BADGE used in this chapter, received from Sigma Aldrich, is liquid, although pure BADGE is a colorless, wax-like solid at room temperature). Among the anhydrides, A2 and A7 are liquid at room temperature, all other anhydrides are solids. Each diepoxide was combined with each anhydride in the ratio of 100 to 200. If dianhydrides were used, a ratio of diepoxide to dianhydride of 100 to 100 was used. Within all cases 8 equivalents of **5u-Me-CO₂** were employed relative to 100 equivalents of the diepoxide. Thus, 0.04 mol **5u-Me-CO₂** are present per mole oxirane moiety or per mole anhydride. Homogenization was commonly executed at 40°C for about 30 min under constant stirring.

Some of the resin combinations form homogeneous solutions; however, most combinations stay heterogeneous mixtures or slurries. Subsequently a small sample was submitted to DSC analysis. Table 6 summarizes the T_{max} values found for the various reactions performed by DSC.
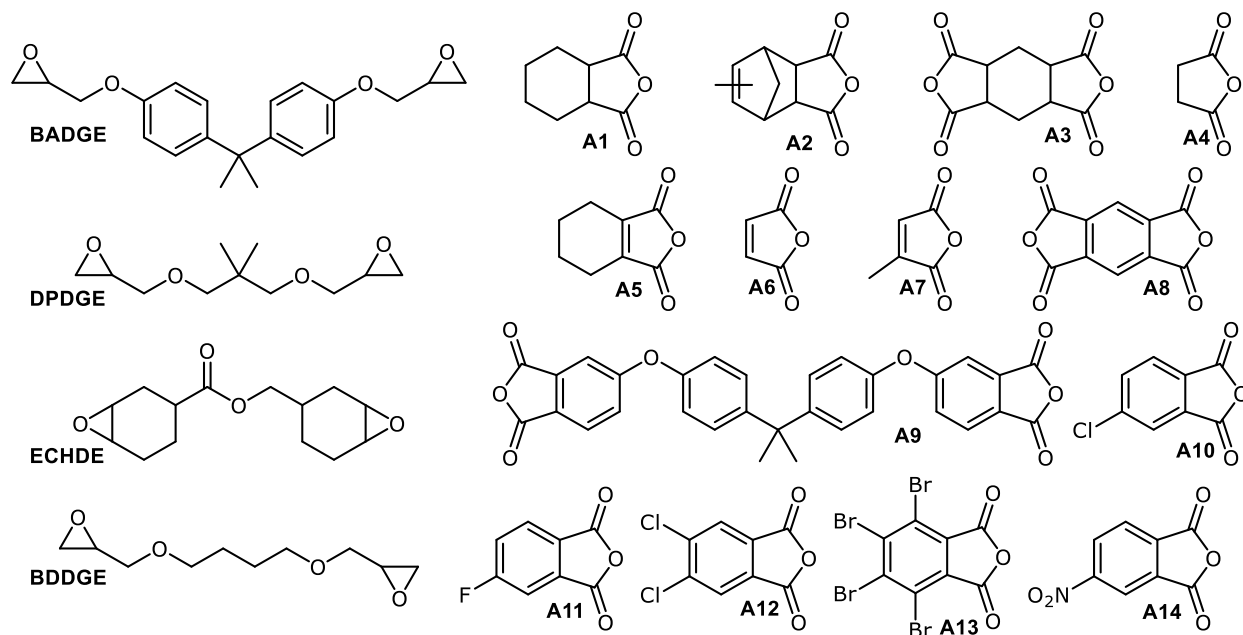
Scheme 59: Structure of the diepoxides and (di-)anhydrides that were applied. Table 6 provides a summary of the T_{max} values of the various combinations of epoxides and anhydrides cured with **5u-Me-CO₂**.

Table 6: T_{max} values of epoxide/anhydride mixtures cured with **5u-Me-CO₂** in DSC with 5 K/min (ratio: oxirane groups:anhydride groups:**5u-Me-CO₂** 200:200:8).

	BADGE	DPDGE	ECHDE	BDDGE
A1	125	133	133	131
A2	146	145	149	146
A3	146[a]	101[a]	98[a]	165[a]
A4	124[a]	108[a]	117[a]	132[a]
A5	131	135[a]	131[a]	132
A6	152	116[a]	115	142
A7	125	126	113	125
A8	110[a]	91[a]	n.d.	96[a]
A9	130[a]	n.d.	135[a]	108[a]
A10	134[a]	120[a]	117[a]	122[a]
A11	126[a]	117[a]	n.d.	121[a]
A12	129[a]	101[a]	93[a]	104[a]
A13	114[a]	91[a]	95[a]	114[a]
A14	105[a]	n.d.	n.d.	n.d.

[a] inhomogeneous mixtures were used.

Anhydrides with electron-withdrawing substituents were selected in order to increase electrophilicity and thus increase reactivity. The selection comprised the (di-)anhydrides A8 to A14 in Table 6. Chlorides, bromides, a second anhydride moiety, ethers and nitro group substitutions on 2-benzofuran-1,3-dione effectively decrease the electron density. Judging from the observed T_{max} values, this approach was successful. T_{max} values below 100°C were found in many cases. The impact is obvious within this group if for example A10 bearing on chlorine substituent is compared to A12 bearing two chlorine substituents. In addition, the comparison of A10 bearing one chlorine atom to A11 bearing one fluorine atom or A14 bearing a nitro group underlines the impact of electron-withdrawing moieties on the reactivity. Aside from the disadvantage that these electron-poor anhydrides do not form clear, homogeneous resins, some do not allow to form latent mixtures but polymerize at ambient conditions. Thus, from a latency

point of view these electron-deficient anhydrides turned out to be unusable. Despite their aliphatic character, A3 and A4 were also found to dissolve incompletely in one of the four diepoxies. Especially A3 shows large differences between the T_{max} values for the different diepoxides. For the cyclohexene oxide-based ECHDE a T_{max} of 98°C was found whereas for BDDGE a value of 165°C was observed. This temperature gap of 67°C presents the largest difference between two epoxides hardened with the same anhydride. In addition, with respect to the heterogeneous mixtures, DPDGE and ECHDE display a tendency to lower T_{max} values compared to BADGE and BDDGE. However, less differences in the T_{max} for a specific anhydride were found if the anhydride and the diepoxide compound formed homogeneous solutions. Unexceptional homogeneous solutions with the investigated diepoxides were only formed if A1, A2 or A7 were used. For those anhydrides, the largest difference in T_{max} was found to be 13°C in case A7 was applied. Other fully homogeneous systems were formed from BADGE/A5, BADGE/A6, ECHDE/A6, BDDGE/A5 and BDDGE/A6.

Noteworthy, for the system BADGE/A1/**5u-Me-CO₂**, reduction of the heat rate from 5 to 1 K/min in DSC lowered the T_{max} from 125°C to 103°C. On the one hand this finding underlines the impact of time necessary for the decarboxylation, initiation and polymerization. Avoidance of "overheated" temperature programs is generally beneficial. One explanation for the huge influence of the heat rate on T_{max} is the absence of significant latency and an occurring, slow polymerization already at room temperature.

Thus, suitable, homogeneous mixtures from Table 6 were selected and investigated, first under isothermal conditions at various temperatures followed by a heat ramp to check for released energy as control for completeness of resin curing. To further investigate latency and reactivity rheological measurements were executed. Systems consisting of DPDGE/A6, DPDGE/A7,

ECHDE/A6 and ECHDE/A7 were selected because of their low viscosity and high reactivity. In addition, a system made of 50 equivalents BADGE, 100 equivalents 2-(phenoxymethyl)oxirane, 100 equivalents A1 and 100 equivalents A10 was prepared. This multi-component mixture was researched with the aim to increase the reactivity of BADGE/A1 by substituting half of A1 by A10 (even though not dissolving in BADGE in a 100 to 200 ratio), which dissolves in the given mixture. To decrease viscosity, half of the BADGE was substituted with 2-(phenoxymethyl)oxirane, a low viscosity monoepoxide. In all following experiments **5u-Me-CO₂** was applied.
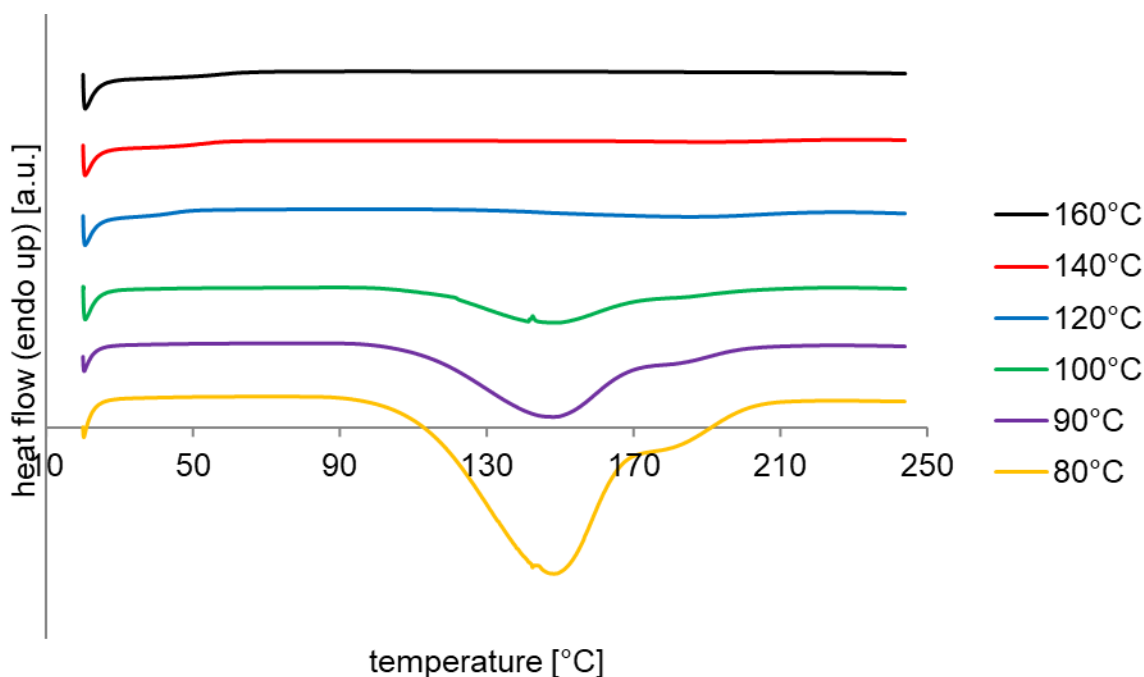
Scheme 60: Stacked DSC thermograms of post-isothermal heat ramp from 20 to 250°C with a heat rate of 20 K/min for the resin system DPDGE/A7/**5u-Me-CO₂** (ratio 100:200:8). The temperatures in the legend represent the temperature of the isothermal pre-curing (20 min).

In Scheme 60 the post-isothermal heat ramps of DPDGE/A7/**5u-Me-CO₂** are summarized. The temperatures applied in the isothermal runs were applied to the resins for 20 min. No energy was released in the control cycle for isothermal curing at 120°C and higher, consequently full curing can be assumed. 127 J/g were observed in the control cycle after isothermal curing at 100°C,

236 J/g at 90°C and 324 J/g at 80°C. This increase of released energies from 0 to 320 J/g within a temperature span of only 40°C from 120 to 80°C points towards useful latent behavior. All the more since the energy released from non-preheated anhydride-hardened epoxide curing reactions is typical between 260 and 400 J/g and 80°C is already an elevated temperature, far from ambient conditions. Other homogeneous resin systems show latency up to 80°C, too. Latent behavior is even better presented by rheology. Hence, the rheological behavior of the system DPDGE/A7/**5u-Me-CO$_2$** (100:200:8) was investigated (Scheme 61). Data for 25, 45, 65 and 85°C were collected in a row not changing the sample starting from 25°C whereas for 120 and 140°C fresh resin was used. No increase of viscosity was observed at 25 (~27 mPa·s) and 45°C (~19 mPa·s) within 30 min. Although slight increases in viscosity were observed at 65 and 85°C, the viscosity was still below 1 Pa·s after 30 min of applied heat. This is in stark contrast to measurements at 120 and 140°C where a fast increase of the viscosities to about 100000 Pa·s was observed. The viscosities increased with increasing degrees of polymerization (DP). Viscosity increase is enhanced for the formation of crosslinked materials compared to linear polymers.
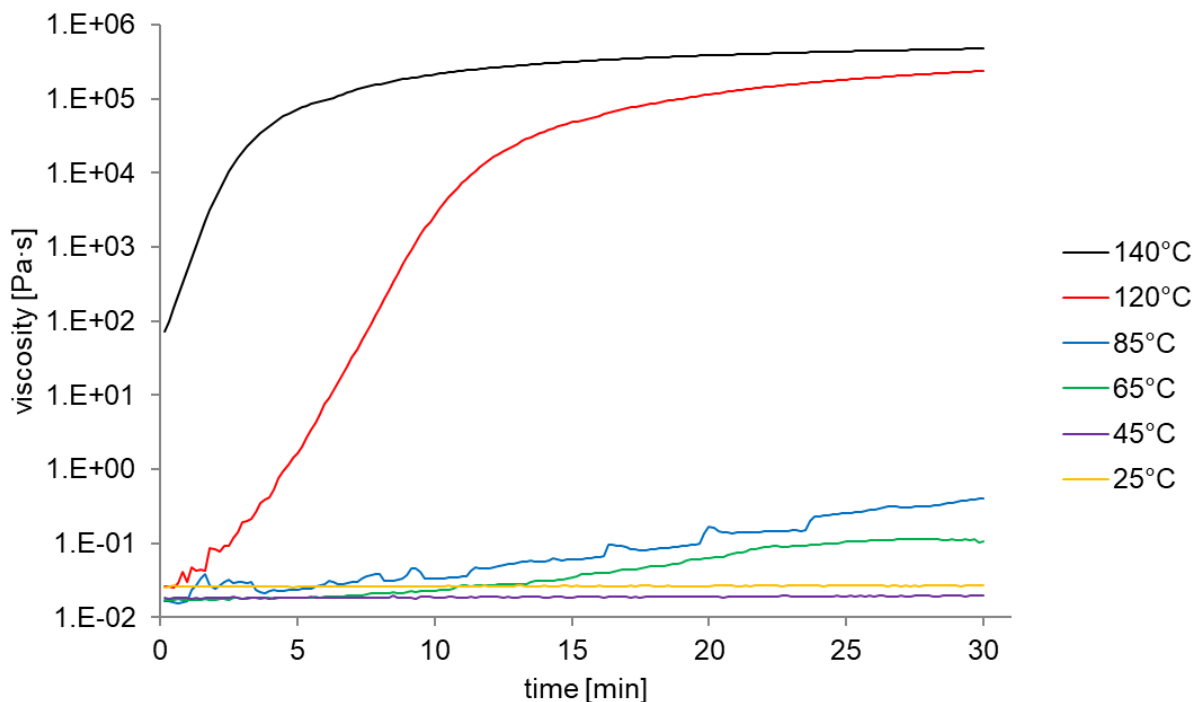
Scheme 61: Viscosities of the system DPDGE/A7/**5u-Me-CO₂** (100:200:8) determined by rheology at various temperatures.

The viscosities resulting from the reaction of the resin system ECHDE/A7/**5u-Me-CO₂** at various temperatures are depicted in Scheme 62. No or a low increase in viscosity was observed at 25°C (orange), 45°C (violet) and 65°C (green). At 85°C, a strong increase was observed (blue). Consequently latency was not as successful as for the system DPDGE/A7/**5u-Me-CO₂**. Most interesting is the step-effect around 15 min that was found for both rheological investigations concerning ECHDE. As discussed in the introduction, epoxides based on cyclohexene oxide tend to a certain degree to epoxide homopolymerization, although anhydrides are still present in the reaction.[240] The resulting polyether formation is one explanation for this step-effect. However, fast curing was observed again at temperatures of 120°C or higher (red and black, respectively).
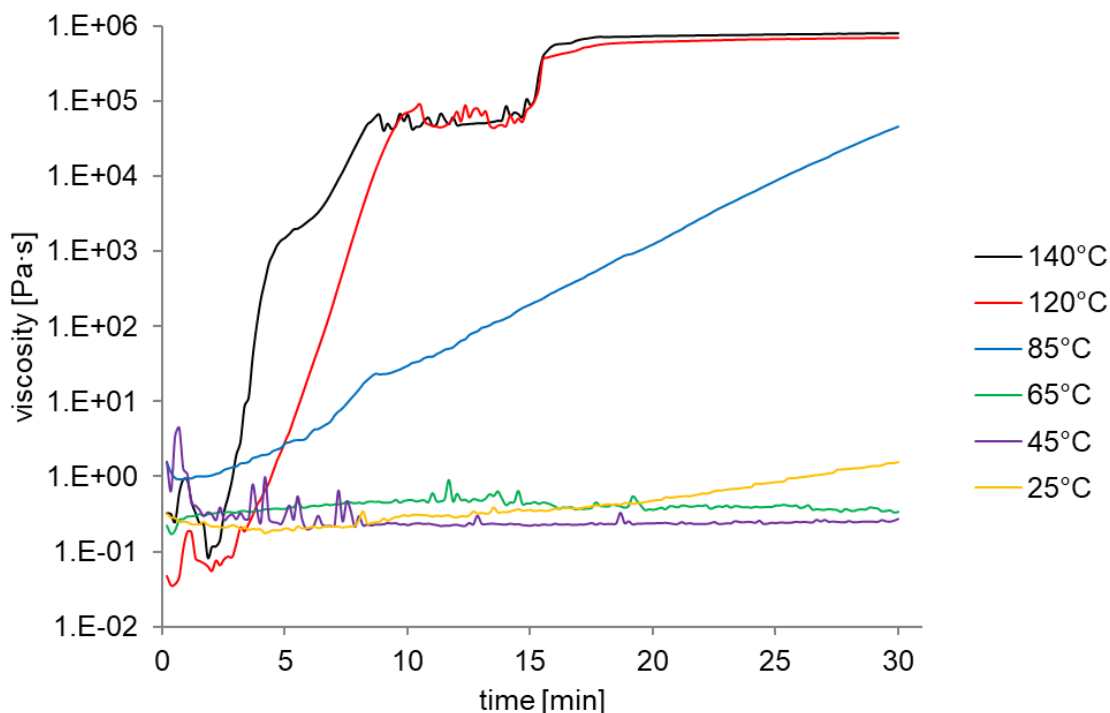
Scheme 62: Viscosities of the system ECHDE/A7/**5u-Me-CO$_2$** (100:200:8) determined by rheology at various temperatures.

Viscosities for the system BADGE/2-(phenoxymethyl)orxiraneA1/A19/**5u-Me-CO$_2$** showed no second step-like increase but fast curing below 5 min at 140°C (black). While a moderate increase in viscosity was observed at 85°C (blue), no, or no significant increase was found at temperatures below. The viscosity remained constant, both at 25°C (125 mPa·s, orange) and at 45°C (59 mPa·s, violet). At 65°C (green) initially the lowest viscosity of 32 mPa·s was found, however increasing slightly to 55 mPa·s within 30 min.
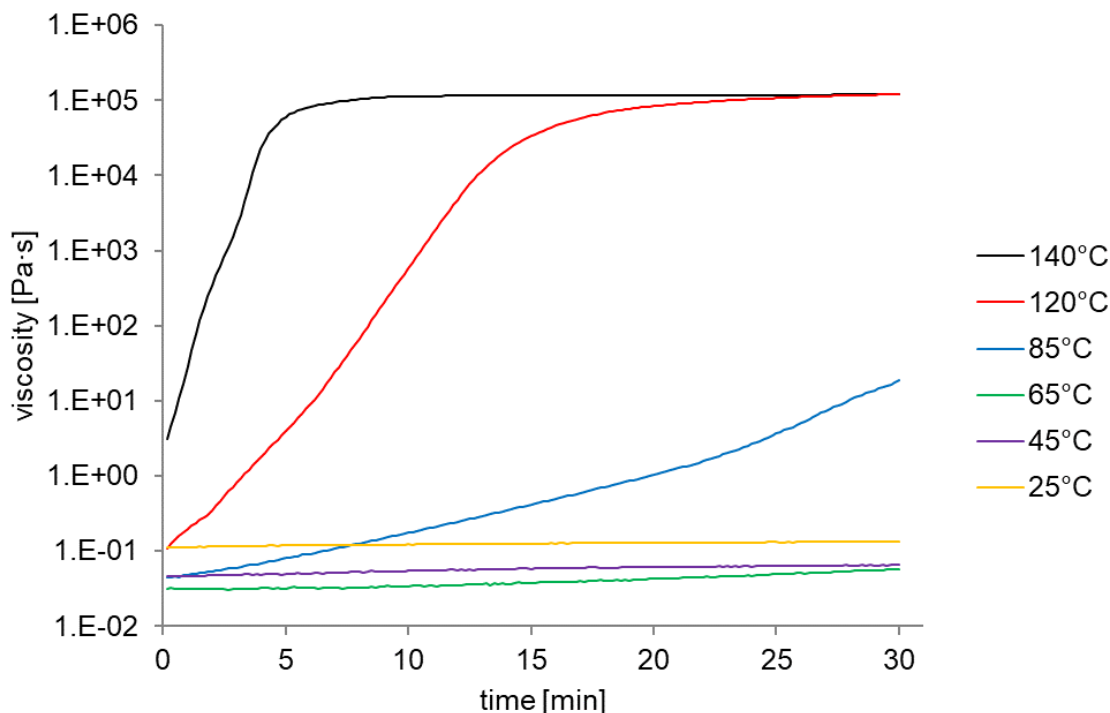
Scheme 63: Viscosities of the system BADGE/2-(phenoxymethyl)oxirane/A1/A10/**5u-Me-CO₂**
(50:100:100:100:8) determined by rheology at various temperatures

All reaction profiles determined by DSC at 120 and 140°C of mixtures containing terminal epoxides showed no induction periods. In contrast, the mixtures containing ECHDE, which is based on cyclohexene oxide and thus an internal epoxide, displayed a certain induction period of 2 to 5 min. This is consistent with the literature according to which the electrophilic carbon atoms of the oxirane ring are almost exclusively attacked at the sterically less hindered position.[393-395] This suggests eased and thus faster reaction, which in turn leads to the induction period for ECHDE. This observation is basically independent of the question whether the initial reaction of the released carbene ring-opens an oxirane moiety or an anhydride. All experiments show satisfying latent behavior at ambient temperatures, but the induction period could be especially useful for applications that need an extended delay or pot life time even at elevated temperatures.

Concluding, anhydride-hardened epoxide resins with latent initiators based on NHCs were investigated. After an initial screening of different NHC precursor structures, Lewis acid additives and initiator loadings in conjunction with a BADGE/A1 system, a screening of four diepoxides and fourteen (di-)anhydrides was performed. From the NHC precursor screening a reactivity boost caused by sterically demanding (cyclic) side groups was deduced. Despite the minimal steric demand of the nitrogen substituents, **5u-Me-CO₂** was used as an initiator due to its favorable synthesis and robustness. Loadings of 8 equivalents of precursor to 100 equivalents of diepoxide were found to be suitable (1 equivalent precursor per 25 oxirane moieties and 25 equivalents anhydride). Latent resins were not formed in case very strong electron-withdrawing moieties were connected to the anhydrides; instead, gelation was observed already at room temperature. Further, the solubility of electron-deficient anhydrides in the diepoxides was limited resulting in heterogeneous mixtures, which are hardly sprayed (clogged nozzles) and bear unfavorable mechanical properties. On the contrary, liquid and low melting anhydrides form homogeneous mixtures, which are apparently latent. Isothermal DSC as well as rheological measurements showed the latency of the systems more quantitatively. Stabile latent behavior was found below 65°C for all resins investigated by rheology. Temperature increase decreased the viscosities, which were well below 1 Pa·s, in many cases below 100 mPa·s. Slow to moderate curing was observed between 65 and 100°C. Here, 65°C might be an advantageous temperature for the handling of some resins as their viscosity is remarkably low for a certain time period after the temperature was applied. Above 100°C, rapid curing reactions were observed. In some cases full curing at 140°C was observed within 3 min and in all cases with temperatures of 120 the polymerization was complete after 30 min according to the viscosities determined by rheology.

A final remark on the experiments conducted in conjunction with anhydride-cured epoxide resins concerns anhydride mixtures. As seen for the mixture BADGE/2-(phenoxymethyl)oxirane/A1/A10/**5u-Me-CO$_2$** the application of different anhydrides can be advantageous from a reactivity, a viscosity and a preparation (liquid-liquid mixing) point of view. Thus, three anhydrides that are solid at room temperature, namely A1, A4 and A6, were selected to search for eutectic mixtures that are liquid at room temperature. For this purpose the samples were weighed in in various ratios and heated in a closed vial to 60°C for several minutes. Mixtures of A1/A4 as well as mixtures of A4/A6 resulted in compositions that were solid at room temperature. Mixtures from 100 equivalents A6 and 30 equivalents A1 to mixtures of 100 equivalents A6 and 200 equivalents A1 were found to remain liquid after cooling to room temperature.

The approach to mix anhydrides with the intension to optimize reactivity, viscosity, handling, flame retardancy or the mechanical properties after curing offers many possibilities for future scientific work and applications. All the more if the epoxide compounds are additionally taken into account. Further, the starting materials were stored and the resins were mixed inside the glove box. However, homogenization and polymerizations were executed under ambient atmosphere. Depending on the application it would be interesting to identify whether the polymerizations can be conducted with various amounts of additional water and the impact on the carboxylate and the free carbene, respectively, could be investigated. Further, the incorporation of other additives like carbon black, silver, polyurethanes and other materials to adjust the final properties of the cured resin must be reinvestigated for the special reactivity of latent NHCs. Upstream investigations applying monoepoxides and anhydrides, to form linear

114

polyesters, could facilitate mechanistic investigations, the research for suitable additives and latent resins for the formation of thermoplastic polyesters.

7.2 Polyoxazolidin-2-ones

In this chapter the synthesis of polyoxazolidin-2-ones from diepoxides and diisocyanates catalyzed by NHCs and Lewis acids is described. Many of the results of this chapter are published: H. J. Altmann, M. Clauss, S. König, E. Frick-Delaittre, C. Koopmans, A. Wolf, C. Guertler, S. Naumann, M. R. Buchmeiser, Synthesis of Linear Poly(oxazolidin-2-one)s by Cooperative Catalysis Based on N-Heterocyclic Carbenes and Simple Lewis Acids, *Macromolecules* **2019**, *52*, 487-494.[5] Special attention was spent on the aims in the following.

- Although different synthesis routes, starting from other monomers than diisocyanates and diepoxides were established and offer advantages like reduced reaction temperature and high chemoselectivity, the most atom economic synthesis for polyoxazolidin-2-ones comprises commercially available diisocyanates and diepoxides.[254-255, 268-277]

- The avoidance of isocyanurate formation is essential for the synthesis of an exclusively linear, thermoplastic polyoxazolidin-2-ones since triisocyanates, which result from the trimerization of diisocyanates, act as crosslinking agents.

- Homopolymerization of both, diisocyanates and diepoxides had to be avoided due to its impact on the stoichiometry of the reaction, which is important to reach high molecular weight polymers from polyaddition reactions.

- NHCs were selected as catalysts because they were supposed to provide side-product-free polymers.

- To exploit the full potential of the polymer class of polyoxazolidin-2-ones both, aliphatic and aromatic diisocyanates should be used.

- A solvent, innocent at the harsh reaction conditions and suitable for the monomers and the polymer, had to be found.

- Clarification on the regioisomerism of polyoxazolidin-2-ones was aimed at since the repeating oxazolidin-2-one rings can be substituted in four or five position, which was supposed to affect the polymer properties.
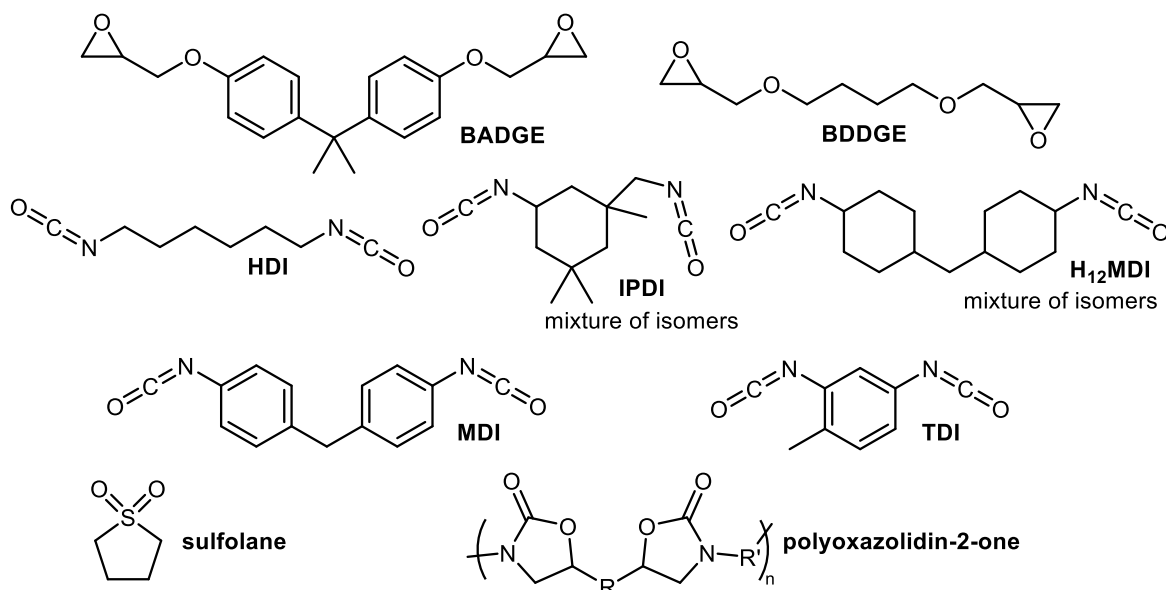
Scheme 64: Monomers used for the synthesis of polyoxazolidin-2-one, the solvent (sulfolane), and a general polymer structure.

Initial experiments were performed applying BADGE (100 equivalents) and TDI (100 equivalents) in conjunction with various NHC carboxylates (1 equivalent) at 60°C (or room temperature), in bulk, DMSO or sulfolane. NHC carboxylates were chosen as pre-catalysts because of the increased temperatures that are necessary to release the carbene thus avoiding side reactions like trimerization at low temperatures.[118] The initially employed reaction temperature and time were chosen according to reports on NHC catalyzed oxirane ring-opening reactions.[396] However, irrespective of the NHC used, IR spectroscopy of the isolated colorless substances only showed signals at 1690 to 1710 cm^{-1} indicating formation of the isocyanate trimer instead of the oxazolidin-2-one for which no evidence was found (Scheme 66). The trimer yields after either precipitation of the reaction mixture, centrifugation, decanting off supernatant solution and drying or intensive washing and drying (for gelly material) ranged from <5 to 37%.
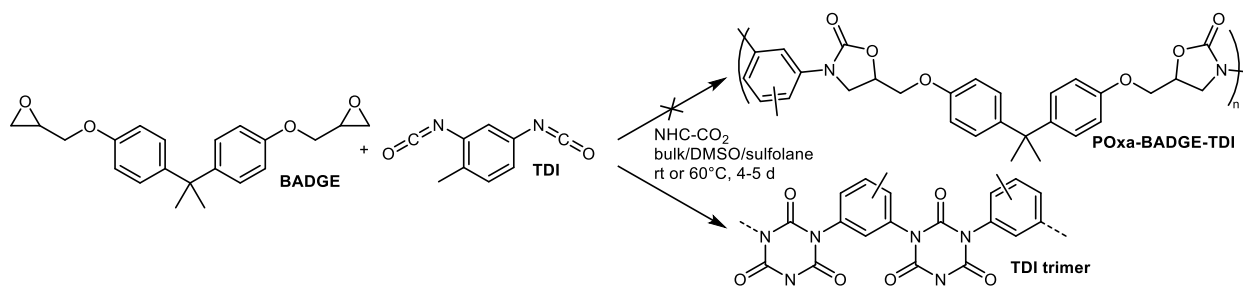
Scheme 65: Reactions of BADGE and TDI lead to the trimer at rt/60°C catalyzed by NHC-CO$_2$.
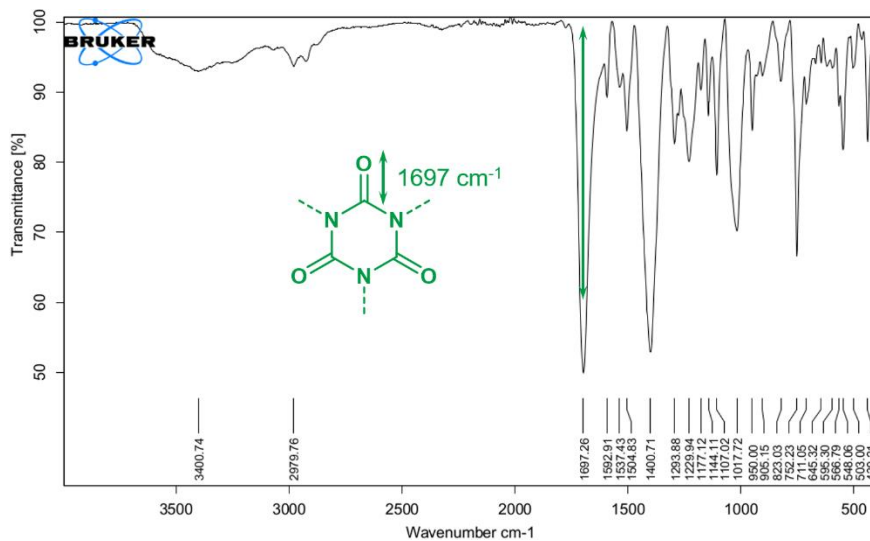
Scheme 66: IR spectrum of the product resulting from an one-pot reaction of BADGE and TDI catalyzed by **5s-Ad-CO$_2$** at 60°C for 5 days in sulfolane. The carbonyl vibration of the trimer is labeled green.

A different picture was found when **6-Mes-MgCl$_2$** was applied at 60°C in sulfolane over a period of 4 days. An intensive oxazolidin-2-one carbonyl vibration (1748 cm^{-1}) was found next to a peak caused by the isocyanurate (1697 cm^{-1}) (Scheme 67). The formation of oxazolidin-2-one was attributed to the MgCl$_2$ protecting group and the NHC, since the sole application of MgCl$_2$ under the same reaction conditions also led to isocyanurate products (compare chapter 9.3). The product resulting from the reaction with **6-Mes-MgCl$_2$** was partially soluble in common organic solvents like DMSO, DMF and DMAc.
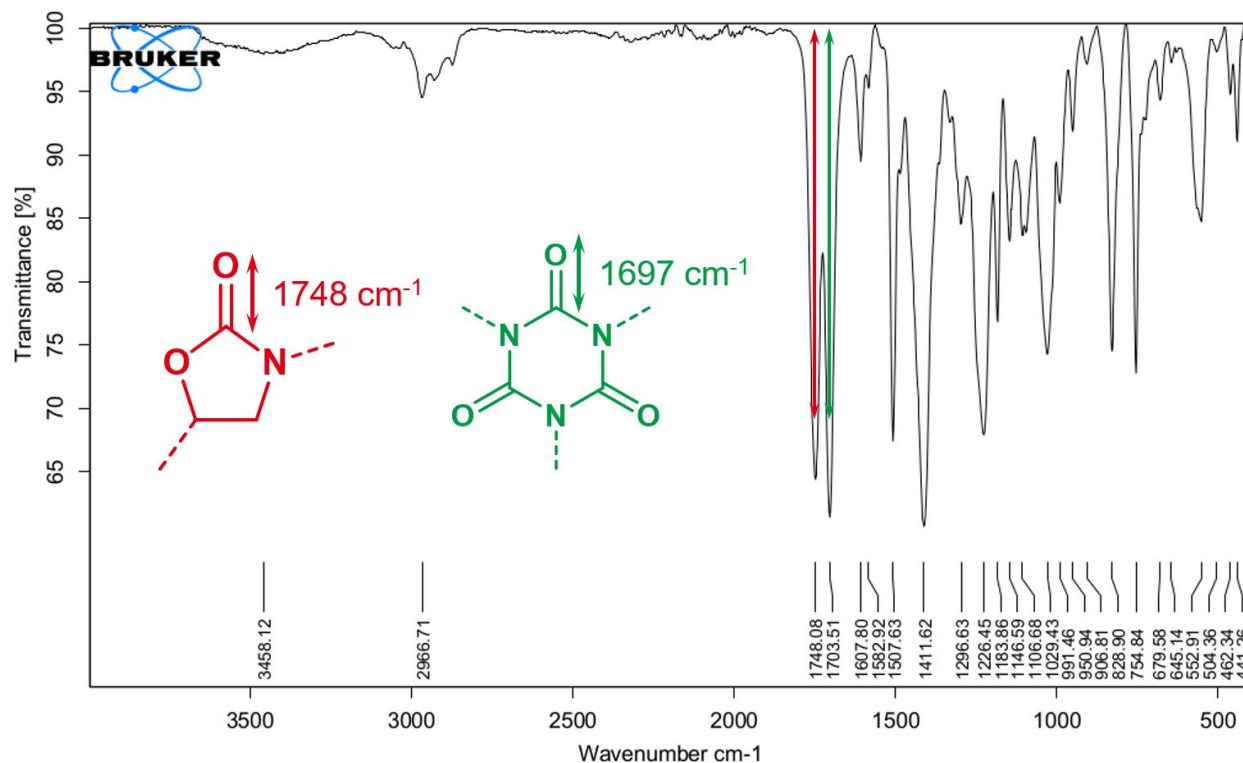
Scheme 67: IR spectrum of the product resulting from an one-pot reaction of BADGE and TDI catalyzed by **6-Mes-MgCl₂** at 60°C for 5 days in sulfolane. Carbonyl vibration of oxazolidin-2-one moieties is labeled in red, isocyanurates in green.

Oxazolidin-2-one and isocyanurate carbonyl vibrations were also observed if **5u-Me-CO₂** was applied as catalyst in conjunction with MgCl₂ (each 1 equivalent) in polyaddition reactions of BADGE and TDI (each 100 equivalents) in a one-pot reaction in sulfolane at 60°C after 6 h.

Lower trimerization rates and lower tendencies for side reactions were reported for alkyl isocyanates compared to aryl isocyanates.[118, 285, 397] Therefore, TDI was exchanged by HDI as monomer for the following investigations. An overview of most polyoxazolidin-2-one structures synthesized in this work is given in Scheme 71. The polyaddition reactions were heated since elongated reaction periods at higher temperatures were shown to enable reopening of isocyanurate rings and concurrent transformation into oxazolidin-2-one rings by conversion with oxirane moieties.[264, 278] The reaction system consisted of equimolar BADGE and HDI as well as **5u-Me-CO₂** and MgCl₂ in sulfolane. The one-pot reaction was heated to 220°C for 15 h and

gave 48% isolated yield of a solid with oxazolidin-2-one (1738 cm^{-1}) and isocyanurate (1683 cm^{-1}) signals in the IR spectrum (Scheme 68). The wave numbers of both signals are lower compared to polymers containing TDI. The product was fully soluble in organic solvents like DMF, DMSO and CHCl$_3$.
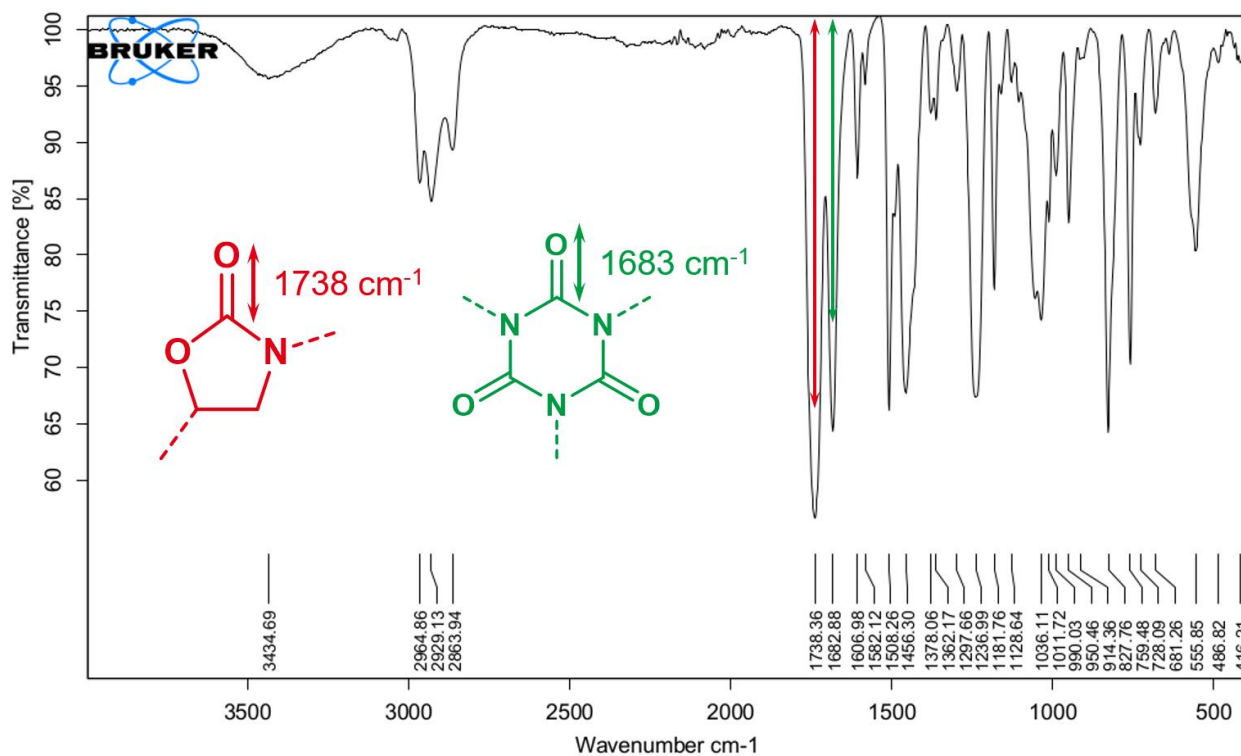
Scheme 68: IR spectrum of the product resulting from an one-pot reaction of BADGE and HDI catalyzed by **5u-Me-CO₂** and MgCl₂ at 220°C for 15 h in sulfolane. Carbonyl vibration of oxazolidin-2-one moieties is labeled in red, isocyanurates in green

In a further modification of the reaction setup, two solutions were prepared. Solution 1 contained 1 equivalent **5u-Me-CO₂**, 2 equivalents MgCl₂ and 100 equivalents BADGE dissolved in sulfolane. Solution 2 was made of 100 equivalents of HDI in sulfolane. Solution 1 was heated to 200°C and solution 2 was added dropwise within 1 h, and the combined solutions were kept at reaction temperature for 2 h. The IR spectrum of the product isolated in 76% yield displays no isocyanurate signal but an intensive oxazolidin-2-on carbonyl vibration (1735 cm^{-1}).
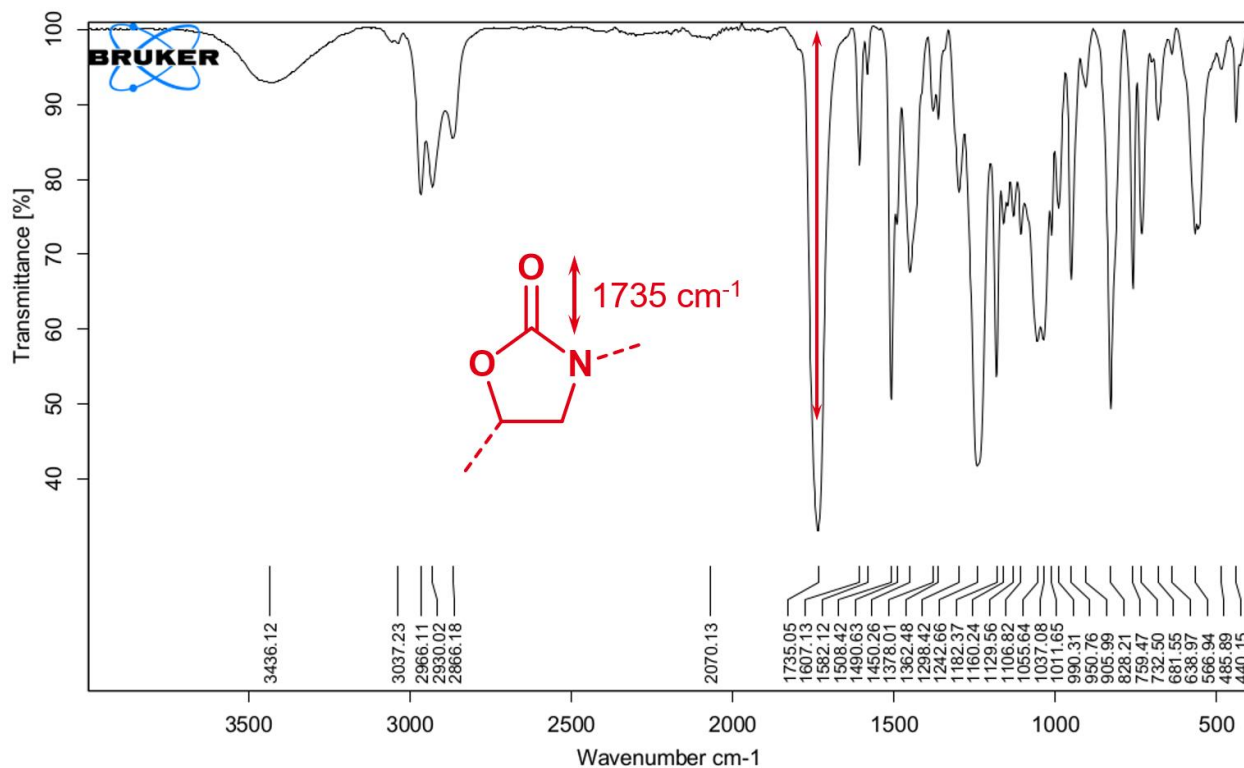
Scheme 69: IR spectrum of a polymer synthesized from BADGE and HDI. An HDI solution in sulfolane was added to a solution of **5u-Me-CO$_2$**, MgCl$_2$ and BADGE in sulfolane at 200°C over a period of 1 h. The combined mixture was kept at 200°C for 2 h. Carbonyl vibration of oxazolidin-2-one moieties is labeled in red.

The polymers presented in Scheme 68 and Scheme 69, both consisting of BADGE and HDI, were submitted to NMR analysis. Comparison of the carbonyl areas from δ=140 to 160 ppm in ^{13}C NMR is shown in Scheme 70. The upper spectrum was received from the polymer synthesized in one-pot. A signal at δ=149 ppm results from the isocyanurate carbonyl carbon (green), underlining the findings by IR. The lower spectrum was received from the polymer synthesized by portionwise addition of a sulfolane solution containing the isocyanate to the residual reaction mixture at reaction temperature (200°C). It does not show any peaks besides the expected oxazolidn-2-one signal and the two aromatic signals. Which in turn means this POxa-BADGE-HDI is isocyanurate-free (Scheme 70). The molecular weight of 9000 g/mol was determined by DMAc-GPC and translates into 18 BADGE-HDI repeat units. A broad molecular weight distribution of 4.8 was found.
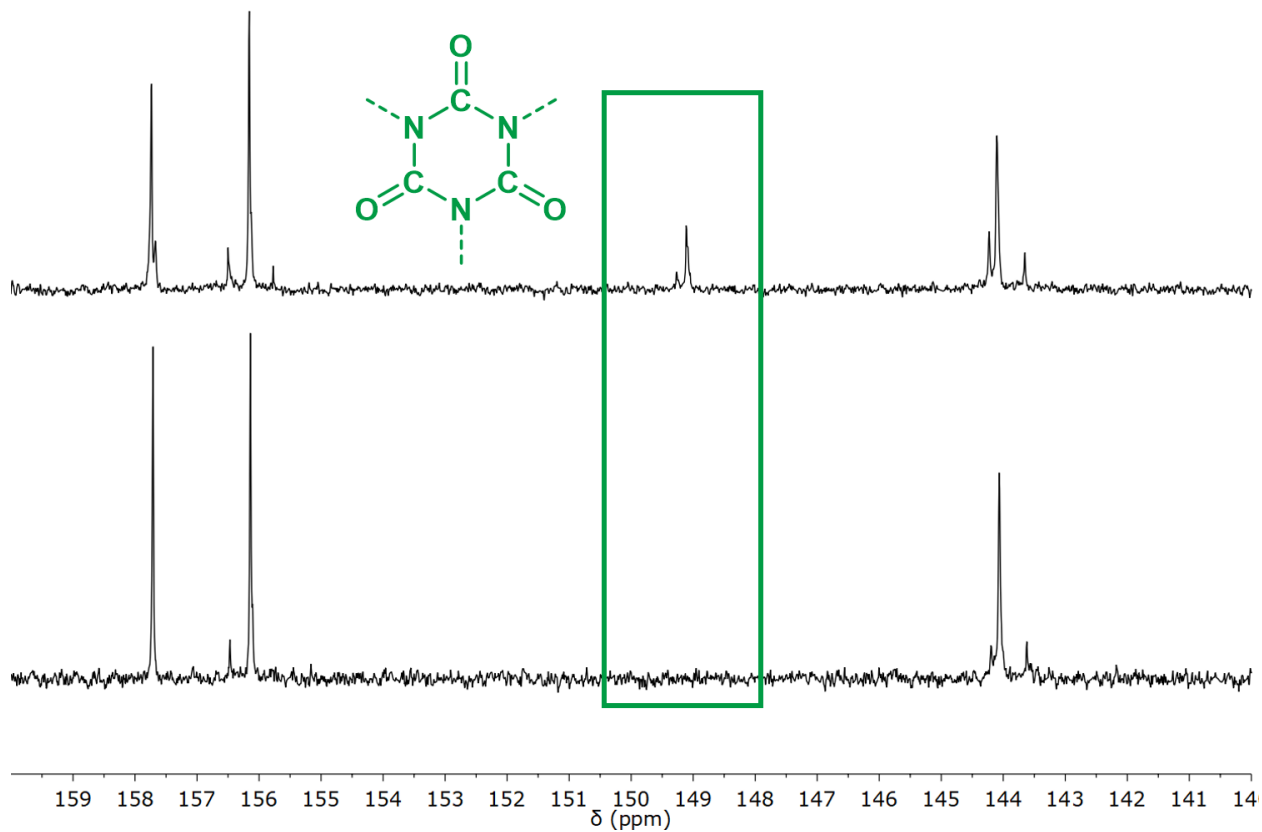
Scheme 70: Stacked ^{13}C NMR (CDCl$_3$) spectra of two polyoxazolidin-2-ones made from BADGE and HDI catalyzed by **5u-Me-CO$_2$** and MgCl$_2$. The polymer on top was synthesized in an one-pot reaction at 220°C within 15 h. The bottom polymer was synthesized by dropwise addition of the isocyanate to the reaction mixture over a period of

1
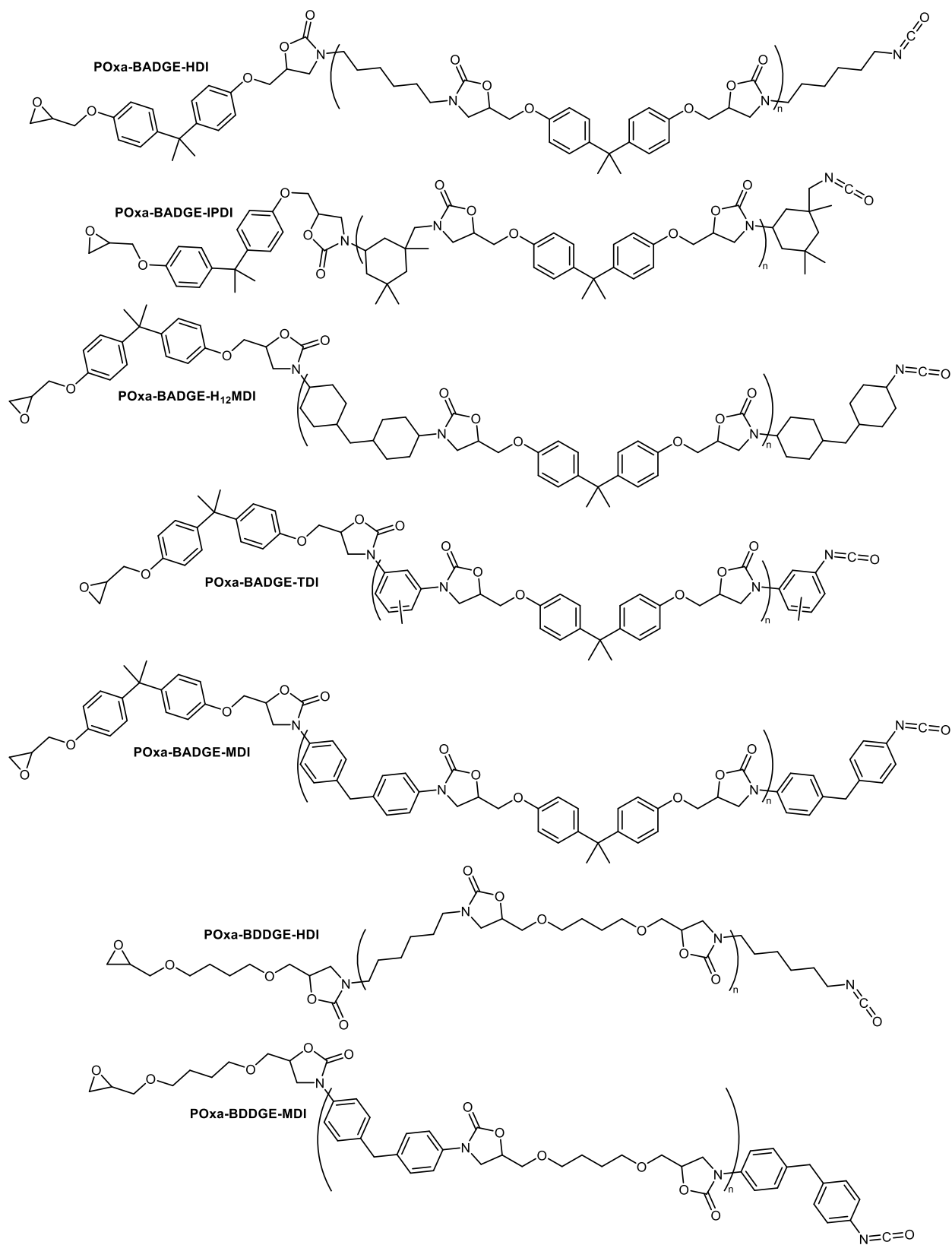
Scheme 71: Overview of the polyoxazolidin-2-ones synthesized in this work.

The successful isocyanurate-free synthesis approach was extended to other carbenes and LiCl. The results are summarized in Table 7. In all cases sole application of either NHC carboxylate or Lewis acid resulted in a certain degree of trimerization (entries 1, 2, 5, 8 and 11). Exclusively linear polymers were found for **6-iPr-CO₂** and **5u-Me-CO₂**, irrespective of the Lewis acids used (entries 3, 4, 9 and 10). In contrast, **6-Mes-CO₂** in conjunction with MgCl₂ delivered a crosslinked polymer (entry 7). The reasons remain speculative. Nonetheless, in conjunction with LiCl an isocyanurate-free polymer was synthesized (entry 6). Therefore, experiments hereafter were executed with LiCl. The molecular weights in the range of 5000 to 22000 g/mol correspond to 18 - 43 BADGE-HDI repeat units (508.62 g/mol per unit).

Table 7: POxa-BADGE-HDI synthesized by portionwise addition (within 1 h) of a solution containing the diisocyanate (100 equivalents) to the reaction mixture at 200°C containing BADGE (100 equivalents), **5u-Me-CO₂** (1 equivalent) and MgCl₂ or LiCl (2 equivalents). Post-heating 2 h.

entry	NHC	Lewis acid	M_n [g/mol][a]	$Đ_M$[a]
1	-	LiCl	crosslinked	-
2	-	MgCl₂	crosslinked	-
3	**6-iPr-CO₂**	LiCl	12000	5.3
4	**6-iPr-CO₂**	MgCl₂	10000	5.4
5	**6-iPr-CO₂**	-	crosslinked	
6	**6-Mes-CO₂**	LiCl	22000	5.4
7	**6-Mes-CO₂**	MgCl₂	crosslinked	
8	**6-Mes-CO₂**	-	crosslinked	
9	**5u-Me-CO₂**	LiCl	5000	8.3
10	**5u-Me-CO₂**	MgCl₂	9000	4.8
11	**5u-Me-CO₂**	-	crosslinked	

[a] determined by DMAc-GPC.

Interestingly the molecular weights follow a trend within the carbenes. An increase in the Tolman electronic parameter (TEP) resulted in lower molecular weights. The TEP of **5u-Me** was determined to be 2052.4 cm⁻¹ (5000 g/mol), the TEP of **6-iPr** 2048.3 cm⁻¹ (12000 g/mol) and the

TEP of **6-Mes** 2042.6 cm^{-1} (22000 g/mol).[133] Nevertheless, the decarboxylation and thus the basicity of the carbene and the NHC-H$^+$ salt, respectively, as well as the steric situation and NHC ring size must also be considered.

Although higher molecular weights were reached with other carbenes, **5u-Me-CO₂** was chosen for further experiments due to its favorable synthesis and robustness. The reaction setup was optimized. Instead of adding the isocyanate to the reaction mixture, both monomers were added to a mixture of **5u-Me-CO₂** and LiCl in sulfolane at 200°C. Further, the time span during which the monomers were added was elongated to 2 h. In turn, the subsequent heating phase was reduced to 1 h. The ratio of monomers : catalyst system (diepoxide:diisocyanate:**5u-Me-CO₂**:LiCl) was varied from 50:50:1:2 over 200:200:1:2 to 400:400:1:2. For high catalyst loadings, slightly increased yields of 80% were found, while the latter two ratios resulted in 50 and <10% yield, respectively. Consequently, the ratio was kept at 100:100:1:2. DMSO and 1,2,4-trichlorbenzene caused major issues (isocyanurate formation and crosslinking). In contrast sulfolane and 1,3-dimethylimidazol-2-one were successfully applied in the process. Lowering the reaction temperature (175°C) resulted in the formation of trimer and 200°C were set as standard. This setup was applied to five diisocyanates and two diepoxides. The results and the monomers are summarized in Table 8. The improved reaction setup resulted in an increased molecular weight for POxa-BADGE-HDI of 32000 g/mol and narrower molecular weight distributions (entry 1). The measured molecular weights can be categorized by the type of monomers that were used. For all combinations of BADGE and aliphatic isocyanates molecular weights are in the range of 30000 g/mol. For BADGE and aromatic isocyanates values of 11000 and 14000 g/mol were found. Lowest molecular weights were found for BDDGE and the differences between aromatic and aliphatic diisocyanate vanished in terms of molecular weights. Molecular

weight distributions between 1.9 and 3.0 are acceptably low for polyadditions, especially for polymers synthesized at 200°C. For the production of polyoxazolidin-2-ones from MDI and TDI the monomer addition times were doubled to 4 h and in the case of TDI it was also found favorable to change the solvent from sulfolane to 1,3-dimethylimidazol-2-one since POxa-BADGE-TDI from sulfolane contained small amounts of isocyanurates. Polymers consisting of former aromatic isocyanates were soluble in typical polymer solvents like DMF, DMSO and DMAc in addition to those used in their synthesis. For polymers made from HDI, H_{12}MDI and IPDI additional solubility in CH_2Cl_2 and $CHCl_3$ was found. This affected the workup procedure. Once the polymerization samples were cooled down the reaction solution was precipitated into iPrOH, centrifuged, the supernatant solution decanted and the polymer dried under reduced pressure. Eventually the polymer was redissolved and the workup process was repeated. This was needed in several cases especially to remove the remaining sulfolane. The glass transition temperatures for polymers based on BADGE were found to be high if cyclic structures were incorporated in the diisocyanate monomer. POxa-BADGE-HDI displayed a little lower value for T_g. The substitution of BADGE by BDDGE further reduced the T_g to 83°C for POxa-BDDGE-MDI and no signal was found for fully aliphatic and acyclic POxa-BDDGE-HDI, respectively. The broad range of 83 to 178°C implied the possibility to adjust the glass transition temperature to a temperature of choice by mixing more than two monomers. In entry 8 a mixture of BADGE:HDI:MDI (100:50:50) was added within 4 h to the reaction mixture to form a copolymer. Indeed the T_g was in-between POxa-BADGE-HDI and POxa-BADGE-MDI. An experiment to synthesize a block-copolymer by adding first BADGE and MDI over 4 h and after an 1 h break second BADGE and HDI did not lead to a clear result. Although the polymer was isocyanurate-free only one T_g was found at 129°C. For block-copolymers two values, close to

126

those of the homopolymers were expected. A molecular weight of 35000 g/mol ($Đ_M$=2.9) and a yield of 85% were determined. In comparison to the literature, the measured molecular weights are reasonable. Azechi and Endo observed number-average molecular weights up to 5000 g/mol.[290] In a study by Wolf *et al.* for POxa-BADGE-MDI a molecular weight of 9000 g/mol was found by DMAc-GPC.[283] If, additionally, molecules with a molecular weight below 2000 g/mol were excluded a molecular weight of as high as 18000 g/mol was observed. All polymers were found to be amorphous.

Table 8: Polymerization results of various monomers synthesized according to the improved reaction setup.

entry	epoxide	isocyanate	M_n [g/mol][a]	$Đ_M$[a]	DP[b]	T_g [°C]	yield [%]
1	BADGE	HDI	32000	2.7	63	110	72
2	BADGE	IPDI	31000	1.9	55	178	69
3	BADGE	H_{12}MDI	32000	2.5	53	148	73
4[c]	BADGE	MDI	14000	2.7	24	151	71
5[c,d]	BADGE	TDI	11000	2.4	21	156	89
6	BDDGE	HDI	9000	2.0	24	-	52
7	BDDGE	MDI	9000	3.0	20	83	76
8	BADGE	HDI/MDI	31000	2.5	56	145	>90

[a] determined by DMAc-GPC; [b] calculated from the molecular weight results; [c] the monomer addition period was extended to 4 h; [d] 1,3-dimethylimidazol-2-one was used as solvent.

With the optimized reaction setups at hand, additional NHC carboxylates were selected to investigate the influence of the carbene on the reaction. The selection was made according to the TEP of the free carbenes. There were 2052.4 cm^{-1} for **5u-Me₂**, 2050.7 for **5u-Mes**, 2045.5 for **6-Dipp** and 2042.6 for **6-Mes**.[133] The selected NHCs were used to synthesize POxa-BADGE-HDI (Table 9) and POxa-BADGE-MDI (Table 10).

Table 9: Polyoxazolidin-2-ones synthesized from BADGE/HDI/NHC/LiCl (100:100:1:2) at 200°C.

entry	NHC	M_n [g/mol][a]	$Đ_M$[a]	DP[b]	yield [%]
1	**5u-Me-CO₂**	20000	1.9	39	73
2	**5u-Mes-CO₂**	14000	1.7	28	78
3	**6-Dipp-CO₂**	12000	1.9	24	74
4	**6-Mes-CO₂**	10000	1.6	20	78

[a] determined by DMSO-GPC; [b] calculated from the molecular weight results.

To prevent confusion, it must be mentioned that the DMSO-GPC system was used to determine the values in Table 9 and Table 10 instead of the DMAc-GPC system used before. The changed GPC system influences the molecular weights determined e.g. the M_n of POxa-BADGE-HDI in the DMAc system was 32000 g/mol (Table 8, entry 1), whereas with the DMSO-GPC a M_n of 20000 g/mol was found (Table 9, entry 1). Similarly, the molecular weight changed for POxa-BADGE-MDI from 14000 g/mol for the DMAc system to 42000 g/mol with the DMSO system. The reasons are mostly attributed the solvent, which has a strong impact on the polymer geometry. However, within the respective system the values appear trustworthy and comparable.

For POxa-BADGE-HDI the molecular weights increase with increasing TEP (Table 9). On the contrary, albeit less pronounced, for POxa-BADGE-MDI the opposite behavior was observed (Table 10). Both polymers, POxa-BADGE-HDI and POxa-BADGE-MDI had narrow molecular weight distributions in common. The differences between the polymers are attributed to the interaction of the NHC with the monomer in the initiation reaction. Hence, trimerization experiments were executed for phenyl-, 4-methylphenyl-, cyclohexyl- and n-hexyl isocyanate. The isocyanates were mixed with **6-Cy-CO₂** at room temperature. Under these conditions aromatic isocyanates react rapidly to the isocyanurate whereas aliphatic isocyanates do not undergo trimerization. If the same applies to the diisocyanates during the polymerization, two different reaction pathways are conceivable for aromatic and aliphatic diisocyanates,

respectively. One starts from NHC-activated isocyanates and Lewis acid-activated oxirane moieties. The other starts from either isocyanurates ring-opened by alkoxides resulting from epoxide ring-opening or by Lewis acid activated epoxides that are ring-opened by NHCs and subsequently undergo a nucleophilic attack at the isocyanate. The mechanism will be discussed in detail at the end of this chapter.

Table 10: Polyoxazolidin-2-ones synthesized from BADGE/MDI/NHC/LiCl (100:100:1:2) at 200°C.

entry	NHC	M_n [g/mol][a]	$Đ_M$[a]	DP[b]	yield [%]
1	**5u-Me-CO₂**	42000	1.4	71	80
2	**5u-Mes-CO₂**	46000	1.4	70	82
3	**6-Dipp-CO₂**	47000	1.4	80	84
4	**6-Mes-CO₂**	51000	1.5	86	83

[a] determined by DMSO-GPC; [b] calculated from the molecular weight results.

In order to simplify the reaction and facilitate the use of a variety of NHCs, a process circumventing the synthesis of carboxylates and the associated deprotonation and elaborate inert gas proceedings was developed. Here, the catalyst system is formed *in situ* from NHC-HX and a metal hydride (Scheme 72). For demonstration purposes **5u-Mes-HCl** and LiH were chosen. Both were mixed together with sulfolane and heated to 200°C for 1 h to form the free carbene **5u-Mes** and the Lewis acid LiCl *in situ* under hydrogen evolution before a solution of BADGE and HDI in sulfolane was added portionwise to form POxa-BADGE-HDI (Scheme 72). In addition, a control experiment was conducted applying **5u-Mes** and LiCl as dual catalytic system under the same conditions. Isocyanurate-free polymers with an M_n of 13000 g/mol ($Đ_M$=3.7, DMAc-GPC) for the *in situ* system and an M_n of 15000 g/mol ($Đ_M$=3.1 DMAc-GPC) in the control experiment were found. The similar outcomes suggest successful *in situ* formation of the dual catalyst system. There are two explanations for the observed reduced molecular weights in both experiments. On the one hand the LiCl loading was halved compared to the POxa-BADGE-

HDI (Table 8, entry 1), on the other hand the built up molecular weight was lower for **5u-Mes**

than for **5u-Me** (Table 9, entries 1 and 2). In addition it must be mentioned that side reactions

e.g. with the solvent or impurities during the *in situ* dual catalyst formation or during the heating

of the control experiment to 200°C for 1 h cannot be excluded. Nonetheless, the potential of this

approach is high since basically any NHC-H^{+} and other metal hydrides like NaH, KH, CsH,

MgH$_2$ or other could be used. Further, the addition of other Lewis acids in order to reach a ratio

of carbene to metal salt of 1 to 2 is possible.
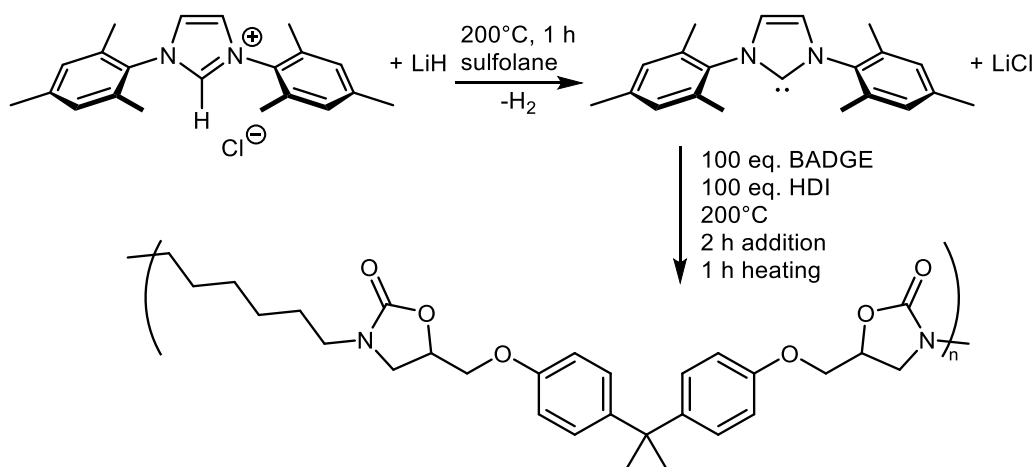
Scheme 72: *In situ* formation of the catalyst system **5u-Mes** and LiCl and subsequent monomer addition and polymerization.

Regioisomerism has an eminent impact on polymer properties. In the context of polyoxazolidin-

2-ones the substitution of the oxazolidin-2-one ring in position four or five must be discussed. A

comparison of the polymer structures with monofunctional molecules promised to be insightful.

The reaction of phenyl isocyanate with 2-(phenoxymethyl)oxirane catalyzed by **5u-Me-CO$_2$** and

LiCl was chosen to synthesize 4-(phenoxymethyl)-3-phenyloxazolidin-2-one (**4-Oxa**) and 5-

(phenoxymethyl)-3-phenyloxazolidin-2-one (**5-Oxa**) in sulfolane at 200°C in a one-pot reaction

(Scheme 73). The consumption of 2-(phenoxymethyl)oxirane was followed by GC-MS (Scheme

73). 2,5,8,11-Tetraoxadodecane was used as internal standard. The oxirane derivative was

consumed to more than 80% within the first 15 min indicating a fast reaction with the isocyanate.

Aside from oxazolidin-2-one formation 1,3,5-triphenyl-1,3,5-triazin-2,4,6-trione was observed. Its relative signals decreased with decreasing 2-(phenoxymethyl)oxirane signals. However, after 60 min it was still detected, albeit in minor concentrations. Unfortunately, one oxazolidin-2-one regioisomer (**5-Oxa**) was produced almost exclusively, thereby precluding comparison with the polymers for regioisomer determination.
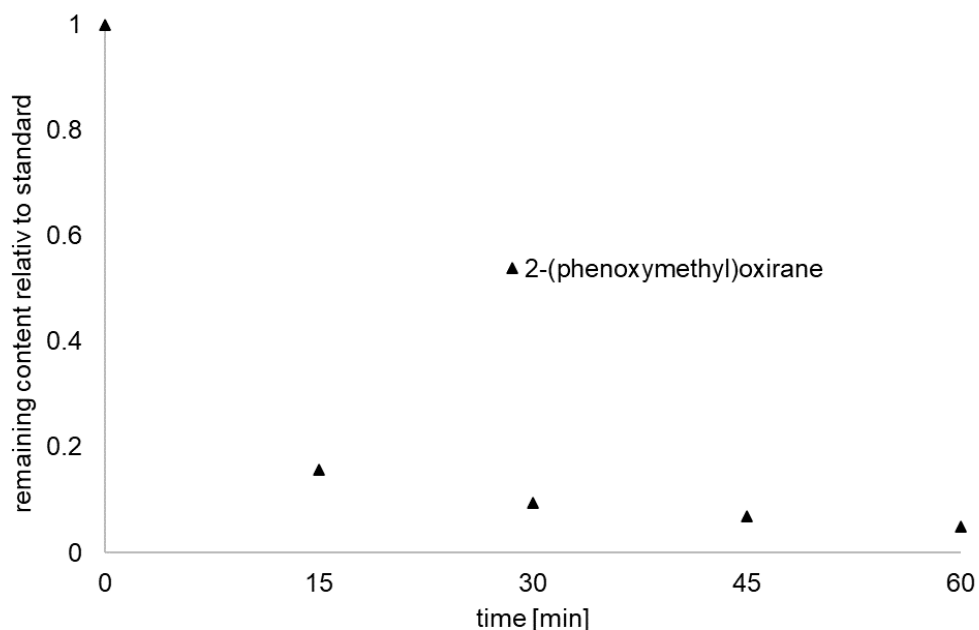
Scheme 73: Consumption of 2-(phenoxymethyl)oxirane relative to the internal standard 2,5,8,11-tetraoxadodecane in an addition reaction with phenylisocyanate. The sample at 0 min was taken directly before heating to 200°C.

Thus, **4-Oxa** and **5-Oxa** were synthesized starting from 1,3,5-triphenyl-1,3,5-triazin-2,4,6-trione and 2-(phenoxymethyl)oxirane. The used catalyst systems were either sole LiCl or sole **5u-Me-CO$_2$** or dual catalysis with both in sulfolane at 200°C (Scheme 74 and Table 11). The reaction period was extended to 4 h to ensure conventionally high conversions.
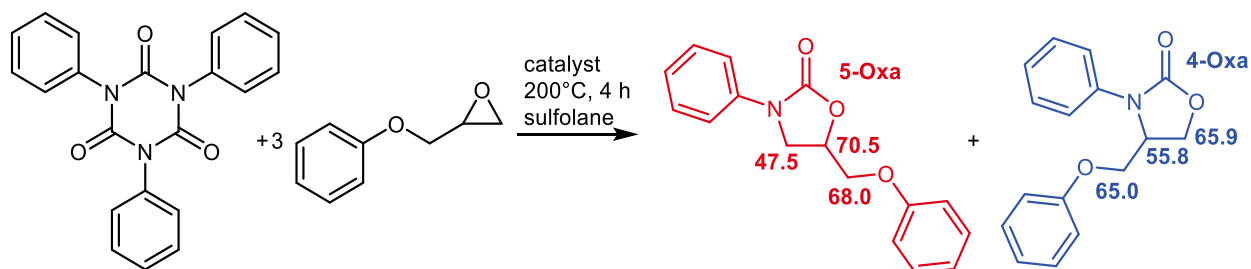
Scheme 74: Synthesis of monofunctional 4-(phenoxymethyl)-3-phenyloxazolidin-2-one (**4-Oxa**, blue) and 5-(phenoxymethyl)-3-phenyloxazolidin-2-one (**5-Oxa**, red). The ^{13}C NMR shifts of the carbon atoms originating from the oxirane are given in ppm (compare Scheme 75). The used catalytic systems are summarized in Table 11.

Table 11: Different catalytic systems employed in the production of monofunctional regioisomers according to Scheme 74.

entry	NHC	Lewis acid	formed product [%]	ratio [**4-Oxa**:**5-Oxa**]
1	-	-	<5	n.d.
2	-	LiCl (2 eq.)	65	10:90
3	**5u-Me-CO₂** (1 eq.)	-	66	9:91
4	**5u-Me-CO₂** (1 eq.)	LiCl (2 eq.)	85	12:88

The ratios of **4-Oxa** to **5-Oxa** were determined by GC-MS. Independent of the catalytic system a ratio of the regioisomers of about 1 : 9 was observed. The dual approach resulted in the highest productivity (Table 11, entry 4). After separation and isolation of **4-Oxa** and **5-Oxa** the ^{13}C NMR spectra were compared to those of the respective polymers. A magnification of the area from δ=45 to 75 ppm of the stacked spectra can be found in Scheme 75. Spectra of polymers containing an aromatic diisocyanate were measured in DMSO-d6, all other spectra were recorded in CDCl₃. POxa-BADGE-HDI, polymers from BDDGE and polymers from BADGE in conjunction with MDI or TDI, respectively, showed no signals around δ=55 ppm, which represent nitrogen-neighbored CH groups of oxazolidin-2-one moieties with a substitution at C₄. Also the signals for oxygen neighbored aliphatic carbons were very similar to those of **5-Oxa** and occur with a chemical shift of about δ=68.0 and 70.5 ppm. Hence, these polymers are

substituted at C_5 and bear only one regioisomer. In contrast, for POxa-BADGE-H_{12}MDI and POxa-BADGE-IPDI peaks around δ=69.5 or 65.0 ppm, respectively, were additionally found, suggesting formation of both, 4- and 5-oxazolidin-2-one moieties. Further, these two polymers showed downfield shifted signals for the nitrogen-neighbored carbons around δ=55.8 ppm, indicating substitution at C_4. However, no exclusive substitution at C_4 was observed, as obvious from the downfield shifted peaks for the oxygen neighbored carbon atoms, indicating C_5 substituted rings.
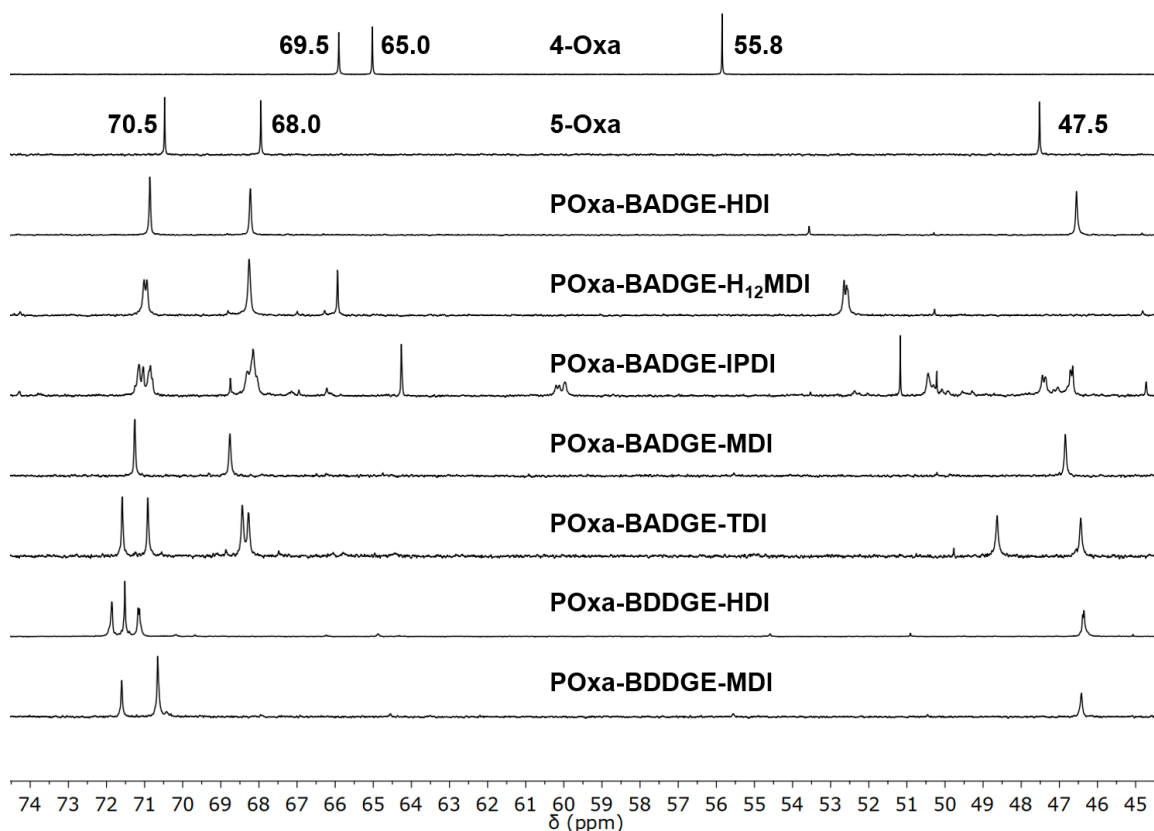
Scheme 75: Magnification of the ^{13}C NMR spectra of 4-(phenoxymethyl)-3-phenyl oxazolidin-2-one (CDCl$_3$), 5-(phenoxymethyl)-3-phenyl oxazolidin-2-one (CDCl$_3$), POxa-BADGE-HDI (CDCl$_3$), POxa-BADGE-H$_{12}$MDI (CDCl$_3$), POxa-BADGE-IPDI (CDCl$_3$), POxa-BADGE-MDI (DMSO-d6), POxa-BADGE-TDI (DMSO-d6), POxa-BDDGE-HDI (CDCl$_3$) and POxa-BDDGE-MDI (DMSO-d6). The chemical shifts for **4-Oxa** and **5-Oxa** are given in ppm.
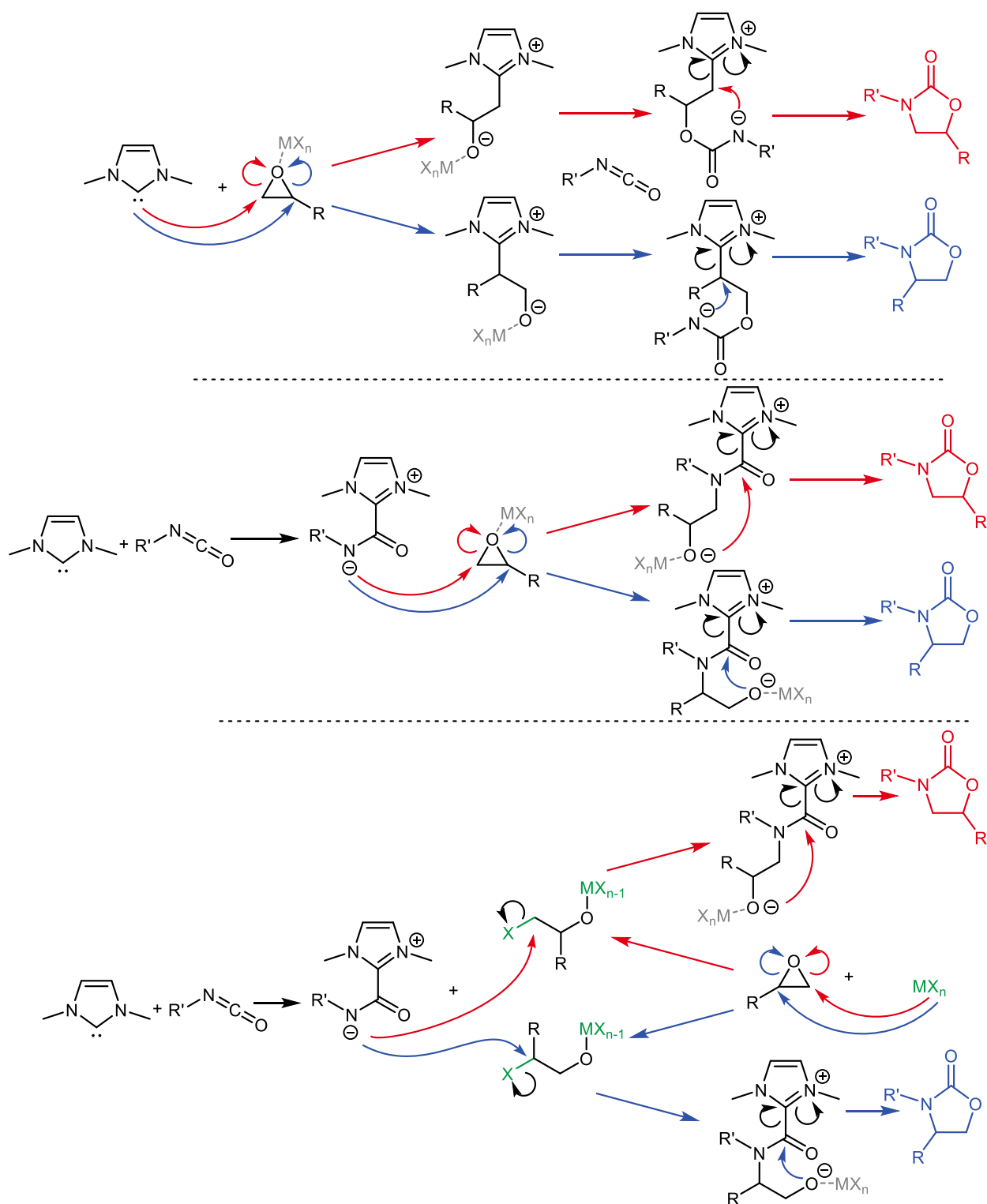
Scheme 76: Plausible NHC-catalyzed and Lewis acid-accelerated reaction pathways. Initiation at the oxirane (top) and at the isocyanate (middle) moiety are conceivable. Lewis acid ring-opening by the Lewis acid and isocyanate activation by the NHC (bottom). The red pathway leads to substitution in ring position five, the blue pathway to substitution in ring position four.

Mechanisms for the formation of oxazolidin-2-one moieties, substituted in position 4 and 5, respectively, have been discussed in the literature, however, not for NHCs serving as nucleophiles in the synthesis of polyoxazolidin-2-ones (Scheme 76). The Lewis acid (grey) is depicted in several cases as electron-withdrawing activator coordinated to the oxirane moieties or to the alcoholates formed by ring-opening as suggested by the literature (top and middle).[346] However, the oxirane ring-opening by, e.g. the halide of a Lewis acid was reported as well (green, bottom).[264, 288] In addition, the oxirane ring-opening by NHCs was described.[243-244, 396]. Trimerization must be discussed especially with regards to the differences between aromatic and aliphatic isocyanates.[118] The reaction of monofunctional phenylisocyanide and 2-(phenoxymethyl)oxirane displayed rapid consumption of the oxirane derivative although the reaction was carried out one-pot. For portionwise monomer addition to a reaction system at 200°C almost quantitative consumption of isocyanates and oxiranes and formation of oxazolidin-2-ones seems likely. The trimerization tendency is probably lower too, since the isocyanate concentration is lower at all times. Nonetheless, isocyanurate formation must not be excluded and as demonstrated by the conversion of 1,3,5-triphenyl-1,3,5-oxazine-2,4,6-trione to **4-Oxa** and **5-Oxa** small amounts will not disturb the formation of trimer-free, linear polymers. The impact of the dual approach was demonstrated not only by the higher product formation of the dual approach in trimer-opening, but even more important by the production of isocyanurate-free polymers in contrast to polymers obtained from the sole application of either the NHC or the Lewis acid. The high activity of **6-Cy-CO$_2$** in the trimerization of aromatic isocyanates and the higher trimerization tendency for aromatic isocyanates reported in the literature catalyzed by NHCs and the increased monomer addition times necessary for the isocyanurate-free polymerization of aromatic isocyanates are in accordance. Together, these findings indicate that

an initiation of the NHC at the isocyanate and subsequent trimerization take place as one pathway of the reaction, and is least pronounced for aromatic isocyanates competing with the direct addition of isocyanate and oxirane derivative. This means for aromatic isocyanates that both pathways, i.e. the direct addition and trimerization happen simultaneously and both lead to oxazolidin-2-ones although with different rates. The initial reaction is probably the betaine adduct formation from the NHC and the isocyanate (Scheme 76, middle). Whether the Lewis acid coordinates or ring-opens the oxirane moiety remains unclear. However, both result in an eased nucleophilic attack. The same considerations are valid for aliphatic isocyanates although less indicated by experimental data and trimerization seems to be less pronounced.

In conclusion, NHCs in conjunction with Lewis acids as catalytic system allowed for the preparation of isocyanurate-free, exclusively linear polyoxazolidin-2-ones. Sulfolane and 1,3-dimethylimidazol-2-one were not found to undergo side reactions with the monomers in concentrations up to 15 wt.-%. Polyoxazolidin-2-ones were synthesized successfully from two different diepoxides and five different diisocyanates. All polymers were found to be fully amorphous. The reaction setup was optimized in terms of temperature, monomer addition process and catalyst/monomer ratio. High molecular weights up to 50000 g/mol as well as acceptable molecular weight distributions were found. Copolymers of BADGE with HDI and MDI were synthesized and were also proven to be isocyanurate-free. The impact of the NHCs was investigated and a correlation between molecular weight and TEP was assumed. To lower the hurdles of applying NHCs, an approach for the application of NHC-HX salts in conjunction with metal hydrides was presented for the synthesis of POxa-BADGE-HDI. By ^{13}C NMR the regio-constitution was investigated. It was found that most POxa were substituted at C_5, however, those produced from IPDI and H_{12}MDI also contained oxazolidin-2-one rings with

substitutions at C_4. The mechanism was discussed by including the experimental data but could not be unambiguously determined.

Therefore, the application of NHCs as catalyst in conjunction with Lewis acids to produce polyoxazolidin-2-ones should be further investigated. Especially experiments on a multi-gram scale and high resolution *in situ* kinetics could contribute to elucidate the mechanism. In this context, aromatic and aliphatic isocyanates must be considered separately. Introduction of crystallinity into the polymers could possibly be achieved by the incorporation of other monomers like naphthalene-1,4-diisocyanate and improve the material properties. Further, despite the suitable solvents used, bulk polymerizations would be desirable since removing high boiling solvents is time and energy consuming.

7.3 Polyamide 6 Synthesis

Herein, the synthesis of PA6 using **5u-Me-CO₂** under the assistance of Lewis acids and activators is described. Previously, Buchmeiser *et al.* did not use any activators in their attempt to synthesize polyamide 6 in a ring-opening fashion from azepan-2-one in conjunction with latent (mostly CO_2-protected) *N*-heterocyclic carbenes.[7-9] Most of the results described in this chapter are published: H. J. Altmann, M. Steinmann, I. Elser, M. J. Benedikter, S. Naumann, M. R. Buchmeiser, Dual catalysis with an N-heterocyclic carbene and a Lewis acid: Thermally latent precatalyst for the polymerization of ε-caprolactam, *J. Polym. Sci.* **2020**, *58*, 3219-3226.[6]

Buchmeiser *et al.* discussed a correlation between the activity of latent NHC initiators and their basicity.[7-8] The starting point for comparison of the pK_a values is reasonably the pK_a of the monomer, azepan-2-one which is 27.2 in DMSO.[303, 305] Six-membered NHCs with aliphatic nitrogen substituents show pK_a values of 27 to 29 whereas imidazole-based NHCs with aliphatic side groups range from 22 to 24.[105, 107-109] For instance, the pK_a of **6-Me-H⁺** is 27.6 whereas the pK_a of **5u-Me-H⁺** is 21.5, both according to DFT calculations by Ji *et al.*[108-109] Thus, the amount of lactamate anions that initiate the chain-growth reaction, formed in mixtures of carbene and monomer, is higher for **6-Me** compared to **5u-Me** by about a factor of one million with respect to the NHC concentration. A situation as depicted in Scheme 77 is conceivable in addition to common discourse based on equilibriums. It was assumed that mostly protonated **6-Cy-H⁺** and deprotonated lactamate is formed from the reaction of **6-Cy** and AEO (bottom).[7-9] In contrast, the results of the reaction of **5u-Me** and AEO could also be proposed as an activated "proton complex" (top). However, the huge excess of AEO monomer over the initiator, which is used in the polymerization reactions will contribute to force the equilibrium to the right side of the equation, either with separated charges or in an activated state.
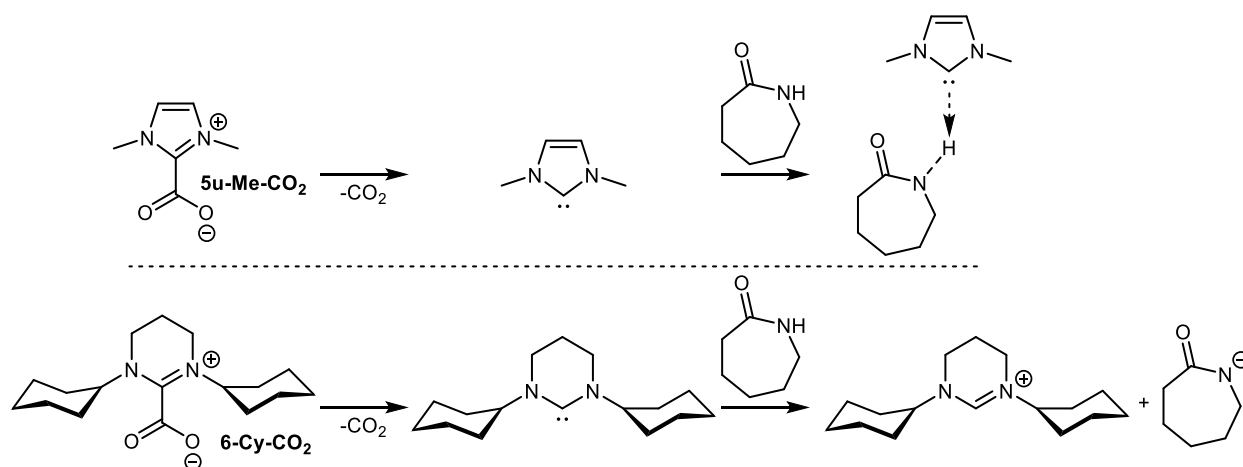
Scheme 77: Conceivable difference between **6-Cy** being predominantly protonated by AEO (bottom) and in contrast **5u-Me** activating the monomer (top).

As a consequence of the reduced basicity of **5u-Me** (especially with respect to most polymerization active **6-Cy**) a further activation of the reactants was necessary in order to apply **5u-Me-CO₂**. However, for comparison reasons, two initial reactions were conducted applying sole **5u-Me-CO₂** as initiator of interest and sole **6-Cy-CO₂** as benchmark. In the literature the ratio of AEO : **6-Cy-CO₂** was 160 : 1 and the reaction run for 45 min at 180°C producing 85% yield.[7] Here, the monomer : NHC ratio was 100 : 1, the temperature was 200°C and the reaction period 1 h. Rapid solidification and quantitative yield resulted for the reaction with **6-Cy-CO₂** after a workup that included dissolving of the polymer in methanoic acid (1 to 3 days, 4 to 12 mL/g_polymer), precipitation from propan-2-one (30 to 150 mL/g_polymer), centrifugation at 4500 rpm for 15 to 99 min, decanting the supernatant solution and drying under reduced pressure. With **5u-Me-CO₂**, however, only an increased viscosity of the reaction mixture and 17% yield were observed after workup (Table 12, entries 1 and 2). Control experiments with LiCl, MgCl₂ or 1-acetylazepan-2-one (AEO-Ac) without **5u-Me-CO₂** did not lead to the formation of polymer (entries 3 to 5). In contrary, the combined use of **5u-Me-CO₂** and LiCl resulted in an increased productivity expressed by an increased yield of 33% (entry 6). The most obvious explanation would be an increased electrophilicity of the carbonyl carbon of the attacked

monomer by coordinating the Lewis acidic LiCl, easing both initiation and chain-growth. This effect was exploited further if three or even five equivalents of LiCl were used in the experiments yielding 52 or 58%, respectively (entries 7 and 8). An upper limit for the productivity enhancement by further addition of LiCl is reached at around ten equivalents of LiCl and 60% yield (entry 9). 72% polymer were isolated if 100 equivalents monomer were treated with each 1 equivalent of **5u-Me-CO$_2$**, LiCl and AEO-Ac (entry 10). When compared to entry 6 (1 equivalent NHC and 1 equivalent LiCl) the addition of the acetylated monomer resulted in a more than doubled polymer yield. This is all the more interesting since a combination of an NHC and activator without any Lewis acid resulted in no productivity (entry 11), probably due to terminating side reactions with the activator. However, AEO converted with MgCl$_2$ and **5u-Me-CO$_2$** resulted in the formation of PA6 in 37% yield (entry 12). Further increased MgCl$_2$ equivalents, in contrast to LiCl, resulted in lower polymer yields (entries 13 to 15). One explanation is the formation of stable NHC-MgCl$_2$ complexes preventing polymerization or slowing down the reaction velocity. Another explanation is the more pronounced formation of **5u-Me-HCl** by simultaneous formation of MgCl-AEO, showing a decreased reactivity in the absence of activators. Although both explanations are also applicable when only 1 equivalent of MgCl$_2$ is added to the reaction mixture, increased MgCl$_2$ concentration are expected to have a higher impact. Deduced from the isolated polyamide 6 yield the combination of **5u-Me-CO$_2$**, AEO-Ac and MgCl$_2$ results in the highest yields (entry 16).
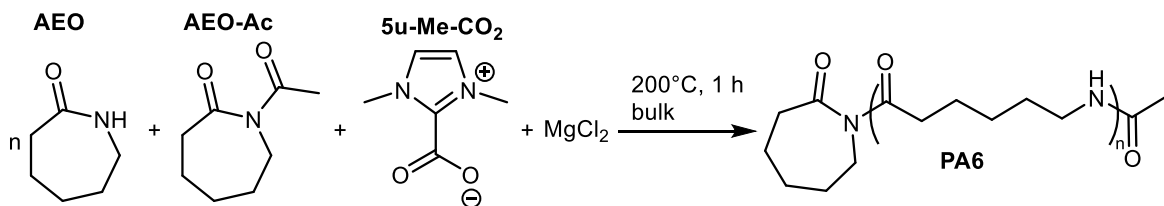
Scheme 78: Bulk polymerization of azepan-2-one to PA6 at 200°C applying **5u-Me-CO$_2$**, MgCl$_2$ and AEO-Ac as initiator and activators, respectively.

Table 12: Polymerizations of azepan-2-one at 200°C, reaction time 1 h. All substances were mixed in a 4 mL glass vial equipped with a magnetic stir bar. The vial was sealed and injected to a pre-heated metal block with drill holes place on a magnetic heating plate.

entry	NHC-CO$_2$ ([eq.])	Lewis acid ([eq.])	AEO-Ac [eq.]	AEO [eq.]	yield [%]
1	6-Cy-CO$_2$ (1)	-	-	100	>96
2	5u-Me-CO$_2$ (1)	-	-	100	17
3	-	LiCl (1)	-	100	<1
4	-	MgCl$_2$ (1)	-	100	<1
5	-	-	1	100	<1
6	5u-Me-CO$_2$ (1)	LiCl (1)	-	100	33
7	5u-Me-CO$_2$ (1)	LiCl (3)	-	100	52
8	5u-Me-CO$_2$ (1)	LiCl (5)	-	100	58
9	5u-Me-CO$_2$ (1)	LiCl (10)	-	100	60
10	5u-Me-CO$_2$ (1)	LiCl (1)	1	100	72
11	5u-Me-CO$_2$ (1)	-	1		<1
12	5u-Me-CO$_2$ (1)	MgCl$_2$ (1)	-	100	37
13	5u-Me-CO$_2$ (1)	MgCl$_2$ (3)	-	100	<5
14	5u-Me-CO$_2$ (1)	MgCl$_2$ (5)	-	100	<5
15	5u-Me-CO$_2$ (1)	MgCl$_2$ (10)	-	100	6
16	5u-Me-CO$_2$ (1)	MgCl$_2$ (1)	1	100	≥96

All substances were mixed in a 4 mL glass vial equipped with a magnetic stir bar. The vial was sealed and injected to a pre-heated metal block with drill holes place on a magnetic heating plate.

In order to gain a better understanding of the activation caused by the interaction of MgCl$_2$ and AEO-Ac, both substances were combined in a mixture of CH$_2$Cl$_2$ and THF. After the solvents were removed under reduced pressure, a colorless solid was obtained, which was dissolved in CD$_3$CN and submitted to NMR analysis. Scheme 79 shows the reaction mixture as well as the magnified carbonyl area of the ^{13}C NMR spectra of AEO-Ac (black) and the formed product [AEO-Ac-Mg-Cl$_2$] (red). The downfield shifted signals of [AEO-Ac-Mg-Cl$_2$] compared to the signals of AEO-Ac indicate a reduced electron density at the carbonyl carbons of the complex. An increased electrophilicity is the consequence which, in this case, goes along with an enhanced

reactivity in this case. This conclusion can further be underpinned with previous findings concerning the lactamolytic and the ion-coordinative mechanism as outlined in the introduction (chapter 6.5 Polyamide 6 Synthesis).[291, 294]
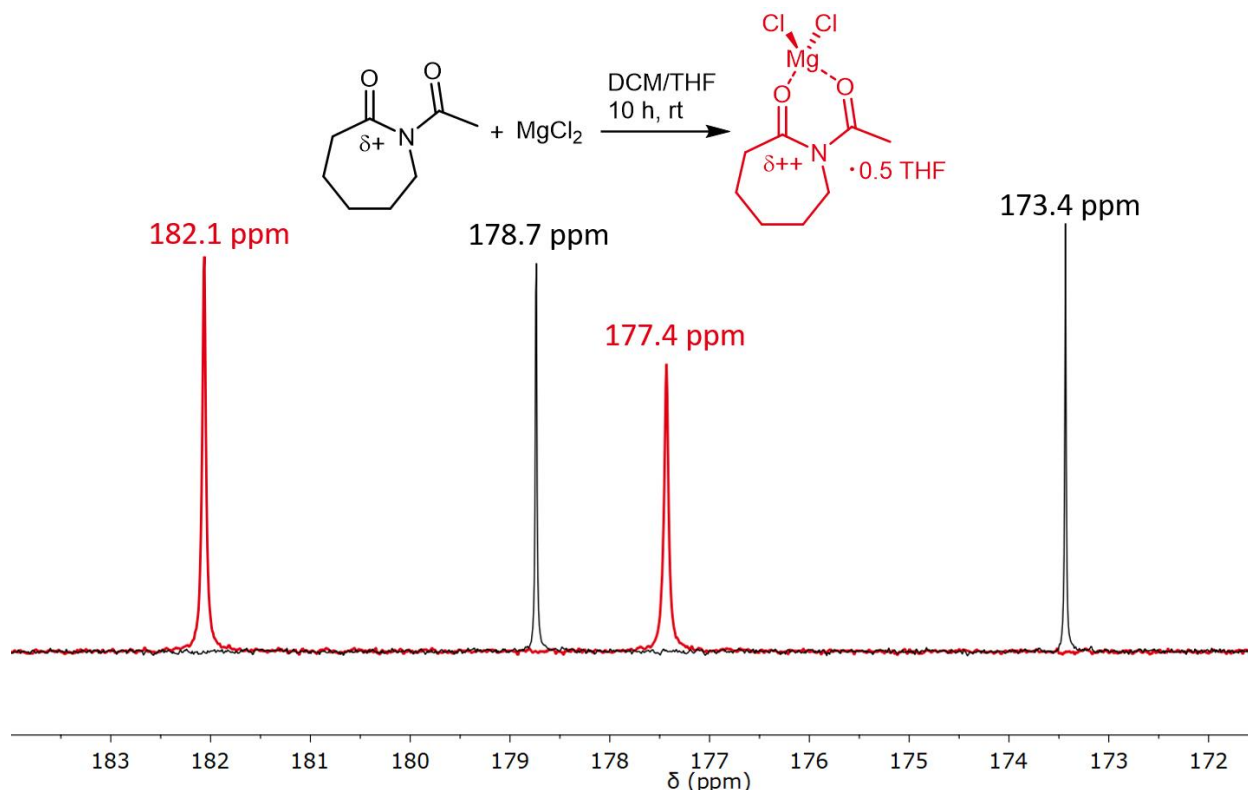
Scheme 79: Reaction of AEO-Ac and MgCl$_2$ to the corresponding complex [AEO-Ac-MgCl$_2$] (in red) with half an equivalent of THF (top). Comparison of the carbonyl area of the ^{13}C NMR spectra of AEO-Ac in black and [AEO-Ac-MgCl$_2$] in red recorded in CD$_3$CN (bottom).

The mixtures for the polymerization reactions in Table 12 were weighed into the same glass vial and then exposed to the reaction temperature (200°C) to form a homogeneous solution in the molten AEO before solidifying due to polymer formation (in cases of high yields). Before polymerization these mixtures were not homogenized. With respect to stoichiometry, heterogeneous mixtures cannot be divided into multiple smaller polymerization samples or at least some inaccuracies in the composition must be expected. Aiming at the formation of a truly homogeneous, latent polymerization system, the reaction mixture was homogenized by dissolving NHC, MgCl$_2$ and AEO-Ac in molten AEO without initiating the polymerization. The

latent behavior was enabled by latent **5u-Me-CO$_2$**. In contrast to previous experiments (Table 12), the monomer : catalyst system ratio was increased to 500 : 1. NHC, MgCl$_2$, AEO-Ac and AEO were weighed in and stirred for >1 h at 75°C until all substances were dissolved in the molten monomer. The resulting homogeneous solution was allowed to cool to ambient temperatures, upon whicha colorless solid was formed, and stored inside the glove box. This mixture was polymerized in small portions after different time periods of 1, 3 and 9 days as well as after 3 months. Quantitative yields were found in all cases after heating the polymerization system to 200°C for 1 h as summarized in Table 13.

Table 13: Experiments with a latent polymerization system for polyamide 6 synthesis homogenized at 75°C for >1 h and polymerized at 200°C within 1 h.

entry	**5u-Me-CO$_2$** [eq.]	MgCl$_2$ [eq.]	AEO-Ac [eq.]	AEO [eq.]	time[a]	yield [%]
1	1	1	1	500	1 day	≥96
2	1	1	1	500	3 days	≥96
3	1	1	1	500	9 days	≥96
4	1	1	1	500	3 month	≥96

[a] time between homogenization and polymerization, in the meantime the mixtures were stored inside the glove box (N$_2$, ambient temperature).

These latent polymerization systems proved to be stable as solid at ambient temperatures and in the absence of air. Quantitative yields were also isolated if the monomer content was increased to 1000 equivalents with respect to the catalyst system consisting of **5u-Me-CO$_2$**, MgCl$_2$ and AEO-Ac. Moreover, a latent mixture stored as liquid at 75°C (above the melting point of AEO) for five days with increased catalyst system loading (200 eq. AEO to each 1 eq. of **5u-Me-CO$_2$**, MgCl$_2$ and AEO-Ac) were investigated. After five days at 75°C the mixture was found to be slightly turbid. Again, samples were taken from the ready to use mixture and polymerized at different temperatures (160, 180 and 200°C, Table 14, entry 4). In addition, prehomogenized polymerization systems with 100, 200 and 400 equivalents monomer loading were prepared and

converted to PA6 at the same temperatures (Table 14, entries 1 to 3). Furthermore, prehomogenized polymerization systems with monomer loadings of 100 equivalents were prepared but in contrast to the above-mentioned reactions reacted under ambient atmosphere (Table 14, entry 5). The solidification times are summarized in Table 14. In some cases the relative viscosities were additionally determined (entries 1 to 3).

Table 14: Solidification times in minutes of PA6 polymerization reactions of 1 g prehomogenized systems conducted at different temperatures, with different loadings and different reaction conditions. Solidification times of 0.5 g in square brackets, relative viscosities, in round brackets, are referring to solidification values without brackets.

entry	AEO[a]	160°C[b]	180°C[b]	200°C[b]
1	100	6 [4] (2.04)	3 [2] (2.10)	2 [2] (2.19)
2	200	7 [6] (2.75)	4 [3] (2.84)	3 [3] (2.65)
3	400	10 [7] (3.10)	6 [5] (2.94)	5 [4] (3.27)
4[c]	200	7 [5]	4 [3]	4 [3]
5[d]	100	10	8	5

[a] amount of AEO relative to each 1 equivalent **5u-Me-CO$_2$**, MgCl$_2$ and AEO-Ac; [b] polymerization temperature; [c] the homogenized polymerization mixture was stored 5 days in liquid state at 75°C; [d] polymerized under ambient atmosphere.

Comparison of the results in entries 1 to 3 in Table 14 show increasing solidification times with decreasing temperatures and increasing monomer loadings. This is unsurprising since increased reaction times must be expected for lower reaction temperatures and higher monomer loadings. The relative viscosities increased with increasing monomer loadings and indicate higher molecular weights as per equivalent of initiator more equivalents of monomer are available, which results in longer polymer chains. It must be noted that solidification times are (reaction) mass sensitive within the given reaction setup because a given quantum of energy per gram (or mole) is necessary to increase the temperature of the mixture (heat capacity) and an amount of time is needed to transport the energy into the system. This is illustrated by the solidification times in square brackets (0.5 g sample mass) if compared to those without brackets (1 g sample

mass). In addition, 1 g of a polymer system based on 200 equivalents with respect to the catalyst system was reacted at 140°C and a solidification time of 12 min was observed. Melting points of the polyamides synthesized e.g. at 200°C were 218°C for 100 equivalents, 219°C for 200 equivalents and 220°C for 400 equivalents. The values were determined as average of the second and third heating cycle in DSC with a heating rate of 10 K/min. Although these values show a tendency that goes along with what would be expected from the molecular weights the small differences between the melting points must not be overinterpreted. Despite the observation of minor turbidity for the polymerization systems after storage at 75°C for 5 days (Table 14 entry 4), in all cases a colorless, clear and homogeneous solution was observed before solidifying. In comparison, the solidification times did not differ significantly, accordingly no major changes of the polymerization system led to expected while being stored in the liquid state at 75°C, underlining the latency of the catalyst system (Table 14, entry 2). This is further strengthened by the solidification times found for 0.5 g (Table 14 entry 4 square brackets), which show the same behavior as the mixture stored as solid (Table 14, entry 2). In conjunction with the low viscosity of the AEO melt this finding offers access to potential applications for the polymer system where extended pot live times are beneficial, like liquid composite molding (LCM) or thermoplastic resin transfer molding (T-RTM).[398-399] The experiments summarized in entry 5 in Table 14 were conducted as follows: The homogeneous mixtures were molten and stirred at 75°C before the screw caps of the vials were removed and the reaction mixtures were exposed to ambient atmosphere. Without any delay the vials were placed in an aluminum heating block (on a magnetic stirrer) preheated to the respective reaction temperature to induce the polymerization. Clearly the solidification times increased compared to the reactions executed under inert gas atmosphere. When compared to entry 1 (Table 14) where the same monomer to

catalyst system ratio was used the time to solidify roughly doubled for all three temperatures. The effect is attributed to the uptake of water from ambient humidity, which partially quenches the activated monomers or anions, respectively. Nonetheless, quantitative conversion of the monomer deduced from quantitative yields were observed underlining the robustness of **5u-Me-CO₂** also in comparison to **6-Cy-CO₂** and other terahydropyrimidine-based carbenes and their precursors.

GPC measurements were conducted for PA6 received from two reactions at 200°C (1 h). The first polymer was synthesized from a mixture consisting of 100 equivalents AEO, 1 equivalent **5u-Me-CO₂**, 1 equivalent $MgCl_2$ and 1 equivalent AEO-Ac and displayed a number-average molecular weight of 59 kg/mol and a polydispersity of 1.9 (theoretical molecular weight 11 kg/mol). The second polymer was received from the polymerization of 500 equivalents AEO, 1 equivalent **5u-Me-CO₂**, 1 equivalent $MgCl_2$ and 1 equivalent AEO-Ac. The molecular weight was determined to 238 kg/mol with a polydispersity of 2.1 (theoretical molecular weight 57 kg/mol). The stark deviation from the theoretical molecular weight can be explained to some extent by the calibration of the GPC column versus polystyrene having a structure that is very different from PA6. The factor between 238 and 59 kg/mol is 4 whereas the monomer : initiator ratio was increased by a factor of 5. The uncomplete translation of the monomer : initiator ratio into molecular weight cannot be attributed to the GPC system again; instead, a certain degree of transamidation must be expected, too, present for all polymerizations but pronounced at higher monomer loadings. On the whole, a molecular weight increase must be noted with increasing monomer loading, as observed in conjunction with the relative viscosities.

Commercially available activators are often based on (di)isocyanates or their addition products with azepan-2-one. As described in the introduction (6.5 Polyamide 6 Synthesis) isocyanate-

based activators also result e.g. for Na-AEO in faster polymerization reactions than AEO-Ac.[294] The structures of HDI-AEO$_2$ and MDI-AEO$_2$, which were used in due course, are depicted in Scheme 80.
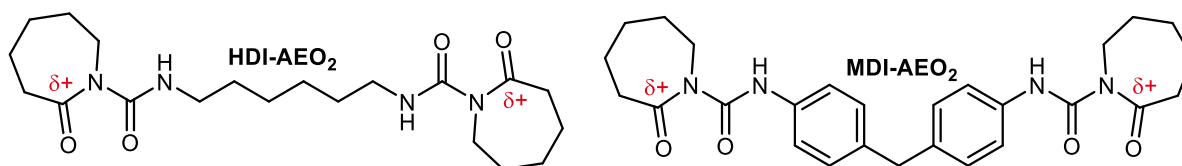
Scheme 80: Chemical structure of the diisocyanate based activators HDI-AEO$_2$ an MDI-AEO$_2$.

Mixtures of 300 equivalents monomer were mixed and homogenized at 75°C each with 1 equivalent **5u-Me-CO$_2$**, MgCl$_2$ and 1 equivalent of either HDI-AEO$_2$ or MDI-AEO$_2$ (Table 15). The observed solidification times for 140, 160 and 180°C were comparably long and in the range from 21 to 73 min compared to the solidification times of 7 and 6 min at a temperature of 200°C, respectively.

Table 15: Solidification times of prehomogenized (75°C) PA6 polymerization systems consisting of 300 equivalents AEO, 1 equivalent **5u-Me-CO$_2$**, 1 equivalent MgCl$_2$ and 1 equivalent of either HDI-AEO$_2$ or MDI-AEO$_2$, respectively, at different temperatures.

entry	activator	140°C	160°C	180°C	200°C
1	HDI-AEO$_2$	73	35	26	7
2	MDI-AEO$_2$	55	25	21	6

In all cases where diisocyanates were applied as activators, workup was hampered by low solubility of the resulting polymers in methanoic acid. Polymer solubility decreased with increasing reaction temperature, probably due to very high molecular weights. An argument pointing towards high molecular weights is the activator structure that in principle allows chain-growth at both ends. However, the more suitable, but speculative explanation is tremendous crosslinking by side reactions. It must also be assumed that dissolution within several weeks in

methanoic acid did not result in a true solution of the polymerization product but rather in bond breaking either of the amide or the formed crosslinkages. Noteworthy, swelling was very pronounced for the majority of the samples and the synthesized polymers were able to take up ≥ 30 mL$_{\text{methanoic acid}}$/g$_{\text{polymer}}$ while becoming gelly. It is questionable whether the diisocyanate-AEO$_2$ adducts form complex structures with MgCl$_2$ comparable to [AEO-Ac-MgCl$_2$].

This question must be addressed in the future along with various others, like the influence of the NHC to activator ratio. Further it is interesting to investigate if shorter solidification times are accessible under preservation of the molecular weight by increasing the amount of NHC while keeping the amount of activator constant. Another issue to tackle are the end-groups of the resulting polymer namely the cyclic imide formed in the last insertion and the acetyl group moiety on the other side since both are difficult to address in chain-extension reactions.

To sum up, the successful application of **5u-Me-CO$_2$** in conjunction with Lewis acids and activators in PA6 synthesis was accomplished. ^{13}C NMR downfield shifts of the carbonyl signals of [AEO-Ac-MgCl$_2$] compared to AEO-Ac show the beneficial influence of the Lewis acid resulting in increased electrophilicity and higher reactivity. MgCl$_2$ is assumed to shift after each nucleophilic, ring-opening attack to the newly formed imide end-group, thereby providing constant activation throughout the reaction. Latency and storability of the prehomogenized polymerization systems over days in the liquid state and over months in the solid state were demonstrated. Also, solidification times at various temperatures, monomer to catalyst ratios under ambient atmosphere were determined. Molecular weights were found to be mainly influenced by the monomer to catalyst ratio.

Additionally, an initial contribution to the flame retardancy of PA6 was developed with the benefit of combining activator and flame retardancy. Flame retardancy can be provided in various ways. One is the integration of phosphorus, offering several modes of action regarding flame suppression.[400-401] Beneficially fire protection is integrated covalently, which among other things leads to better wash fastness compared to non-covalently bound flame retardants. The design strategy follows the idea to combine activator and flame retardant by substitution of the acetyl group of AEO-Ac by a phosphorus-containing group (Scheme 81).
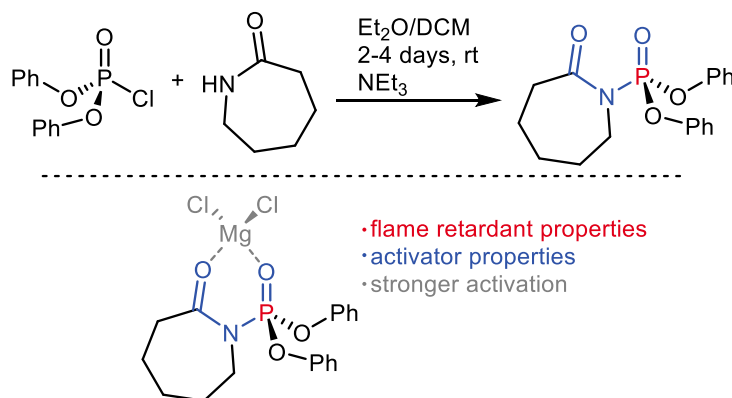
Scheme 81: Synthesis (top) and modes of action (bottom) of AEO-P(O)(OPh)$_2$.

The simple one-step synthesis manipulating the most accessible group of the AEO molecule under mild conditions comes with a disadvantage. The phosphorylated molecule can only be incorporated to the polymer in the initial step. Due to the missing substituted proton no deprotonation and consequently no nucleophilic attack can be expected from this flame retardant. Nonetheless, it is designed precisely for this purpose (Scheme 81 bottom, where additionally the coordination by MgCl$_2$ is indicated). The hypothesis was investigated by ^{13}C NMR spectroscopy where a chemical shift of 178.4 ppm was found for AEO-P(O)(OPh)$_2$, which is very close to the carbonyl shift of AEO-Ac at 178.7 ppm. Further, the flame retardant was used in polymerization reactions (Scheme 82).
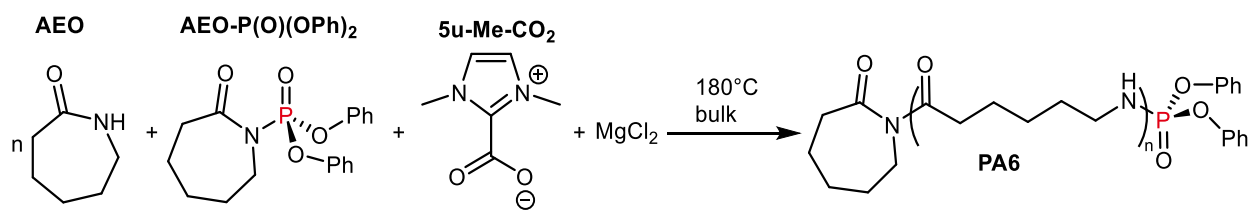
Scheme 82: Synthesis of PA6 with incorporated flame retardant.

The polymerization system consisting of 100 equivalents AEO, 1 equivalent **5u-Me-CO₂**, 1 equivalent AEO-P(O)(OPh)₂ and 1 equivalent $MgCl_2$ was prehomogenized at 90°C overnight and subsequently polymerized at 180°C for 4 h. However, no solidification at reaction temperature was observed. After cooling to ambient temperature and workup the workup cycle was repeated in order to remove any non-covalent by bound phosphorus. The phosphorus content of the isolated polymer was investigated by ^{31}P NMR spectroscopy. For these purposes a defined amount of P(O)(Ph)₂(Mes) was mixed as reference with a defined amount of the polymer, dissolved in D_2SO_4 and submitted to NMR analysis (Scheme 83). The signal at δ=-7.81 ppm belongs to the polymer, the signal at δ=-15.06 ppm to the reference. An average of two measurements revealed a phosphorus content of 0.275 wt.-% which is close to the maximum content calculated from the starting material composition of 0.266 wt.-%. Although this analysis method is not absolutely accurate, the presence of covalently incorporated phosphor was proven, thereby opening the field for future investigations.
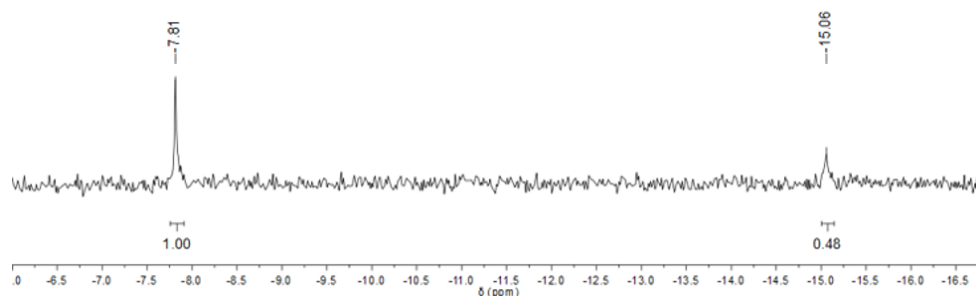

Scheme 83: ^{31}P NMR of the phosphorus containing polymer and P(O)(Ph)₂(Mes) in D_2SO_4.

7.4 Spirocyclic NHC Precursors

In this chapter the synthesis of 1,3-dicyclohexyl-6,9-dimethyl-1,3,6,9-tetraazaspiro[4.4]non-7-ene-2,4-dione (**5u-Me-(OCN-Cy)₂**) and application as initiator for anhydride-hardened epoxide resins and PA6 synthesis is discussed. Although the polymerizations initiated by NHCs were discussed in the former chapters (7.1 Anhydride-hardened Epoxide Resins and 7.3 Polyamide 6 Synthesis), the application of an isocyanate-protected carbene offers many new possibilities and reaction pathways. The content of this chapter was majorly published: H. J. Altmann, W. Frey, M. R. Buchmeiser, A Spirocyclic Parabanic Acid Masked *N*-Heterocyclic Carbene as Thermally Latent Pre-Catalyst for Polyamide 6 Synthesis and Epoxide Curing, *Macromol. Rapid. Commun.* **2020**, e2000338.[10]

In the previous chapter (7.2) on polyoxazolidin-2-ones the question arose whether the initiation reaction catalyzed by an NHC initially attacks the isocyanate or the oxirane moiety under ring-opening (a comparable issue appears for epoxides and anhydrides). Both, attack on the isocyanate and attack on the oxirane, result in betaines as discussed above. Building on related studies on the interaction of NHCs and isocyanates the spirocyclic **5u-Me-(OCN-Cy)₂** (Scheme 84) was isolated.[45, 181, 192-196, 199-202]
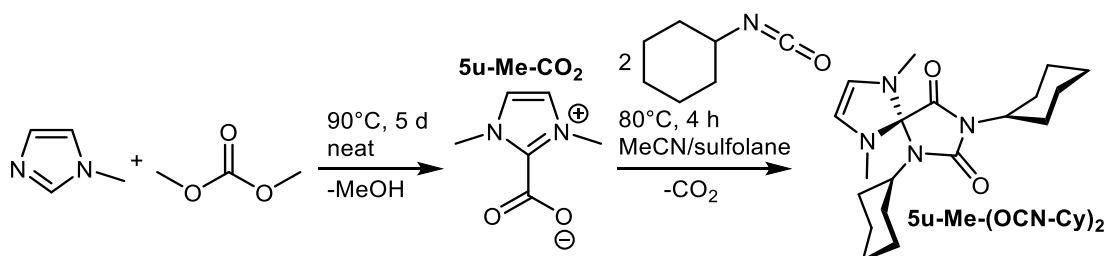

Scheme 84: Synthesis of **5u-Me-CO₂** and **5u-Me-(OCN-Cy)₂**.[3]

5u-Me-(OCN-Cy)₂ was synthesized in a simple approach from **5u-Me-CO₂** and cyclohexyl isocyanate in a mixture of MeCN and sulfolane at elevated temperatures. The intense red

reaction mixture was extracted with pentane, resulting in a biphasic mixture. The pentane extracts were collected, filtered over celite and concentrated before the product was crystallized from pentane in the freezer. The yellow crystals were isolated and the structure determined by proton and carbon NMR as well as single crystal X-ray structure analysis. Although different solvents were used for ^{1}H NMR spectroscopy of **5u-Me-CO$_2$** (D$_2$O) and **5u-Me-(OCN-Cy)$_2$** (C$_6$D$_6$) a comparison of the chemical shifts seems worthwhile. For **5u-Me-CO$_2$** the signal in the ^{1}H NMR spectrum corresponding to the imidazolium ring backbone appears at δ=7.38 ppm, the one for the methyl groups at δ=3.99 ppm whereas for **5u-Me-(OCN-Cy)$_2$** the imidazole backbone signals can be found at δ=5.21 ppm and the methyl groups at δ=2.33 ppm. The high field shift of **5u-Me-(OCN-Cy)$_2$** compared to **5u-Me-CO$_2$** is caused by the absence of the cationic charge located in the former imidazolium ring. In ^{13}C NMR the backbone signals are moderately shifted to high field from δ=123.1 ppm (**5u-Me-CO$_2$**, D$_2$O) to δ=116.6 ppm (**5u-Me-(OCN-Cy)$_2$**, C$_6$D$_6$). The CO$_2$-protected carbenoid C$_2$ carbon for **5u-Me-CO$_2$** shows a signal at δ=139.9 ppm, the spirocyclic central carbon of **5u-Me-(OCN-Cy)$_2$** is strongly shifted to high field to δ=101.7 ppm. This is a remarkably downfield signal for a sp^3 carbon, caused, aside from the spirocyclic nature, by three neighboring electronegative nitrogen atoms. **5u-Me-(OCN-Cy)$_2$** crystallizes in the monoclinic space group *P2$_1$/c* with the unit cell dimensions a=1909.01 pm, b=691.33 pm, c=1466.25 pm, α=90°, β=99.127° and γ=90° (Scheme 85). The NCN angle of the imidazole moiety was determined to 107.15° and 103.35° for **5u-Me-CO$_2$** and **5u-Me-(OCN-Cy)$_2$**, respectively.[3] **5u-Me-CO$_2$** displays a torsion angle of 29° between C$_2$ and CO$_2$, whereas the two planes of the spirocycle are almost orthogonal to each other. However, the release of **5u-Me** from **5u-Me-(OCN-Cy)$_2$** probably proceeds stepwise from the spirocycle via the monoisocyanate-protected NHC to the free carbene, thus the torsion angle of the intermediate

152

would be more interesting. From the literature an almost orthogonal torsion angle was reported for the adduct of 1,3-dimethylbenzimidazol-2-ylidene and benzoyl isothiocyanate (see introduction 6.2.4).[201] In addition, the formation of a double-isocyanate protected carbene from an aliphatic isocyanate fits the trimerization experiments with isocyanates in chapter 7.2 Polyoxazolidin-2-ones.
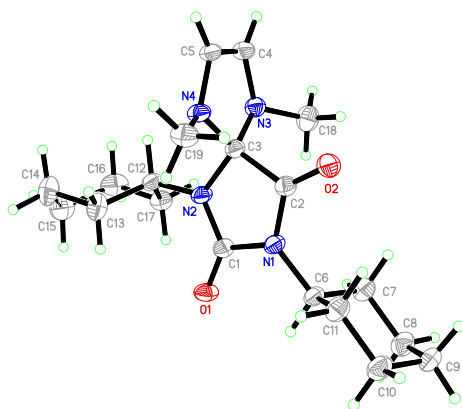
Scheme 85: Plot of the crystal structure of **5u-Me-(OCN-Cy)₂**.

From the literature and previous investigations, each two diepoxides and anhydrides were selected to perform epoxide curing experiments by DSC (Scheme 86).[2, 4]
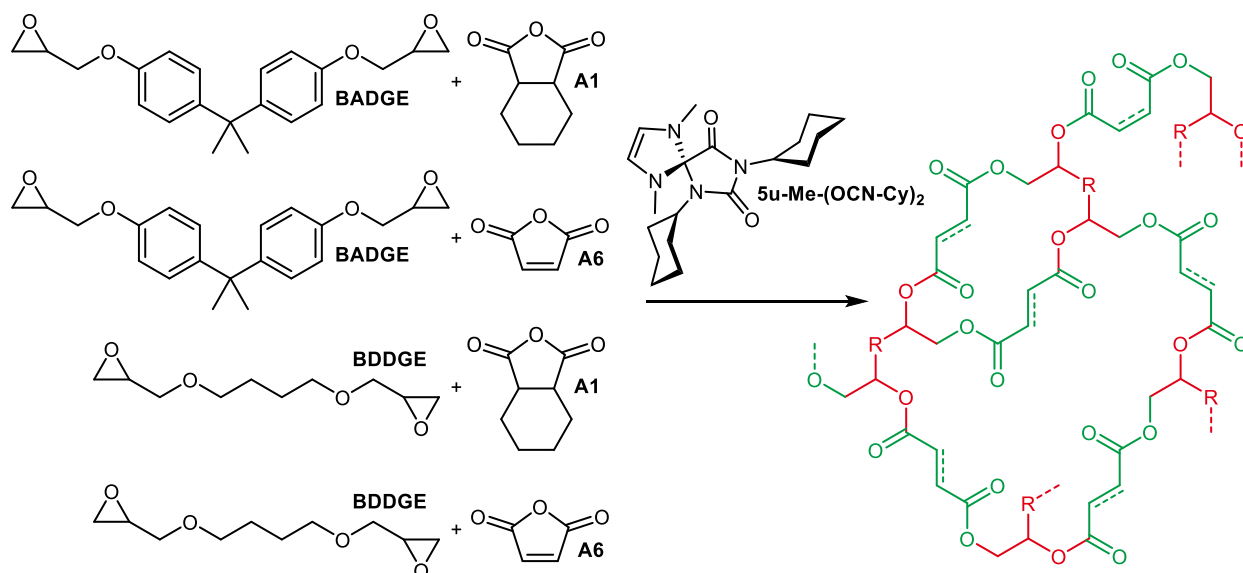
Scheme 86: Anhydride-hardened epoxide curing reaction initiated by **5u-Me-(OCN-Cy)₂**. Former epoxide groups in the generalized product are colored red, anhydrides green.

153

For the experiments the epoxide and anhydride compound were combined and homogenized (up to 60°C if necessary) before the precursor was added at room temperature and stirred until a homogeneous solution resulted. Ratios of 100 equivalents diepoxide, 200 equivalents of anhydride and 8 equivalents **5u-Me-(OCN-Cy)₂** were weighed in. Mixtures containing compound A1 remained colorless or became slightly yellowish, mixtures containing A6 became reddish or brown.

Table 16 summarizes the curing experiments with **5u-Me-(OCN-Cy)₂** and offers a comparison to the curing experiments executed with **5u-Me-CO₂** with the same monomers. T_{max} values for **5u-Me-CO₂** ranged broadly from 125 to 152°C. In contrast for **5u-Me-(OCN-Cy)₂** a narrower distribution from 131 to 144°C was found. Further, for the latter initiator T_{max} values decreased for experiments containing A6 whereas for A1 the opposite behavior was observed. Although the differences are small it is interesting that this trend seemingly goes along with the anhydride applied. On the contrary, the amount of released energy seems to be mainly connected to the diepoxide. Full curing can be assumed due to the similar reaction enthalpies that were measured during curing for both initiators and no additional energy releases were found in subsequent control cycles.

Table 16: Comparison of the released energies (ΔH) and temperatures of maximum of energy release (T_{max}) for **5u-Me-CO₂** and **5u-Me-(OCN-Cy)₂**. Molar ratio: diepoxide:anhydride:initiator 100:200:8.

entry	monomers	5u-Me-(OCN-Cy)₂		5u-Me-CO₂	
		T_{max} [°C]	ΔH [J/g]	T_{max} [°C]	ΔH [J/g]
1	BADGE/A1	140	-281	125	-279
2	BADGE/A6	141	-301	152	-263
3	BDDGE/A1	144	-395	131	-400
4	BDDGE/A6	131	-390	142	-399

Isocyanates are problematic due to their impact on human health and the environment. Therefore, some considerations on the whereabouts of the isocyanates after the release of carbene and cyclohexyl isocyanates are summarized and discussed in the following (Scheme 87). Katritzky *et al.* found the single isocyanate-protected carbene and 1 equivalent of released isocyanate at 70°C.[202] For higher temperatures, the free carbene and 2 equivalents of isocyanate were observed. The same reaction path is assumed here (Scheme 87, top). Formation of isocyanurates (cyclic isocyanate trimers) in the presence of NHCs as reported by Louie *et al.* but was not described by Katritzky and is unlikely for aliphatic derivatives.[118, 202] However, free NHC is available for the initiation of the anhydride epoxide curing reaction. Another possible initiation pathway starts from the single isocyanate-protected carbene. A nucleophilic attack at the oxirane ring results in the formation of a betaine with the positive charge located at the imidazolium ring and an alkoxide. Two possible reaction pathways can occur. First, an intramolecular ring-closing reaction that results in the release of a free carbene, ready to initiate the curing reaction, and an oxazolidin-2-one. In case of a monoepoxide this would be a non-addressable chain-end, for diepoxides the crosslinkage density might be slightly reduced. Second, an anhydride is incorporated and the anhydride-hardened epoxide curing reaction proceeds. In a downstream step the carbene can be released by a nucleophilic attack of an alkoxide and thus fixate the isocyanate stronger in the macromolecular structure. Further, growing chain-end alkoxies attack free isocyanates and incorporate them into the polymer structure. However, from a stoichiometric point of view, an excess of oxirane moieties over anhydrides is needed or either isocyanate or anhydride remain unreacted in the mixture.
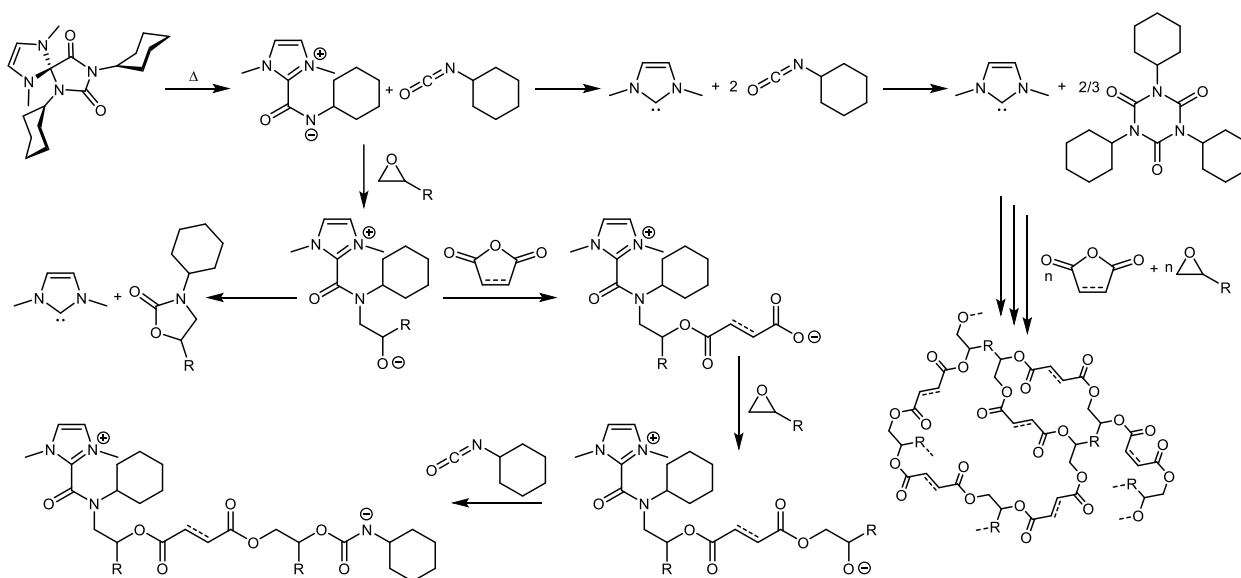
Scheme 87: Various conceivable reaction pathways for anhydride-hardened epoxide resins cured by **5u-Me-(OCN-Cy)₂**.

As described in chapter 7.3 the synthesis of polyamide 6 was achieved from pre-homogenized (75°C) mixtures. These were consisting of **5u-Me-(OCN-Cy)₂**, the monomer azepan-2-one (AEO), AEO-Ac and MgCl₂ (Table 17, entries 1 to 3). In addition, one experiment containing 2 equivalents of cyclohexyl isocyanate and 1 equivalent **5u-Me-CO₂** was executed (entry 4). All reactions were heated for 1 hour to 180°C to ensure quantitative conversion.
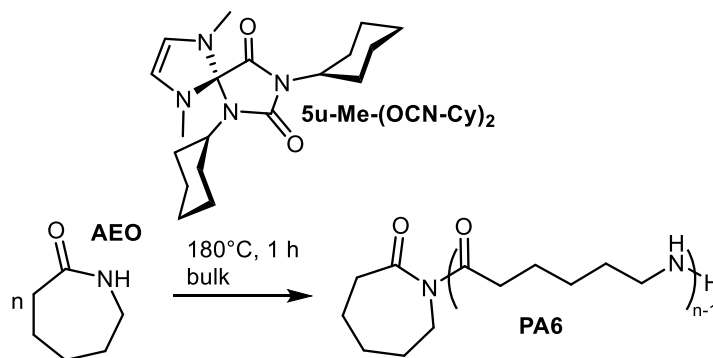
Scheme 88: Polyamide 6 synthesis initiated by **5u-Me-(OCN-Cy)₂**. The use of different activator is not depicted.

Table 17: Composition of PA6 polymerization mixtures, solidification times and T_m. (samples were homogenized at 75°C before polymerization at 180°C for 1 h).

entry	AEO [eq.]	5u-Me-(OCN-Cy)$_2$ [eq.]	MgCl$_2$ [eq.]	AEO-Ac [eq.]	5u-Me-CO$_2$ [eq.]	Cy-NCO [eq.]	solidification time [min]	T_m [°C]	yield [%]
1	250	1	1	1	-	-	3	208	≥96
2	250	1	1	-	-	-	9	215	≥96
3	250	1	-	-	-	-	7	211	≥96
4	250	-	-	1	1	2	3	205	≥96

Rapid solidification was found for all experiments (Table 17). Solidification times are in the same range as observed for experiments in chapter 7.3. Remarkably, the solidification time in the entries 1 and 4 are shorter than in the entries 2 and 3. This is attributed to adduct formation of released isocyanates with the monomers. This assumption is strengthened by the literature-known synthesis of *N*-cyclohexyl-2-oxoazepane-1-carboxamide from an addition reaction of AEO and cyclohexyl isocyanate.[302, 307-308] In the formed adduct, electron density is withdrawn from the carbonyl carbon within the AEO ring. Consequently, an increased electrophilicity eases the nucleophilic attack followed by ring-opening. The adduct of cyclohexyl isocyanate and AEO acts as activator. Noteworthy, the sole use of **5u-Me-(OCN-Cy)$_2$** leads to good polymerization results as well (entry 3). Solidification times are increased but still below 10 min in all experiments (Table 17). In contrast, sole application of **5u-Me-CO$_2$** did not result in quantitative polymer yields although a higher loading of 100 to 1 AEO to initiator was used. This further strengthens the assumption of AEO and cyclohexyl isocyanate adduct formation. The reason for the extended solidification time for the reaction in entry 2 (Table 17) must be MgCl$_2$. Whether a complex comparable to [AEO-Ac-MgCl$_2$] is formed or if other conceivable side reactions are responsible remains speculative (Scheme 89, bottom). Isocyanate adducts of AEO are commonly used as activators even without Lewis acid. In addition, the melting points (T_m), determined at 30 K/min, do not differ greatly but again values in entries 1 and 4 are lower than in entries 2 and 3 (Table 17), which is a possible consequence of lower molecular weights resulting from a higher molar amount of activators which act as chain-starter. The resulting polymer with end-groups is depicted in Scheme 89 (middle).
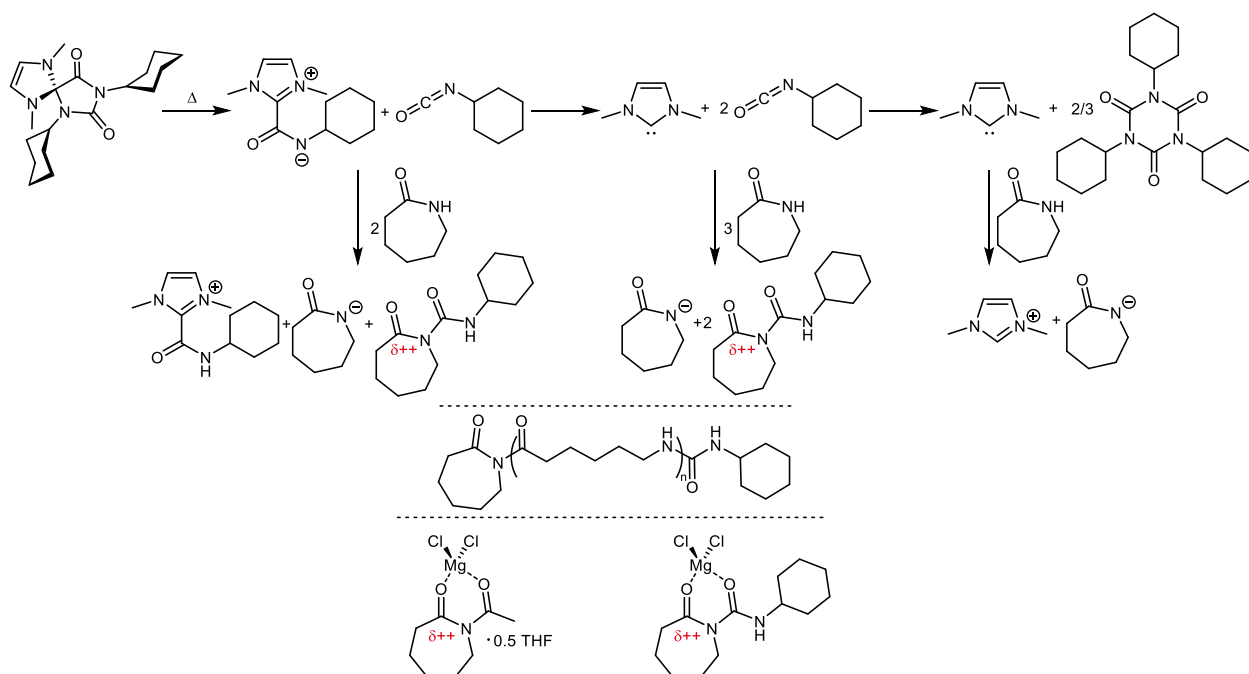
Scheme 89: Various conceivable reaction pathways for polyamide 6 synthesis initiated by **5u-Me-(OCN-Cy)₂**. The adducts of AEO and cyclohexyl isocyanate are used as activators (top).[302, 308] Isocyanurate formation is unlikely. Polymer structure with the end-groups after initiation at *N*-cyclohexyl-2-oxoazepane-1-carboxamide is depicted (middle). The structure of [AEO-Ac-MgCl₂] and the conceivable pendant of the isocyanate adduct are also depicted.

The synthesis of a new double-isocyanate protected NHC precursor from accessible and inexpensive educts was shown and the structure solved by NMR spectroscopy and single crystal X-ray structure analysis. The latent initiator was applied for the curing of anhydride-hardened epoxide resins as well as for polyamide 6 synthesis. Although satisfying reaction behavior, like latency, solubility, high activity and presumably beneficial activator formation were observed mechanistic details remain unsolved.

Again, the synthesis of linear polyester from monoepoxides and anhydrides is expected to be beneficial to clarify the curing mechanism and shed light on the structure responsible for the initiation as well as the fate of the isocyanate protecting groups. Low molecular weight polymers (degree of polymerization <10) would allow for a detailed end-group structure analysis. In a first step the shift of isocyanates moieties from **5u-Me-(OCN-Cy)₂** to AEO could be observed in

reactions with a molar ratio of one equivalent **5u-Me-(OCN-Cy)₂** to two equivalents AEO. Moreover, double-isocyanate protected NHCs as latent initiators find limited attention. This is probably due to the simultaneous release of carbene and toxic isocyanates and potential side reactions. However, as demonstrated, a thoughtful application might lead to harmless and even beneficial reactivities. Therefore, the synthesis of **5u-Me-(OCN-Cy)₂** should be optimized and extended to other NHCs and isocyanates. The solvent mixture, the concentration and the temperature program could be improved. Probably synthesis in a less polar solvent under reflux conditions would be a suitable approach since the solubility of **5u-Me-(OCN-Cy)₂** is, due to its neutral character, high in apolar solvents whereas **5u-Me-CO₂**, and other NHC carboxylates, are commonly soluble in polar media. Instead of extraction of **5u-Me-(OCN-Cy)₂** and subsequent crystallization only filtration and removal of the solvent and other volatiles under reduced pressure could lead to the final product. Direct synthesis of **5u-Me-(OCN-Cy)₂** could further be achieved *in situ* within selected monomers (monoepodixes for examples) serving as solvent.

7.5 Oligomerization of 4-Methyloxetan-2-one to Diols

The synthesis of difunctional oligoesters of 4-methyloxetan-2-one (4MO) catalyzed by titanium(IV) alkoxides is discussed in this chapter. The particular reactivity of 4MO must therefore be recapitulated. The ring strain of 4MO is -59.2 kJ/mol.[335] Therefore 4MO, depending on the catalyst or initiator used, can be polymerized in a ring-opening fashion by either O-acyl cleavage or O-alkyl cleavage.[301] The active chain-end after O-acyl cleavage is an alkoxide (or alcohol), after O-alkyl cleavage the active chain-end is a carboxylate (or carboxylic acid) (Scheme 90). Although polymerizations of 4MO proceeds via anionic, cationic and metal-insertion mechanisms, depending on the catalyst or initiator used, the ring-opening fashion (O-acyl or O-alkyl cleavage) is not predetermined by the catalyst or initiator class.[301, 354-355, 365, 371-373] For example, aluminum alkoxides polymerize 4MO by O-acyl cleavage whereas the polymerization catalyzed by aluminum chlorides proceeds via O-alkyl cleavage.[301, 331, 369] Crotonate formation can occur after O-alkyl cleavage by elimination of the initiator and after O-acyl cleavage by elimination of water.[301] In addition, thermally-induced crotonic acid formation from 4MO was reported. In terms of polymer chemistry, crotonate-like end-group represent non-addressable chain-ends, which are not accessible for further monomer incorporation.
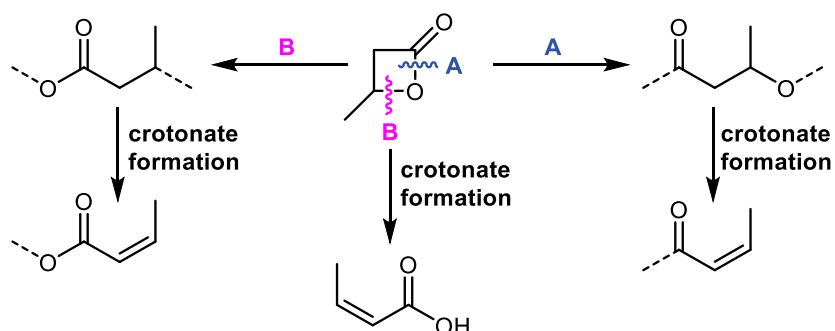

Scheme 90: O-acyl cleavage (A, blue) and O-alkyl cleavage (B, pink) were observed in ring-opening polymerizations of 4MO. Crotonate formation is one of the most important side reactions of 4MO polymerizations.

Within this project special attention was devoted on the following goals.

- synthesis of polymers from 4-methyloxetan-2-one via O-acyl cleavage

- realization of low molecular weights (5 to 20 repeat units)

- formation of α,ω-dihydroxy telechelic products

- high end-group fidelity (avoidance of elimination and acid formation)

- control over the molecular weight

- realization of a solvent-free approach

- demonstration of copolymerizability with other difunctional monomers

The content of this chapter is majorly published: H. J. Altmann, M. R. Machat, A. Wolf, C. Gürtler, D. Wang, M. R. Buchmeiser, Synthesis of dihydroxy telechelic oligomers of β-butyrolactone catalyzed by titanium(IV)-alkoxides and their use as macrodiols in polyurethane chemistry, *J. Polym. Sci.*, **2021**, *59*, *3*, 274-281.[11]

A ratio of 4MO : butanediol (BDO), serving as initiator, of 10 : 1 (Scheme 91) was chosen to synthesize α,ω-dihydroxy telechelic oligomers with a number-average molecular weight of approximately 1000 g/mol (Scheme 91). 0.1 equivalents of Ti(OiPr)$_4$ were added as catalyst (4MO:BDO:Ti(OiPr)$_4$ 100:10:1). Ti(OiPr)$_4$ was selected for initial polymerization experiments due to its high electrophilicity and commercial availability. The reaction was carried out at 60°C as bulk polymerization and was monitored by NMR and THF-GPC for 5 h. To determine conversion the monomer signal at δ=4.7 ppm and the product signal at δ=5.3 ppm were monitored by ^{1}H NMR spectroscopy.
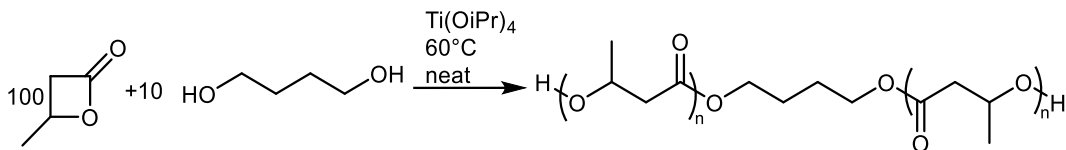
Scheme 91: Oligomerization of 4MO with BDO to a dihydroxy telechelic oligoester.

A continuous increase of product over time up to a conversion of 91% after 5 h with no crotonate formation (5.8 ppm) at any stage and a molecular weight of 900 g/mol ($Đ_M$=1.47) was found. At earlier stages of the reaction, conversion of 58% (2 h) and 76% (3 h) lower molecular weights of 600 ($Đ_M$=1.11) and 800 g/mol ($Đ_M$=1.18), respectively, were found. Next, for further investigations the starter diol was changed. In most cases, (2-hydroxyethyl)ether (DEG) and for some experiments 1,2-di(2-hydroxyethoxy)ethane (TEG) were used. In order to optimize the reaction, a temperature screening was conducted. Again, reactions were executed in bulk. After 2 hours the reactions were stopped and the product submitted to NMR analysis. A magnification of the stacked spectra is shown in Scheme 92. The red area highlights the olefinic region for crotonate-like structures (as known from a literature comparison).[402] No crotonate derived resonances were found for reaction temperatures of 80 and 100°C whereas at 120 and 140°C small amounts of elimination and thus crotonate formation occurred. Although the crotonate signals wereminor (~1:100 relative to the proton at the tertiary carbon) they must be noted since they represent the end-groups that are not addressable for further ring-opening or step-growth polymerizations.
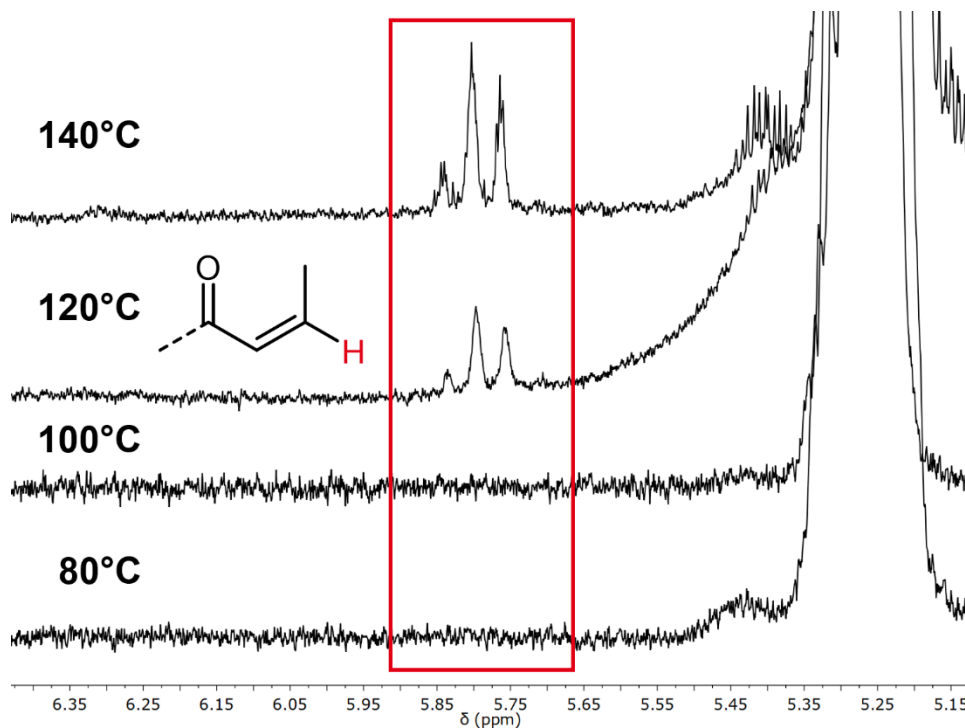
Scheme 92: Stacked ^{1}H NMR spectra of oligomerizations of 4-methyloxetan-2-one and DEG at various temperatures (CDCl$_3$). The red labeled area shows the proton signal that occurs after hydroxide elimination.

In a subsequent optimization step the catalyst : monomer : initiator ratio was investigated with the goal to reduce catalyst loading. This was combined with reactions at different temperatures. Additionally, the acid values were determined by titration with NaOH. The acid value in industrial application is given in milligram KOH that are necessary to neutralize the carboxylic acid groups of one gram of the sample. Here, the value is given in µmol/g. Further, the monomer to initiator ratio was varied to determine the impact on the molecular weight. Results are summarized in Table 18. The polymers synthesized at 80, 90 and 100°C, respectively, had similar molecular weights all of which were close to the theoretical molecular weight (Table 18, entries 1 to 3). The same applies to the polymer in entry 4 (Table 18) which is distinguished from entry 2 only by the different starter TEG that was used instead of DEG. An increase of monomer and initiator loading did not affect the molecular weight (Table 18, entries 5 and 6). In turn the chain length followe the monomer to initiator ratio. The higher the initiator loading, the lower

the resulting molecular weights were. The determined polydispersities were high compared to other metal complexes used for the polymerization of lactones, but not uncommon for titanium catalysts.[340, 374, 379, 381] However, comparison to literature data suffers from the different molecular weights of the synthesized polymers, which are higher in the literature. In addition, the two-fold initiator character of the diols is assumed to broaden the molecular weight distributions since the chain-growth takes place on both ends. The acid values display the concentration of possibly present carboxylic acid. These can be formed during the reaction by O-alkyl cleavage (compare introduction chapter 6.6). As described in the introduction, this is uncommon for the coordination insertion mechanism, especially for alkoxide complexes like used here. This is reflected by the low acid values that were found by titration. However, elongated reaction periods (9 h) at 80°C seemingly reduced the acid value whereas higher temperatures (100°C) over time (4 h) seemed to induce the formation of carboxylic acids, probably by transesterification. Monomer conversions >96% were found.

Table 18: Variation of the temperatures, catalyst to monomer and initiator and monomer to initiator ratio of the oligomerization reaction of 4MO.

entry	4MO:DEG:Ti(OiPr)$_4$	T [°C]	t [h]	M_n[a] [g/mol]	$M_{n, theo}$	$Đ_M$[a]	acid value[b] [µmol/g]
1	100:10:1	80	2	900	967	1.3	23
2	100:10:1	90	2	1000	967	1.4	20
3	100:10:1	100	2	1000	967	1.6	21
4[c]	100:10:1	90	2	900	1011	1.5	25
5	250:25:1	80	9	800	967	1.4	12
6	250:25:1	100	4	1000	967	1.6	37
7	100:25:1	80	2	300	450	1.2	-
8	100:17:1	80	2	400	622	1.3	-

[a] determined by THF-GPC; [b] determined by titration [µmol$_{COOH}$/g$_{oligomer}$]; [c] TEG was used instead of DEG.

The oligomers were investigated by MALDI-ToF-MS and NMR spectroscopy to elucidate the polymerstructure in detail (Scheme 93). The crude ^{1}H NMR spectra show the repeat units (b, c, d), the end-groups (a, b', c', d') and the initiator signals (e, f). No crotonate signal is visible at δ=5.8 ppm. Further, a peak labeled with g can be found which corresponds to a prop-2-yl group. Consequently, it must be assumed that the 2-propoxide ligands of the titanium catalyst at least partially initiate oligomerization. This finding is underlined by the mass spectrum (Scheme 93). Aside from the main signals caused by the dihydroxy telechelic oligoester of different chain lengths (labeled with the respective mass in several cases) a further substance was identified, which again corresponds to the oligomer initiated by the 2-propoxide ligand. The spectrum resulting from both initiators has distances between the separate peaks of 86 g/mol corresponding to the molecular mass of the monomer. This is exemplified by the peak with the mass of 903.436 g/mol. After subtraction of the cation (Na$^+$) a mass of 880.447 g/mol remains, from which again after subtraction of the initiator (DEG) a mass of 774.333 g/mol remains. This mass precisely fits the mass of nine monomer molecules.
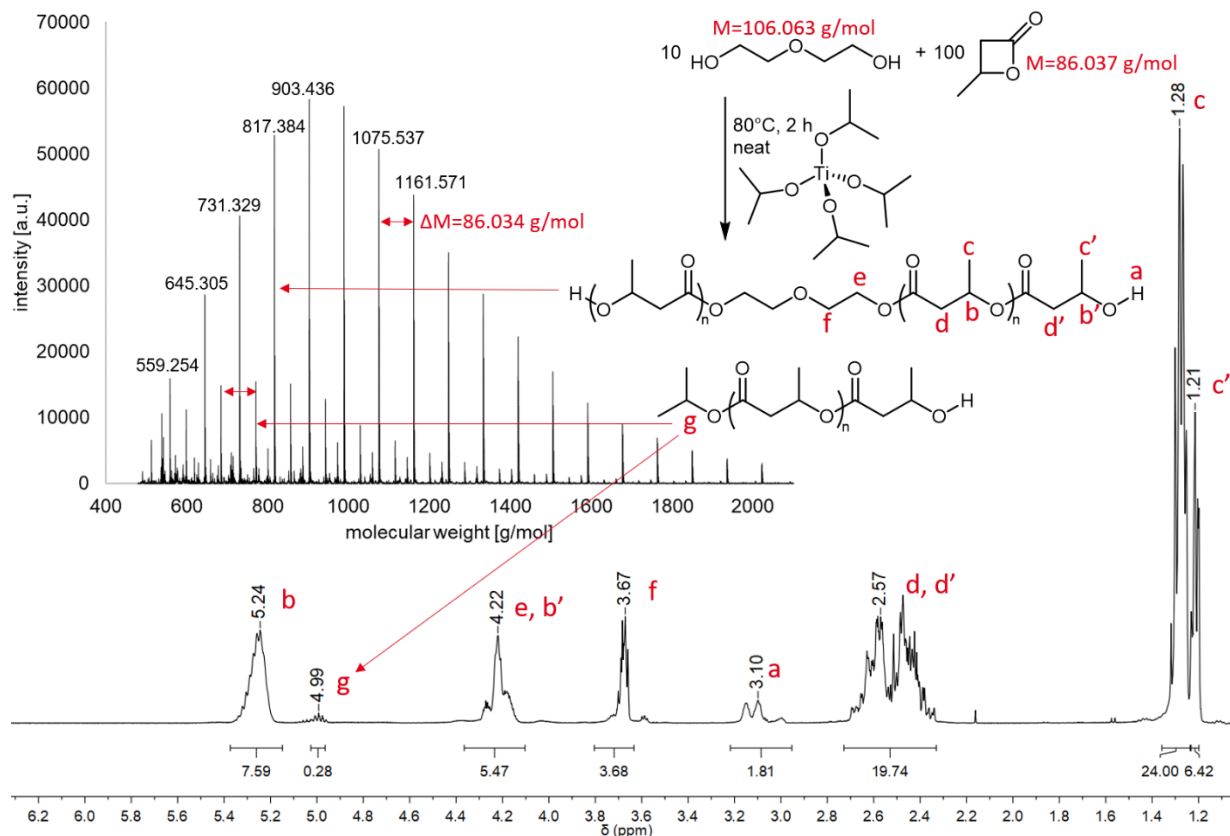
Scheme 93: ^{1}H NMR (CDCl$_3$), MALDI-ToF-MS and structure of a oligo(4MO) initiated by DEG.

To overcome the drawback of 2-propoxy end-groups a final optimization step in which the alkoxide ligands of the titanium catalysts were varied (Ti(OiPr)$_4$, Ti(OMe)$_4$ and Ti(OtBu)$_4$) and higher monomer and initiator (4MO:DEG:Ti(OR)$_4$ 500:50:1) loadings were used in conjunction with increased reaction times (Table 19). As determined by NMR spectroscopy the intensity of the signal at δ=4.99 ppm, corresponding to the 2-propoxy end-groups, was reduced by a factor of 4. Unfavorable methoxide and tertbutoxide signals are overlayed with the oligomer signals. Molecular weights found by GPC remain close to the theoretical molecular weights (967 g/mol), underlining the dependence of the molecular weight on the monomer to initiator ratio. The polydispersities are similar to those observed for higher loadings of Ti(OiPr)$_4$. Monomer conversion was quantitative for all titanium alkoxides and all oligomers were found to be

crotonate-free by NMR spectroscopy. Catalyst loadings as low as 0.2 mol-% (Table 19) resulted

in less than 1 $mg_{titanium}/g_{oligomer}$ in the final product, calculated without any workup.

Table 19: Oligo(4MO) synthesis initiated by DEG and catalyzed by titanium catalysts with different alkoxide ligands.

| entry	4MO:DEG:cat	catalyst	T [°C]	t [h]	M_n[a] [g/mol]	$Đ_M$[a]
1	500:50:1	Ti(OMe)$_4$	100	13	1000	1.6
2	500:50:1	Ti(OiPr)$_4$	100	13	1100	1.4
3	500:50:1	Ti(OtBu)$_4$	100	13	1100	1.4

[a] determined by THF-GPC.

In order to polymerize the macrodiols with diisocyanates to polyurethane, pre-experiments with

phenyl isocyanate were executed. Ti(OiPr)$_4$ was applied in conjunction with 100 equivalents

4MO and 10 equivalents DEG at 80°C for 2 h. Since phenyl isocyanate is liquid it was added

(20 equivalents) to the reaction mixture after cooling to room temperature. The molecular weight

increased to 1500 g/mol ($Đ_M$=1.7) and the hydroxyl signal in the ^{1}H NMR spectrum vanished

and new signals were found in the aromatic region (7.40, 7.29 and 7.04 ppm). Thus, for the first

polymerization experiment the liquid diisocyanate TDI was chosen. The molar ratio was

equivalent to the molar ratio of the initially applied diol for the oligomerization. Solvent-free

addition resulted in a fast, exothermic reaction and formation of a partially brownish, crosslinked

material. The reaction was repeated with TDI added as THF solution. A rapid increase in

viscosity was observed. After 4 h the reaction mixture was poured into pentane and a colorless

solid precipitated. The molecular weight of the worked up polymer was 7100 g/mol and the

dispersity 1.6 (CHCl$_3$-GPC). In the following experiments TDI was replaced by MDI since a

solvent had to be used for smoother reaction conditions as well as improved material properties

were expected. In addition, the investigations were extended to the three titanium alkoxides at

ratios of 4MO:DEG:Ti(OR)$_4$:MDI of 100:10:1:10 and 500:50:1:50 (Scheme 94).
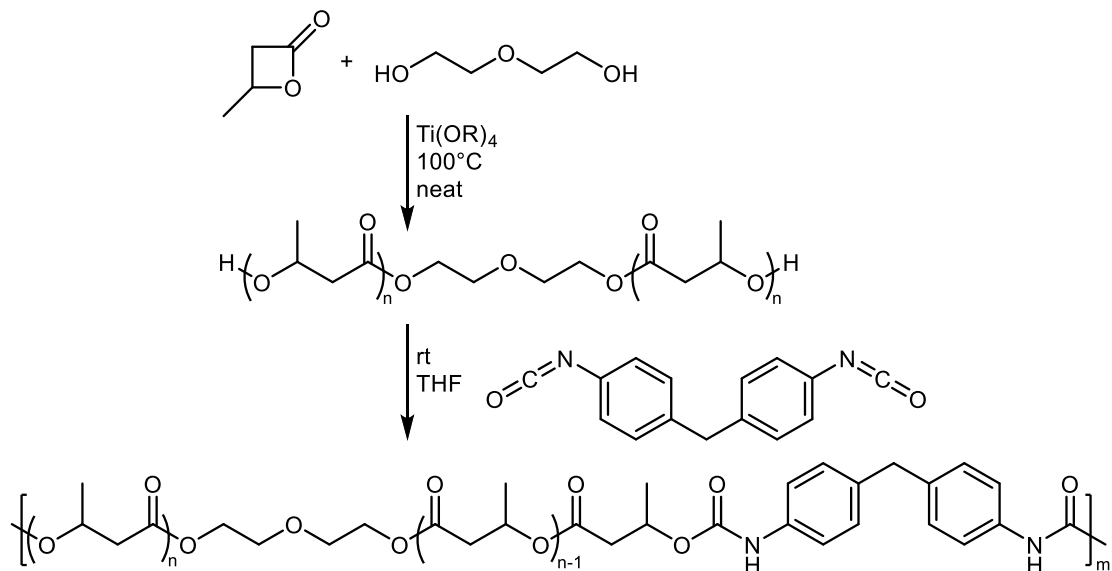
Scheme 94: Bulk synthesis of dihydroxy telechelic oligo(4-methyloxetan-2-one) and subsequent polymerization with MDI in THF.

The oligomerization reaction of 4MO initiated by DEG and catalyzed by three different titanium alkoxides at 100°C in the ratio of 100:10:1 and 500:50:1 were allowed to cool to room temperature after the appropriate reaction time of 2 and 13 hours, respectively. A THF solution containing 10 equivalents MDI was added under continued stirring and a rapid increase in viscosity was observed within 30 minutes. Note, that the polyurethane synthesis was not catalyzed by any other substance than the respective titanium catalyst applied for the ring-opening polymerization of 4MO. After 12 h the reaction solution was precipitated into pentane and a typical workup containing centrifugation, decanting the volatiles and drying was conducted. The analytical results of the reaction products are summarized in Table 20. In all cases (compare entry 1 and 2, 3 and 4 and 5 and 6, Table 20) a reduced catalyst loading in the ring-opening reaction allows for the preparation of higher molecular weight polyurethanes. Further, with Ti(OtBu)$_4$, bearing bulky tertbutoxide ligands, the highest molecular weights were found. Even the oligo(4MO) prepared with a ratio of 100:10:1 (4MO:DEG:Ti(OR)$_4$) outrivals the other catalysts at ratios of 500:50:1. Both, the higher molecular weights at lower catalyst

loading and the higher molecular weights for bulky ligands point towards a coordination insertion polymerization mechanism and ligands that are incorporated into the oligomer as observed by NMR and MALDI-ToF-MS analysis. Furthermore, a rapid exchange of titanium coordinating alkoxides must be expected, supported by the relatively narrow molecular weight distributions of the oligomers. The molecular weight distributions for the polyurethanes are similarly narrow for a polyaddition reaction. In the ^{1}H NMR spectrum the hydroxyl groups vanished again and the carbamate signals were found in the aromatic region overlayed by MDI derived signals. In addition, the signal for the proton of the tertiary carbon end-group shifted from δ=~4.2 to 5.2 ppm and the CH$_3$ end-group signal shifted from δ=1.2 to 1.3 ppm. Further, the CH$_2$ groups in-between the two aromatic moieties arise at δ=3.84 ppm.
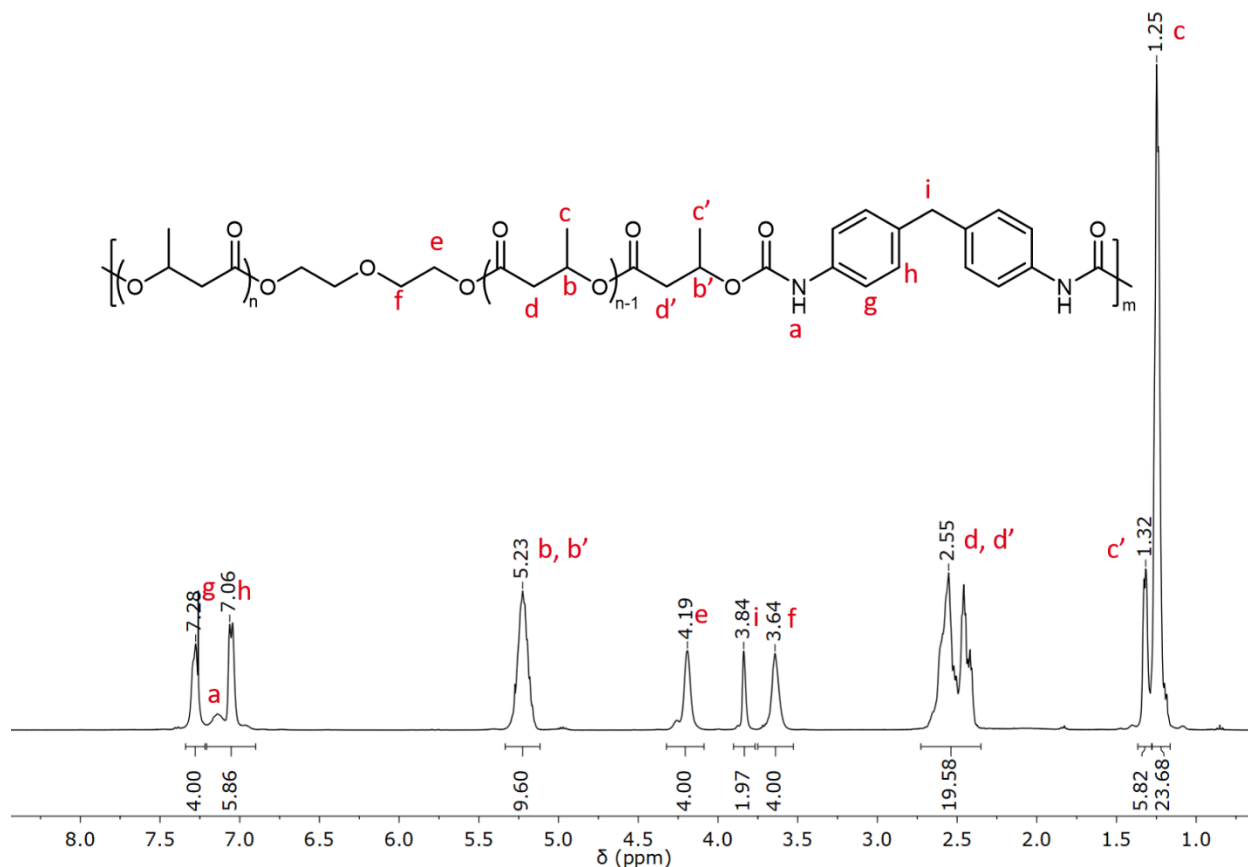
Scheme 95: ^{1}H NMR spectrum of a polyurethane synthesized from MDI and a α,ω-dihydroxy telechelic oligo(4-methyloxetan-2-one) based on DEG with structure and labeled signals.

Table 20: Polyurethanes synthesized from MDI and a α,ω-dihydroxy telechelic oligo(4-methyloxetan-2-one) based on DEG.

entry	monomer	DEG	cat	MDI	T_1/T_2 [°C]	t_1/t_2 [h]	yield [%]	M_n^a [g/mol]	$Đ_M$	DP
1	100	10	Ti(OiPr)$_4$	10	100/rt	2/12	79	8000	1.6	13
2	500	50	Ti(OiPr)$_4$	50	100/rt	13/12	90	20000	1.7	33
3	100	10	Ti(OMe)$_4$	10	100/rt	2/12	76	12000	2.2	20
4	500	50	Ti(OMe)$_4$	50	100/rt	13/12	83	20000	1.8	33
5	100	10	Ti(OtBu)$_4$	10	100/rt	2/12	82	29000	1.4	48
6	500	50	Ti(OtBu)$_4$	50	100/rt	13/12	89	53000	1.5	87

[a] determined by CHCl$_3$-GPC.

Post-reaction determination of, both the quality and quantity of the functional groups of the used monomer can be interesting e.g. in case the monomer was synthesized *in situ*. This can be

achieved after a polymerization, if the molecular weight of a polymer, and thus the degree of polymerization X_n, is determined for example by using GPC or other methods, and by transforming Carothers equation (equation 2) to r as demonstrated below in equation 3 to 6.

$$X_n = \frac{1+r}{1+r-2rp} \tag{2}$$

$$X_n + rX_n - 2rpX_n = 1 + r \tag{3}$$

$$X_n - 1 = r - rX_n + 2rpX_n \tag{4}$$

$$X_n - 1 = r(1 - X_n + 2pX_n) \tag{5}$$

$$\frac{X_n - 1}{1 - X_n + 2pX_n} = r \tag{6}$$

An example from Table 20, entry 6 is given in equation (7).

$$r = \frac{87 - 1}{1 - 87 + 2 \cdot 1 \cdot 87} = 0.98 \tag{7}$$

The ratio r allows an estimation on the monomer quality, for example dysfunctional groups i.e., the ratio of AX to AA monomers within the reaction mixture, whereby a molecule AX bears one X group that is not able to react with a B group of the BB monomer in a manner that it forms a covalent bond.

172

Table 21: Selected results from Table 20 in the same order and r calculated according to equation (7).

entry	M_n [g/mol]	$Đ_M$	DP	r
1	8000	1.6	13	0.86
2	20000	1.7	33	0.94
3	12000	2.2	20	0.90
4	20000	1.8	33	0.94
5	29000	1.4	48	0.96
6	53000	1.5	87	0.98

However, this method has some disadvantages and inaccuracies or requirements, respectively. The basic assumptions are the quantitative conversion of one of the functional groups and a satisfying yield of the isolated polymer. Further, GPC results were used to determine the number-average molecular weight, which was thenused to determine the degree of polymerization. This is not fully accurate since the GPC system was calibrated with polystyrene. For this calculation a mass of 1217 g/mol per repeat unit was assumed on the basis of the summarized mass of 1 equivalent MDI and 1 equivalent macrodiols. The latter was assumed to consist of 10 equivalents 4-methyloxetan-2-one and 1 equivalent DEG. However, these uniformity is not given for polymers with a molecular weight dispersity of >1.0. Nonetheless, these calculations can be helpful for the comparison with diols in other/future approaches.

In conclusion, α,ω-dihydroxy telechelic poly(4-methyloxetan-2-one)s were synthesized in bulk with adjustable molecular weights and high end-group fidelity in conjunction with diols. Titanium catalysts with different alkoxides were used and their impact on the polymerization was discussed. Bulky titanium tertbutyl alkoxides were found to be the most innocent. The structure of the oligomers was elucidated by NMR, IR and MALDI-ToF-MS analysis, further the

acid value was determined for some examples. Reaction parameters like time, temperature and catalyst loading were optimized. A low catalyst loading of 500 equivalents monomer per titanium tetratertbutoxide, 100°C and 13 h reaction time were found satisfying. Finally, polymerization of the macrodiols with MDI led to polyurethanes with molecular weights up to 50000 g/mol with no additional catalyst.

The developed method convinces by the simplicity and commercial availability of all chemicals used. Lower catalyst loadings are always beneficial but are of even higher importance to achieve higher end-group fidelity. The application of the metal organic framework introduced by Davidson *et al*. for the marcodiol synthesis from 4MO could be interesting for future work since the catalyst is stable at ambient conditions.[381] It must be noted that polyurethanes typically consist of hard and soft segments.[344] Thus the conducted polymerization experiments could be extended. Mixing the synthesized macrodiols with an excess of diisocyanate leads to macrodiisocyanates, which upon addition of a short chained diol (and eventually further diisocyanate) would allow for the introduction of hard segments and result in increased molecular weights.

8 Experimental Section

8.1 General

8.1.1 Characterization and Equipment

NMR spectra were recorded on a Bruker Avance III 400. For proton NMR a frequency of 400 MHz and for carbon NMR a frequency of 101 MHz was used. Chemical shifts are given in ppm relative to the solvent shifts, taken from the literature.[403-404] The topspin and MestreNova software were used. The following multiplet assignments were used: singlet (s), doublet (d), triplet (t), quartet (q), broad (b) and multiplet (m). Infrared (**IR**) spectra were recorded on a Bruker Platinum ATR spectrometer after 24 background scans. 24 scans were recorded in the range of 4000 to 400 cm^{-1} with a resolution of 4 cm^{-1}. IR spectra were analyzed using the Opus software. IR spectra are baseline corrected. Gas chromatography mass spectrometry analysis (**GC-MS**) was executed with an Agilent Technologies system consisting of a 7890A GC system, a 5975 inert MSD with Triple-Axis Detector and 7693 Autosampler. The **DMAc-GPC** system was a 1260 Infinity System from Agilent Technologies Inc. and was run at a flow rate of 0.75 mL/min. A precolumn (PolarSil 8x50 mm at 35°C) and a column (PolarSil S linear 8x300 mm) were used, together with a refractive index detector (40°C). The system was calibrated in the range from M_p 800 to 200000 g/mol with PMMA. Cirrus was used as software. **DMSO-GPC** was executed with a system consisting of a Waters 515 HPLC Pump, a Waters 2707 autosampler and a Waters 2414 Refractive Index Detector at a flow rate of 0.75 mL/min. A GRAM 8x50 mm precolumn and a GRAM LINEAR 8x300 mm were used at 35°C. The system was calibrated with PMMA samples in the range M_p 602 to 900000 g/mol. Empower 3 was used as software. The **THF-GPC** system consisted of a Waters 515 HPLC Pump, a Waters Pump Control Module II, a Waters 2707 Autosampler and a Waters2414 Refractive Index Detector and

was equipped with a SDV 3 µm 8x50 mm pre-column and two SDV 100 Å 3 µm 8x300 mm columns provided by PPS. Columns were operated at 30°C. PS standards from 162 to 7930 g/mol were used for calibrations. A flow rate of 1 mL/min was used. Empower 3 software was used. The **CHCl$_3$-GPC** system was purchased from Agilent with a 1200 Series G 1362A detector (refractive index). An SDV 5 µm 8x50 mm pre-column and three SDV 100000 Å 5 µm 8x50 mm columns, provided by PSS, were used and operated at 40°C. PS standards in the range from 200 to 1000000 g/mol were used for calibration. Software: WinGPC UniChrome. The **Cresol-GPC** system consisted of a precolumn (SDV, 20 µm, 8x50 mm 1000 Å) and an SDV, 20 µm, 8x300 mm, 10000 Å column from PSS operated at 70°C. A flow rate of 1 mL/min and calibration versus PS were applied. **DSC** measurements were executed on a Perkin Elmer Differential Scanning Calorimeter DSC 400 under a constant nitrogen flow of 20 mL/min and 50 µL pans or on a TA Instruments Q2000 and 40 µL pans. Software from Pyrris or TA Instruments was used. **MALDI-ToF-MS** (matrix-assisted laser desorption ionization time-of-flight mass spectrometry) spectra were recorded on a Bruker Autoflex III in the positive ion mode with a smart ion beam laser (337 nm). The reflector mode was used. A mixture of 20:5:2 of matrix (2,5-dihydroxybenzoic acid, 10 mg/mL), polymer (5 mg/mL) and NaOSO$_2$CF$_3$ (17 mg/mL) in THF was used to prepare the sample. MALDI-ToF-MS was executed by Dr. Dongren Wang.

Inert gas manipulations were executed using standard **Schlenk technique** or in an **MBraun glove box** filled with nitrogen. Connected to the glove box was a solvent purification system (**SPS**, MB SPS-800) from MBraun, which provided dry and degassed THF, pentane, dichloromethane, toluene and diethyl ether. A Hettich Universal 320 **centrifuge** was used to separate precipitated polymers. **Crystal structures** were measured and solved by Dr. Wolfgang

Frey from the Institute of Organic Chemistry of the University of Stuttgart. High resolution mass spectrometry (**HRMS**) was executed at the Institute of Organic Chemistry of the University of Stuttgart. Viscosities of epoxide resins were determined with a Phsica R 301 **rheometer** from Anton Paar. A Peltier element adjusted the temperature. Oscillation measurements were executed at a frequency of 1 Hz and a deformation of 10%.

### 8.1.2 Solvents, Chemicals and Materials

Deuterated solvents were purchased from Eurisotop. For use under ambient conditions deuterated solvents were used as received. For glove box use they were dried and stored over molecular sieves 0.3 or 0.4 nm. Glove box solvents (pentane, toluene, diethyl ether, THF, dichloromethane) were purchased from VWR. Solvents were degassed by passing through nitrogen and dried by passing the solvents through columns with molecular sieves and aluminum oxide. Sulfolane was purchased from abcr and dried and distilled from CaH_2 before freeze-pump-thaw degassing and storage inside the glove box. 1-Methylimidazole was purchased from abcr and used as received. Dimethyl carbonate was received from abcr and used as received. $MgCl_2$ was purchased from Merck, used as received and stored inside the glove box. LiCl was received from Grüssing, used as received and stored inside the glove box. BADGE (2,2-di-4,4'(oxiranylmethoxyphenyl)propane) for anhydride-hardened epoxide resins was received from Sigma Aldrich (D.E.R. 332) and used as received. For all other manipulations, BADGE was received from Covestro AG as colorless solid under inert gas, used as received and stored inside the glove box. 3,4-Epoxycyclohexylmethyl-3',4'-epoxycyclohexaneoate (ECHDE) was purchased from TCI and used as received. 1,4-Dioxiranylmethoxy butane (BDDGE) was purchased from TCI and used as received for synthesis of anhydride-hardened epoxide resins whereas for the synthesis of polyoxazolidinones it was dried and distilled under reduced pressure

177

from CaH$_2$ before degassing and storage inside the glove box. 2-(Phenoxymethyl)oxirane was received from TCI and used as received for anhydride-hardened epoxide resins whereas for the synthesis of oxazolidinones it was dried and distilled under reduced pressure from CaH$_2$ before degassing and storage inside the glove box. MDI was received from Covestro AG as colorless solid under inert gas, used as received and stored at -18°C under inert gas. TDI was received from Covestro AG as colorless liquid under inert gas, used as received and stored at -18°C under inert gas. HDI was received from Covestro AG as colorless liquid under inert gas, used as received and stored under inert gas. IPDI was received from TCI, distilled under reduced pressure and degassed. H$_{12}$MDI was received from TCI, distilled under reduced pressure and degassed. AEO was supplied by Brüggemann GmbH & Co. KG and used without further purification and stored inside the glove box or under an atmosphere of argon. AEO-Ac was received from Sigma Aldrich and dried over CaH$_2$ before distilling and degassing by three freeze-pump-thaw cycles. AEO-Ac was stored at ambient temperature inside the glove box over 0.4 nm molecular sieves. HDI-AEO$_2$ (Brueggolen C20P) and MDI-AEO$_2$ (Brueggolen C25) were received from Brüggemann GmbH & Co. KG, used without further purification and stored inside the glove box. 4-Methyloxetan-2-one (4MO) was purchased from TCI or Merck, dried and distilled under reduced pressure from CaH$_2$, degassed (3 freeze-pump-thaw cycles) and stored inside the glove box freezer at -35°C. (2-Hydroxyethyl) ether (DEG) was received from Sigma Aldrich, distilled under reduced pressure, dried over molecular sieves 0.4 nm overnight, filtered, degassed by 3 freeze-pump-thaw cycles and stored inside the glove box at ambient temperature. 1,2-Di(2-hydroxyethoxy)ethane (TEG) was received from Sigma Aldrich, distilled under reduced pressure, dried over 0.4 nm molecular sieves overnight, filtered, degassed by 3 consecutive freeze-pump-thaw cycles and stored inside the glove box at ambient temperature.

Ti(OMe)$_4$ was purchased from Alfa Aesar, stored and used inside the glove box at ambient temperatures. Ti(OiPr)$_4$ was purchased from Sigma Aldrich, distilled and degassed by 3 freeze-pump-thaw cycles and stored and used inside the glove box at ambient temperatures. Ti(OtBu)$_4$ was purchased from Acros Organics, stored and used inside the glove box at ambient temperatures. *N*-heterocyclic carbenes and derivatives like carboxylates and others were synthesized according to the literature and in several cases received from coworkers within the Buchmeiser group.[2, 7-8, 111-112, 120, 188] Molecular sieves 0.3 nm and molecular sieves 0.4 nm were both received from Carl Roth GmbH & Co. KG. All molecular sieves were dried *in vacuo* over night at 150°C and stored inside the glove box. Celite was received from Carl Roth GmbH and Co. KG. Before usage inside the glove box, it was dried *in vacuo* over night at 150°C.

8.1.3   5u-Me-CO$_2$

The carbene precursor **5u-Me-CO$_2$** was mainly used in this thesis why its synthesis shall be described here in advance of the following chapters. The synthesis follows a publication from 2003 with minor modifications.[3]
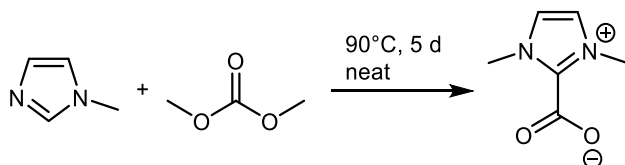
Scheme 96: Synthesis of 1,3-dimethylimidazolium-2-carboxylate (**5u-Me-CO$_2$**) from 1-methylimidazole and dimethyl carbonate.

In a 2000 mL flask equipped with a magnetic stir bar 500 g 1-methylimidazole (1 eq., 6.1 mol) were mixed with 768 g dimethyl carbonate (1.4 eq., 8.5 mol) at ambient temperatures and sealed with a stopper. The mixture was heated to 90°C. Within in a few hours a colorless precipitate formed, which increased steadily over time. After five days the reaction was cooled to room temperature. (The product mass formed did not allow for continuous stirring.) Yield: 78%
^{1}H NMR (D$_2$O, ppm): δ=7.38 (2 H, s, N-C*H*=C*H*-N), 3.99 (6 H, s, *H*$_3$C-N).

179

8.2 Anhydride-hardened Epoxide Resins

The content of this chapter is mostly published: H. J. Altmann, S. Naumann, M. R. Buchmeiser, Protected *N*-heterocyclic carbenes as latent organocatalysts for the low-temperature curing of anhydride-hardened epoxy resins, *Eur. Polym. J.* **2017**, *95*, 766-774.[4]

General procedure for the preparation, synthesis and DSC measurements of anhydride-hardened epoxide resins. The samples were weighed in inside the glove box and had a total mass of about 1 g. Then, a magnetic stir bar was added. The sample was brought outside the glove box and homogenized under constant stirring (at elevated temperatures up to 40°C if necessary) for at least 30 min. Samples of 0.5 to 10 mg were submitted to DSC. The aluminum pans used for DSC had a volume of 40 or 50 μL.

T_{max} measurements were executed by heating the sample to 20°C for 1 min before heating from 20 to 250°C applying a heat rate of 5 K/min. Isothermal measurements were executed by equilibrating the sample for 1 to 4 min at 20°C or 100°C below the final temperature. Next, the sample was heated within 1 min to the final temperature, which was kept for 20 min. Afterwards, the sample was cooled to 20°C before starting the control cycle by heating to 250°C with 20 K/min. If further energy was released during the control cycle, the area was integrated from 64 to 244.5°C.

The isothermal rheological behavior was investigated with the ai of a Phsica R 301 rheometer from Anton Paar. A Peltier element adjusted the temperature. Oscillation measurements were executed at a frequency of 1 Hz and a deformation of 10%. Measurements at 25, 45, 65 and 85°C were collected from the same sample. Recording was started at 25°C and increased stepwise to 85°C. For measurements at 120 and 140°C a fresh sample of the resin was used.

8.3 Polyoxazolidin-2-ones

Many of the results of this chapter are published: H. J. Altmann, M. Clauss, S. König, E. Frick-Delaittre, C. Koopmans, A. Wolf, C. Guertler, S. Naumann, M. R. Buchmeiser, Synthesis of Linear Poly(oxazolidin-2-one)s by Cooperative Catalysis Based on N-Heterocyclic Carbenes and Simple Lewis Acids, *Macromolecules* **2019**, *52*, 487-494.[5]

Unless otherwise noted polymerization experiments were conducted under inert gas atmosphere either inside a glove box or by using standard Schlenk technique.

8.3.1 Synthesis of POxa-BADGE-HDI

Solution 1 containing **5u-Me-CO₂** (1 eq., 0.0008 g, 0.006 mmol), LiCl (2 eq., 0.0005 g, 0.012 mmol) and sulfolane (0.5 g) was weighed into a 4 mL vial equipped with a PTFE-coated stir bar. Solution 2 consisting of BADGE (100 eq., 0.2000 g, 0.588 mmol), HDI (100 eq., 0.0988 g, 0.588 mmol) and sulfolane (1.75 g) was taken up by a syringe with a needle. Solution 2 was added within 2 h (rate of ~0.1 mL/7 min) to the stirred solution 1 at 200°C. After the addition was finished the reaction was kept at 200°C for 1 h. The orange/brownish reaction mixture was poured into propan-2-ol (35 mL) and a precipitate was obtained, which was separated by centrifugation. The supernatant solution was discarded and the remaining substance dried under reduced pressure. If necessary, the polymer was dissolved in CH_2Cl_2 and again precipitated, centrifuged, decanted and dried under reduced pressure.

Yield: 72%. M_n=32000 g/mol; DP=63; PDI=2.7. ^{1}H NMR (CDCl$_3$, ppm): δ=7.12 (4 H, d, J=8.0 Hz, $H_{arom.}$), 6.78 (4 H, d, J=8.0 Hz, $H_{arom.}$), 4.79 (2 H, s, HC-O$_{oxa\ ring}$), 4.07 (4 H, s, H_2C-O-C$_{arom.}$), 3.66 (2 H, m, H_2C-N$_{oxa\ ring}$), 3.50 (2 H, m, H_2C-N$_{oxa\ ring}$), 3.26 (4 H, s, C-CH_2-N), 1.65-1.48 (10 H, m, C(CH_3)$_2$ and N-CH$_2$-CH_2), 1.36 (4 H, s, N-CH$_2$-CH$_2$-CH_2). ^{13}C NMR (CDCl$_3$,

ppm): δ=157.7 (C=O), 156.1 ($C_{arom.\ ipso}$), 144.0 ($C_{arom.}$), 127.9 ($C_{arom.}$), 114.1 ($C_{arom.}$), 70.9 (C-O$_{oxa\ ring}$), 68.2 (C-O-C$_{arom.}$), 46.6 (C-N$_{oxa\ ring}$), 43.9 (C-CH_2-N), 41.8 (C(CH$_3$)$_2$), 31.1 (C(CH_3)$_2$), 27.2 (N-CH$_2$-CH_2), 26.1 (N-CH$_2$-CH$_2$-CH_2). IR [cm^{-1}]: 2966, 2930, 2866, 1735, 1607, 1582, 1508, 1491, 1450, 1361, 1243, 1182, 1055, 1037, 951, 828, 759, 733, 567.

8.3.2 Synthesis of POxa-BADGE-IPDI

Solution 1 containing **5u-Me-CO₂** (1 eq., 0.0008 g, 0.006 mmol), LiCl (2 eq., 0.0005 g, 0.012 mmol) and sulfolane (0.5 g) was weighed into a 4 mL vial equipped with a PTFE-coated stir bar. Solution 2 consisting of BADGE (100 eq., 0.2000 g, 0.588 mmol), IPDI (100 eq., 0.1306 g, 0.588 mmol) and sulfolane (1.75 g) was taken up by a syringe with a needle. Solution 2 was added within 2 h (rate of ~0.1 mL/7 min) to the stirred solution 1 at 200°C. After the addition was finished the reaction was kept at 200°C for 1 h. The orange/brownish reaction mixture was poured into propan-2-ol (35 mL) and a precipitate was obtained, which was separated by centrifugation. The supernatant solution was discarded and the remaining substance dried under reduced pressure. If necessary, the polymer was dissolved in CH$_2$Cl$_2$ and again precipitated, centrifuged, decanted and dried under reduced pressure.

Yield: 69%. M_n=31000 g/mol; DP=55; 1.9. ^{1}H NMR (CDCl$_3$, ppm): δ=7.10 (4 H, s, $H_{arom.}$), 6.77 (4 H, m, $H_{arom.}$), 4.76 (2 H, s, HC-O$_{oxa\ ring}$), 4.3-3.3 (8 H, m), 1.60 (7 H, s), 1.5-0.7 (14 H, m). ^{13}C NMR (CDCl$_3$, ppm): δ=159.0 (C=O, d), 156.9, 156.0, 143.9 ($C_{arom.\ ipso}$, d), 127.9 ($C_{arom.\ ortho}$, d), 114.0 ($C_{arom.}$, d), 113.9, 71.3-70.8 (m), 68.6-67.9 (m), 60.4-59.8 (m), 50.7-50.1 (m), 47.7-47.3 (m), 46.9-46.7 (m), 43.0-42.4 (m), 41.8 (C(CH$_3$)$_2$), 41.1, 39.2-38.6 (m), 38.4-37.9 (m), 35.5-35.1 (m), 32.1-31.8 (m), 31.1 (C(CH_3)$_2$), 27.7, 27.6, 24.0-23.7 (m). IR [cm^{-1}]: 2960, 1737, 1607, 1508, 1431, 1234, 1182, 1058, 1031, 951, 829, 761, 736, 694, 565.

8.3.3 Synthesis of POxa-BADGE-H$_{12}$MDI

Solution 1 containing **5u-Me-CO$_2$** (1 eq., 0.0008 g, 0.006 mmol), LiCl (2 eq., 0.0005 g, 0.012 mmol) and sulfolane (0.5 g) was weighed into a 4 mL vial equipped with a PTFE-coated stir bar. Solution 2 consisting of BADGE (100 eq., 0.2000 g, 0.588 mmol), H$_{12}$MDI (100 eq., 0.1541 g, 0.588 mmol) and sulfolane (1.75 g) was taken up by a syringe with a needle. Solution 2 was added within 2 h (rate of ~0.1 mL/7 min) to the stirred solution 1 at 200°C. After the addition was finished the reaction was kept at 200°C for 1 h. The orange/brownish reaction mixture was poured into propan-2-ol (35 mL) and a precipitate was obtained, which was separated by centrifugation. The supernatant solution was discarded and the remaining substance dried under reduced pressure. If necessary, the polymer was dissolved in CH$_2$Cl$_2$ and again precipitated, centrifuged, decanted and dried under reduced pressure.

Yield: 73%. M_n=32000 g/mol; DP=53; PDI=2.5. ^{1}H NMR (CDCl$_3$, ppm): δ=7.12 (4 H, d, J=7.4, Harom.), 6.78 (4 H, d, J=7.4, Harom.), 4.78 (2 H, m, HC-O$_{oxa\ ring}$), 4.06 (3 H, s), 3.67 (3 H, m), 3.48 (2 H, m), 1.90-0.90 (26 H, m). ^{13}C NMR (CDCl$_3$, ppm): δ=157.0, 156.1, 144.0, 127.9, 114.0, 71.0 (C-O$_{oxa\ ring}$), 68.2, 52.7-52.3 (m), 43.9, 43.5, 43.4, 42.8, 41.8 (C(CH$_3$)$_2$), 38.2, 34.3, 33.7, 32.2-31.8, 31.1 (C(CH_3)$_2$), 29.9, 29.8, 29.2-28.7 (m), 25.2-24.8 (m). IR [cm^{-1}]: 2924, 2854, 1734, 1607, 1508, 1430, 1377, 1299, 1233, 1182, 1106, 1057, 951, 902, 828, 761, 734, 700, 567.

8.3.4 Synthesis of POxa-BADGE-MDI

Solution 1 containing **5u-Me-CO$_2$** (1 eq., 0.0008 g, 0.006 mmol), LiCl (2 eq., 0.0005 g, 0.012 mmol) and sulfolane (0.5 g) was weighed into a 4 mL vial equipped with a PTFE-coated stir bar. Solution 2 consisting of BADGE (100 eq., 0.2000 g, 0.588 mmol), MDI (100 eq., 0.1470 g, 0.588 mmol) and sulfolane (1.75 g) was taken up by a syringe with a needle. Solution 2 was added within 4 h (rate of ~0.1 mL/14 min) to the stirred solution 1 at 200°C. After the

addition was finished the reaction was kept at 200°C for 1 h. The orange/brownish reaction mixture was poured into propan-2-ol (35 mL) and a precipitate was obtained, which was separated by centrifugation. The supernatant solution was discarded and the remaining substance dried under reduced pressure. If necessary, the polymer was dissolved in DMF or DMSO and again precipitated, centrifuged, decanted and dried under reduced pressure.

Yield: 71%. M_n=14000 g/mol; DP=24; PDI=2.7. ^{1}H NMR (DMSO-d6, ppm): δ=7.48 (4 H, d, J=7.4 Hz, $H_{arom.}$), 7.22 (4 H, s, $H_{arom.}$), 7.09 (4 H, br, $H_{arom.}$), 6.83 (4 H, br, $H_{arom.}$), 4.99 (2 H, s, HC-O$_{oxa\ ring}$), 4.17 (6 H, m), 3.87 (4 H, s), 1.54 (6 H, s, C(CH_3)$_2$). ^{13}C NMR (DMSO-d6, ppm): δ=156.3 (C=O), 154.6 ($C_{arom.}$), 143.6 (d, $C_{arom.}$), 137.1 ($C_{arom.\ mdi}$), 136.9 ($C_{arom.\ mdi}$), 129.5 ($C_{arom.\ mdi}$), 128.0 ($C_{arom.}$), 118.6 ($C_{arom.\ mdi}$), 114.5 ($C_{arom.}$), 71.3 (C-O$_{oxa\ ring}$), 68.8 (C-O-$C_{arom.}$), 46.8 (C-N$_{oxa\ ring}$), 41.7 (C(CH$_3$)$_2$), (40.8 ($C_{arom.}$-CH$_2$-$C_{arom.}$) overlapping with DMSO), 31.1 (C(CH_3)$_2$). IR [cm^{-1}]: 2964, 1741, 1697, 1509, 1430, 1406, 1309, 1220, 1183, 1133, 1030, 983, 950, 828, 751, 571, 511.

8.3.5   Synthesis of POxa-BADGE-TDI

Solution 1 containing **5u-Me-CO₂** (1 eq., 0.0008 g, 0.006 mmol), LiCl (2 eq., 0.0005 g, 0.012 mmol) and 1,3-imethylimidazol-2-one (0.5 g) was weighed into a 4 mL vial equipped with a PTFE-coated stir bar. Solution 2 consisting of BADGE (100 eq., 0.2000 g, 0.588 mmol), TDI (100 eq., 0.1023 g, 0.588 mmol) and 1,3-imethylimidazol-2-one (1.75 g) was taken up by a syringe with a needle. Solution 2 was added within 4 h (rate of ~0.1 mL/14 min) to the stirred solution 1 at 200°C. After the addition was finished the reaction was kept at 200°C for 1 h. The orange/brownish reaction mixture was poured into propan-2-ol (35 mL) and a precipitate was obtained, which was separated by centrifugation. The supernatant solution was discarded and the

remaining substance dried under reduced pressure. If necessary, the polymer was dissolved in DMF or DMSO and again precipitated, centrifuged, decanted and dried under reduced pressure.

Yield: 89%. M_n=11000 g/mol; DP=21; PDI=2.4. ^{1}H NMR (DMSO-d6, ppm): δ=7.63 (1 H, s, $H_{\text{arom. tdi}}$), 7.48 (1 H, d, J=7.8, $H_{\text{arom. tdi}}$), 7.32 (1 H, d, J=7.8, $H_{\text{arom. tdi}}$), 7.11 (4 H, br, $H_{\text{arom.}}$), 6.87 (4 H, m, $H_{\text{arom.}}$), 5.04 (2 H, s, HC-O$_{\text{oxa ring}}$), 4.19 (6 H, m), 3.90 (1 H, s), 3.79 (1 H, s), 2.23 (3 H, s, CH_3-C$_{\text{arom.}}$), 1.56 (6 H, s, C(CH_3)$_2$). ^{13}C NMR (DMSO-d6, ppm): δ=156.0, 155.8, 155.2, 154.1, 143.2, 137.1, 136.6, 131.2, 130.7, 127.6, 127.5, 117.4, 116.4, 114.0, 113.9, 71.6, 70.9, 68.4, 68.3, 48.6, 46.4, 41.2, 30.7, 16.8. IR [cm^{-1}]:2966, 1742, 1608, 1507, 1410, 1222, 1183, 1093, 1025, 950, 828, 754, 684, 555.

8.3.6 Synthesis of POxa-BDDGE-HDI

Solution 1 containing **5u-Me-CO₂** (1 eq., 0.0008 g, 0.006 mmol), LiCl (2 eq., 0.0005 g, 0.012 mmol) and sulfolane (0.5 g) was weighed into a 4 mL vial equipped with a PTFE-coated stir bar. Solution 2 consisting of BDDGE (100 eq., 0.1188 g, 0.588 mmol), HDI (100 eq., 0.0988 g, 0.588 mmol) and sulfolane (1.75 g) was taken up by a syringe with a needle. Solution 2 was added within 2 h (rate of ~0.1 mL/7 min) to the stirred solution 1 at 200°C. After the addition was finished the reaction was kept at 200°C for 1 h. The yellowish reaction mixture was poured into demineralized water (35 mL) and a precipitate was obtained, which was separated by centrifugation, the supernatant solution was discarded and the remaining substance dried under reduced pressure. If necessary, the polymer was dissolved in CH$_2$Cl$_2$ and again precipitated, centrifuged, decanted and dried under reduced pressure.

Yield: 52%. M_n=9000 g/mol; DP=24; PDI=2.0. ^{1}H NMR (CDCl$_3$, ppm): δ=4.58 (2 H, m, HC-O$_{\text{oxa ring}}$), 3.54 (6 H, br), 3.47 (4 H, m), 3.33 (2 H, m), 3.21, (4 H, m), 1.57 (4 H, m), 1.50 (4 H,

m), 1.30 (4 H, m). ^{13}C NMR (CDCl$_3$, ppm): δ=157.9 (*C*=O), 71.9, 71.5, 71.2, 71.2, 46.4, 46,4, 43.8, 27.1, 26.2, 26.1. IR [cm^{-1}]: 2928, 1731, 1490, 1444, 1358, 1254, 1121, 1057, 762, 682.

8.3.7 Synthesis of POxa-BDDGE-MDI

Solution 1 containing **5u-Me-CO$_2$** (1 eq., 0.0008 g, 0.006 mmol), LiCl (2 eq., 0.0005 g, 0.012 mmol) and sulfolane (0.5 g) was weighed into a 4 mL vial equipped with a PTFE-coated stir bar. Solution 2 consisting of BDDGE (100 eq., 0.1188 g, 0.588 mmol), MDI (100 eq., 0.1470 g, 0.588 mmol) and sulfolane (1.75 g) was taken up by a syringe with a needle. Solution 2 was added within 4 h (rate of ~0.1 mL/14 min) to the stirred solution 1 at 200°C. After the addition was finished the reaction was kept at 200°C for 1 h. The yellowish reaction mixture was poured into demineralized water (35 mL) and a precipitate was obtained, which was separated by centrifugation. The supernatant solution was discarded and the remaining substance dried under reduced pressure. If necessary, the polymer was dissolved in CH$_2$Cl$_2$ and again precipitated, centrifuged, decanted and dried under reduced pressure.

Yield: 76%. M_n=9000 g/mol; DP=20; PDI=3.0. ^{1}H NMR (CDCl$_3$, ppm): δ=7.43 (4 H, br, *H*$_{arom.}$), 7.20 (4 H, br, *H*$_{arom.}$), 4.72 (2 H, s, *H*C-O$_{oxa\ ring}$), 3.99 (2 H, s), 3.83 (2 H, s), 3.68 (2 H, s), 3.48 (4 H, m), 3.38 (4 H, s), 1.45 (4 H, s). ^{13}C NMR (CDCl$_3$, ppm): δ=162.5 (*C*=O), 154.4, 136.6, 136.6, 129.1, 118.1, 71.6, 70.7, 46.4, 35.9, 30.9, 25.8. IR [cm^{-1}]: 2866, 1738, 1612, 1513, 1481, 1429, 1405, 1311, 1219, 1129, 983, 856, 813, 799, 752, 650, 594, 512.

8.3.8 Synthesis of 1,3,5-triphenyl-1,3,5-triazinan-2,4,6-trione

6-Cy-CO$_2$ (1 eq., 0.0610 g, 0.2 mmol) and phenyl isocyanate (200 eq., 5 g, 42.0 mmol) were weighed into a 10 mL screw top vial equipped with a PTFE-coated magnetic stir bar. The reaction was exothermic and a colorless solid precipitated. The reaction was heated to 80°C

overnight. The obtained mixture was diluted into diethyl ether (40 mL), filtered, washed with diethyl ether (2x 25 mL) and dried under reduced pressure. Yield: 90%. ^{1}H NMR (CDCl$_3$, ppm): δ=7.55-7.40 (m, overlapping signals). ^{13}C NMR (CDCl$_3$, ppm): δ=148.8, 133.7, 129.4, 128.5. GC-MS (m/z)= 357.2 g/mol (found); 357.19 g/mol (expected).

8.3.9   Synthesis of 4- and 5-(phenoxymethyl)-3-phenyl oxazolidin-2-one

A closed 250 mL Schlenk flask under inert gas equipped with 1,3,5-triphenyl-1,3,5-triazinane-2,4,6-trione   (25 eq.,   2.15 g,   6.02 mmol),   2-(phenoxymethyl)oxirane   (75 eq.,   2.71 g, 18.05 mmol), LiCl (2 eq., 0.020 g, 0.48 mmol), **5u-Me-CO$_2$** (1 eq., 0.034 g, 0.241 mmol), a PTFE-coated stir bar and 60 mL sulfolane were heated to 200°C for 4 h. After cooling to rt 200 mL water were added before the addition of 100 mL diethyl ether resulted in the precipitation of a colorless substance which was filtered off. The water phase was extracted five times with 100 mL diethyl ether, the combined organic phases were washed 2x with 100 mL water, dried over MgSO$_4$, filtered and the volatiles removed under reduced pressure. The remaining solid was extracted 5 times with 100 mL of hot pentane. The combined pentane phases were reduced to dryness under vacuum. The remaining substance was purified by column chromatography (hexane/ethyl ethanoate 2 to 1). 4-(Phenoxymethyl)-3-phenyl oxazolidin-2-one phases were collected (R$_f$=0.33), combined, the solvent removed and the product crystallized from CH$_2$Cl$_2$ and pentane in the fridge. The solid remaining from the hot pentane extraction was dissolved in CH$_2$Cl$_2$, mixed with silica, concentrated to dryness, placed on fresh silica and flushed with 200 mL diethyl ether to afford 5-(phenoxymethyl)-3-phenyl oxazolidin-2-one as a colorless solid after the solvent was removed. Again, the residue was crystallized from CH$_2$Cl$_2$ and pentane in the fridge to afford 5-(phenoxymethyl)-3-phenyloxazolidin-2-one.

4-(Phenoxymethyl)-3-phenyl oxazolidin-2-one: ^{1}H NMR (CDCl$_3$, ppm): δ=7.38 (2 H, m), 7.27 (2 H, m), 7.15 (2 H, m), 7.09 (1 H, tt, J=7.4 Hz, J=1.1 Hz), 6.86 (1 H, tt, J=7.4 Hz, J=1.0 Hz), 6.72 (2 H, m), 4.63 (1 H, m), 4.51 (1 H, t, J=8.7 Hz), 4.39 (1 H, m), 3.92 (2 H, m). ^{13}C NMR (CDCl$_3$, ppm): δ=158.0 (*C*=O), 155.9, 136.4, 129.7, 129.5, 125.8, 122.3, 121.8, 144.6, 65.9 (*C*-O$_{oxa\ ring}$), 65.0 (*C*-O-C$_{arom}$), 55.9 (*C*-N). IR [cm^{-1}]: 2907, 2875, 1736, 1593, 1491, 1474, 1459, 1415, 1379, 1363, 1295, 1281, 1247, 1217, 1166, 1139, 1088, 1068, 1042, 1003, 985, 965, 915, 902, 841, 752, 723, 692, 675, 623, 614, 582, 521, 508, 489. HRMS (ESI, positive) (m/z): 269.11 (calc.), 561.20 (found, 2M+Na$^+$), 292.10 g/mol (found, M+Na$^+$) and 270.11 (found, M+H$^+$).

5-(Phenoxymethyl)-3-phenyl oxazolidin-2-one: ^{1}H NMR (CDCl$_3$, ppm): δ=7.59 (2 H, m), 7.40 (2 H, m), 7.30 (2 H, m), 7.16 (1 H, t, J=7.4 Hz), 7.00 (1 H, t, J=7.4 Hz), 6.92 (2 H, m), 4.99 (1 H, m), 4.22 (3 H, m, overlaying signals), 4.08 (1 H, m. ^{13}C NMR (CDCl$_3$, ppm): δ=158.1 (*C*=O), 154.5, 138.2, 129.8, 129.3, 124.3, 121.9, 118.4, 114.7, 70.5 (*C*-O$_{oxa\ ring}$), 68.0 (*C*-O-C$_{arom}$), 47.5 (*C*-N$_{oxa\ ring}$). IR [cm^{-1}]: 3038, 2961, 1735, 1600, 1583, 1500, 1456, 1444, 1410, 1336, 1291, 1248, 1221, 1162, 1144, 1131, 1095, 1085, 1043, 1022, 1002, 982, 901, 886, 832, 816, 774, 753, 743, 684, 669, 614, 572, 518, 506. HRMS (ESI, positive) (m/z): 269.11 (calc.), 561.20 (found, 2M+Na$^+$), 292.10 (found, M+Na$^+$), 270.11 (found, M+H$^+$).

8.4 Polyamide 6 Synthesis

Most of the results described in this chapter are published: H. J. Altmann, M. Steinmann, I. Elser, M. J. Benedikter, S. Naumann, M. R. Buchmeiser, Dual catalysis with an N-heterocyclic carbene and a Lewis acid: Thermally latent precatalyst for the polymerization of ε-caprolactam, *J. Polym. Sci.* **2020**, *58*, 3219-3226.[6]

Unless otherwise noted, polymerizations were conducted under inert gas atmosphere in a glove box or using standard Schlenk technique. The same applies to reactions with [AEO-Ac-MgCl$_2$]. Determination of the relative viscosities was conducted at the German Institutes of Textile and Fiber Research applying a Ubbelohde viscosimeters. 1 g of the polyamide was dissolved in 100 mL of H$_2$SO$_4$ (96%, Merck) and the measurements were executed at 25°C. All values were double determined.

8.4.1 Synthesis of [AEO-Ac-MgCl$_2$]

A solution of AEO-Ac (1 eq., 0.0815 g, 0.525 mmol) dissolved in 2 mL CH$_2$Cl$_2$ was combined at room temperature with a mixture of MgCl$_2$ (1 eq., 0.0500 g, 0.525 mmol) in THF: CH$_2$Cl$_2$ (2 mL, 1:1 by volume). The reaction was stirred for 10 h at ambient temperature before the solvent was removed and a colorless solid was received. ^{1}H NMR (D$_3$CCN, ppm): δ=3.94 (2 H, bs, -C*H$_2$*-N-), 3.77 (2 H, m, -O-C*H$_2$* THF), 2.80 (2 h, bm, -C*H$_2$*-C(O)-), 2.43 (3 H, s, *H$_3$*C-C(O)-), 1.83 (2 H, -O-CH$_2$-C*H$_2$*- THF), 1.74 (6 H, bs, -C*H$_2$*-C*H$_2$*-C*H$_2$*-). ^{13}C NMR (D$_3$CCN, ppm): δ=182.1 (-C(O)-), 177.4 (-C(O)-), 69.0 (-O-C*H$_2$*- THF), 47.1, 40.0, 29.0, 28.2, 27.0 (-O-CH$_2$-C*H$_2$*-), 25.9, 23.8.

8.4.2 PA6 Synthesis, Non-homogenized Approach

AEO (0.5 to 6 g) and the respective amount of NHC, Lewis acid and activator were weighed into an oven-dry 4 or 10 mL glass vial equipped with a magnetic stir bar. The vial was closed with a screw top and placed into a drill hole of a preheated aluminum block, placed onto the heating plate of a magnetic stirrer. After the appropriate reaction time the vial was removed from the heat source and allowed to cool to room temperature before workup (see below).

8.4.3 Prehomogenization

AEO (0.5 to 6 g) an the respective amount of NHC, Lewis acid and activator were weighed into an oven-dry 4 or 10 mL glass vial equipped with a magnetic stir bar. The vial was closed with a screw top and heated under constant stirring above the melting point of AEO (typically 75 to 90°C) until a clear, colorless and homogeneous solution was obtained. The time until homogenization varied between 1 and several hours. Typically homogenization was conducted for 1 to 3 h; however, in several cases the mixtures were homogenized overnight.

8.4.4 Direct Polymerization

The vials containing the prehomogenized polymerization systems were taken from the heating plate for homogenization and were placed into the drill holes of an aluminum block preheated to thepolymerization temperature and placed on the heating plate of a magnetic stirrer. After the appropriate reaction time, the vial was removed from the heat source and allowed to cool down to room temperature before workup (see below).

8.4.5 Storage as Solid

The vials containing the prehomogenized polymerization systems were allowed to cool to room temperature and brought inside the glove box where they were stored for later use possibly split

into several charges, which were eventually diluted with additional monomer. To polymerize these mixtures, they were equipped with a magnetic stir bar and placed into the drill holes of an aluminum block preheated to the polymerization temperature and placed on the heating plate of a magnetic stirrer. After the appropriate reaction time, the vial was removed from the heat source and allowed to cool down to room temperature before workup (see below).

8.4.6 Storage as Liquid

The vials containing the prehomogenized polymerization systems were kept at a temperature above the melting point of AEO (typically 75°C) and stirred continuously up to five days. Samples were subsequently placed into the drill holes of an aluminum block preheated to the polymerization temperature and placed on the heating plate of a magnetic stirrer. After the appropriate reaction time, the vial was removed from the heat source and allowed to cool down to room temperature before workup (see below).

8.4.7 Polymer Workup

Polymers were worked up under ambient conditions. Methanoic acid (4 to 12 mL/g_{AEO}) was added to the reaction product in order to dissolve the polymer. Dissolving the polymers typically took 1 to 3 days depending on the molecular weight. After the product was fully dissolved it was precipitated into propan-2-one (30 to 150 mL/g_{AEO}). A colorless precipitate was found in case a polymer had formed during the reaction. The precipitate was separated by centrifugation applying 4500 rpm for 15 to 99 min. The supernatant solution was discarded and the remaining product was dried under reduced pressure in the temperature range between room temperature and 70°C. Drying usually took at least overnight. Finally the polymer yield was determined gravimetrically.

8.4.8 Flame Retardancy

AEO (1 eq., 0.4212 g, 0.3723 mmol) and NEt_3 (1 eq., 0.3767 g, 0.3723 mmol) were dissolved in CH_2Cl_2 (6 mL) before a solution of $P(O)(OPh)_2Cl$ (1 eq., 1.0000 g, 0.3723 mmol) dissolved in diethyl ether (2 mL) was added. The combined mixture was stirred at room temperature for 2 days. During this time a colorless precipitate was formed which was removed by filtration, the remaining solution was reduced to dryness under reduced pressure. The obtained colorless solid was recrystallized from of CH_2Cl_2 (5 drops) and diethyl ether (8 mL) to give colorless crystals. If necessary, the product was recrystallized again. Yield: 63%. ^{1}H NMR (CDCl$_3$, ppm): δ=7.32 (8 H, m, arom.), 7.20 (2 H, m, arom.), 3.71 (2 H, t, CH_2-N), 2.57 (2 H, CH_2-C(O)) 1.54 (4 H, s), 1.36 (2 H, m). ^{13}C NMR (CDCl$_3$, ppm): δ=178.4, 150.1 (d), 129.8, 125.7 (d), 121.0 (d), 47.3 (d), 38.8 (d), 29.3, 29.3 (d), 23.2. ^{31}P NMR (CDCl$_3$, ppm): δ=-5.49.

For polymerizations with AEO-P(O)(OPh)$_2$, all substances (NHC, MgCl$_2$ and AEO) were weighed into an oven-dry 4 or 10 mL glass vial equipped with a magnetic stir bar. The vial was closed with a screw top and heated under constant stirring above the melting point of AEO (typically 75 to 90°C) until a clear, colorless and homogeneous solution was obtained (~2 h).

8.5 Spirocyclic NHC Precursor

The content of this chapter was majorly published: H. J. Altmann, W. Frey, M. R. Buchmeiser, A Spirocyclic Parabanic Acid Masked *N*-Heterocyclic Carbene as Thermally Latent Pre-Catalyst for Polyamide 6 Synthesis and Epoxide Curing, *Macromol. Rapid. Commun.* **2020**, e2000338.[10]

Inside a glove box, 1,3-dimethylimidazolium-2-carboxylate (1 eq., 1.0000 g, 7.136 mmol) weighed into a 50 mL Schleck flask was mixed with cyclohexyl isocyanate (2 eq., 1.7864 g, 14.271 mmol) in acetonitrile (10 mL) and sulfolane (15 mL). The flask was closed, brought outside the glove box and heated to 80°C for 4 h. Within this time a deep red solution formed. The flask was transferred back into the glove box; then was cooled down to room temperature. The solution was extracted several times with pentane, which did not mix with the red phase. The pentane phases were collected. Extraction was continued until pentane washings remained colorless. The collected pentane phases were dried under reduced pressure at ambient temperature. The residuals were dissolved in pentane again, filtered through a pad of celite, concentrated under reduced pressure and crystallized at -35°C after the pentane phase was concentrated under reduced pressure. Yield: 67%. ^{1}H NMR (C_6D_6, ppm): δ=5.21 (2 H, s, -N-CH=), 4.15 (1 H, tt, J=12.3 Hz, J=3.7 Hz, -CO-N(-$C_{ipso}H$-)-CO-), 3.58 (1 H, tt, 12.2 Hz, J=3.9 Hz, -C-N(-$C_{ipso}H$-)-CO-N-), 2.53-2.26 (10 H, m, sum of integrals with 6 protons of the two methyl groups), 1.80 (2 H, m), 1.68 (2 H, m), 1.59 (4 H, m), 1.44 (2 H, m), 1.14 (6 H, m). ^{13}C NMR (C_6D_6, ppm): δ=165.4 (-N-CO-N-), 154.2 (-C-CO-N-), 116.6 (-CH=CH-), 101.7 (C_{spiro}), 51.8, 51.0, 33.0, 31.0, 30.1, 26.1, 25.7, 25.3. IR (cm^{-1}): 2925, 2854, 1705, 1426, 1371, 1175, 1116, 1017, 979, 894, 681, 618, 601. HRMS (m/z): calculated: 346.24 g/mol ($C_{19}H_{30}N_4O_2$), found: 347.24 g/mol ($C_{19}H_{30}N_4O_2$+H$^+$).

General procedure for the preparation of latent epoxide resins: Inside a glove box, the epoxide compound (BADGE or BDDGE, 100 eq.) was mixed with the anhydride compound (A1 and A6, 200 eq.). To homogenize the mixtures they were stirred and heated up to 60°C (1 h) if necessary. Typical sample masses were between 0.5 and 1 g. After cooling the epoxide/anhydride mixture to room temperature, **5u-Me-(OCN-Cy)₂** (1 eq.) was added and the mixture was stirred at room temperature until a homogeneous solution was received. Resins produced from anhydride A1 were colorless or yellowish, resins containing anhydride A6 were reddish to brown. From these mixtures, sample of 1 to 5 mg were submitted under ambient conditions to DSC. A heat rate of 5 K/min from 30 to 250°C was used for resin curing and determination of T_{max}. For the control cycle a heat rate of 30 K/min from 0 to 250°C was applied.

Sample preparation for PA6 synthesis: AEO (250 eq., 1.0000 g, 8.836 mmol) and **5u-Me-(OCN-Cy)₂** (1 eq., 12.3 mg, 0.035 mmol) and eventually additives like $MgCl_2$ (1 eq.) and AEO-Ac (1 eq.) were combined in a vial inside a glove box. Under continuous stirring the mixture was heated to 75°C until a clear solution formed. This process took typically around 1 h. These samples were stored under ambient temperature until they were polymerized at 180°C for 1 h. The mixtures were stirred until the reaction solidified. At ambient conditions, the polymers were dissolved in methanoic acid (typically 10 mL/$g_{polymer}$). The polymer solution was precipitated from propan-2-one (35 mL/$g_{polymer}$), centrifuged (4500 rpm, ≥15 min), the supernatant solution decanted and discarded and the polymer dried under reduced pressure and elevated temperatures of 60°C. Melting points were determined with a heat rate of 30 K/min and 40 K/min.

8.6 Oligomerization of 4-Methyloxetan-2-one to Diols

The content of this chapter is majorly published: H. J. Altmann, M. R. Machat, A. Wolf, C. Gürtler, D. Wang, M. R. Buchmeiser, Synthesis of dihydroxy telechelic oligomers of β-butyrolactone catalyzed by titanium(IV)-alkoxides and their use as macrodiols in polyurethane chemistry, *J. Polym. Sci.*, **2021**, *59*, *3*, 274-281.[11] All polymerizations were executed in a nitrogen filled glove box or under standard Schleck technique, unless otherwise noted.

8.6.1 Synthesis of α,ω dihydroxy telechelic oligo(4-methyloxetan-2-one)

A homogenized solution of 4-methyloxetan-2-one (0.25 to 4 g) and the respective amount of initiator diol was mixed with the appropriate amount of Ti(IV) alkoxide in a 4 or 10 mL vial equipped with a magnetic stir bar. The closed vial was submitted to an aluminum block preheated to the reaction temperature, with drill holes placed on a magnetic stirring heating plate. After the appropriate reaction time, the mixture was allowed to cool down to room temperature and a sample was taken and submitted to NMR analysis. The vial was removed from the glove box and 2 to 6 mL THF and several drops demineralized water (5 to 10 drops) were added. The mixture was stirred for >1 h and filtered. Finally, the solvents were removed under vacuum and a colorless, viscos liquid remained.

^{1}H NMR (CDCl$_3$, ppm): δ=5.25 (8 H, bm, -CH$_2$-C*H*(CH$_3$)-), 4.23 (4 H, bm, -O-C*H*$_2$-CH$_2$-O- overlapping with 2 H, bd, -CH$_2$-C*H*(CH$_3$)-OH), 3.68 (4 H, bm, -O-CH$_2$-C*H*$_2$-O-), 2.58 (16 H, bm, -C*H*$_2$-CH(CH$_3$)- overlapping 4 H, bm, -C*H*$_2$-(CH(CH$_3$)-OH), 1.29 (24 H, bm, -CH$_2$-CH(C*H*$_3$)-), 1.22 (6 H, bm, -CH$_2$-CH(C*H*$_3$)-OH). ^{13}C NMR (CDCl$_3$, ppm): δ=172.8-169.3 (*C*=O), 69.0-63.5 (*C*H-O), 43.6-40.6 (*C*H$_2$), 22.6-19.9 (*C*H$_3$). IR (cm^{-1}): 3447, 2977, 1733, 1457, 1383, 1303, 1261, 1183, 1137, 1103, 1057, 977, 597, 450.

8.6.2 Polyurethane Synthesis -1

General procedure for the PU synthesis in the ratio 4MO:DEG:Ti(OR)$_4$:MDI 100:10:1:10. The respective Ti(IV) alkoxide (1 eq.) was placed in a 10 mL vial equipped with a PTFE-coated magnetic stir bar before a mixture of 4-methyloxetan-2-one (100 eq., 1 g, 11.616 mmol) and DEG (10 eq., 0.1233 g, 1.162 mmol) were added. The closed vials were heated and stirred at 100°C for 2 h and again removed from the heat source. After cooling to ambient temperature, a solution of MDI (10 eq., 0.2907 1.162 mmol) in 5 mL THF was added under constant stirring. A rapid increase in viscosity was observed. After 12 h, the solution was poured into 40 mL pentane and a colorless precipitate formed. The mixture was centrifuged, the supernatant solution decanted and the remaining polymer dried for 12 h under reduced pressure at 50°C. The isolated yields of the slightly orange/brownish polymers are given for each catalyst: Ti(OMe)$_4$ 76%; Ti(OiPr)$_4$ 79% and Ti(OtBu)$_4$ 82%.

8.6.3 Polyurethane Synthesis -2

General procedure for the PU synthesis in the ratio 4MO:DEG:Ti(OR)$_4$:MDI 500:50:1:50. The respective Ti(IV) alkoxide (1 eq.) was placed in a 10 mL vial equipped with a PTFE-coated magnetic stir bar before a mixture of 4-methyloxetan-2-one (500 eq., 1 g, 11.616 mmol) and DEG (50 eq., 0.1233 g, 1.162 mmol) were added. The closed vials were heated and stirred at 100°C for 13 h and again removed from the heat source. After cooling to ambient temperature, a solution of MDI (50 eq., 0.2907 g, 1.162 mmol) in 5 mL THF was added under constant stirring. A rapid increase in viscosity was observed. After 12 h, the solution was poured into 40 mL pentane and a colorless precipitate formed. The mixture was centrifuged, the supernatant solution decanted and the remaining polymer dried for 12 h under reduced pressure at 50°C. The isolated

yields of the slightly orange/brownish polymers are given for each catalyst: Ti(OMe)$_4$ 83%; Ti(OiPr)$_4$ 90% and Ti(OtBu)$_4$ 89%.

^{1}H NMR (CDCl$_3$, ppm): δ=7.28 (4 H, bd, 6.1 Hz, *H*$_{arom.}$), 7.06 (4 H, bd, 6.1 Hz, *H*$_{arom.}$ overlapping with 2 H, bs, N*H*), 5.23 (10 H, bm, -CH$_2$-C*H*(CH$_3$)-), 4.19 (4 H, bm, -O-CH$_2$-C*H*$_2$-O-), 3.84 (2 H, b, -C$_6$H$_4$-C*H*$_2$-C$_6$H$_4$-), 3.64 (4 H, bm, -O-C*H*$_2$-CH$_2$-O-), 2.55 (20 H, bm, C(O)-C*H*$_2$-CH(CH$_3$)-), 1.32 (6 H, bm, -CH(C*H*$_3$)-O-C(O)-NH-), 1.25 (24 H, bm, -CH(C*H*$_3$)-O-C(O)-CH$_2$-). ^{13}C NMR (CDCl$_3$, ppm): δ=170.5-169.3 (-O-*C*(O)-CH$_2$-), 152.9 (-O-*C*(O)-NH-), 136.3 (*C*$_{arom.}$), 129.4 (*C*$_{arom.}$), 118.8 (*C*$_{arom.}$), 68.9-63.5 (-*C*H(CH$_3$)-O-), 41.4-40.5 (-C(O)-*C*H$_2$- and -C$_6$H$_4$-*C*H$_2$-C$_6$H$_4$-), 20.3-19.8 (-CH(*C*H$_3$)-). IR (cm^{-1}): 3346, 2984, 1726, 1597, 1527, 1454, 1412, 1382, 1304, 1260, 1221, 1178, 1131, 1100, 1053, 972, 929, 857, 818, 769, 605, 511.

9 Appendix

9.1 General
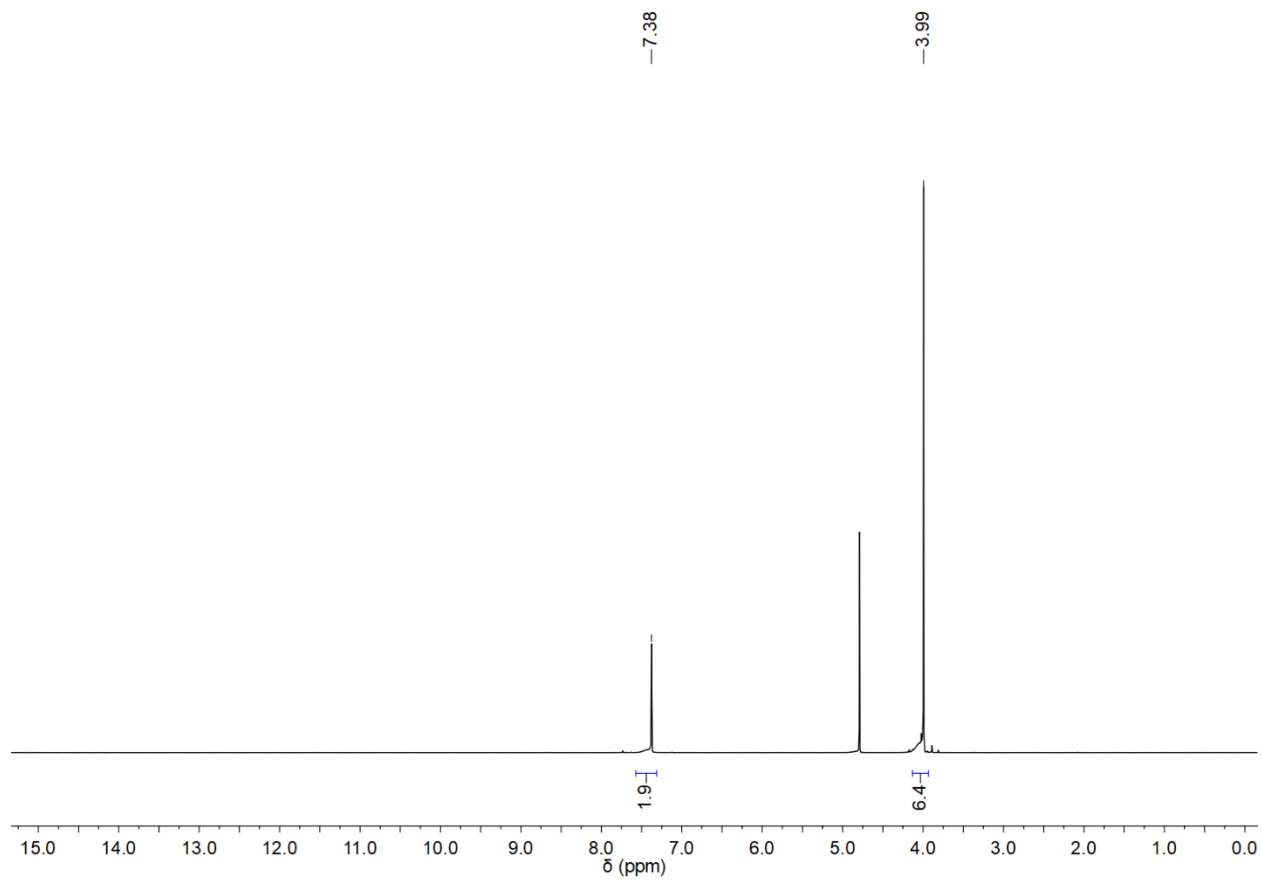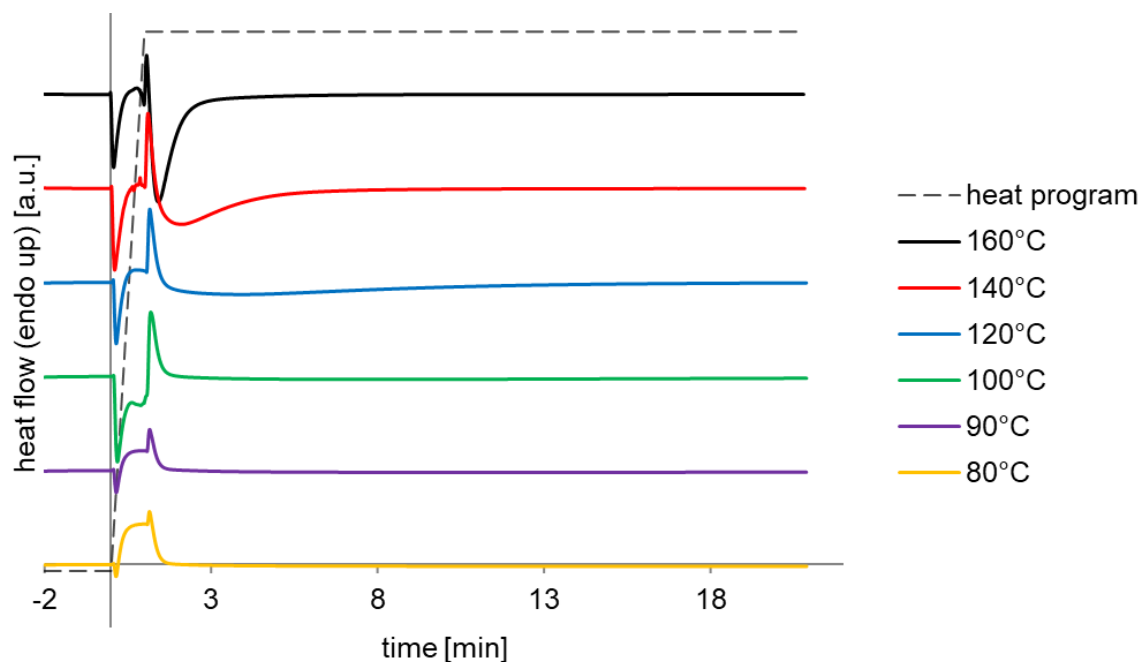

Scheme 97: ^{1}H NMR spectrum of **5u-Me-CO$_2$** in D$_2$O.
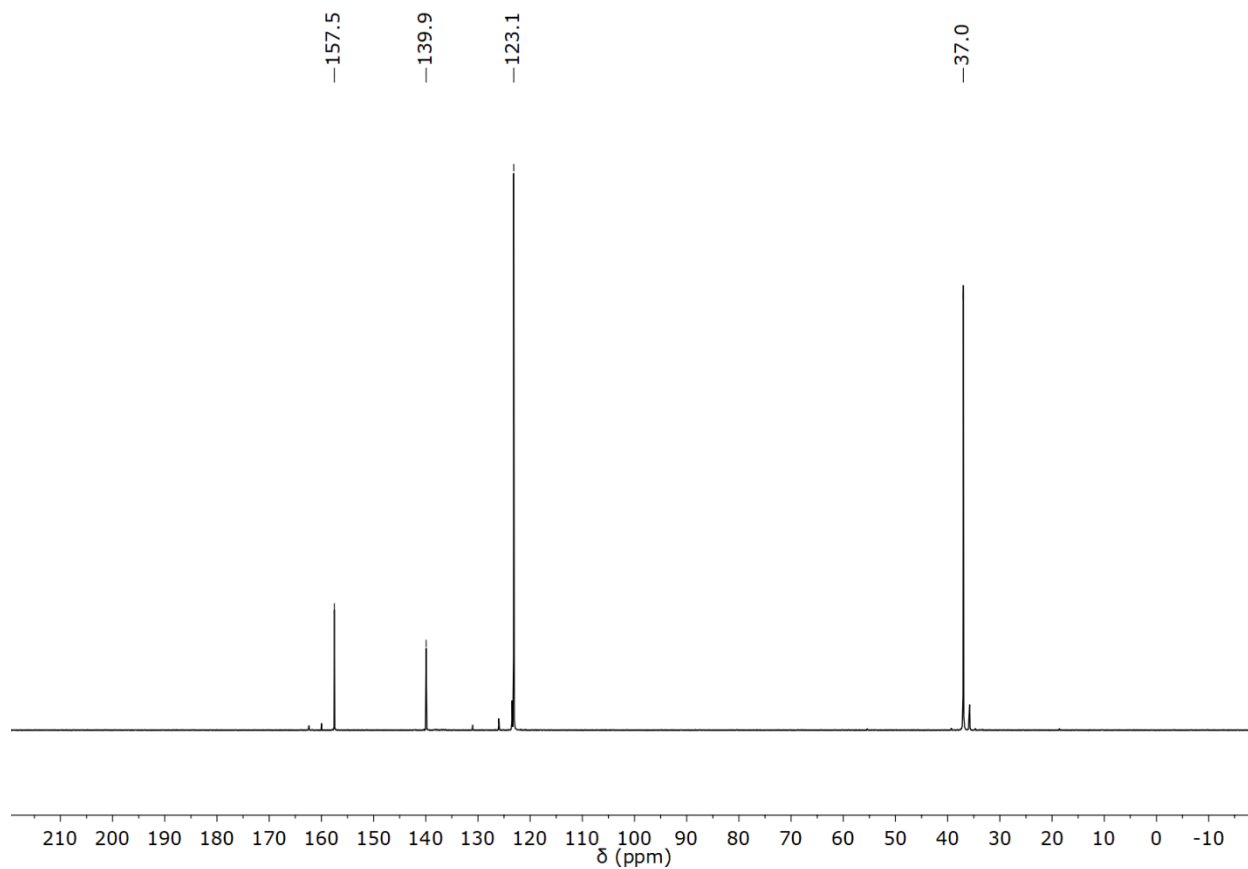
Scheme 98: ^{13}C NMR spectrum of **5u-Me-CO$_2$** in D$_2$O.

## 9.2 Data on Anhydride-hardened Epoxide Resins

Some of these results are published: H. J. Altmann, S. Naumann, M. R. Buchmeiser, Protected *N*-heterocyclic carbenes as latent organocatalysts for the low-temperature curing of anhydride-hardened epoxy resins, *Eur. Polym. J.* **2017**, *95*, 766-774.[4]
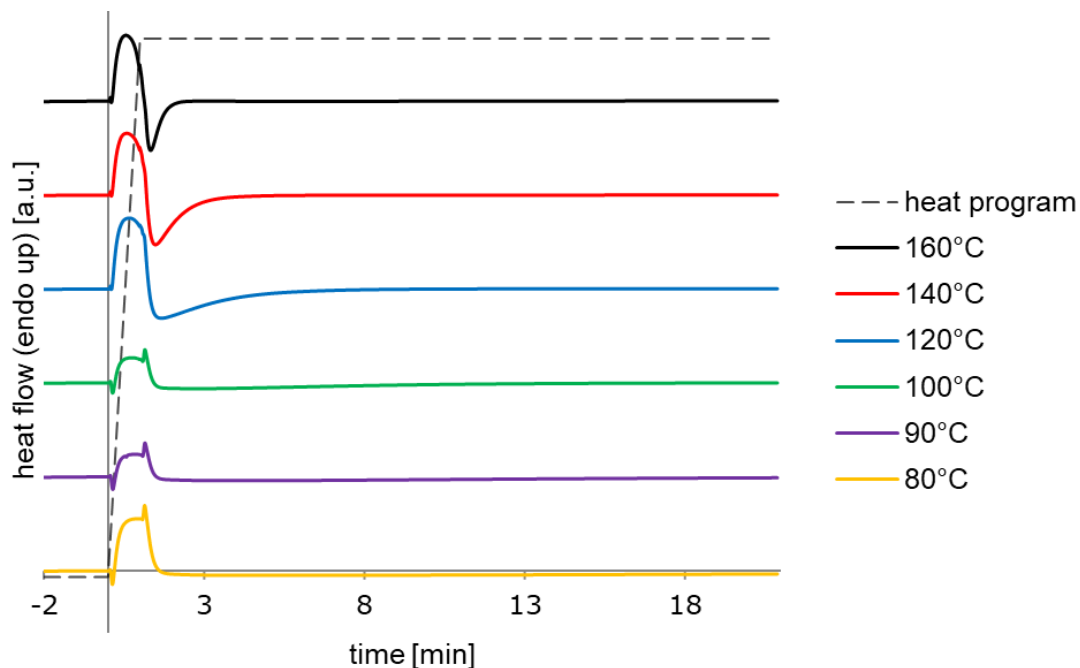

Scheme 99: Stacked isothermal curing curves of the system DPDGE/A7/**5u-Me-CO₂** (100:200:8). The dashed line represents the heat program.
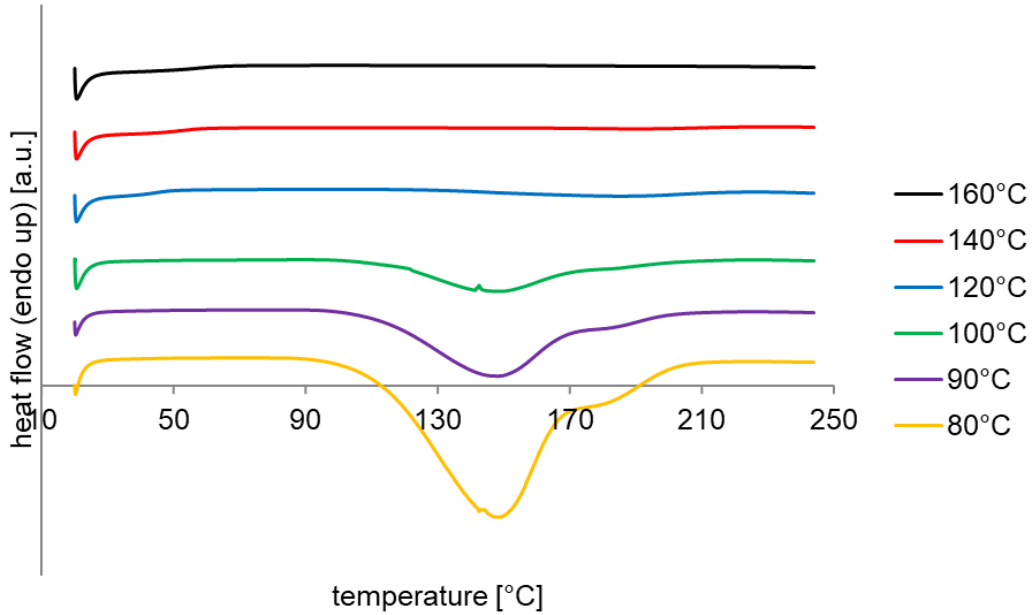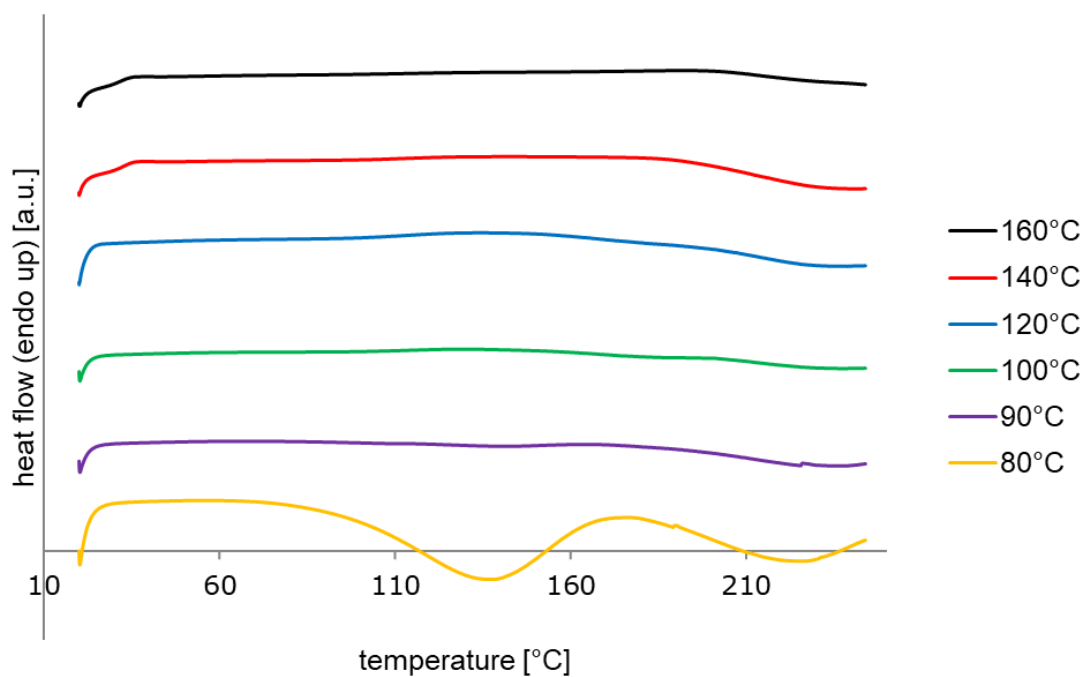
Scheme 100: Stacked DSC thermograms of post-isothermal heat ramp from 20 to 250°C applying a heat rate of 20 K/min for the resin system DPDGE/A7/**5u-Me-CO₂** (ratio 100:200:8). The temperatures in the legend represent the temperature of the isothermal pre-curing of the sample (20 min).
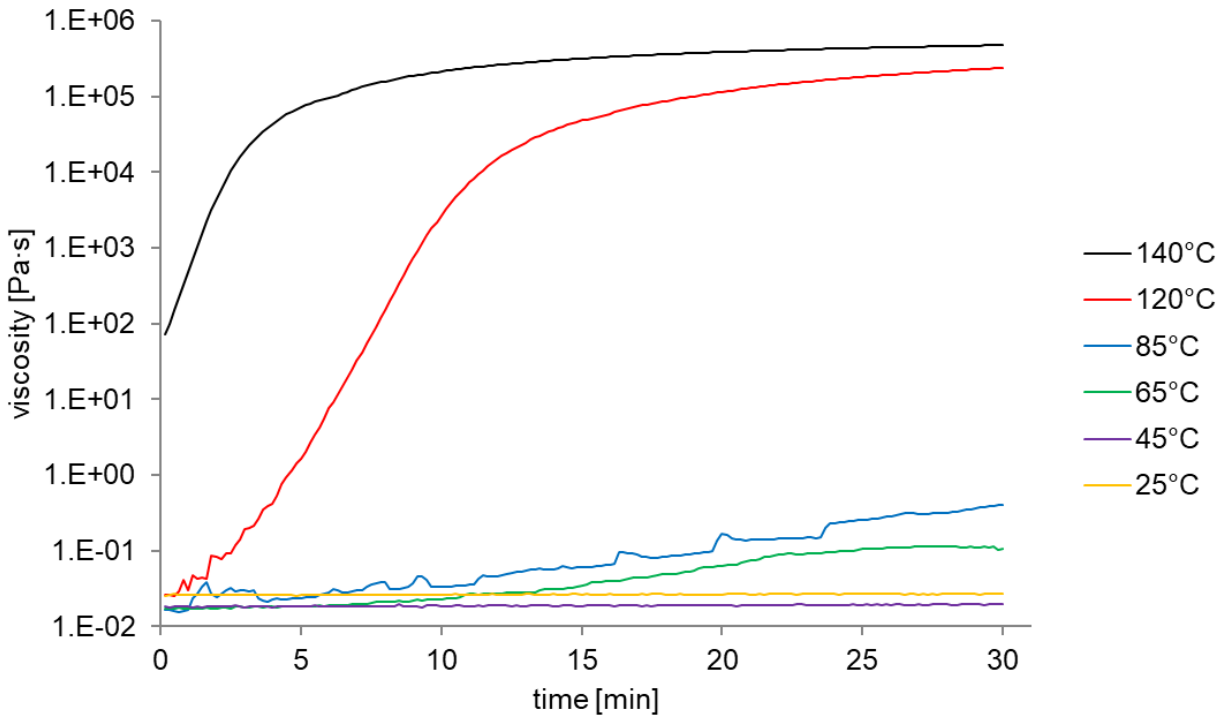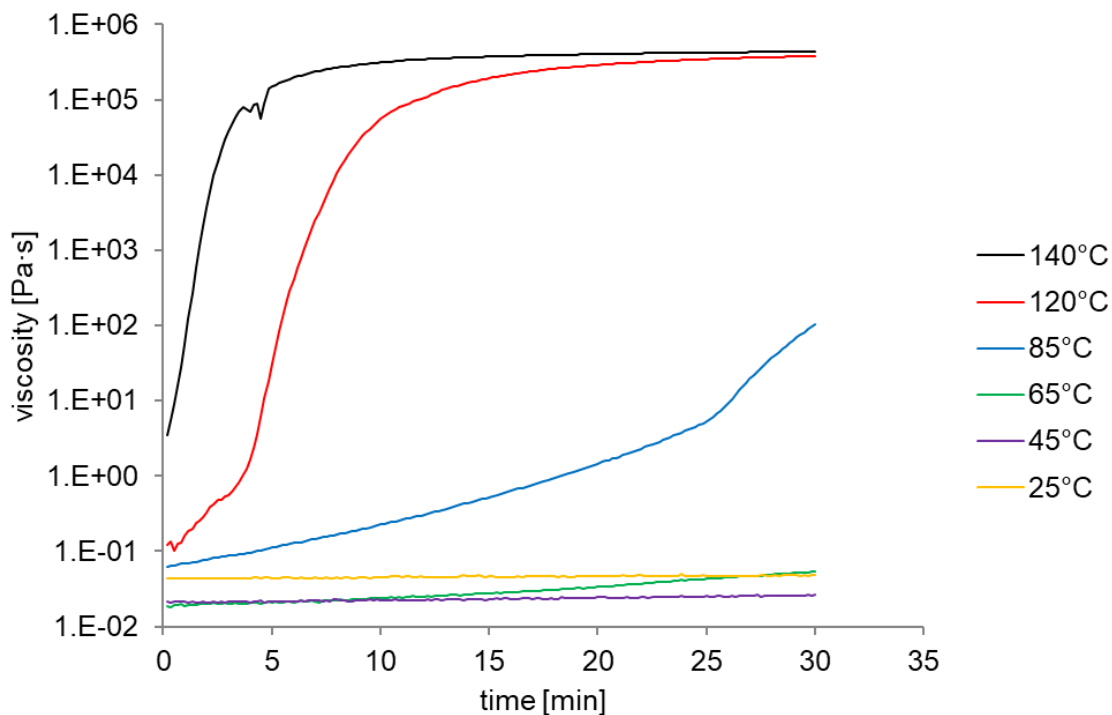

Scheme 101: Viscosities of the system DPDGE/A7/**5u-Me-CO₂** (100:200:8) as determined by rheology measurements at various temperatures.
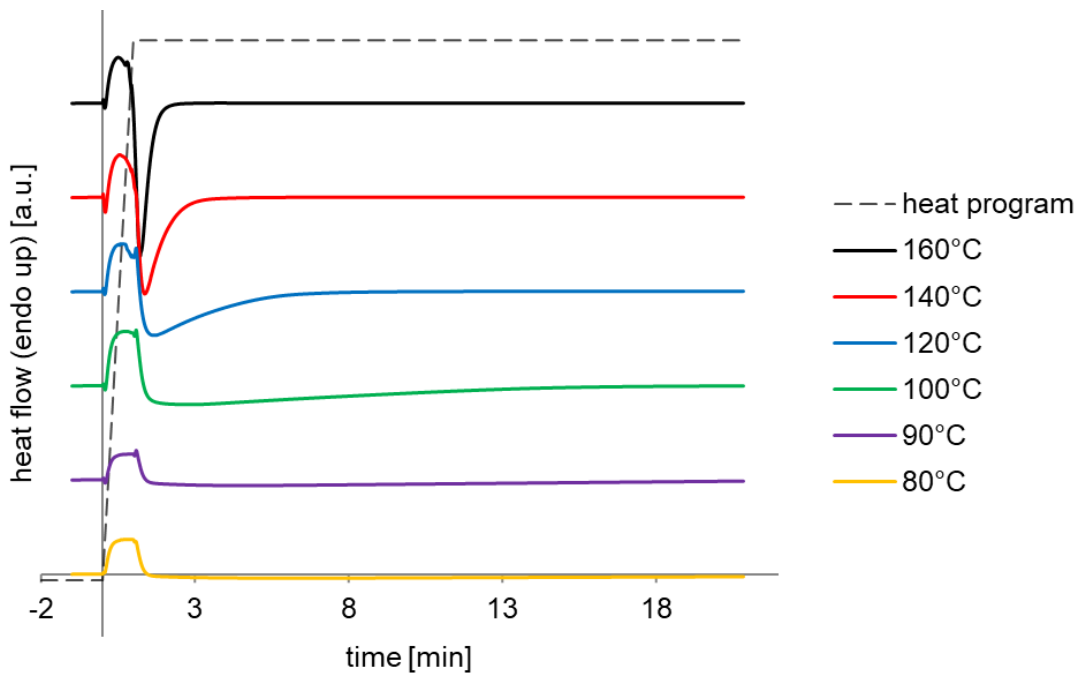
Scheme 102: Stacked isothermal curing curves of the system DPDGE/A6/**5u-Me-CO₂** (100:200:8). The dashed line represents the heat program.

Scheme 103: Stacked DSC thermograms of post-isothermal heat ramp from 20 to 250°C applying a heat rate of 20 K/min for the resin system DPDGE/A6/**5u-Me-CO₂** (ratio 100:200:8). The temperatures in the legend represent the temperature of the isothermal pre-curing of the sample (20 min).

Scheme 104: Viscosities of the system DPDGE/A6/**5u-Me-CO₂** (100:200:8) as determined by
rheology measurements at various temperatures.

Scheme 105: Stacked isothermal curing curves of the system ECHDE/A7/**5u-Me-CO₂**
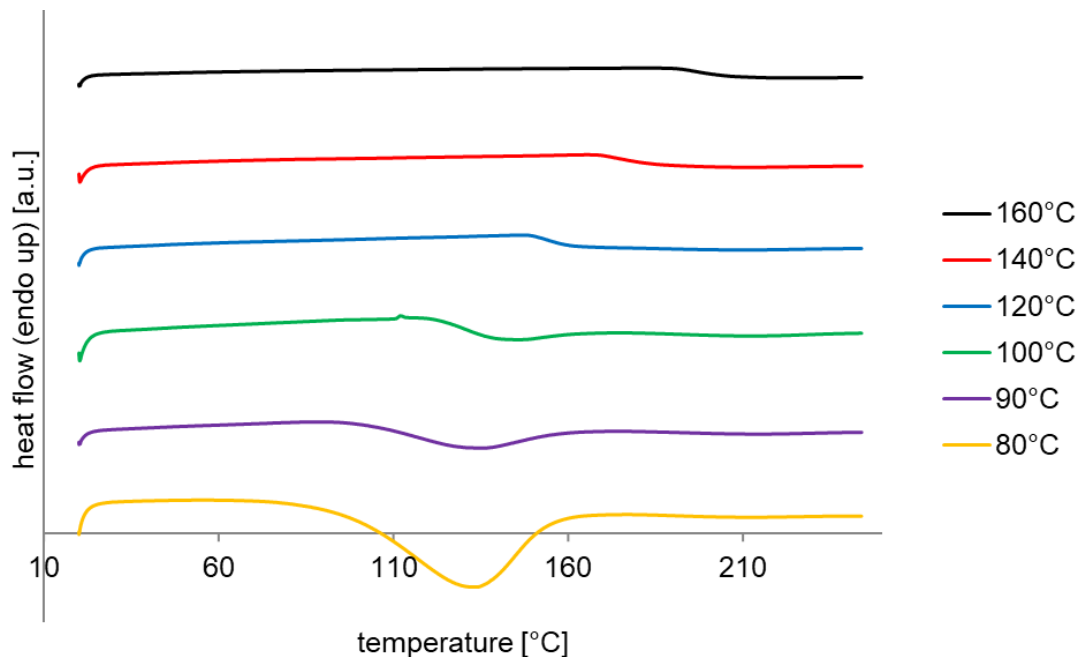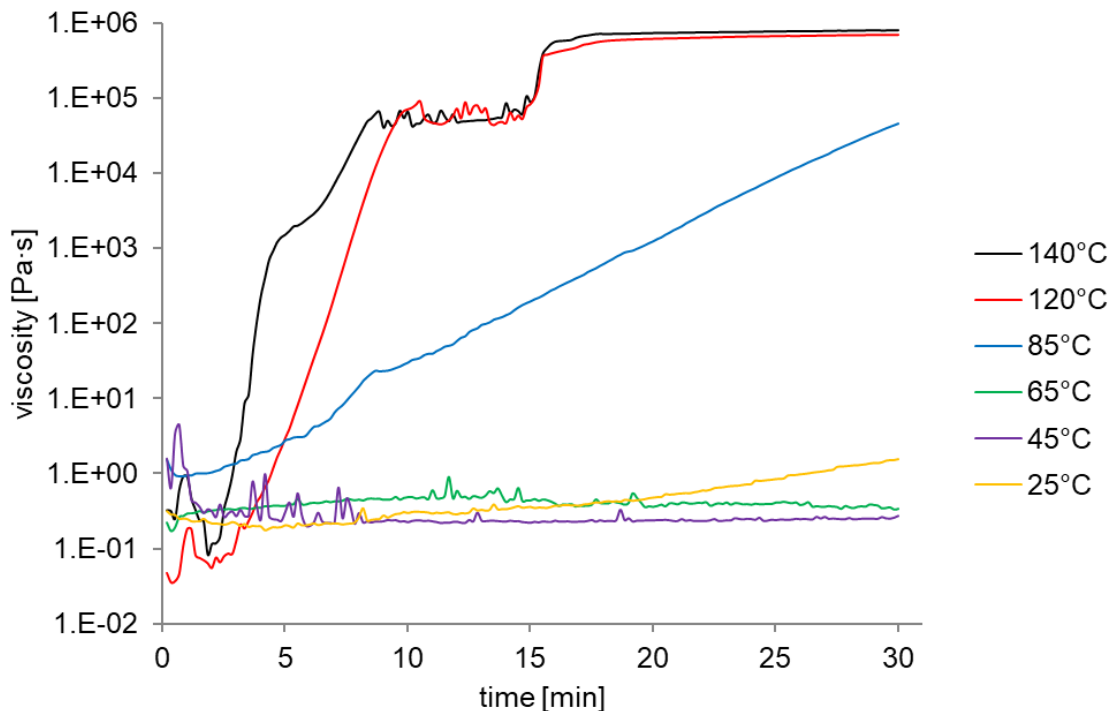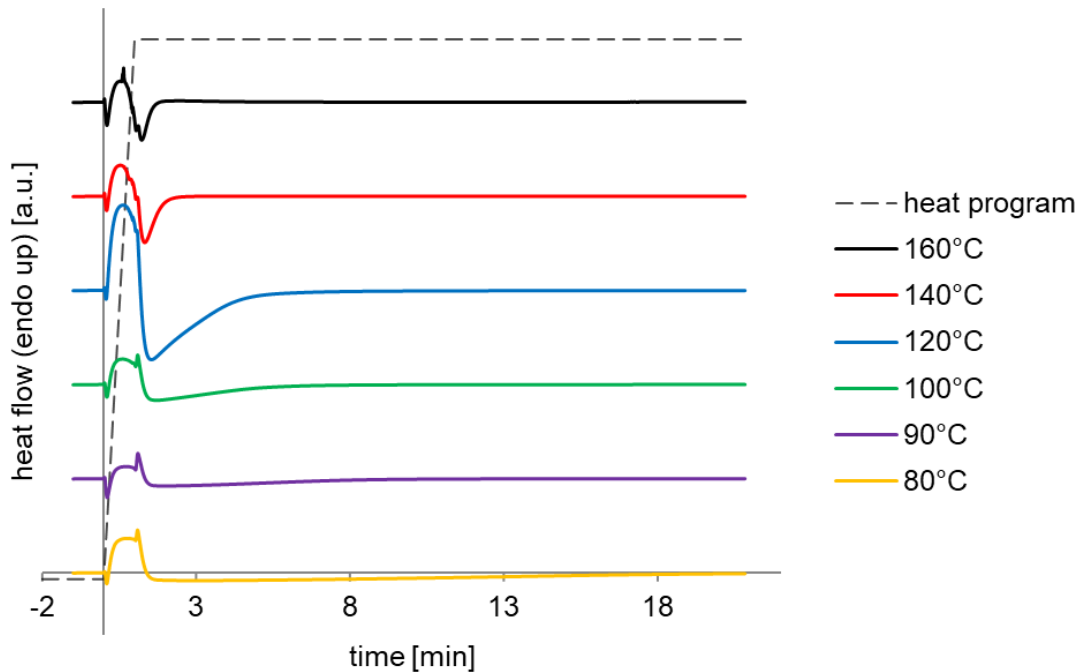(100:200:8). The dashed line represents the heat program.

Scheme 106: Stacked DSC thermograms of post-isothermal heat ramp from 20 to 250°C applying a heat rate of 20 K/min for the resin system ECHDE/A7/**5u-Me-CO$_2$** (ratio 100:200:8). The temperatures in the legend represent the temperature of the isothermal pre-curing of the sample (20 min).

Scheme 107: Viscosities of the system ECHDE/A7/**5u-Me-CO$_2$** (100:200:8) as determined by rheology measurements at various temperatures.

Scheme 108: Stacked isothermal curing curves of the system ECHDE/A6/**5u-Me-CO₂**
(100:200:8). The dashed line represents the heat program.
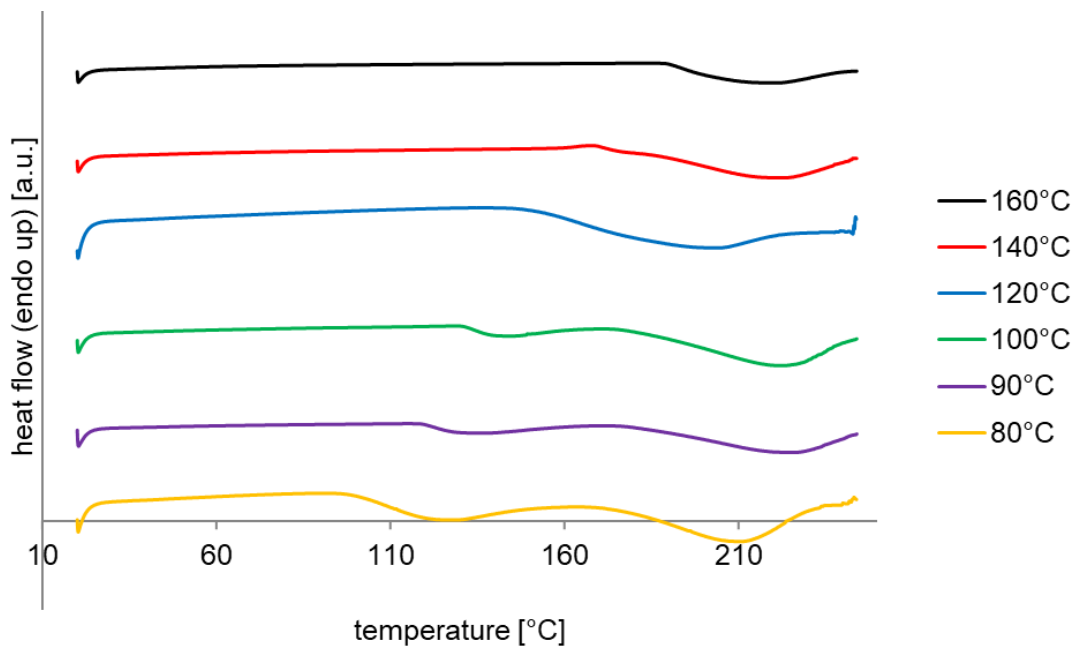

Scheme 109: Stacked DSC thermograms of post-isothermal heat ramp from 20 to 250°C applying
a heat rate of 20 K/min for the resin system ECHDE/A6/**5u-Me-CO₂** (ratio 100:200:8). The
temperatures in the legend represent the temperature of the isothermal pre-curing of the sample
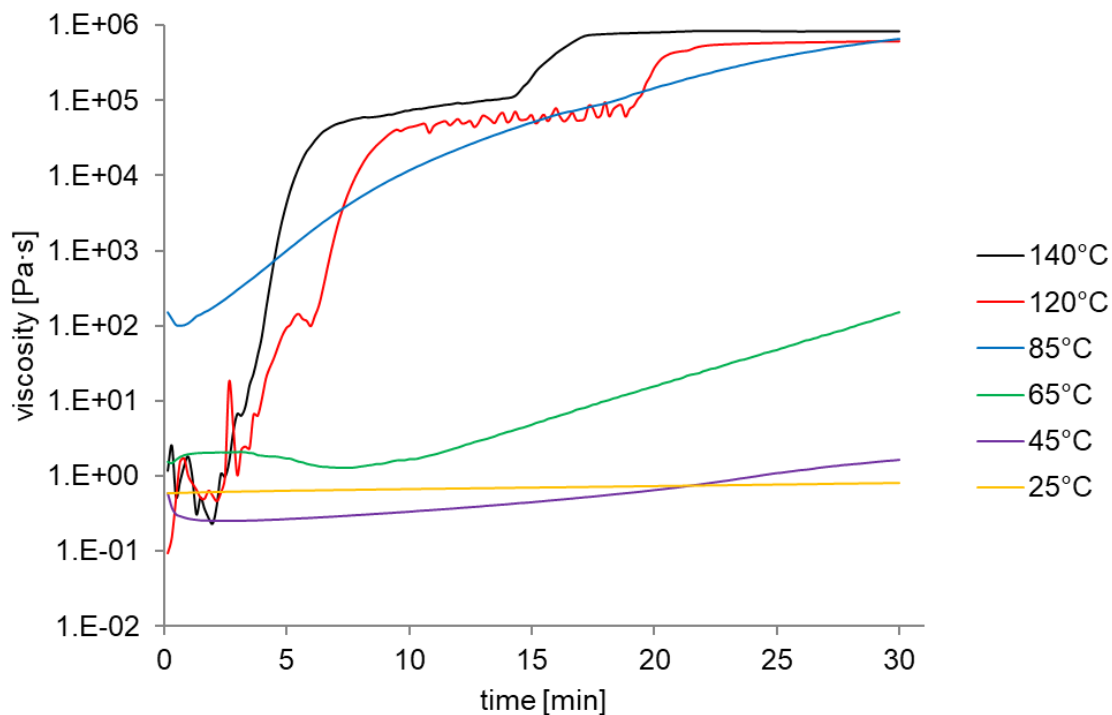(20 min).

Scheme 110: Viscosities of the system ECHDE/A6/**5u-Me-CO$_2$** (100:200:8) as determined by rheology measurements at various temperatures.
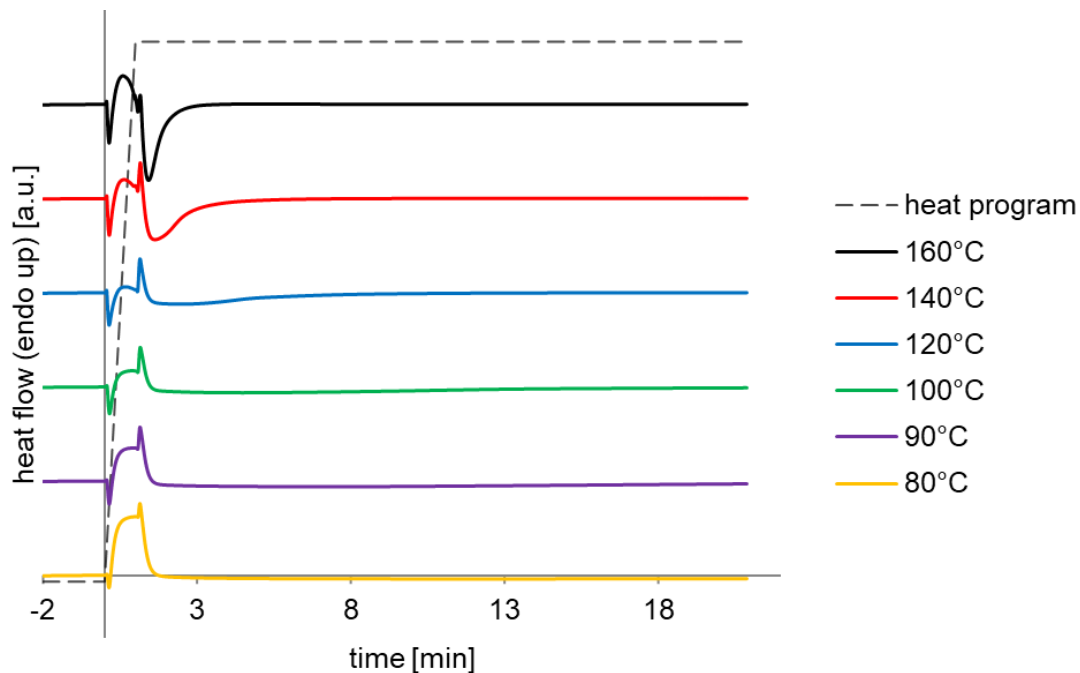

Scheme 111: Stacked isothermal curing curves of the system BADGE/2-(phenoxymethyl)oxirane/A1/A10/**5u-Me-CO$_2$** (50:100:100:100:8). The dashed line represents the heat program.
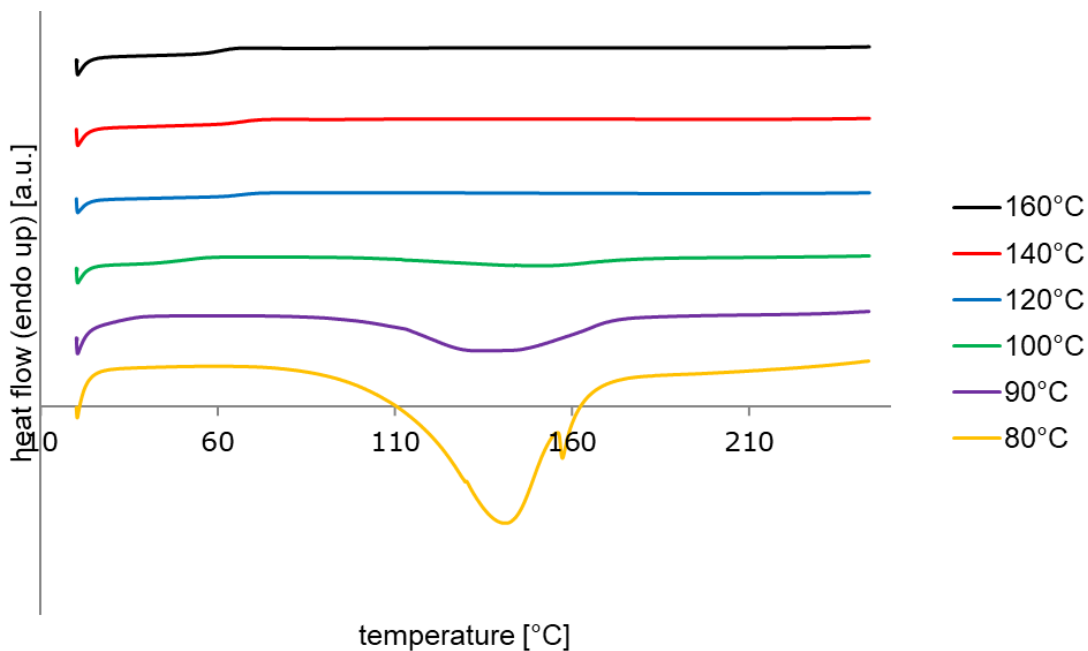
Scheme 112: Stacked DSC thermograms of post-isothermal heat ramp from 20 to 250°C applying a heat rate of 20 K/min for the resin system BADGE/2-(phenoxymethyl)oxirane/A1/A10/**5u-Me-CO₂** (50:100:100:100:8). The temperatures in the legend represent the temperature of the isothermal pre-curing of the sample (20 min).

Scheme 113: Viscosities of the system BADGE/2-(phenoxymethyl)oxirane/A1/A10/**5u-Me-CO₂** (50:100:100:100:8) as determined by rheology measurements at various temperatures.

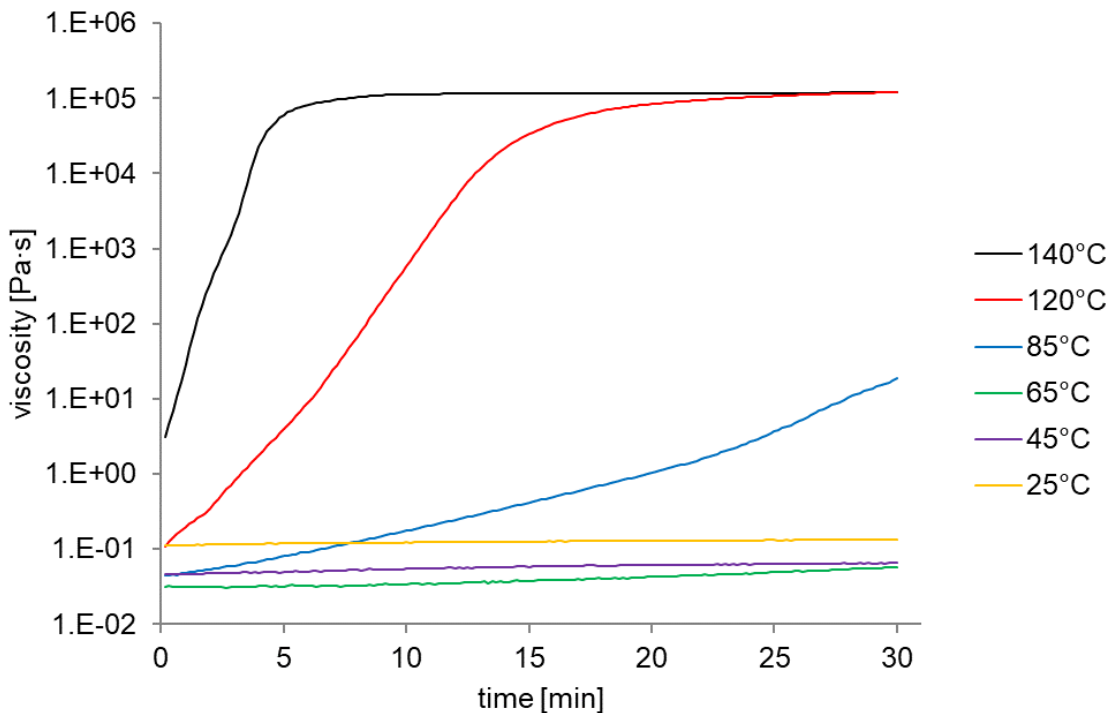## 9.3 Data on Polyoxazolidin-2-ones

Many of the results of this chapter are published: H. J. Altmann, M. Clauss, S. König, E. Frick-Delaittre, C. Koopmans, A. Wolf, C. Guertler, S. Naumann, M. R. Buchmeiser, Synthesis of Linear Poly(oxazolidin-2-one)s by Cooperative Catalysis Based on N-Heterocyclic Carbenes and Simple Lewis Acids, *Macromolecules* **2019**, *52*, 487-494.[5]
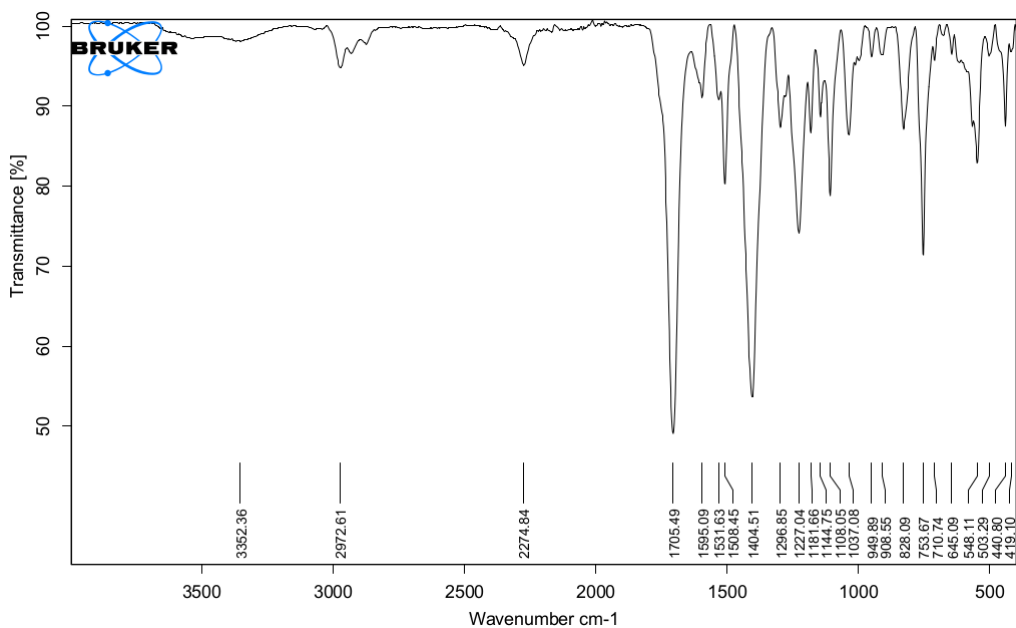
Scheme 114: IR spectrum of the product resulting from an one-pot reaction of BADGE (100 equivalents) and TDI (100 equivalents) catalyzed by $MgCl_2$ (1 equivalent) at 60°C for 5 days in sulfolane.
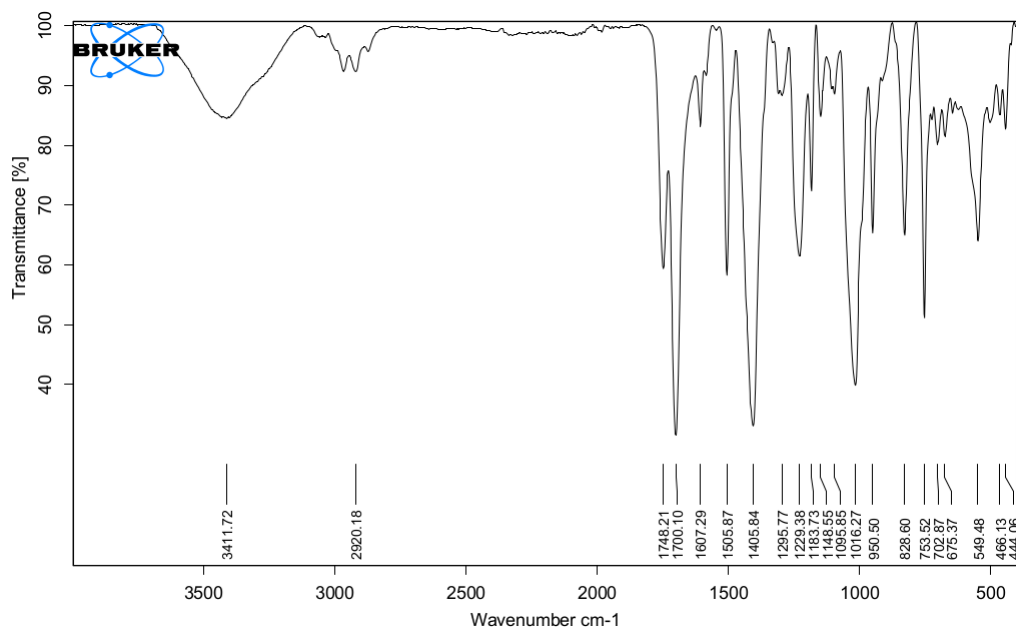
Scheme 115: IR spectrum of the product resulting from an one-pot reaction of BADGE (100 equivalents) and TDI (100 equivalents) catalyzed by **5u-Me-CO₂** (1 equivalent) and MgCl₂ (1 equivalent) at 60°C for 6 hours in sulfolane.
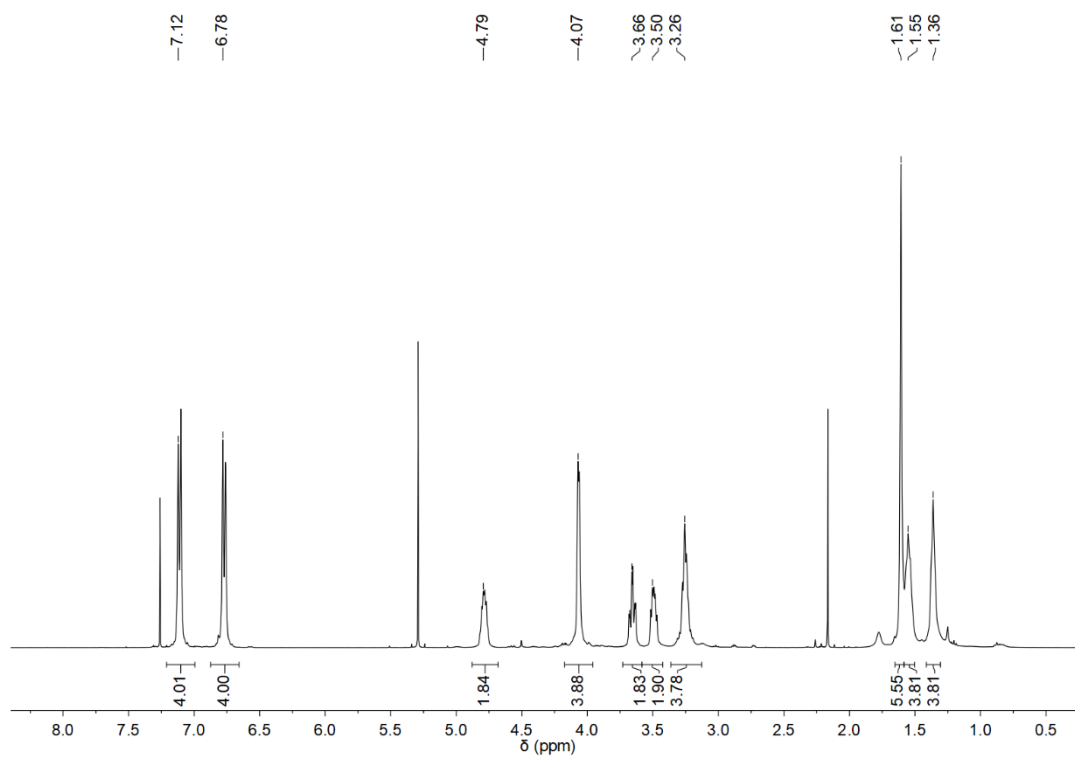
Scheme 116: ^{1}H NMR spectrum of POxa-BADGE-HDI (CDCl₃).
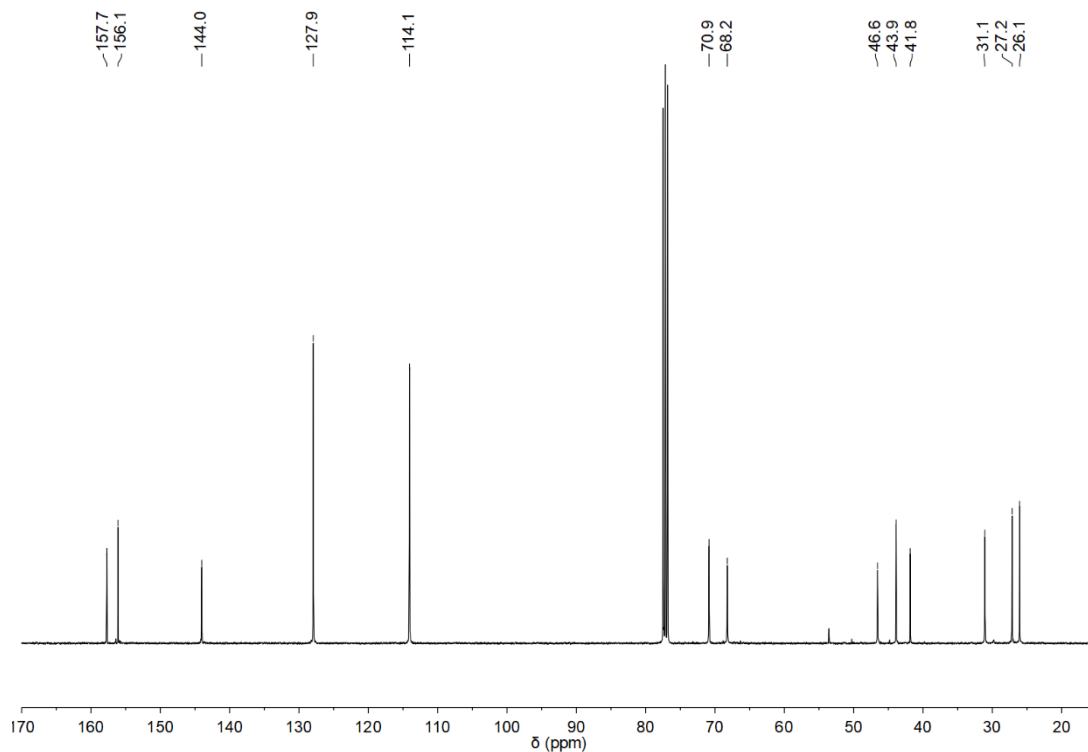
Scheme 117: ^{13}C NMR spectrum of POxa-BADGE-HDI (CDCl$_3$).
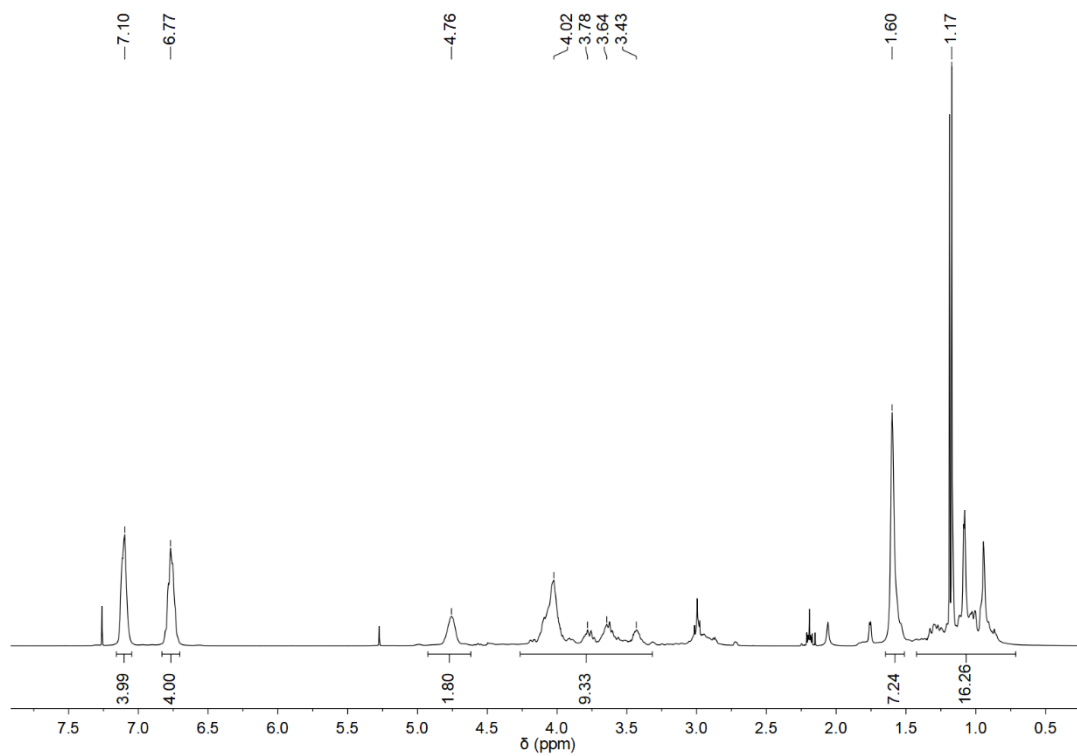
Scheme 118: ^{1}H NMR spectrum of POxa-BADGE-IPDI (CDCl$_3$).
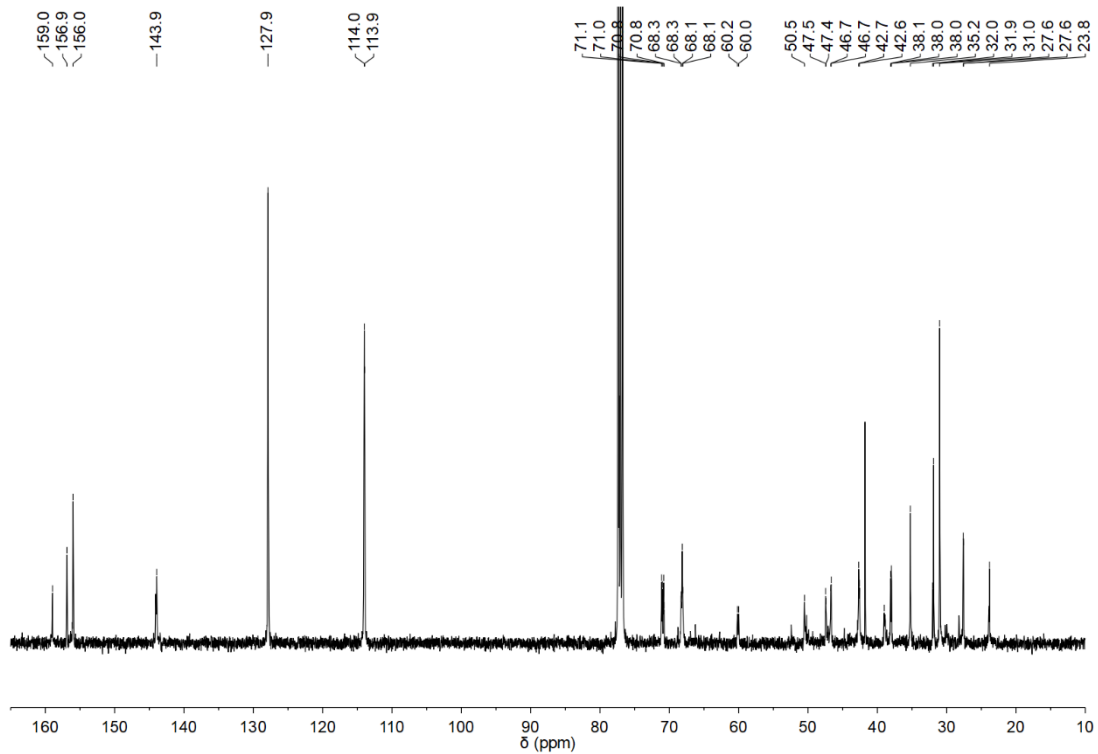
Scheme 119: ^{13}C NMR spectrum of POxa-BADGE-IPDI (CDCl$_3$).
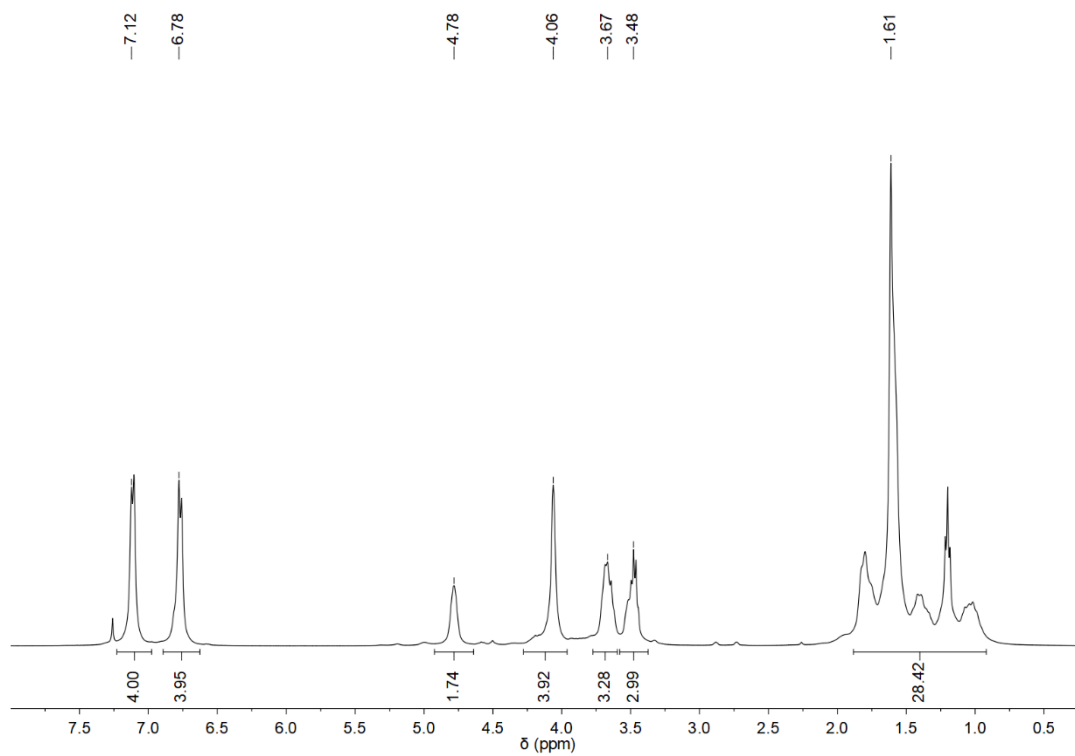
Scheme 120: ^{1}H NMR spectrum of POxa-BADGE-H$_{12}$MDI (CDCl$_3$).
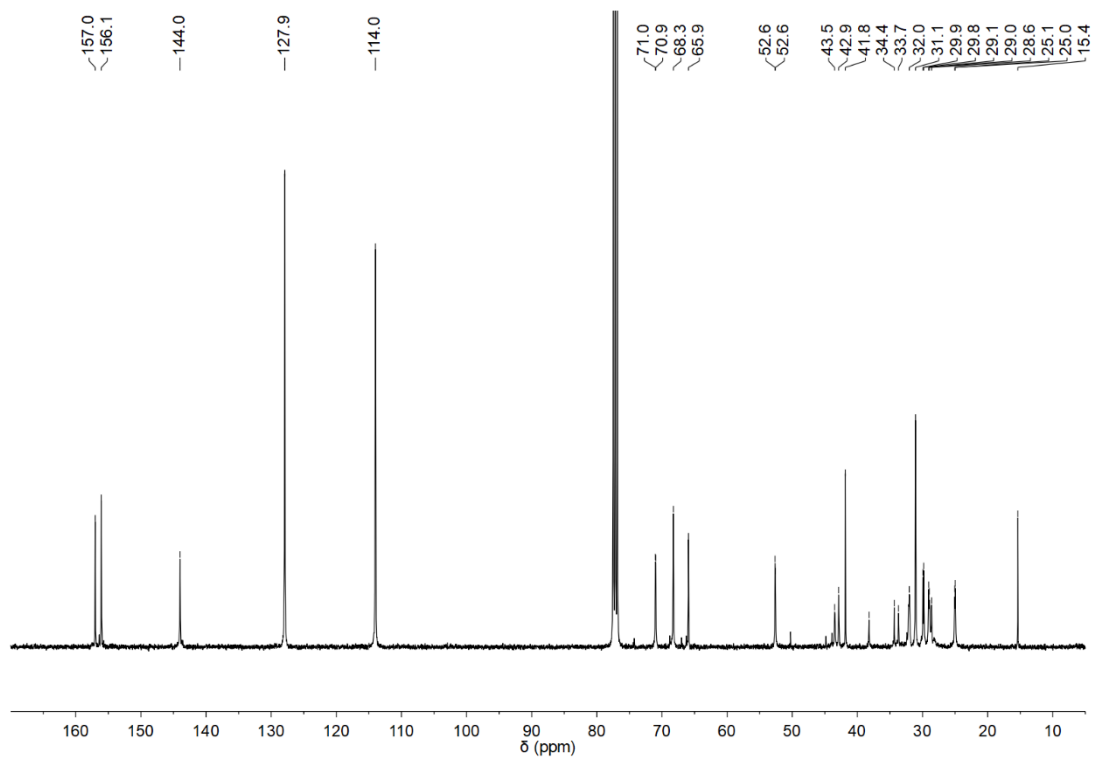
Scheme 121: ^{13}C NMR spectrum of POxa-BADGE-H$_{12}$MDI (CDCl$_3$).
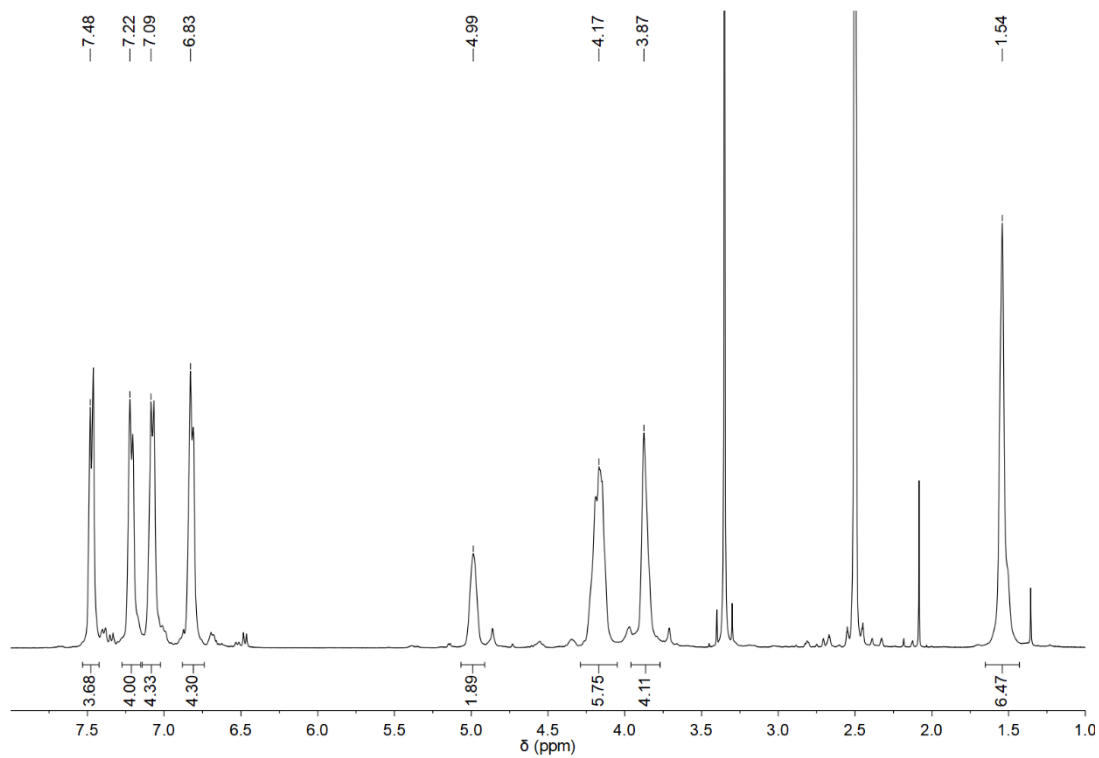
Scheme 122: ^{1}H NMR spectrum of POxa-BADGE-MDI (DMSO-d6).
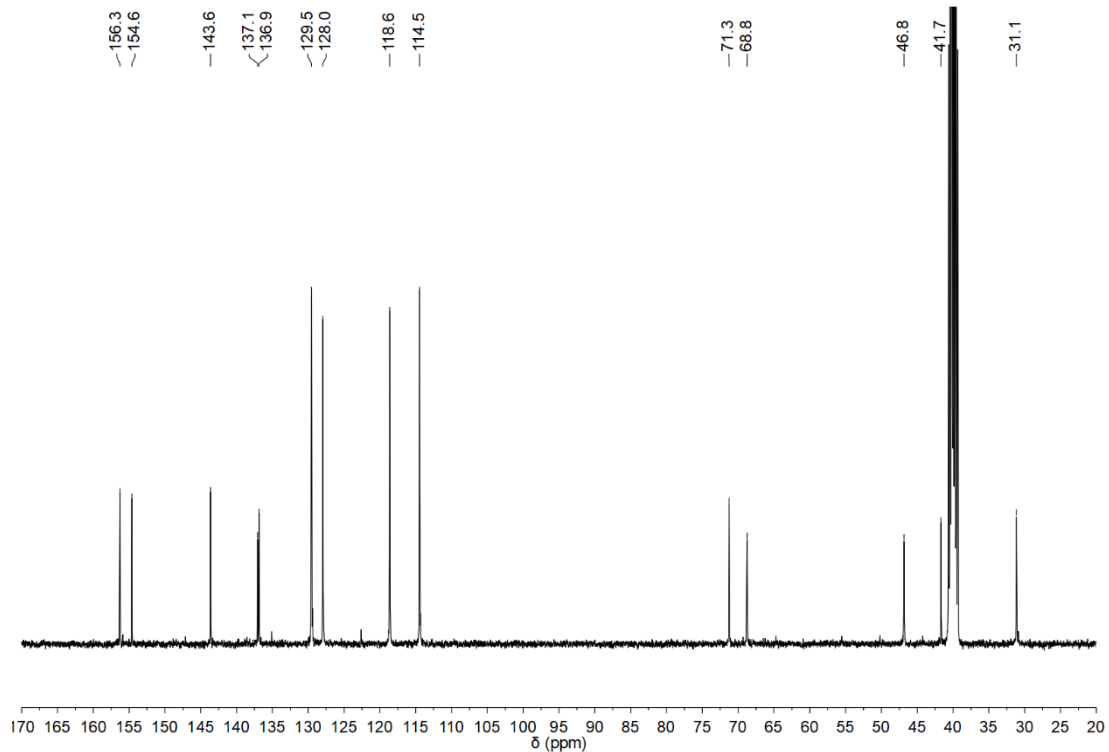
Scheme 123: ^{13}C NMR spectrum of POxa-BADGE-MDI (DMSO-d6).
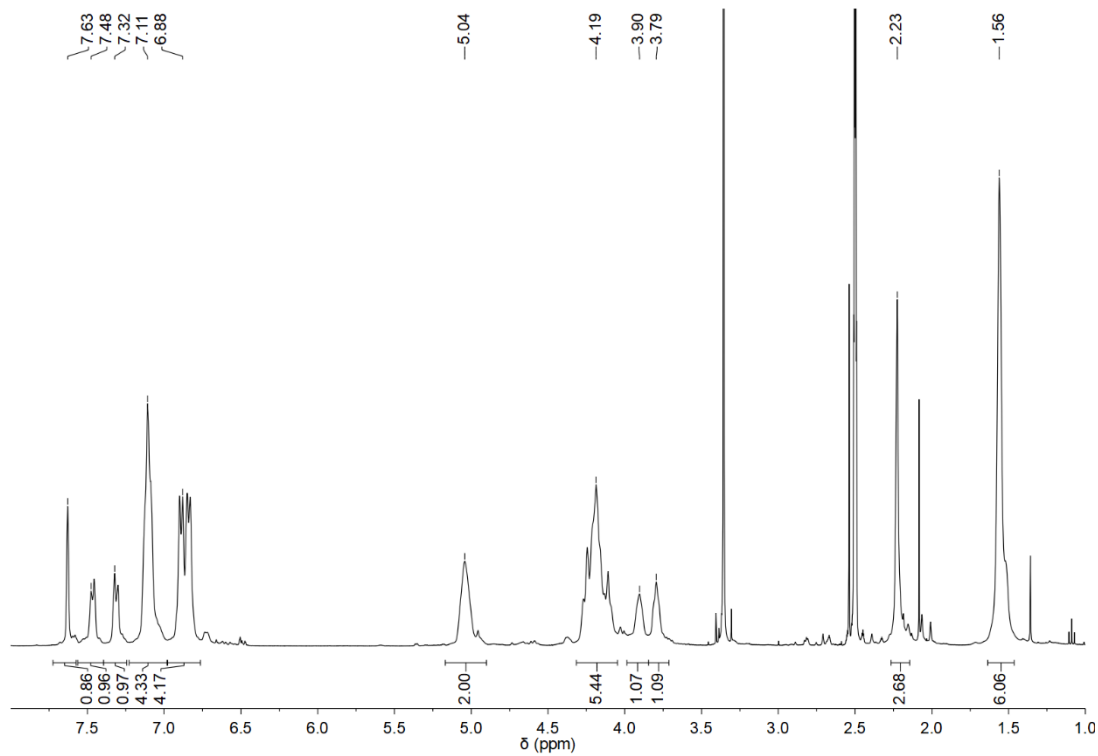
Scheme 124: ^{1}H NMR spectrum of POxa-BADGE-TDI (DMSO-d6).
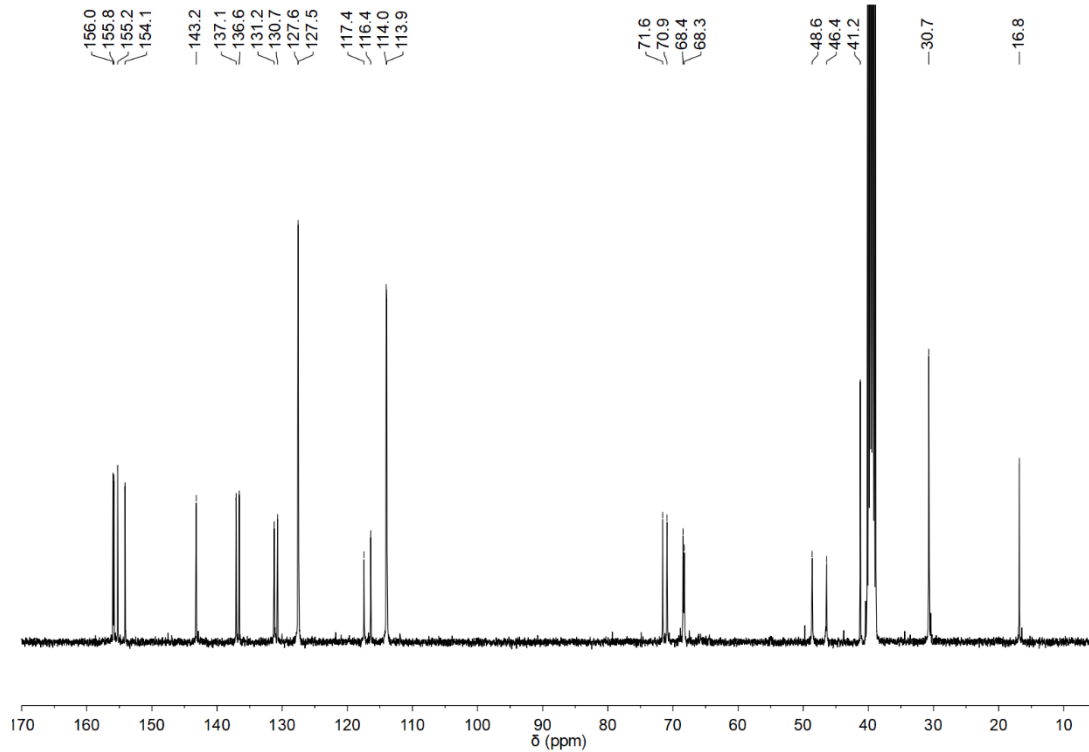
Scheme 125: ^{13}C NMR spectrum of POxa-BADGE-TDI (DMSO-d6).
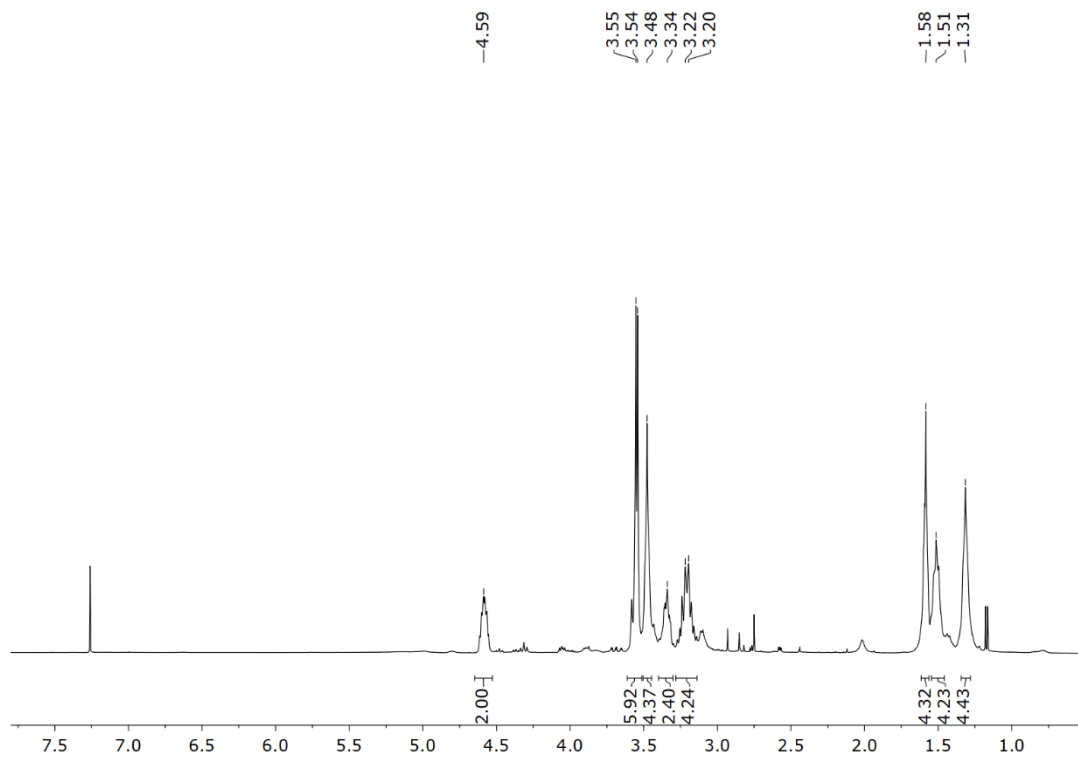
Scheme 126: ^{1}H NMR spectrum of POxa-BDDGE-HDI (CDCl$_3$).
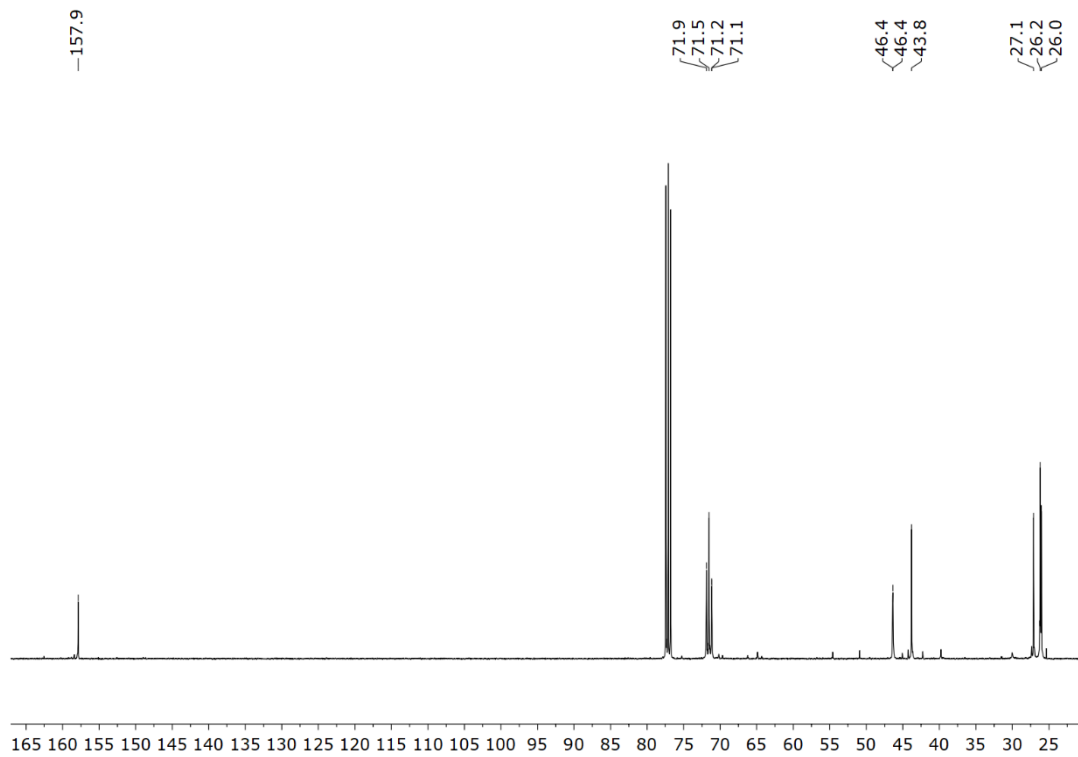
Scheme 127: ^{13}C NMR spectrum of POxa-BDDGE-HDI (CDCl$_3$).
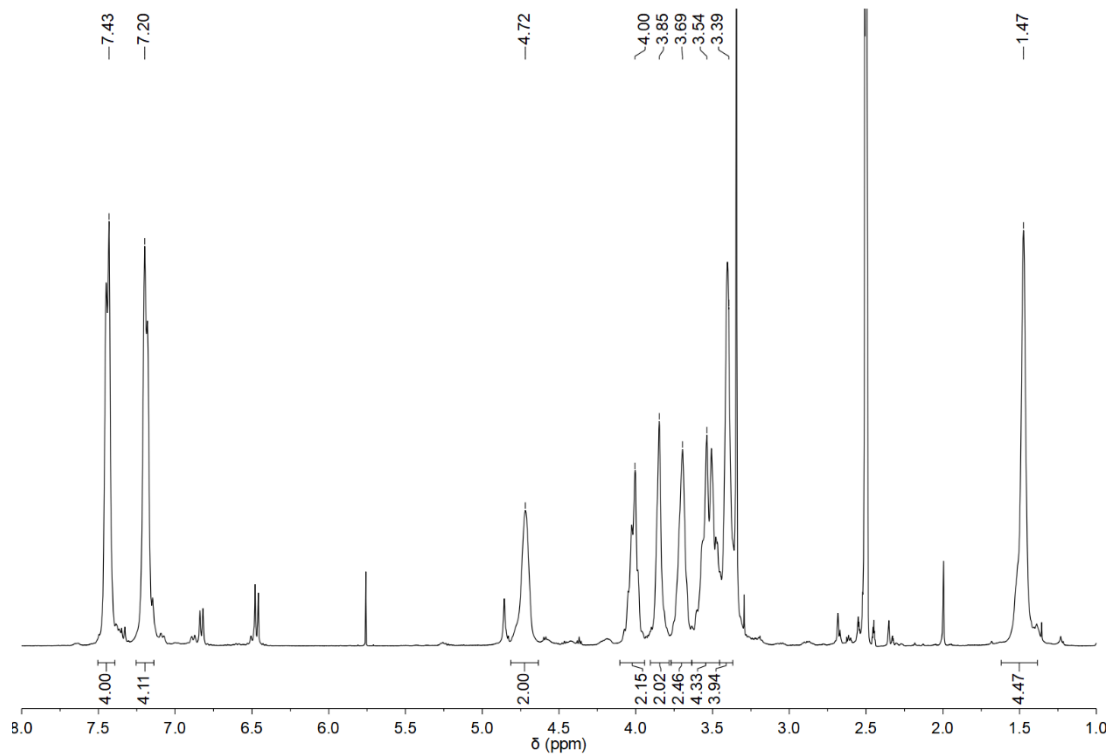
Scheme 128: ^{1}H NMR spectrum of POxa-BDDGE-MDI (DMSO-d6).

Scheme 129: ^{13}C NMR spectrum of POxa-BDDGE-MDI (DMSO-d6).

Scheme 130: ^{1}H NMR spectrum of coPOxa-BADGE-HDI/MDI (CDCl$_3$).

Scheme 131: ^{13}C NMR spectrum of coPOxa-BADGE-HDI/MDI (CDCl$_3$).

Scheme 132: ^{1}H NMR spectrum of block-coPOxa-BADGE-HDI/MDI (CDCl$_3$).

217

Scheme 133: ^{13}C NMR spectrum of block-coPOxa-BADGE-HDI/MDI (CDCl$_3$).

Scheme 134: ^{1}H NMR spectrum of 4-(phenoxymethyl)-3-phenyloxazolidin-2-one (CDCl$_3$).
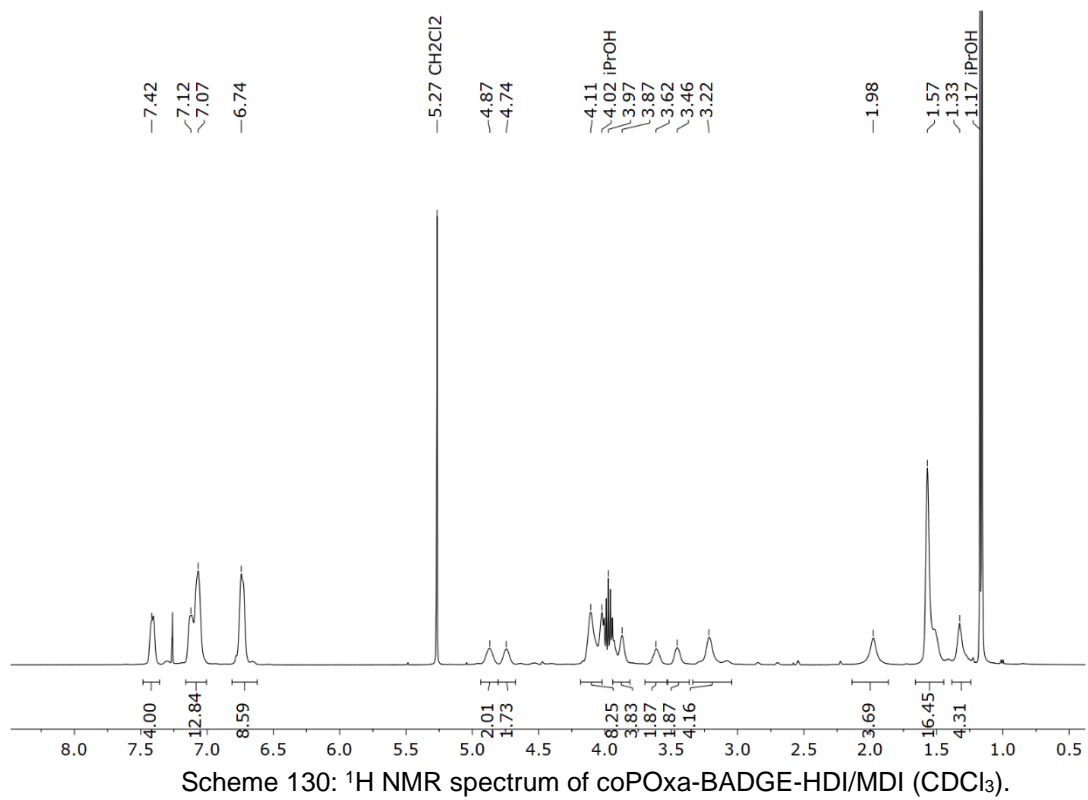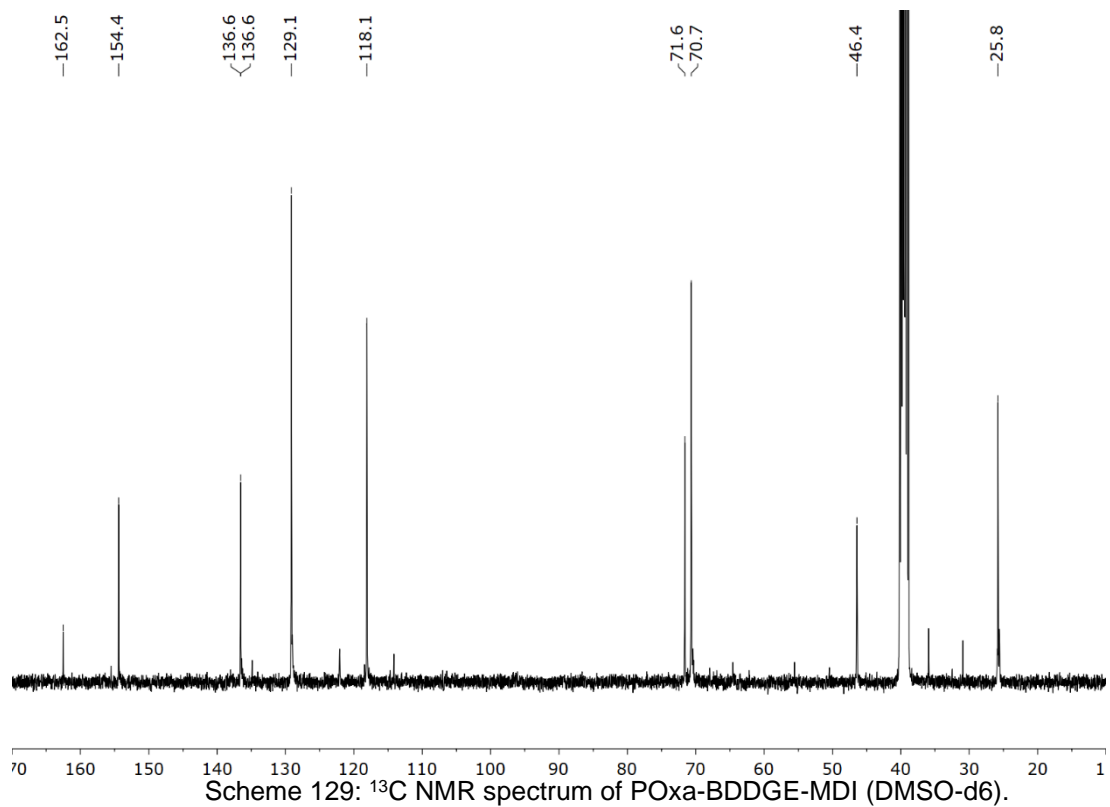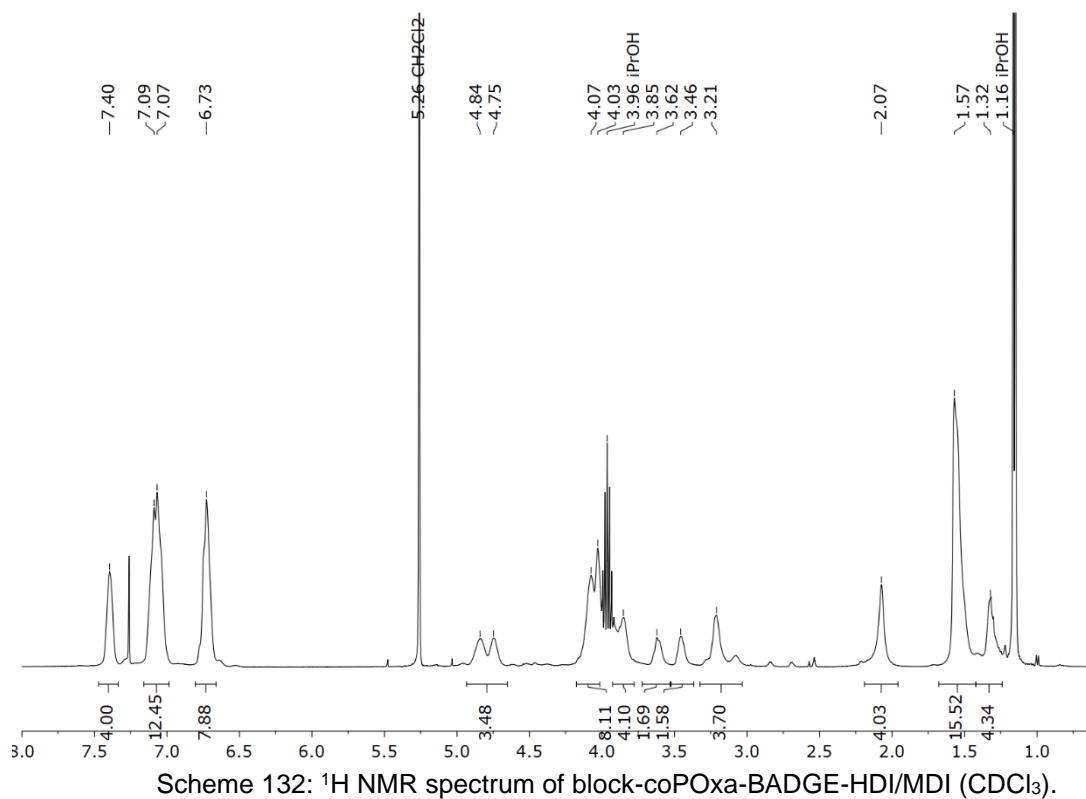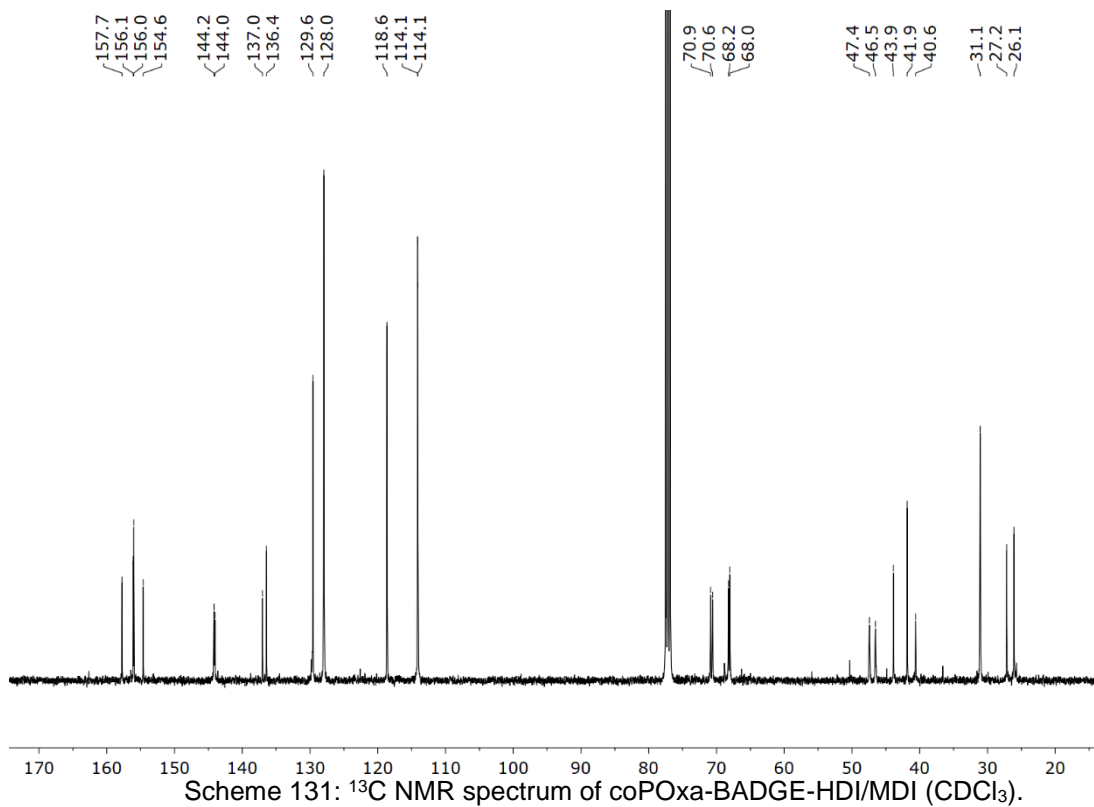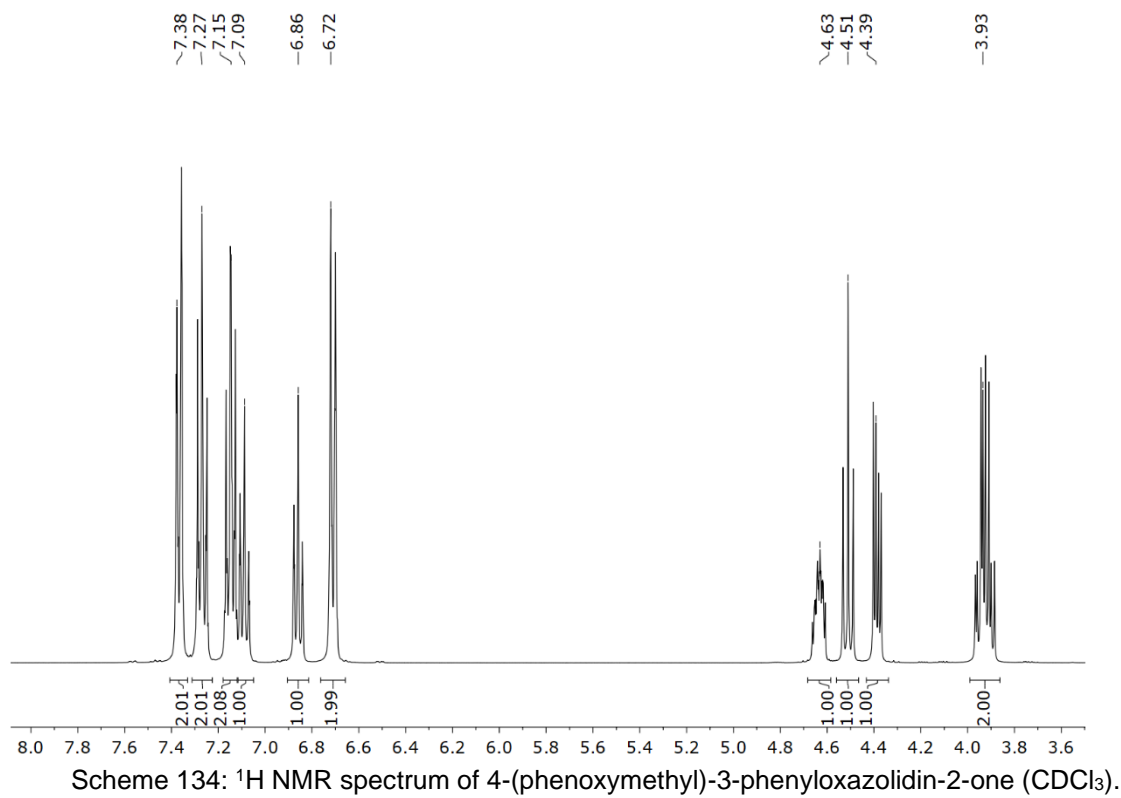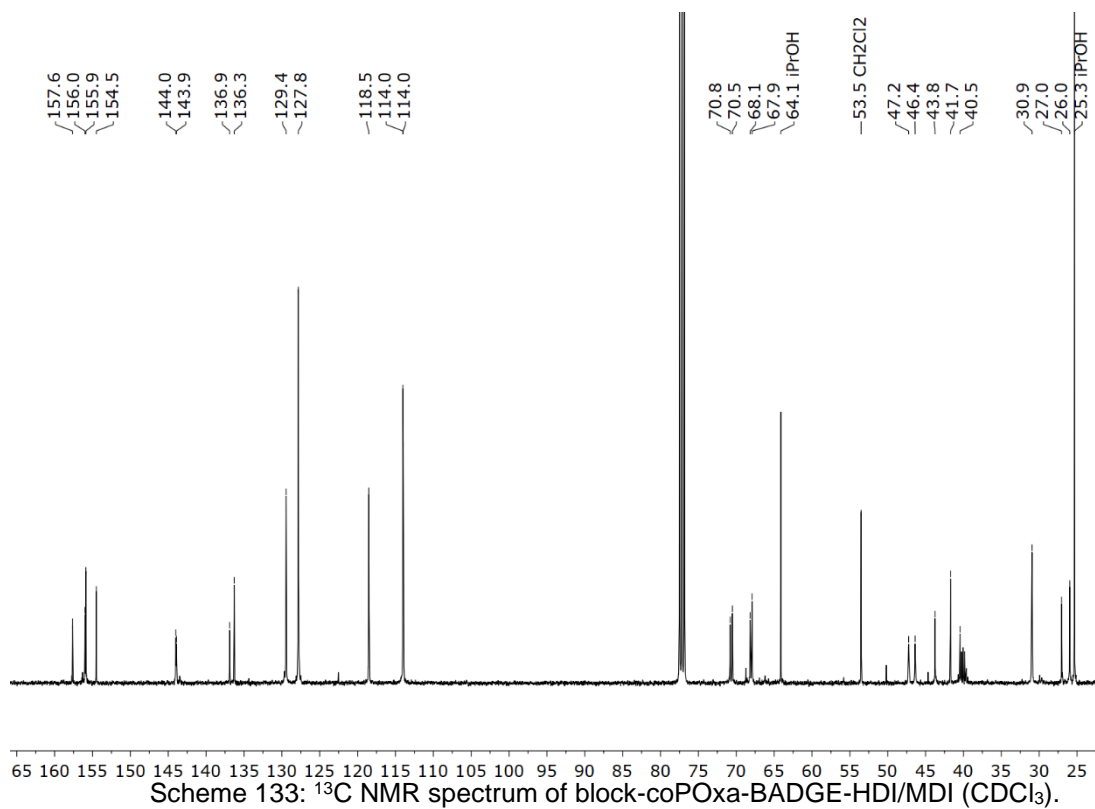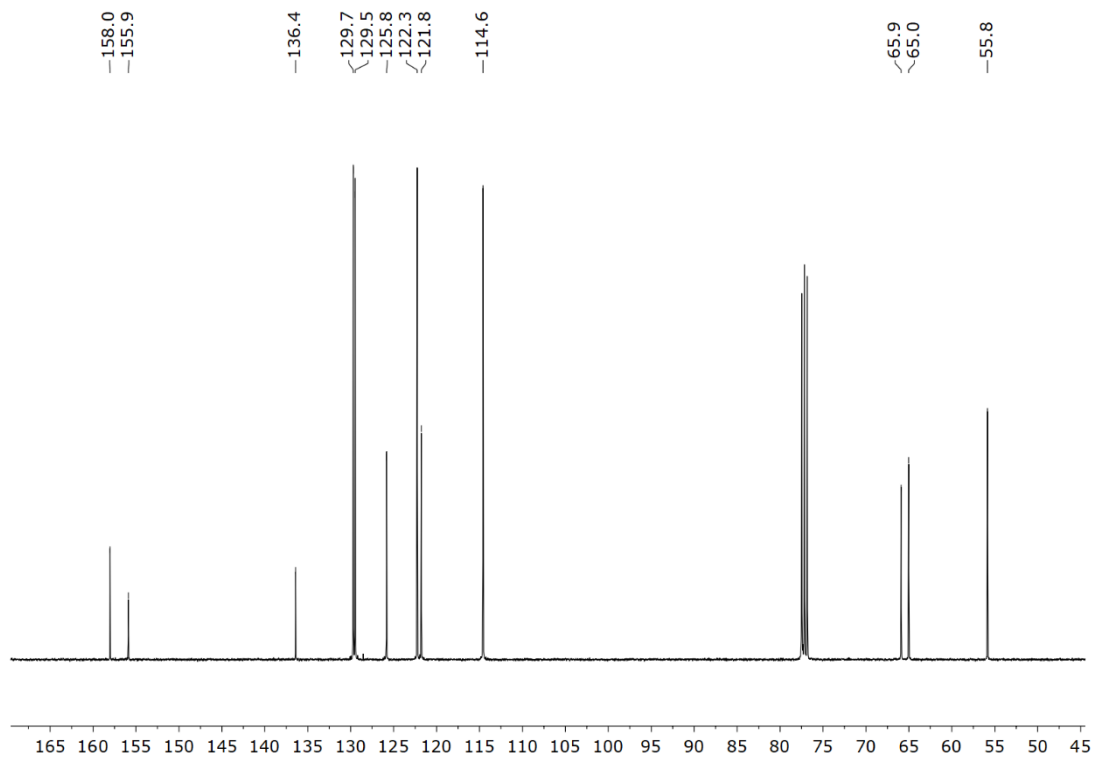
Scheme 135: ^{13}C NMR spectrum of 4-(phenoxymethyl)-3-phenyloxazolidin-2-one (CDCl$_3$).
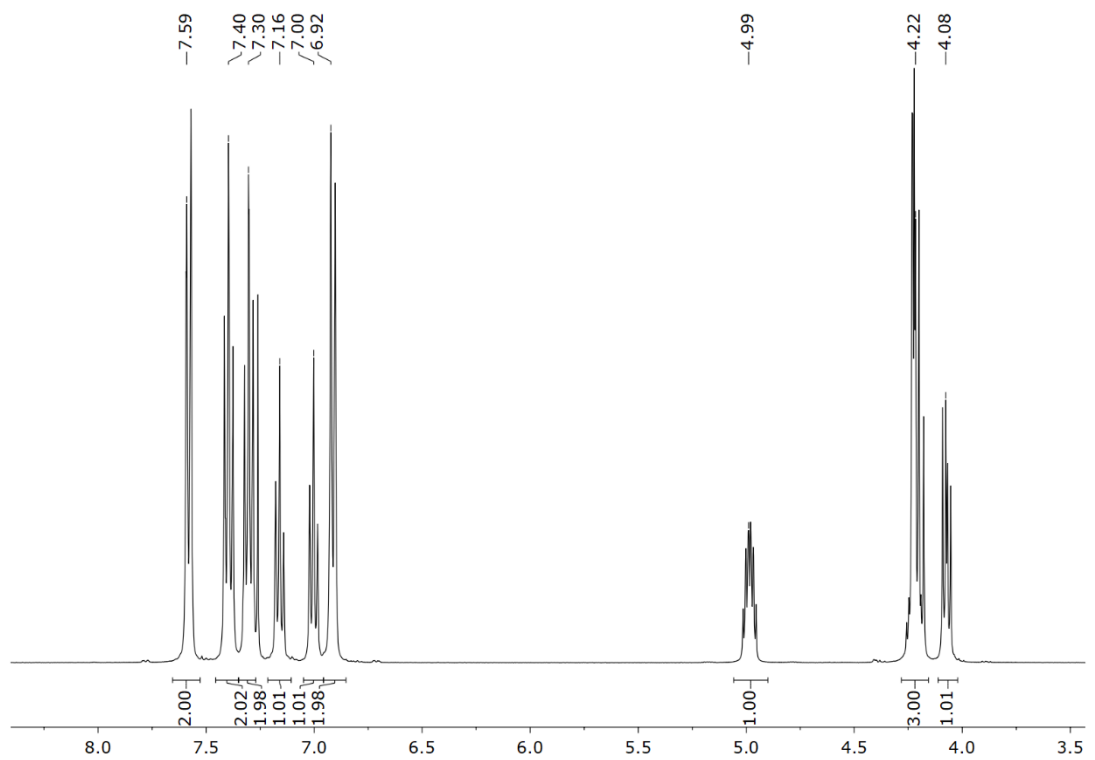
Scheme 136: ^{1}H NMR spectrum of 5-(phenoxymethyl)-3-phenyloxazolidin-2-one (CDCl$_3$).
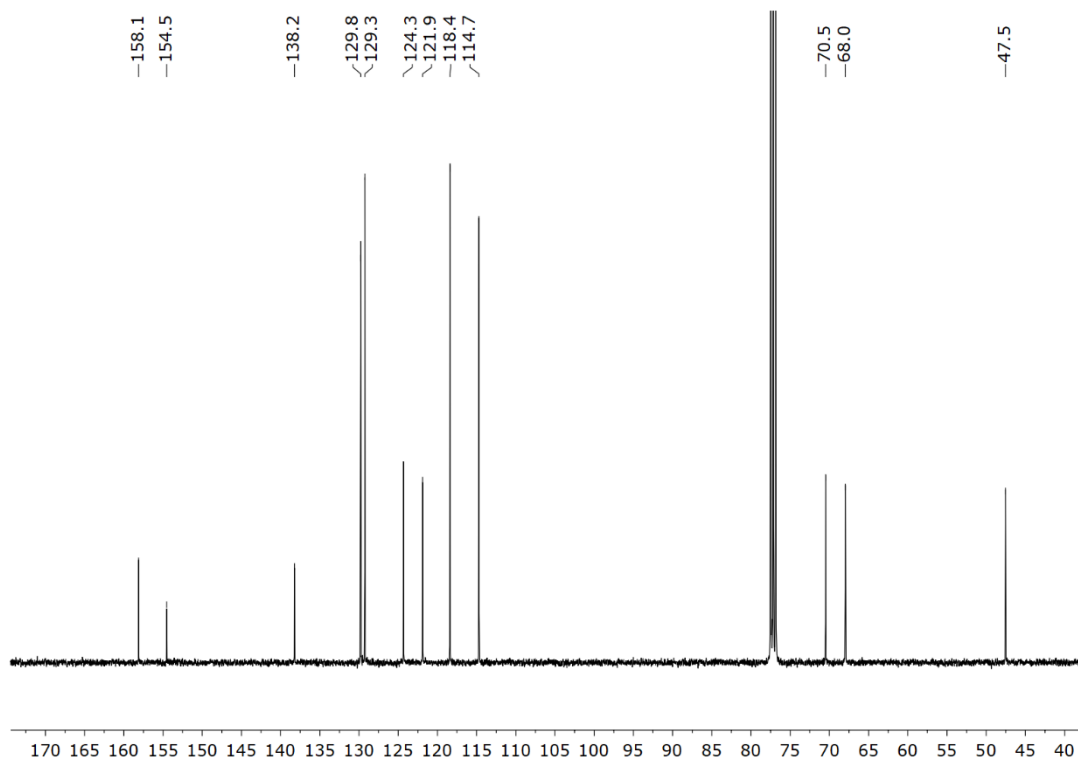
Scheme 137: ^{13}C NMR spectrum of 5-(phenoxymethyl)-3-phenyloxazolidin-2-one (CDCl$_3$).

9.4 Data on Polyamide 6

Most of the results described in this chapter are published: H. J. Altmann, M. Steinmann, I. Elser, M. J. Benedikter, S. Naumann, M. R. Buchmeiser, Dual catalysis with an N-heterocyclic carbene and a Lewis acid: Thermally latent precatalyst for the polymerization of ε-caprolactam, *J. Polym. Sci.* **2020**, *58*, 3219-3226.[6]
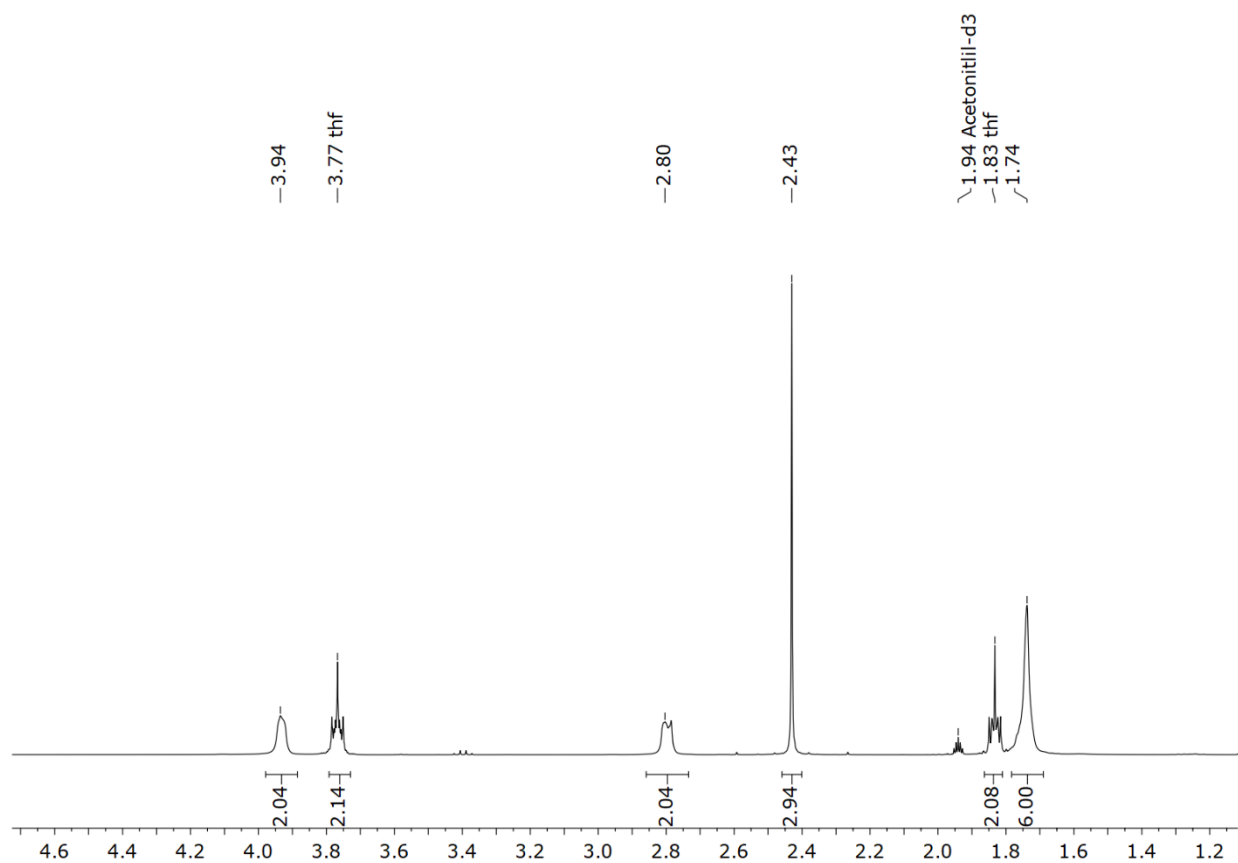
Scheme 138: ^{1}H NMR spectrum of AEO-Ac-MgCl$_2$ in D$_3$CCN.
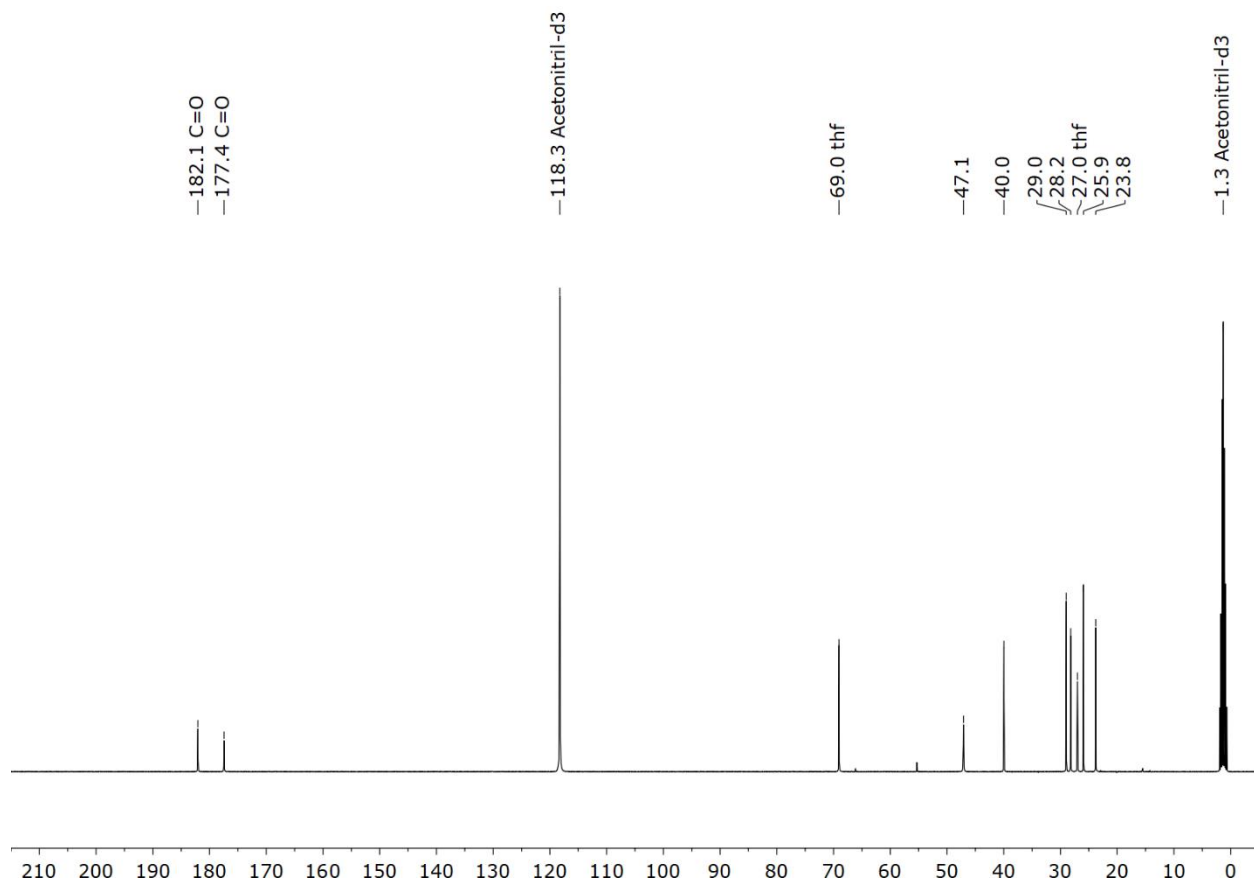
Scheme 139: ^{13}C NMR spectrum of AEO-Ac-MgCl$_2$ in D$_3$CCN.
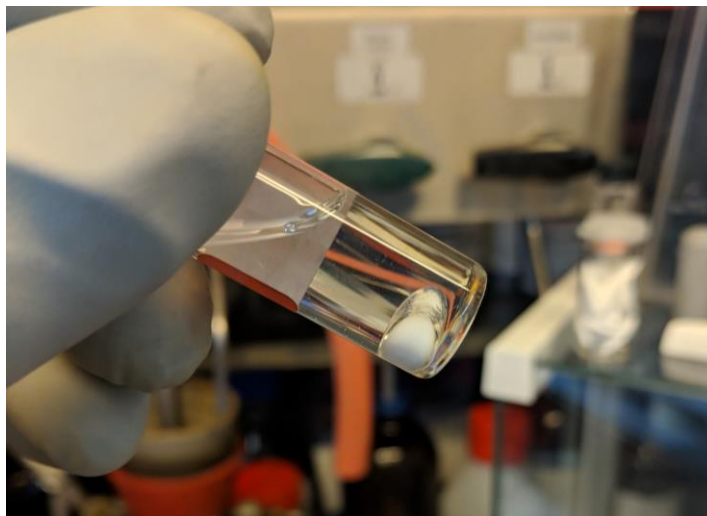
Scheme 140: Homogenized mixture of 100 eq. AEO, 1 eq. **5u-Me-CO$_2$**, 1 eq. MgCl$_2$ and 1 eq. AEO-Ac in the molten state (~75°C).
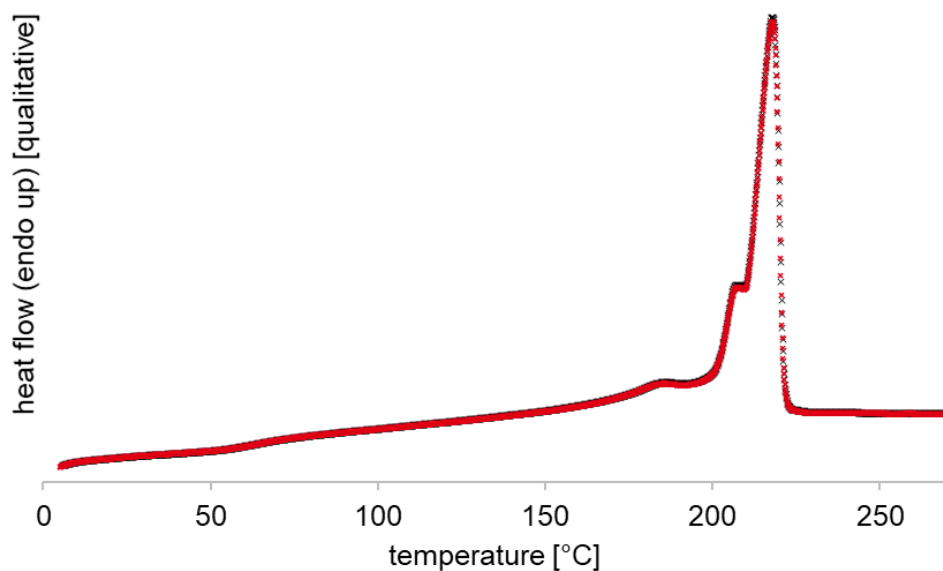
Scheme 141: DSC heating curves (2nd and 3rd cycle, conducted with a heating rate of 10 K/min) of a polyamide 6 synthesized at 200°C from a mixture consisting of 100 equivalents AEO, 1 equivalent **5u-Me-CO$_2$**, 1 equivalent MgCl$_2$ and 1 equivalent AEO-Ac.
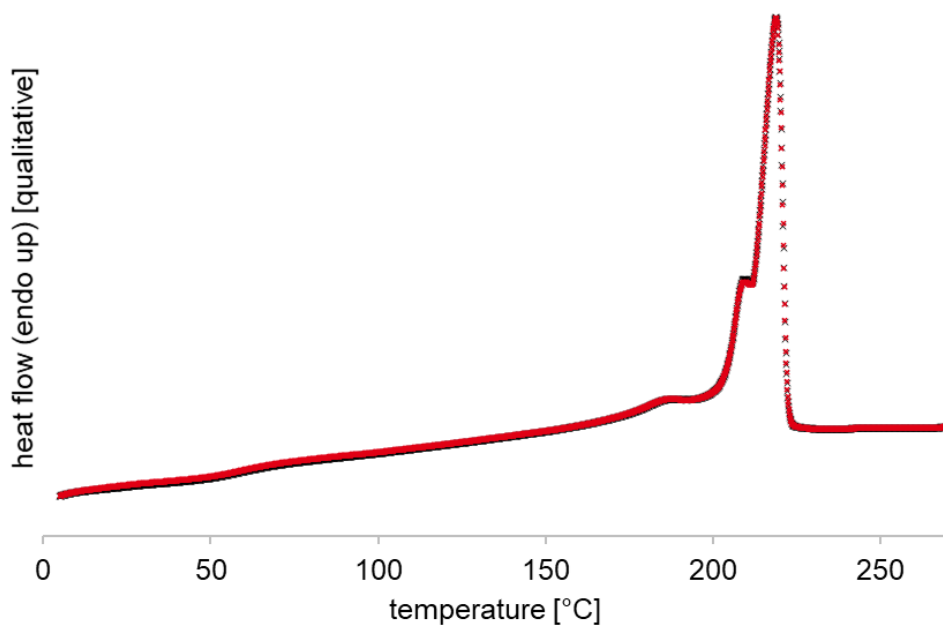
Scheme 142: DSC heating curves (2nd and 3rd cycle, conducted with a heating rate of 10 K/min) of a polyamide 6 synthesized at 200°C from a mixture consisting of 200 equivalents AEO, 1 equivalent **5u-Me-CO$_2$**, 1 equivalent MgCl$_2$ and 1 equivalent AEO-Ac.
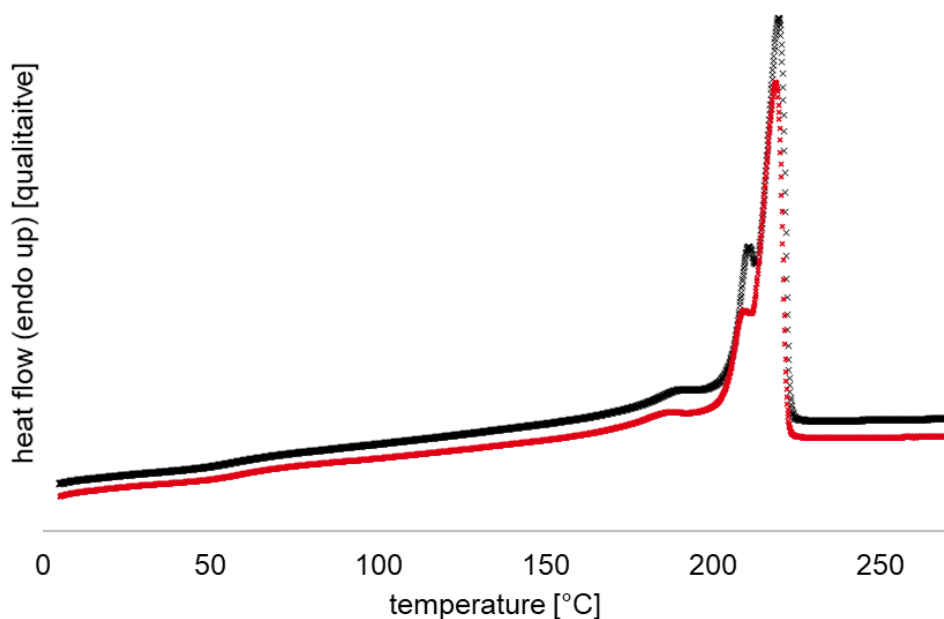
Scheme 143: DSC heating curves (2nd and 3rd cycle, conducted with a heating rate of 10 K/min) of a polyamide 6 synthesized at 200°C from a mixture consisting of 400 equivalents AEO, 1 equivalent **5u-Me-CO₂**, 1 equivalent $MgCl_2$ and 1 equivalent AEO-Ac.
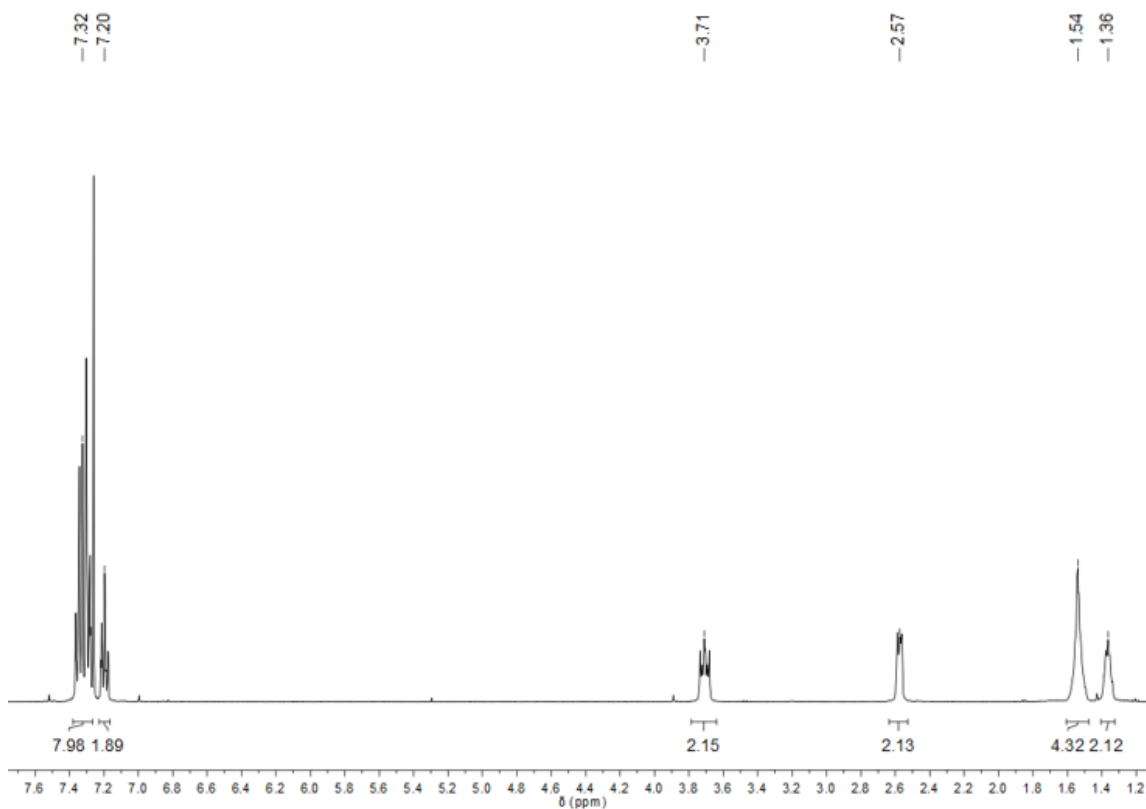
Scheme 144: ^{1}H NMR spectrum of AEO-P(O)(OPh)₂ in CDCl₃.
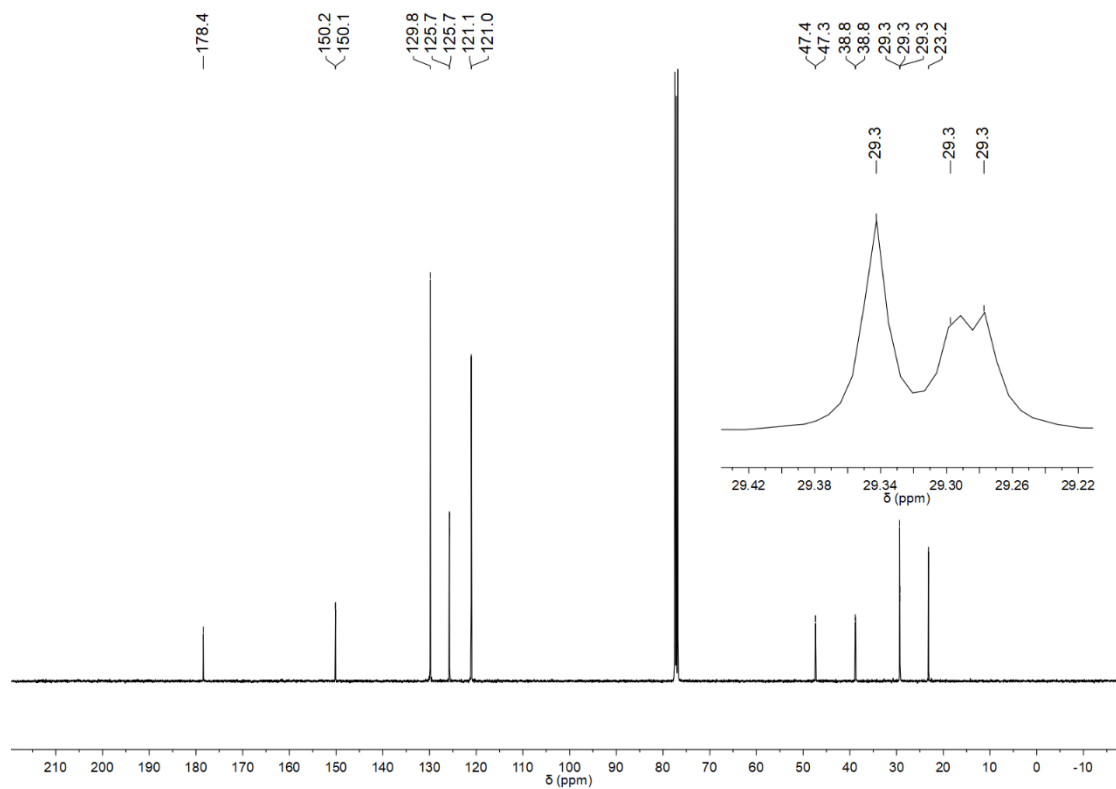
Scheme 145: ^{13}C NMR spectrum of AEO-P(O)(OPh)$_2$ in CDCl$_3$.
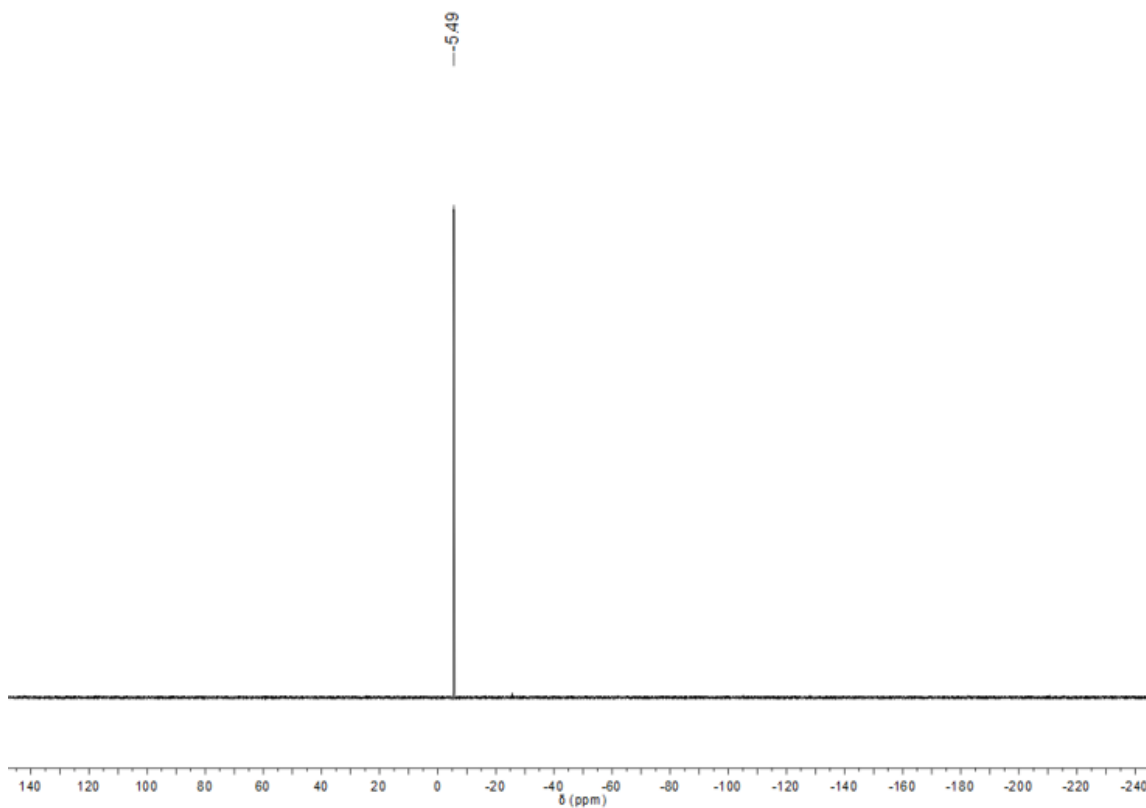
Scheme 146: ^{31}P NMR spectrum of AEO-P(O)(OPh)$_2$ in CDCl$_3$.

Scheme 147: Phosphorescing polyamide 6 synthesized at 200°C from a pre-homogenized (90°C, overnight) polymer system consisting of 400 equivalents AEO, 1 equivalent **5u-Me-CO₂**, 1 equivalent MgCl₂, 1 equivalent AEO-Ac and about 5 to 10 wt.-% of an europium doped aluminum oxide received from lumentics.de.

9.5   Data on Spirocyclic NHC Precursor

The content of this chapter was majorly published: H. J. Altmann, W. Frey, M. R. Buchmeiser, A Spirocyclic Parabanic Acid Masked *N*-Heterocyclic Carbene as Thermally Latent Pre-Catalyst for Polyamide 6 Synthesis and Epoxide Curing, *Macromol. Rapid. Commun.* **2020**, e2000338.[10]
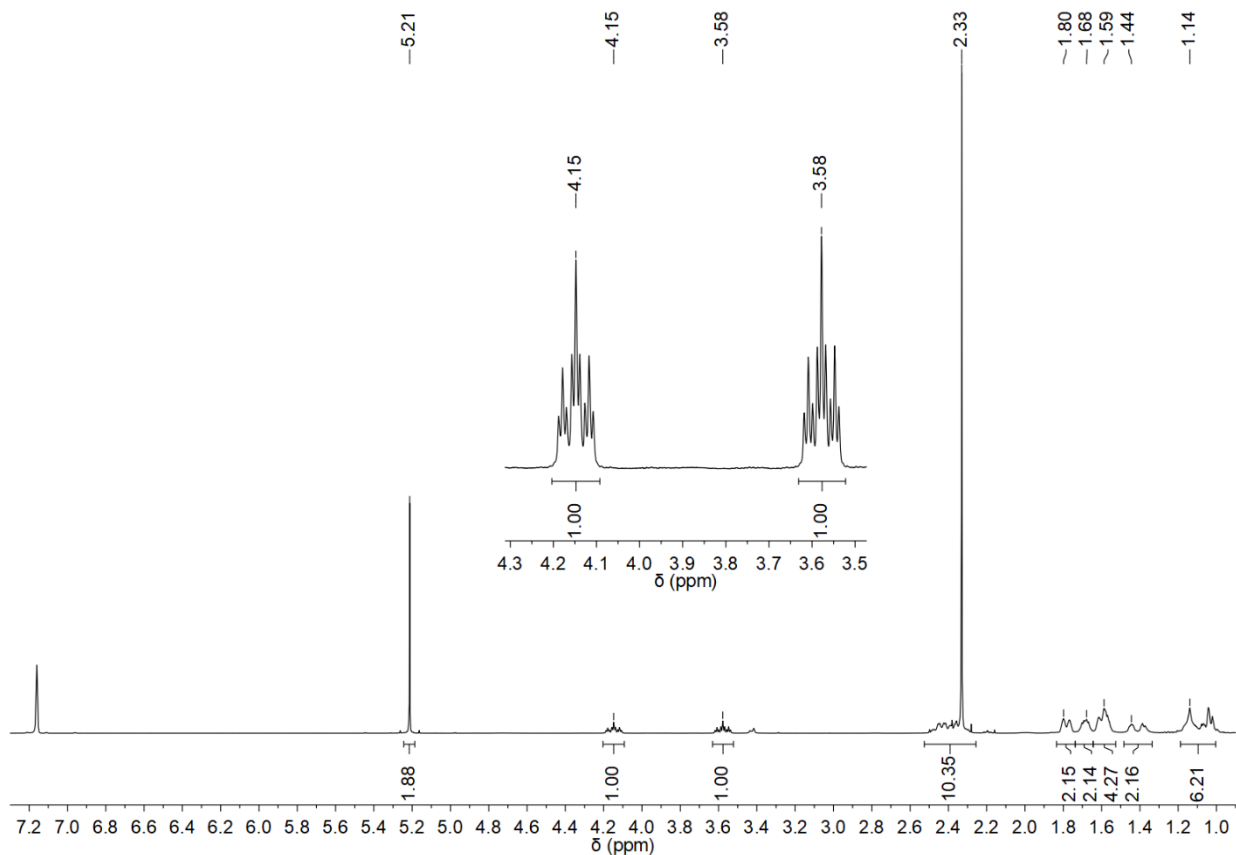
Scheme 148: ^{1}H NMR spectrum of **5u-Me-(OCN-Cy)$_2$** with magnification of the signals of the protons bound to the ipso-carbon of the cyclohexyl rings (C$_6$D$_6$).
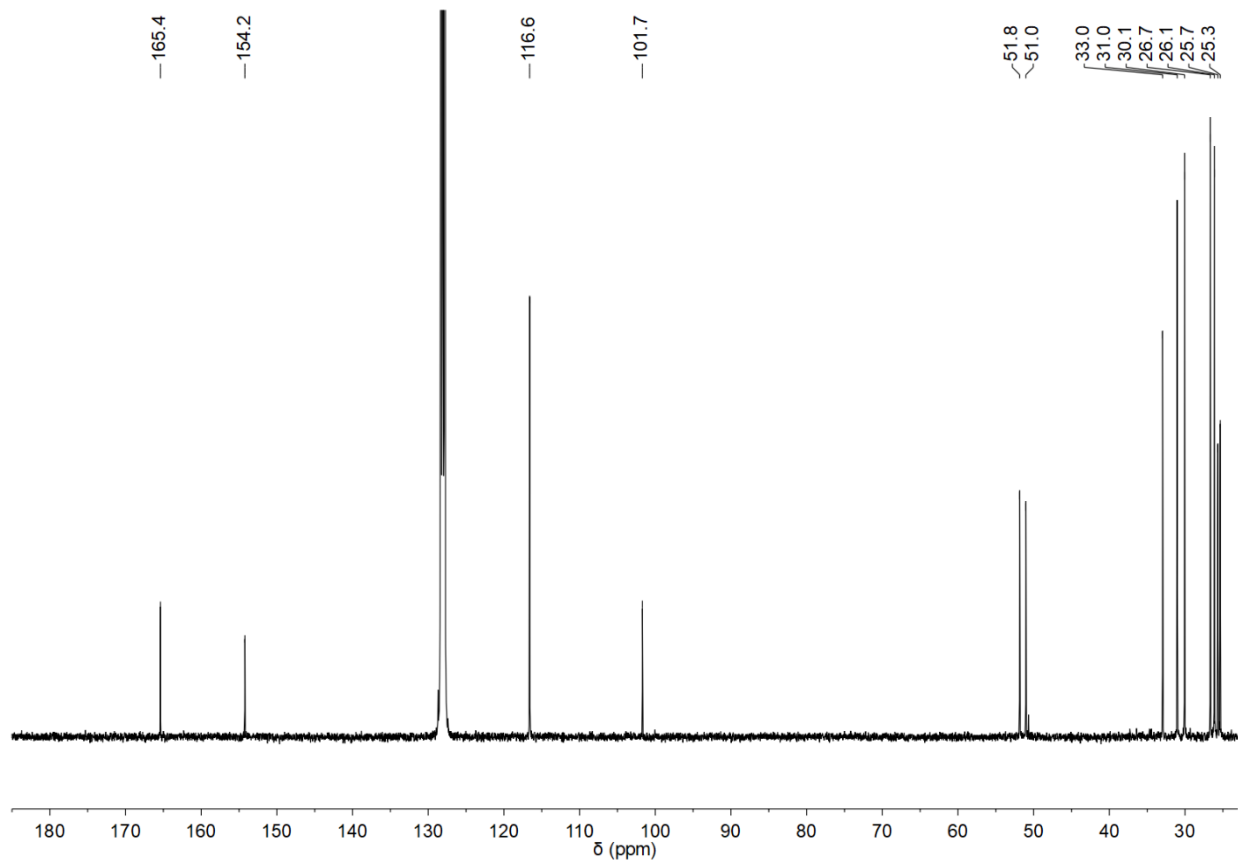
Scheme 149: ^{13}C NMR spectrum of **5u-Me-(OCN-Cy)₂** (C₆D₆).
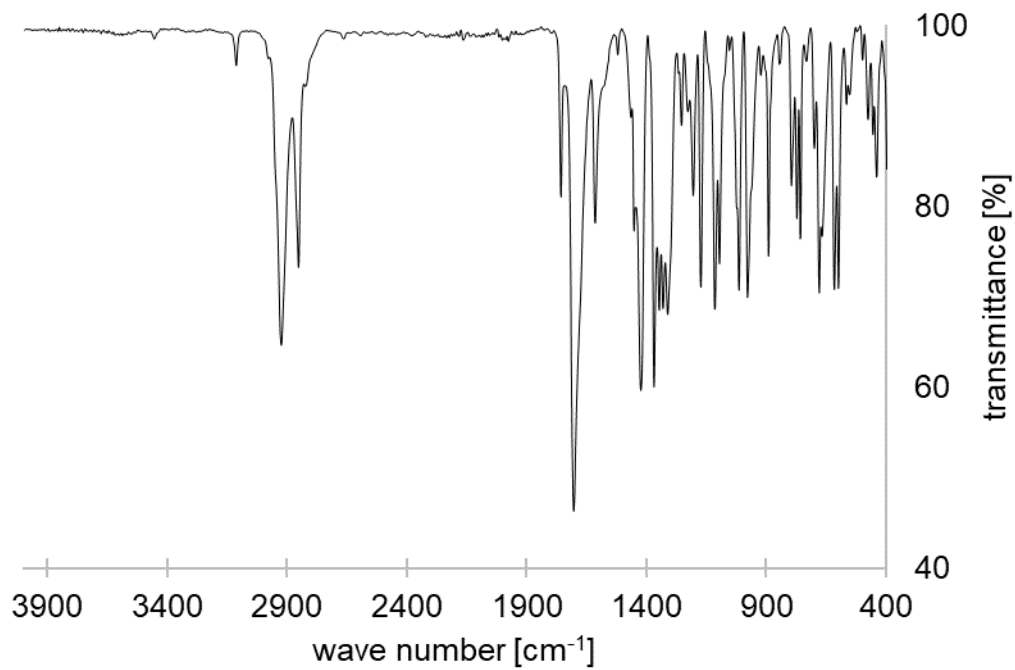
Scheme 150: IR spectrum of **5u-Me-(OCN-Cy)₂**.

The crystal structure was measured and solved by Dr. Wolfgang Frey from the Institute of Organic Chemistry of the University of Stuttgart.
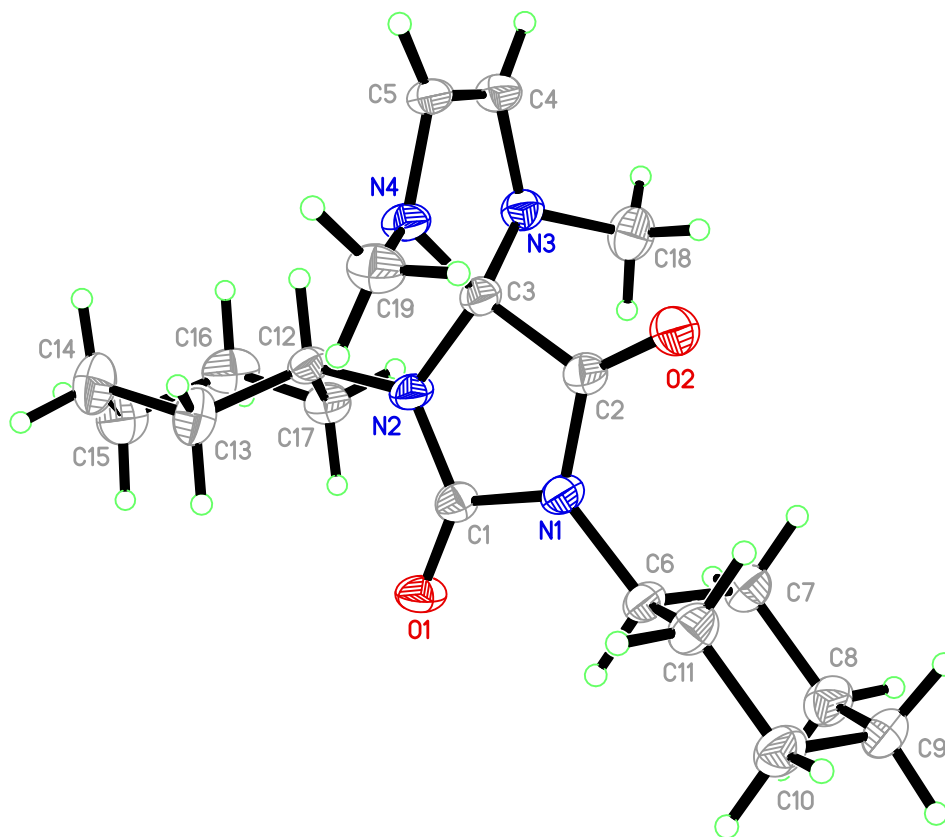
Scheme 151: Plot of the crystal structure of **5u-Me-(OCN-Cy)₂**.

Table 22: Crystal data and structure refinement for spirocyclic **5u-Me-(OCN-Cy)₂**.

empirical formula	$C_{19}H_{30}N_4O_2$
formula weight	346.47 g/mol
temperature	135(2) K
wavelength	71. 073 pm
crystal system	monoclinic
space group	$P2_1/c$
unit cell dimension	

a	1909.01(15) pm
b	691.33(7) pm
c	1466.25(11) pm
α	90°
β	99.127(4)°
γ	90°
volume	1.9106(3) nm^3
Z, calculated density	4, 1.204 Mg/m^3
absorption coefficient	0.080 mm^{-1}
F(000)	752
crystal size	0.467·0.330·0.185 mm
theta range for data collection	2.161 to 28.360°
limiting indices	-25≤h≤25, -9≤k≤9; -19≤l≤19
reflections collected/unique	19578/4749 [R(int)=0.0358]
completeness to Θ=25.242	99.9%
absorption correction	semi-empirical from equivalents
max. and min. transition	0.7457 and 0.7242
refinement method	full-matrix least squares on F^2
data/restraints/parameter	4749/0/228
goodness-of-fit on F^2	1.044
final R indices [I>2σ(I)]	R1=0.0450, wR2=0.1077
R indices (all data)	R1=0.0767, wR2=0.1171
extinction coefficient	n/a
largest peak and hole	0.235 and -0.191 e 10^{-3}nm^3

Table 23: Summary of the atomic coordinates (·10^4) of **5u-Me-(OCN-Cy)$_2$** and equivalent displacement parameters (Å^2·10^3). U(eq) is defined as one third of the trace of the orthogonalized U$_{ij}$ tensor.

atom	x	y	z	U(eq)
O(1)	2141(1)	5383(2)	5355(1)	28(1)
N(1)	2978(1)	6433(2)	4479(1)	23(1)
C(1)	2342(1)	5499(2)	4611(1)	22(1)

O(2)	3571(1)	6911(2)	3237(1)	32(1)
N(2)	2027(1)	4814(2)	3790(1)	24(1)
C(2)	3076(1)	6309(2)	3576(1)	23(1)
N(3)	2616(1)	3450(2)	2593(1)	24(1)
C(3)	2430(1)	5201(2)	3038(1)	22(1)
N(4)	2022(1)	6273(2)	2294(1)	24(1)
C(4)	2452(1)	3737(2)	1631(1)	27(1)
C(5)	2106(1)	5385(2)	1462(1)	24(1)
C(6)	3488(1)	7079(2)	5279(1)	23(1)
C(7)	4085(1)	5608(2)	5503(1)	27(1)
C(8)	4594(1)	6231(2)	6362(1)	33(1)
C(9)	4875(1)	8244(2)	6246(1)	33(1)
C(10)	4277(1)	9691(2)	6017(1)	31(1)
C(11)	3767(1)	9095(2)	5152(1)	28(1)
C(12)	1356(1)	3758(2)	3635(1)	23(1)
C(13)	738(1)	5025(2)	3793(1)	32(1)
C(14)	42(1)	3900(3)	3596(1)	41(1)
C(15)	72(1)	2050(3)	4156(1)	41(1)
C(16)	696(1)	812(2)	3997(1)	36(1)
C(17)	1388(1)	1921(2)	4214(1)	27(1)
C(18)	3265(1)	2451(2)	2979(1)	34(1)
C(19)	1945(1)	8334(2)	2386(1)	30(1)

Table 24: Bond length of **5u-Me-(OCN-Cy)₂**.

bond	length [pm]
O(1)-C(1)	121.45(14)
N(1)-C(2)	136.93(16)
N(1)-C(1)	141.61(16)
N(1)-C(6)	146.98(16)
C(1)-N(2)	134.39(17)
O(2)-C(2)	120.84(14)

N(2)-C(12)	146.13(16)
N(2)-C(3)	146.52(15)
C(2)-C(3)	155.55(19)
N(3)-C(4)	140.91(17)
N(3)-C(3)	144.57(17)
N(3)-C(18)	145.19(18)
C(3)-N(4)	144.14(17)
N(4)-C(5)	139.75(16)
N(4)-C(19)	144.08(18)
C(4)-C(5)	131.9(2)
C(4)-H(4)	95.00
C(5)-H(5)	95.00
C(6)-C(11)	151.37(19)
C(6)-C(7)	152.32(19)
C(6)-H(6)	100.00
C(7)-C(8)	152.6(2)
C(7)-H(7A)	99.00
C(7)-H(7B)	99.00
C(8)-C(9)	151.0(2)
C(8)-H(8A)	99.00
C(8)-H(8B)	99.00
C(9)-C(10)	151.6(2)
C(9)-H(9A)	99.00
C(9)-H(9B)	99.00
C(10)-C(11)	152.87(19)
C(10)-H(10A)	99.00
C(10)-H(10B)	99.00
C(11)-H(11A)	99.00
C(11)-H(11B)	99.00
C(12)-C(13)	151.69(19)
C(12)-C(17)	152.3(2)
C(12)-H(12)	100.00

C(13)-C(14)	152.7(2)
C(13)-H(13A)	99.00
C(13)-H(13B)	99.00
C(14)-C(15)	151.6(2)
C(14)-H(14A)	99.00
C(14)-H(14B)	99.00
C(15)-C(16)	151.5(2)
C(15)-H(15A)	99.00
C(15)-H(15A)	99.00
C(16)-C(17)	151.6(2)
C(16)-H(16A)	99.00
C(16)-H(16B)	99.00
C(17)-H(17A)	99.00
C(17)-H(17B)	99.00
C(18)-H(18A)	98.00
C(18)-H(18B)	98.00
C(18)-H(18C)	98.00
C(19)-H(19A)	98.00
C(19)-H(19B)	98.00
C(19)-H(19C)	98.00

Table 25: Bond angles of **5u-Me-(OCN-Cy)$_2$**.

bond	angle [°]
C(2)-N(1)-C(1)	110.81(11)
C(2)-N(1)-C(6)	127.99(10)
C(1)-N(1)-C(6)	120.28(10)
O(1)-C(1)-N(2)	128.49(12)
O(1)-C(1)-N(1)	123.51(12)
N(2)-C(1)-N(1)	108.00(10)
C(1)-N(2)-C(12)	124.79(10)
C(1)-N(2)-C(3)	113.37(10)

C(12)-N(2)-C(3)	121.83(10)
O(2)-C(2)-N(1)	127.69(12)
O(2)-C(2)-C(3)	124.70(11)
N(1)-C(2)-C(3)	107.61(10)
C(4)-N(3)-C(3)	107.56(11)
C(4)-N(3)-C(18)	119.89(11)
C(3)-N(3)-C(18)	118.53(11)
N(4)-C(3)-N(3)	103.35(10)
N(4)-C(3)-N(2)	112.21(10)
N(3)-C(3)-N(2)	112.47(11)
N(4)-C(3)-C(2)	114.83(11)
N(3)-C(3)-C(2)	114.19(10)
N(2)-C(3)-C(2)	100.20(9)
C(5)-N(4)-C(19)	123.00(11)
C(5)-N(4)-C(3)	108.16(11)
C(19)-N(4)-C(3)	119.24(11)
C(5)-C(4)-N(3)	109.62(12)
C(5)-C(4)-H(4)	125.2
N(3)-C(4)-H(4)	125.2
C(4)-C(5)-N(4)	109.75(12)
C(4)-C(5)-H(5)	125.1
N(4)-C(5)-H(5)	125.1
N(1)-C(6)-C(11)	112.51(11)
N(1)-C(6)-C(7)	110.33(11)
C(11)-C(6)-C(7)	112.10(11)
N(1)-C(6)-H(6)	107.2
C(11)-C(6)-H(6)	107.2
C(7)-C(6)-H(6)	107.2
C(6)-C(7)-C(8)	110.27(12)
C(6)-C(7)-H(7A)	109.6
C(8)-C(7)-H(7A)	109.6
C(6)-C(7)-H(7B)	109.6

C(8)-C(7)-H(7B)	109.6
H(7A)-C(7)-H(7B)	108.1
C(9)-C(8)-C(7)	110.98(12)
C(9)-C(8)-H(8A)	109.4
C(7)-C(8)-H(8A)	109.4
C(9)-C(8)-H(8B)	109.4
C(7)-C(8)-H(8B)	109.4
H(8A)-C(8)-H(8B)	108.0
C(8)-C(9)-C(10)	111.41(12)
C(8)-C(9)-H(9A)	109.3
C(10)-C(9)-H(9A)	109.3
C(8)-C(9)-H(9B)	109.3
C(10)-C(9)-H(9B)	109.3
H(9A)-C(9)-H(9B)	108.0
C(9)-C(10)-C(11)	111.39(12)
C(9)-C(10)-H(10A)	109.3
C(11)-C(10)-H(10A)	109.3
C(9)-C(10)-H(10B)	109.3
C(11)-C(10)-H(10B)	109.3
H(10A)-C(10)-H(10B)	108.0
C(6)-C(11)-C(10)	109.62(12)
C(6)-C(11)-H(11A)	109.7
C(10)-C(11)-H(11A)	109.7
C(6)-C(11)-H(11B)	109.7
C(10)-C(11)-H(11B)	109.7
H(11A)-C(11)-H(11B)	108.2
N(2)-C(12)-C(13)	111.86(12)
N(2)-C(12)-C(17)	111.97(11)
C(13)-C(12)-C(17)	111.11(10)
N(2)-C(12)-H(12)	107.2
C(13)-C(12)-H(12)	107.2
C(17)-C(12)-H(12)	107.2

C(12)-C(13)-C(14)	110.59(13)
C(12)-C(13)-H(13A)	109.5
C(14)-C(13)-H(13A)	109.5
C(12)-C(13)-H(13B)	109.5
C(14)-C(13)-H(13B)	109.5
H(13A)-C(13)-H(13B)	108.1
C(15)-C(14)-C(13)	111.75(13)
C(15)-C(14)-H(14A)	109.3
C(13)-C(14)-H(14A)	109.3
C(15)-C(14)-H(14B)	109.3
C(13)-C(14)-H(14B)	109.3
H(14A)-C(14)-H(14B)	107.9
C(16)-C(15)-C(14)	110.89(12)
C(16)-C(15)-H(15A)	109.5
C(14)-C(15)-H(15A)	109.5
C(16)-C(15)-H(15B)	109.5
C(14)-C(15)-H(15B)	109.5
H(15A)-C(15)-H(15B)	108.1
C(15)-C(16)-C(17)	111.22(13)
C(15)-C(16)-H(16A)	109.4
C(17)-C(16)-H(16A)	109.4
C(15)-C(16)-H(16B)	109.4
C(17)-C(16)-H(16B)	109.4
H(16A)-C(16)-H(16B)	108.0
C(16)-C(17)-C(12)	110.42(12)
C(16)-C(17)-H(17A)	109.6
C(12)-C(17)-H(17A)	109.6
C(16)-C(17)-H(17B)	109.6
C(12)-C(17)-H(17B)	109.6
H(17A)-C(17)-H(17B)	108.1
N(3)-C(18)-H(18A)	109.5
N(3)-C(18)-H(18B)	109.5

		109.5
H(18A)-C(18)-H(18B)		109.5
N(3)-C(18)-H(18C)		109.5
H(18A)-C(18)-H(18C)		109.5
H(18B)-C(18)-H(18C)		109.5
N(4)-C(19)-H(19A)		109.5
N(4)-C(19)-H(19B)		109.5
H(19A)-C(19)-H(19B)		109.5
N(4)-C(19)-H(19C)		109.5
H(19A)-C(19)-H(19C)		109.5
H(19B)-C(19)-H(19C)		109.5

Table 26: Anisotropic displacement parameters ($Å^2 \cdot 10^3$) for **5u-Me-(OCN-Cy)$_2$**. The anisotropic displacement factor exponent takes the form $-2\pi^2[h^2 \cdot a^{*2} U_{11} + \ldots + 2h \cdot k \cdot a^* \cdot b^* \cdot U_{12}]$.

	U_{11}	U_{22}	U_{33}	U_{23}	U_{13}	U_{12}
O(1)	34(1)	32(1)	18(1)	-3(1)	8(1)	-8(1)
N(1)	23(1)	27(1)	18(1)	-1(1)	1(1)	-6(1)
C(1)	24(1)	21(1)	21(1)	1(1)	2(1)	-2(1)
O(2)	28(1)	40(1)	28(1)	-2(1)	8(1)	-11(1)
N(2)	24(1)	35(1)	15(1)	-1(1)	4(1)	-9(1)
C(2)	24(1)	24(1)	21(1)	1(1)	3(1)	0(1)
N(3)	25(1)	24(1)	22(1)	-2(1)	2(1)	1(1)
C(3)	21(1)	25(1)	18(1)	1(1)	2(1)	-2(1)
N(4)	29(1)	25(1)	16(1)	0(1)	1(1)	3(1)
C(4)	28(1)	32(1)	20(1)	-6(1)	3(1)	-3(1)
C(5)	26(1)	32(1)	15(1)	-3(1)	2(1)	-3(1)
C(6)	22(1)	25(1)	19(1)	-2(1)	0(1)	-3(1)
C(7)	28(1)	25(1)	28(1)	-1(1)	-1(1)	0(1)
C(8)	30(1)	36(1)	29(1)	2(1)	-4(1)	6(1)
C(9)	24(1)	42(1)	32(1)	-9(1)	-3(1)	-3(1)
C(10)	31(1)	28(1)	34(1)	-7(1)	0(1)	-4(1)
C(11)	28(1)	23(1)	29(1)	0(1)	-1(1)	-1(1)

C(12)	23(1)	28(1)	18(1)	-2(1)	2(1)	-6(1)
C(13)	25(1)	31(1)	40(1)	7(1)	1(1)	0(1)
C(14)	24(1)	48(1)	51(1)	2(1)	2(1)	-3(1)
C(15)	33(1)	49(1)	42(1)	-2(1)	10(1)	-18(1)
C(16)	48(1)	29(1)	32(1)	-1(1)	8(1)	-14(1)
C(17)	33(1)	22(1)	27(1)	-1(1)	4(1)	0(1)
C(18)	31(1)	31(1)	40(1)	4(1)	1(1)	4(1)
C(19)	39(1)	25(1)	27(1)	0(1)	6(1)	3(1)

Table 27: Hydrogen coordinates ($\cdot 10^4$) and isotropic displacement parameters ($\text{Å}^2 \cdot 10^3$) of **5u-Me-(OCN-Cy)$_2$**.

	x	y	z	U(eq)
H(4)	2571	2876	1175	32
H(5)	1940	5891	864	29
H(6)	3230	7125	5821	27
H(7A)	4346	5496	4973	33
H(7B)	3883	4325	5610	33
H(8A)	4345	6203	6905	39
H(8B)	4996	5310	6476	39
H(9A)	5167	8238	5746	40
H(9B)	5183	8639	6825	40
H(10A)	4478	10980	5918	37
H(10B)	4013	9792	6545	37
H(11A)	3366	10020	5039	33
H(11B)	4016	9120	4609	33
H(12)	1269	3356	2972	28
H(13A)	712	6170	3383	39
H(13B)	813	5487	4440	39
H(14A)	-349	4723	3745	50
H(14B)	-61	3580	2931	50
H(15A)	116	2373	4821	49

H(15B)	-374	1315	3978	49
H(16A)	627	381	3345	44
H(16B)	719	-353	4394	44
H(17A)	1784	1097	4081	33
H(17B)	1477	2261	4878	33
H(18A)	3296	1227	2650	51
H(18B)	3262	2188	3635	51
H(18C)	3674	3262	2913	51
H(19A)	2408	8959	2409	45
H(19B)	1758	8615	2957	45
H(19C)	1616	8830	1856	45

Table 28: Torsions angles of **5u-Me-(OCN-Cy)₂**.

	torsion angle [°]
C(2)-N(1)-C(1)-O(1)	178.83(13)
C(6)-N(1)-C(1)-O(1)	9.0(2)
C(2)-N(1)-C(1)-N(2)	-1.19(16)
C(6)-N(1)-C(1)-N(2)	-171.07(12)
O(1)-C(1)-N(2)-C(12)	0.1(2)
N(1)-C(1)-N(2)-C(12)	-179.91(12)
O(1)-C(1)-N(2)-C(3)	-179.11(14)
N(1)-C(1)-N(2)-C(3)	0.91(16)
C(1)-N(1)-C(2)-O(2)	-178.15(14)
C(6)-N(1)-C(2)-O(2)	-9.3(2)
C(1)-N(1)-C(2)-C(3)	0.97(15)
C(6)-N(1)-C(2)-C(3)	169.87(12)
C(4)-N(3)-C(3)-N(4)	11.90(13)
C(18)-N(3)-C(3)-N(4)	151.98(11)
C(4)-N(3)-C(3)-N(2)	133.14(11)
C(18)-N(3)-C(3)-N(2)	-86.77(14)
C(4)-N(3)-C(3)-C(2)	-113.54(12)

C(18)-N(3)-C(3)-C(2)	26.55(16)
C(1)-N(2)-C(3)-N(4)	-122.63(13)
C(12)-N(2)-C(3)-N(4)	58.17(16)
C(1)-N(2)-C(3)-N(3)	121.35(13)
C(12)-N(2)-C(3)-N(3)	-57.86(16)
C(1)-N(2)-C(3)-C(2)	-0.32(14)
C(12)-N(2)-C(3)-C(2)	-179.53(12)
O(2)-C(2)-C(3)-N(4)	-60.82(18)
N(1)-C(2)-C(3)-N(4)	120.03(12)
O(2)-C(2)-C(3)-N(3)	58.32(18)
N(1)-C(2)-C(3)-N(3)	-120.84(12)
O(2)-C(2)-C(3)-N(2)	178.75(13)
N(1)-C(2)-C(3)-N(2)	-0.40(13)
N(3)-C(3)-N(4)-C(5)	-12.04(13)
N(2)-C(3)-N(4)-C(5)	-133.45(11)
C(2)-C(3)-N(4)-C(5)	112.99(12)
N(3)-C(3)-N(4)-C(19)	-159.22(10)
N(2)-C(3)-N(4)-C(19)	79.36(14)
C(2)-C(3)-N(4)-C(19)	-34.20(15)
C(3)-N(3)-C(4)-C(5)	-7.73(14)
C(18)-N(3)-C(4)-C(5)	-147.18(13)
N(3)-C(4)-C(5)-N(4)	-0.11(15)
C(19)-N(4)-C(5)-C(4)	153.64(13)
C(3)-N(4)-C(5)-C(4)	7.97(15)
C(2)-N(1)-C(6)-C(11)	56.52(18)
C(1)-N(1)-C(6)-C(11)	-135.51(12)
C(2)-N(1)-C(6)-C(7)	-69.49(17)
C(1)-N(1)-C(6)-C(7)	98.48(13)
N(1)-C(6)-C(7)-C(8)	-177.16(11)
C(11)-C(6)-C(7)-C(8)	56.60(14)
C(6)-C(7)-C(8)-C(9)	-55.45(15)
C(7)-C(8)-C(9)-C(10)	55.96(16)

C(8)-C(9)-C(10)-C(11)	-56.45(16)
N(1)-C(6)-C(11)-C(10)	178.47(10)
C(7)-C(6)-C(11)-C(10)	-56.49(14)
C(9)-C(10)-C(11)-C(6)	55.93(15)
C(1)-N(2)-C(12)-C(13)	66.40(17)
C(3)-N(2)-C(12)-C(13)	-114.49(13)
C(1)-N(2)-C(12)-C(17)	-59.07(18)
C(3)-N(2)-C(12)-C(17)	120.04(13)
N(2)-C(12)-C(13)-C(14)	178.18(11)
C(17)-C(12)-C(13)-C(14)	-55.88(16)
C(12)-C(13)-C(14)-C(15)	55.00(17)
C(13)-C(14)-C(15)-C(16)	-55.06(18)
C(14)-C(15)-C(16)-C(17)	56.13(17)
C(15)-C(16)-C(17)-C(12)	-57.10(15)
N(2)-C(12)-C(17)-C(16)	-176.97(11)
C(13)-C(12)-C(17)-C(16)	57.15(15)

Table 29: DSC data of the polyamide 6 in Table 17, entry 1.

heat rate [K/min]	T_m [°C]	T_c [°C]	ΔH [J/g]
-30	-	163	-63.32
-30	-	163	-62.51
+30	208	-	49.90
+30	208	-	50.16
-40	-	159	-61.25
-40	-	159	-60.85
+40	208	-	46.66
+40	208	-	48.13
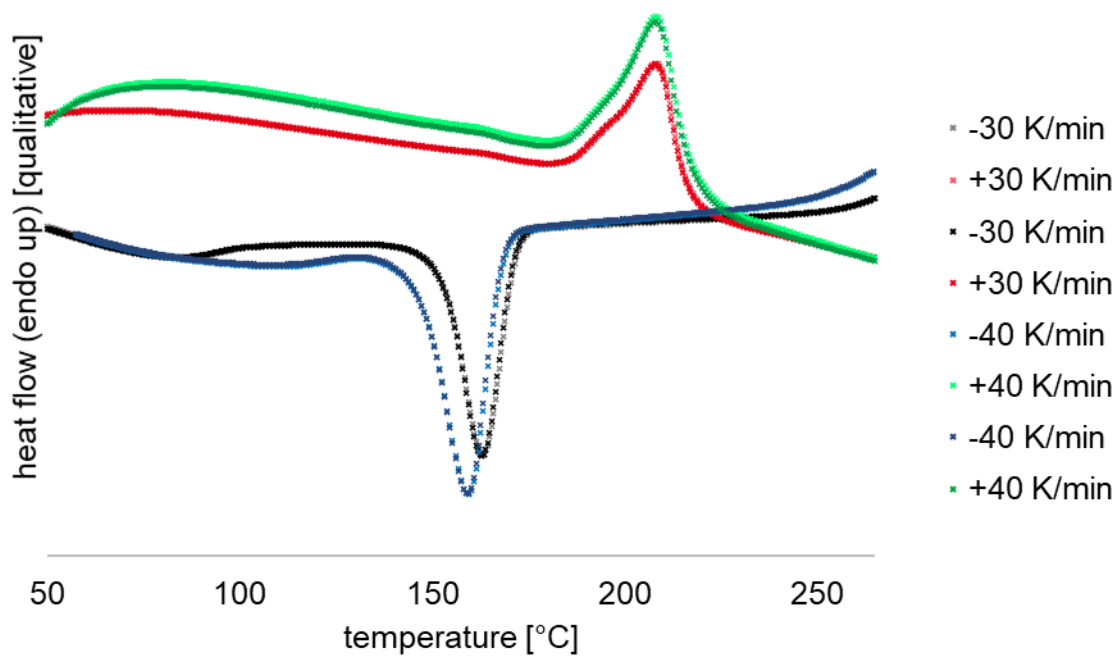
Scheme 152: Thermogram of the polyamide in Table 17, entry 1.

Table 30: DSC data of the polyamide 6 in Table 17, entry 2.

heat rate [K/min]	T_m [°C]	T_c [°C]	ΔH [J/g]
-30	-	171	-58.06
-30	-	171	-58.14
+30	215	-	48.07
+30	215	-	48.07
-40	-	169	-58.16
-40	-	169	-58.12
+40	216	-	46.13
+40	215	-	45.42
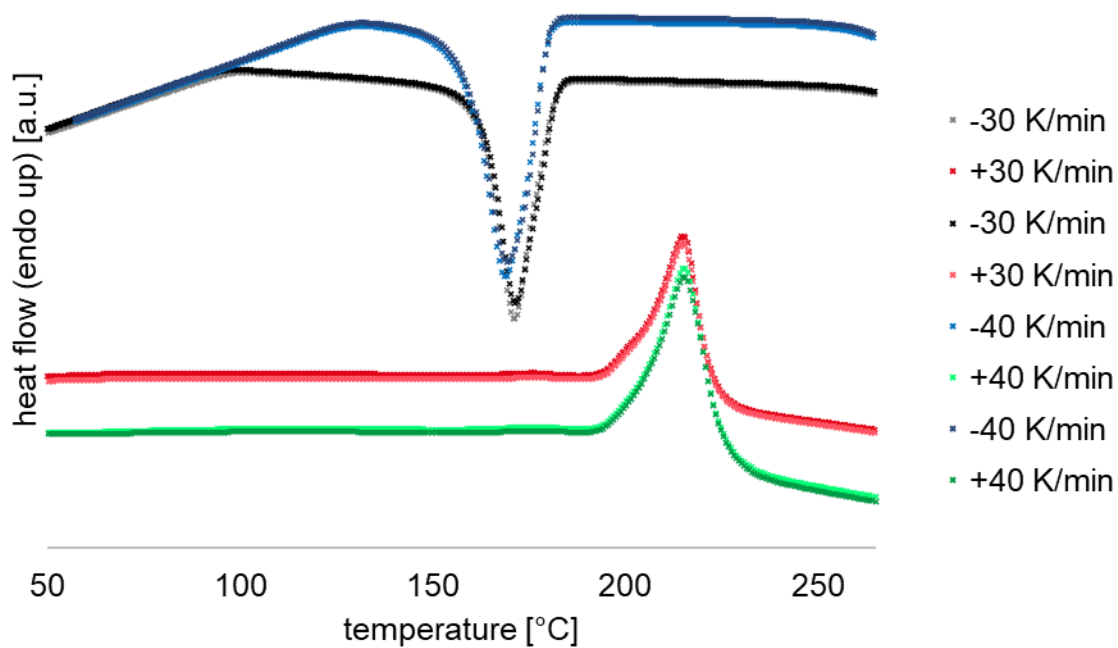
Scheme 153: Thermogram of the polyamide in Table 17, entry 2.

Table 31: DSC data of the polyamide 6 in Table 17, entry 3.

heat rate [K/min]	T_m [°C]	T_c [°C]	ΔH [J/g]
-30	-	167	-68.68
-30	-	167	-66.82
+30	211	-	56.74
+30	211	-	56.56
-40	-	163	-65.02
-40	-	163	-65.26
+40	211	-	56.12
+40	211	-	55.66
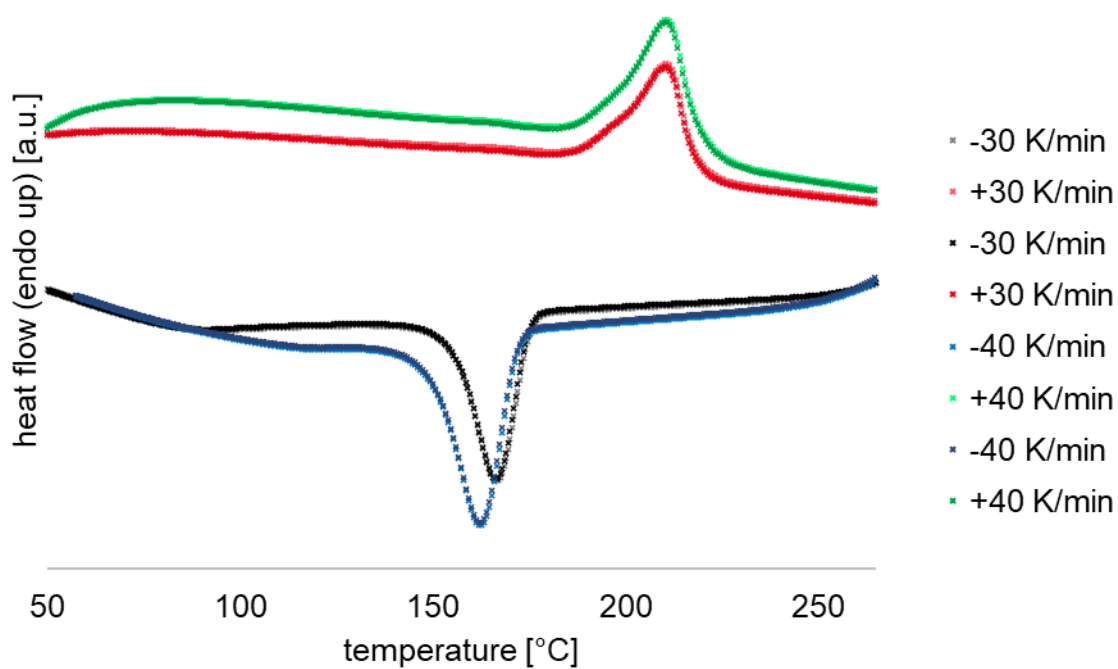
Scheme 154: Thermogram of the polyamide in Table 17, entry 3.

Table 32: DSC data of the polyamide 6 in Table 17, entry 4.

heat rate [K/min]	T_m [°C]	T_c [°C]	ΔH [J/g]
-30	-	160	-68.03
-30	-	162	-68.30
+30	204	-	56.54
+30	205	-	55.43
-40	-	159	-62.72
-40	-	160	-66.18
+40	207	-	51.97
+40	207	-	52.79
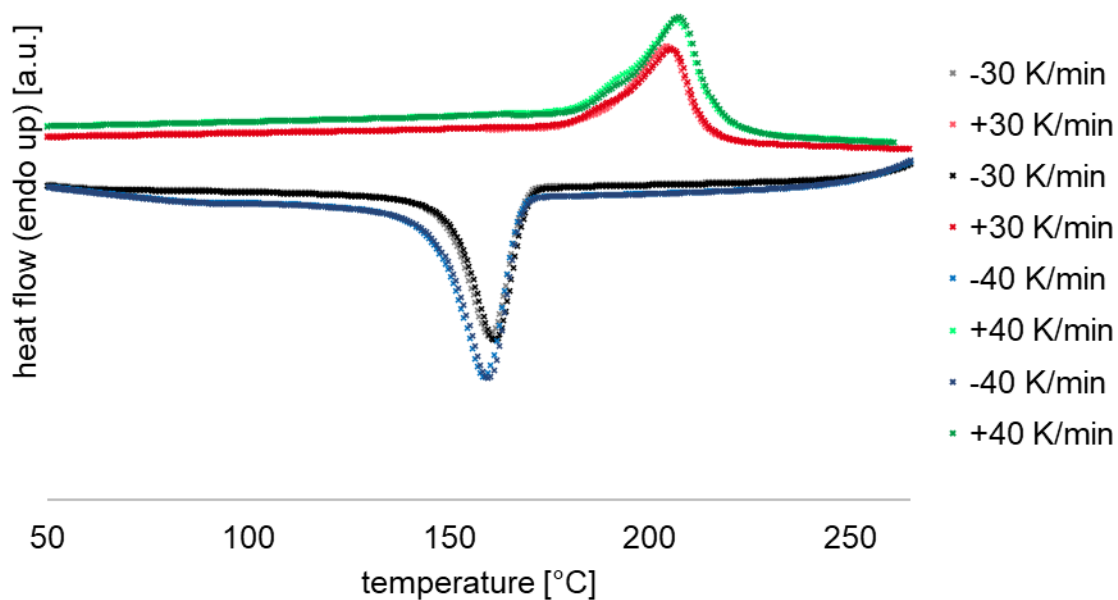
Scheme 155: Thermogram of the polyamide in Table 17, entry 4.

9.6 Data on Oligomerization of 4-Methyloxetan-2-one to Diols

Content of this chapter is majorly published: H. J. Altmann, M. R. Machat, A. Wolf, C. Gürtler, D. Wang, M. R. Buchmeiser, Synthesis of dihydroxy telechelic oligomers of β-butyrolactone catalyzed by titanium(IV)-alkoxides and their use as macrodiols in polyurethane chemistry, *J. Polym. Sci.*, **2021**, *59*, *3*, 274-281.[11]
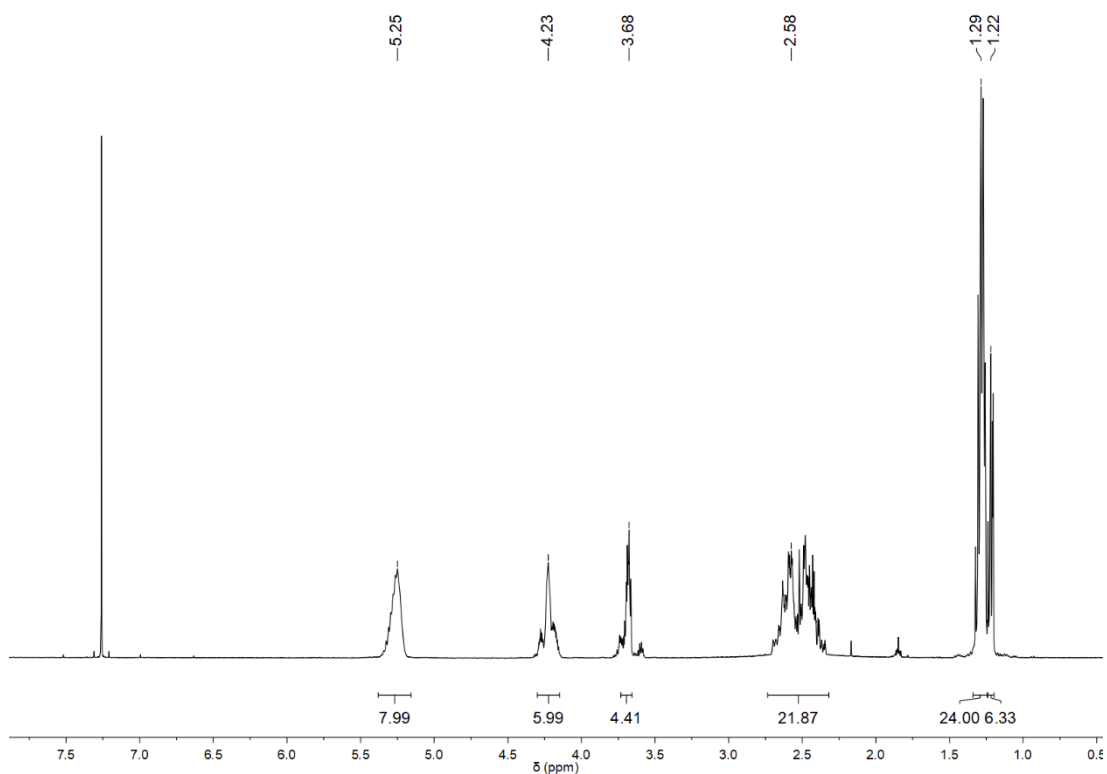
Scheme 156: ¹H NMR spectrum of an α,ω-dihydroxy telechelic oligo(4-methyloxetan-2-one) based on DEG after workup (CDCl₃).

172.8
172.2
171.9
171.8
170.6
170.4
170.2
169.7
169.6
169.6
169.4
169.3

69.0
69.0
67.8
67.7
67.6
67.5
64.5
64.4
64.3
64.3
63.8
63.7
63.5
43.6
43.5
43.4
43.4
43.3
43.0
40.9
40.9
40.8
40.8
40.7
40.6
22.6
22.6
22.5
20.0
20.0
20.0
19.9
19.9
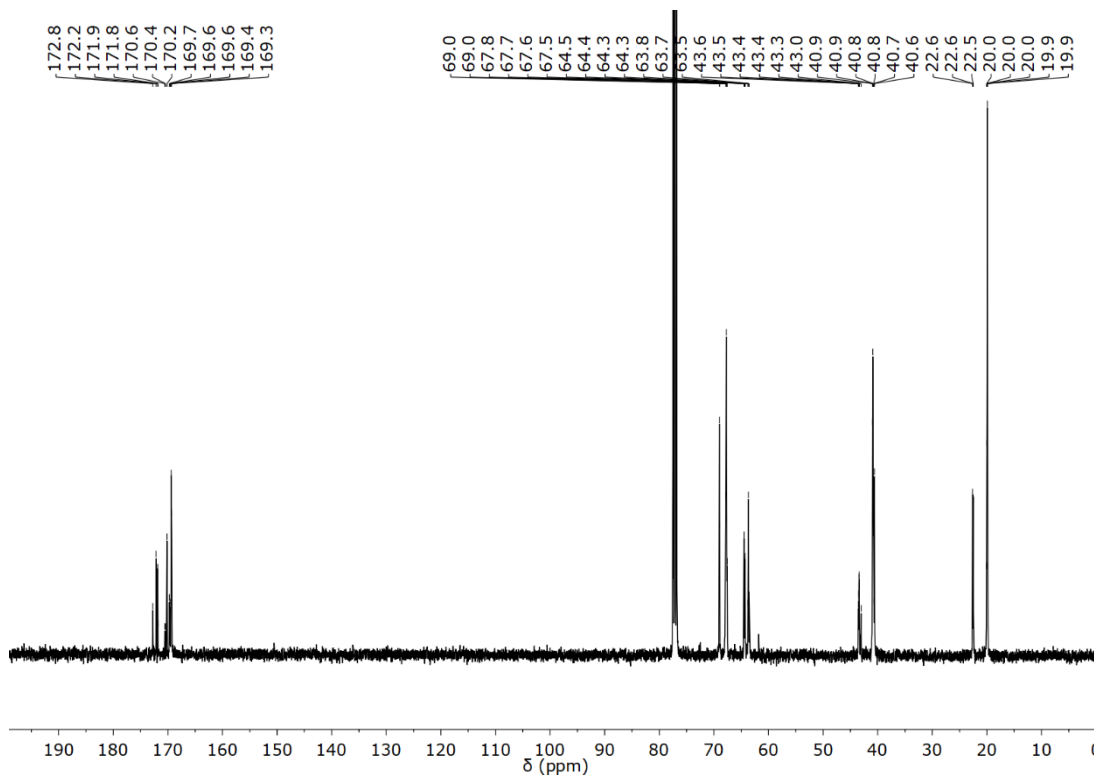
Scheme 157: ^{13}C NMR spectrum of an α,ω-dihydroxy telechelic oligo(4-methyloxetan-2-one) based on DEG (CDCl₃).
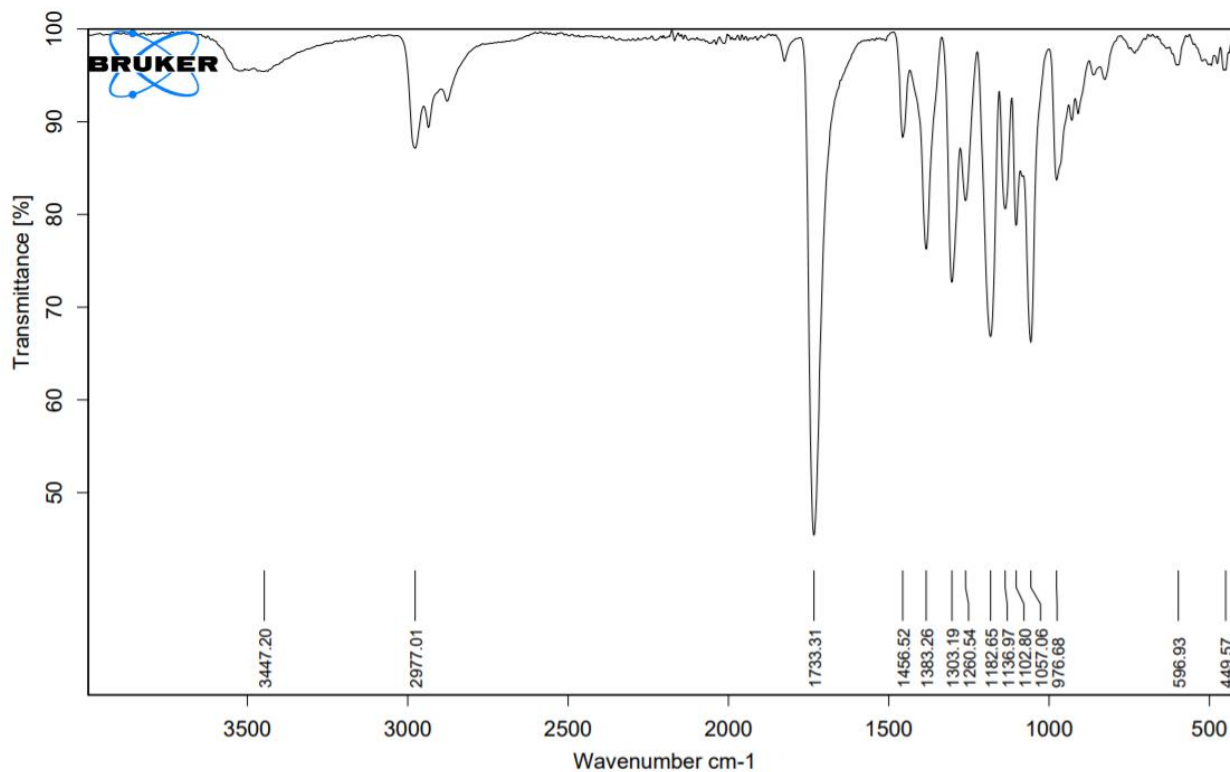
Scheme 158 IR spectrum of an α,ω-dihydroxy telechelic oligo(4-methyloxetan-2-one) based on DEG.

247
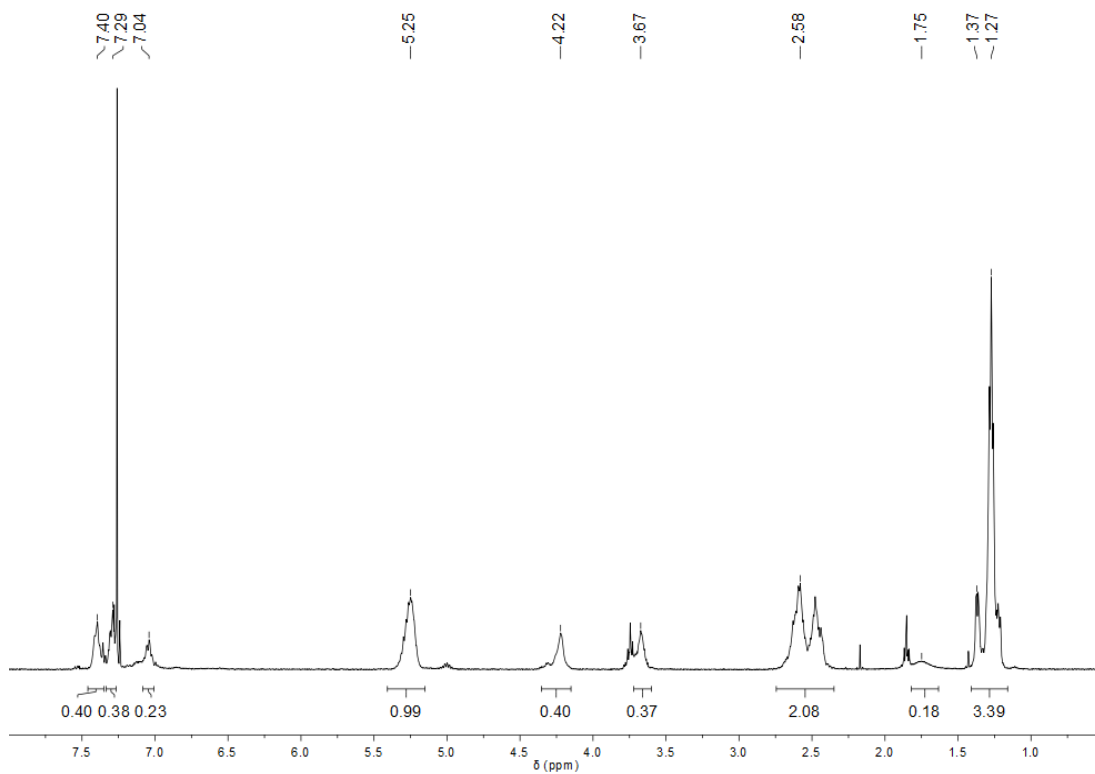
Scheme 159: ¹H NMR spectrum of an α,ω-dihydroxy telechelic oligo(4-methyloxetan-2-one) based on DEG and end-capped with phenyl isocyanate (CDCl₃).
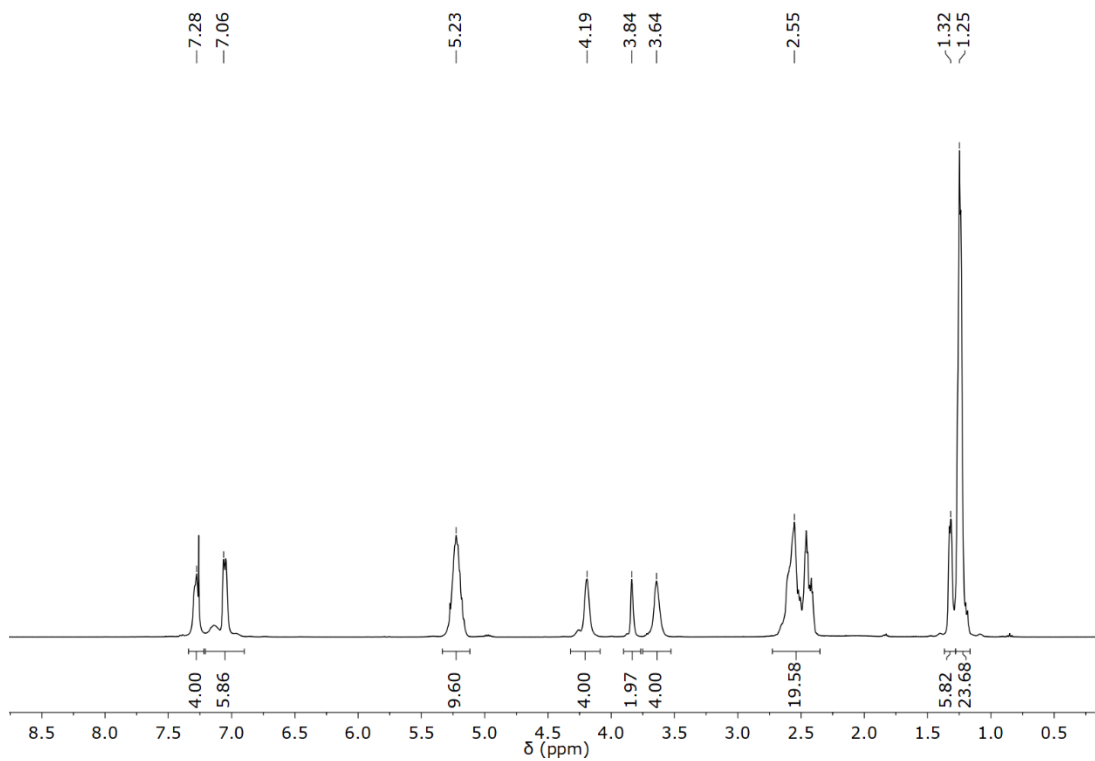
Scheme 160: ¹H NMR spectrum of a polyurethane synthesized from MDI and an α,ω-dihydroxy telechelic oligo(4-methyloxetan-2-one) based on DEG (CDCl₃).
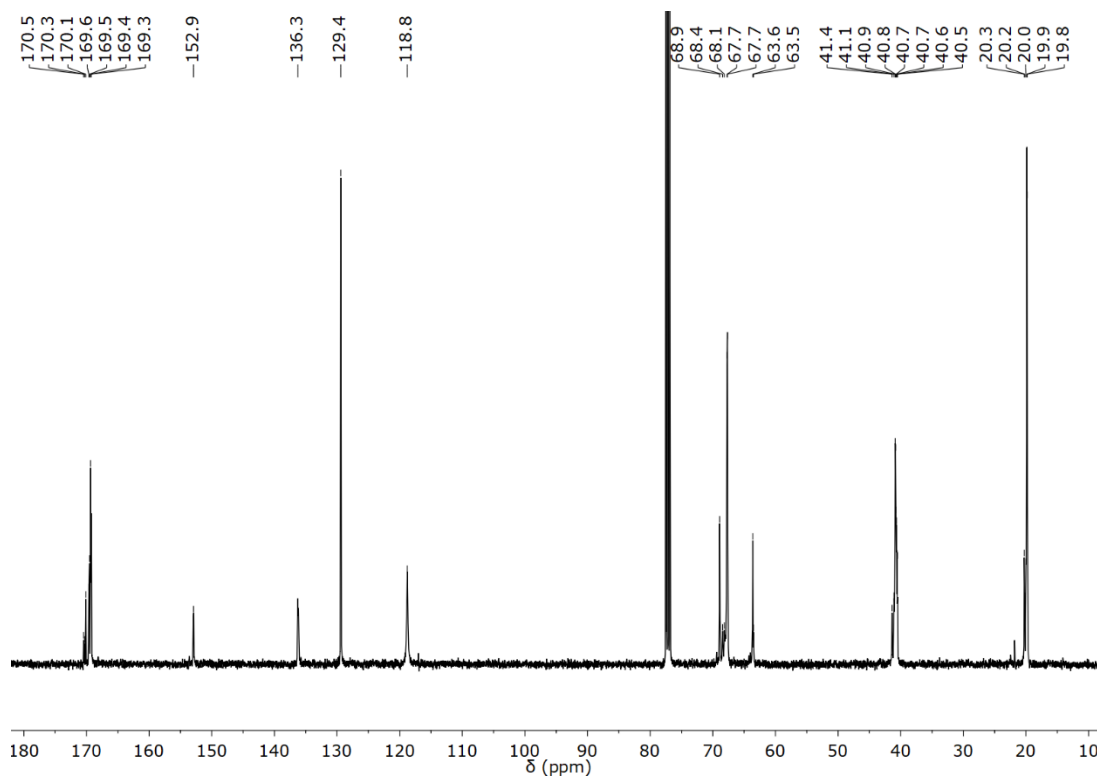
Scheme 161: ^{13}C NMR spectrum of a polyurethane synthesized from MDI and an α,ω-dihydroxy telechelic oligo(4-methyloxetan-2-one) based on DEG (CDCl$_3$).

Scheme 162: IR spectrum of a polyurethane synthesized from MDI and an α,ω-dihydroxy telechelic oligo(4-methyloxetan-2-one) based on DEG.

9.7 Reprint Permissions

Synthesis of Linear Poly(oxazolidin-2-one)s by Cooperative Catalysis Based on N-Heterocyclic Carbenes and Simple Lewis Acids

ACS Publications

Author: Hagen J. Altmann, Manuel Clauss, Simon König, et al

Publication: Macromolecules

Publisher: American Chemical Society

Date: Jan 1, 2019

Copyright © 2019, American Chemical Society

RightsLink®

A Spirocyclic Parabanic Acid Masked N-Heterocyclic Carbene as Thermally Latent Pre-Catalyst for Polyamide 6 Synthesis and Epoxide Curing

Author: Hagen J. Altmann, Wolfgang Frey, Michael R. Buchmeiser

Publication: Macromolecular Rapid Communications

Publisher: John Wiley and Sons

Date: Sep 8, 2020

© 2020 The Authors. Published by Wiley-VCH GmbH

Open Access Article

Wiley offers a professional reprint service for high quality reproduction of articles from over 1400 scientific and medical journals. Wiley's reprint service offers:

- Peer reviewed research or reviews
- Tailored collections of articles
- A professional high quality finish
- Glossy journal style color covers
- Company or brand customisation
- Language translations
- Prompt turnaround times and delivery directly to your office, warehouse or congress.

Please contact our Reprints department for a quotation. Email corporatesaleseurope@wiley.com or corporatesalesusa@wiley.com or corporatesalesDE@wiley.com.

RightsLink®

Dual catalysis with an N-heterocyclic carbene and a Lewis acid: Thermally latent precatalyst for the polymerization of ε-caprolactam

Author: Hagen J. Altmann, Mark Steinmann, Iris Elser, et al

Publication: Journal of Polymer Science

Publisher: John Wiley and Sons

Date: Oct 3, 2020

© 2020 The Authors. Journal of Polymer Science published by Wiley Periodicals LLC.

Synthesis of dihydroxy telechelic oligomers of β-butyrolactone catalyzed by titanium(IV)-alkoxides and their use as macrodiols in polyurethane chemistry

Author: Hagen J. Altmann, Martin R. Machat, Aurel Wolf, et al

Publication: Journal of Polymer Science

Publisher: John Wiley and Sons

Date: Jan 2, 2021

© 2021 The Authors. Journal of Polymer Science published by Wiley Periodicals LLC.

RightsLink

Home   Help   Email Support   Sign In   Create Account

ACSPublications
Most Trusted. Most Cited. Most Read.

Thermodynamics of N-Heterocyclic Carbene Dimerization: The Balance of Sterics and Electronics

Author: Albert Poater, Francesco Ragone, Simona Giudice, et al

Publication: Organometallics

Publisher: American Chemical Society

Date: Jun 1, 2008

Copyright © 2008, American Chemical Society

9.8   Curriculum Vitae

Name:　　　　　　　Hagen Jürgen Altmann

Date of birth:　　　　14. April 1989

Place of birth:　　　　Aalen, Germany

Scientific education

since 2020　　Scientific coworker at the German Institutes of Fiber and Textile Research

2017-2020　　Ph.D. candidate at the Institute of Polymer Chemistry at the University of Stuttgart under supervision of Prof. Buchmeiser

2014-2016　　M.Sc. Chemistry

- University of Stuttgart

- Scientific profile: "Materials and Functional Molecules"

- Master thesis at the Institute of Polymer Chemistry; title: "Synthesis and Reactivity of Molybdenumalkylidenes bearing Chiral, Unsymmetric Carbene Ligands"

2010-2014　　B.Sc. Chemistry

- University of Stuttgart

- Bachelor thesis: "Cationic Ruthenium-Alkylidenes for 2-Phase-Catalysis"

2006-2009　　Certificate of general University Qualification (Abitur)

- Justus von Liebig Schule, Aalen

Scientific publications

2021

H. J. Altmann, M. R. Machat, A. Wolf, C. Gürtler, D. Wang, M. R. Buchmeiser, Synthesis of dihydroxy telechelic oligomers of β-butyrolactone catalyzed by titanium(IV)-alkoxides and their use as macrodiols in polyurethane chemistry, *J. Polym. Sci.*, **2021**, *59*, *3*, 274-281, 10.1002/pol.20200780.

2020

H. J. Altmann, M. Steinmann, I. Elser, M. J. Benedikter, S. Naumann, M. R. Buchmeiser, Dual catalysis with an N-heterocyclic carbene and a Lewis acid: Thermally latent precatalyst for the polymerization of ε-caprolactam, *J. Polym. Sci.* **2020**, *58*, 3219-3226, 10.1002/pol.20200502.

H. J. Altmann, W. Frey, M. R. Buchmeiser, A Spirocyclic Parabanic Acid Masked *N*-Heterocyclic Carbene as Thermally Latent Pre-Catalyst for Polyamide 6 Synthesis and Epoxide Curing, *Macromol. Rapid. Commun.* **2020**, e2000338, 10.1002/marc.202000338.

J. V. Musso, M. J. Benedikter, D. Wang, W. Frey, H. J. Altmann, M. R. Buchmeiser, Reversible N-Heterocyclic Carbene-Induced α-H Abstraction in Tungsten(VI) Imido Dialkyl Dialkoxide Complexes, *Chem. Eur. J.*, **2020**, *26*, 8709-8713, 10.1002/chem.202000840.

2019

H. J. Altmann, M. Clauss, S. König, E. Frick-Delaittre, C. Koopmans, A. Wolf, C. Guertler, S. Naumann, M. R. Buchmeiser, Synthesis of Linear Poly(oxazolidin-2-one)s by Cooperative Catalysis Based on N-Heterocyclic Carbenes and Simple Lewis Acids, *Macromolecules* **2019**, *52*, 487-494, 10.1021/acs.macromol.8b02403.

2018

I. Elser, B. R. Kordes, W. Frey, K. Herz, R. Schowner, L. Stöhr, H. J. Altmann, M. R. Buchmeiser, Latent and Air-Stable Pre-Catalysts for the Polymerization of Dicyclopentadiene: From Penta- to Hexacoordination in Molybdenum Imido Alkylidene N-Heterocyclic Carbene Complexes, *Chem. Eur. J.*, **2018**, *24*, 12652-12659, 10.1002/chem.201801862.

2017

H. J. Altmann, S. Naumann, M. R. Buchmeiser, Protected *N*-heterocyclic carbenes as latent organocatalysts for the low-temperature curing of anhydride-hardened epoxy resins, *Eur. Polym. J.* **2017**, *95*, 766-774, 10.1016/j.eurpolymj.2017.05.032.

2015

M. Koy, H. J. Altmann, B. Autenrieth, W. Frey, M. R. Buchmeiser, Grubbs–Hoveyda type catalysts bearing a dicationic N-heterocyclic carbene for biphasic olefin metathesis reactions in ionic liquids, *Beilstein J. Org. Chem.*, **2015**, *11*, 1632-1638, 10.3762/bjoc.11.178.

Patents

Catalysts for the synthesis of oxazolidinones; Carsten Koopmans, Elena Frick-Delaittre, Aurel Wolf, Christoph Gürtler, Michael Buchmeiser, Hagen Altmann, Stefan Naumann, WO 2020/025805 A1.

Latent catalyst systems and processes for the production of polyamides; H. J. Altmann, I. Elser, M. J. Benedikter, S. Naumann, M. R. Buchmeiser, patent pending.

Oral presentations

2019   Tag der Organischen Chemie der Universität Stuttgart; <u>H. J. Altmann</u>, M. Clauss, S. König, E. Frick-Delaittre, C. Koopmans, A. Wolf, C. Guertler, S. Naumann, M. R. Buchmeiser; title: „Poly(oxazolidin-2-one)s

Poster presentations

2020   Macromolecular Colloquium, Freiburg; H. J. Altmann, M. Clauss, S. König, E. Frick-Delaittre, C. Koopmans, A. Wolf, C. Guertler, S. Naumann, M. R. Buchmeiser, title: "Synthesis of Linear Poly(Oxazolidin-2-one)s by Cooperative Catalysis Based on N-Heterocyclic Carbenes and Simple Lewis Acids"

10 Literature

[1]   *Le Syntème international d'unités The International System of Units, Vol. 2020*, 9 ed., Bureau International des Poids et Mesures, **2019**.

[2]   S. Naumann, M. Speiser, R. Schowner, E. Giebel, M. R. Buchmeiser, Air Stable and Latent Single-Component Curing of Epoxy/Anhydride Resins Catalyzed by Thermally Liberated N-Heterocyclic Carbenes, *Macromolecules* **2014**, *47*, 4548-4556, 10.1021/ma501125k.

[3]   J. D. Holbrey, W. M. Reichert, I. Tkatchenko, E. Bouajila, O. Walter, I. Tommasi, R. D. Rogers, 1,3-dimethylimidazolium-2-carboxylate: the unexpected synthesis of an ionic liquid precursor and carbene-CO_2 adduct, *Chem. Commun.* **2003**, 28-29, 10.1039/b211519k.

[4]   H. J. Altmann, S. Naumann, M. R. Buchmeiser, Protected N-heterocyclic carbenes as latent organocatalysts for the low-temperature curing of anhydride-hardened epoxy resins, *Eur. Polym. J.* **2017**, *95*, 766-774, 10.1016/j.eurpolymj.2017.05.032.

[5]   H. J. Altmann, M. Clauss, S. König, E. Frick-Delaittre, C. Koopmans, A. Wolf, C. Guertler, S. Naumann, M. R. Buchmeiser, Synthesis of Linear Poly(oxazolidin-2-one)s by Cooperative Catalysis Based on N-Heterocyclic Carbenes and Simple Lewis Acids, *Macromolecules* **2019**, *52*, 487-494, 10.1021/acs.macromol.8b02403.

[6]   H. J. Altmann, M. Steinmann, I. Elser, M. J. Benedikter, S. Naumann, M. R. Buchmeiser, Dual catalysis with an N-heterocyclic carbene and a Lewis acid: Thermally latent precatalyst for the polymerization of ε-caprolactam, *J. Polym. Sci.* **2020**, *58*, 3219-3226, 10.1002/pol.20200502.

[7]   S. Naumann, S. Epple, C. Bonten, M. R. Buchmeiser, Polymerization of ε-Caprolactam by Latent Precatalysts Based on Protected N-Heterocyclic Carbenes, *ACS Macro Lett.* **2013**, *2*, 609-612, 10.1021/mz400199y.

[8]   S. Naumann, F. G. Schmidt, M. Speiser, M. Böhl, S. Epple, C. Bonten, M. R. Buchmeiser, Anionic Ring-Opening Homo- and Copolymerization of Lactams by Latent, Protected N-Heterocyclic Carbenes for the Preparation of PA 12 and PA 6/12, *Macromolecules* **2013**, *46*, 8426-8433, 10.1021/ma4018586.

[9]   K. Jovic, J. Unold, S. Naumann, M. Ullrich, F. G. Schmidt, M. R. Buchmeiser, In Situ Copolymerization of Lactams for Melt Spinning, *Macromol. Mater. Eng.* **2016**, *301*, 423-428, 10.1002/mame.201500339.

[10]   H. J. Altmann, W. Frey, M. R. Buchmeiser, A Spirocyclic Parabanic Acid Masked N-Heterocyclic Carbene as Thermally Latent Pre-Catalyst for Polyamide 6 Synthesis and Epoxide Curing, *Macromol. Rapid. Commun.* **2020**, e2000338, 10.1002/marc.202000338.

[11]   H. J. Altmann, M. R. Machat, A. Wolf, C. Gürtler, D. Wang, M. R. Buchmeiser, Synthesis of dihydroxy telechelic oligomers of β-butyrolactone catalyzed by titanium(IV)-alkoxides and their use as macrodiols in polyurethane chemistry, *J. Polym. Sci.* **2021**, *59*, 274-281, 10.1002/pol.20200780.

[12]   *Compendium of Chemical Terminology Goldenbook*, IUPAC, **2014**.

[13]   D. Bourissou, O. Guerret, F. P. Gabbai, G. Bertrand, Stable Carbenes, *Chem. Rev.* **2000**, *100*, 39-92, 10.1021/cr940472u.

[14]   C. Elschenbroic, *Organometallchemie*, Vieweg+Teubner Verlag, **2008**.

[15]   W. A. Herrmann, C. Köcher, N-Heterocyclic Carbenes, *Angew. Chem. Int. Ed.* **1997**, *36*, 2162-2187, 10.1002/anie.199721621.

[16]   E. O. Fischer, A. Maasböl, Zur Frage eines Wolfram-Carbonyl-Carben-Komplexes, *Angew. Chem.* **1964**, *76*, 645-645, 10.1002/ange.19640761405.

[17]   https://www.nobelprize.org/prizes/chemistry/1973/summary/, visitied on 29.06.2020.

[18]   http://nobel-centre.com/wp-content/uploads/2015/01/adolf_otto_fisher.pdf, visitied on 02.07.2020.

[19]   https://www.nobelprize.org/prizes/chemistry/1973/press-release/, visitied on 02.07.2020.

[20]   W. A. Herrmann, Ein neues Verfahren zur Darstellung von Übergangsmetall-Carben-Komplexen, *Angew. Chem.* **1974**, *86*, 556-557, 10.1002/ange.19740861508.

[21]   R. R. Schrock, Alkylcarbene complex of tantalum by intramolecular .alpha.-hydrogen abstraction, *J. Am. Chem. Soc.* **1974**, *96*, 6796-6797, 10.1021/ja00828a061.

[22]   https://www.nobelprize.org/prizes/chemistry/2005/summary/, visitied on 02.07.2020.

[23]   https://www.nobelprize.org/prizes/chemistry/2005/schrock/facts/, visitied on 02.07.2020.

[24]   https://www.nobelprize.org/prizes/chemistry/2005/grubbs/facts/, visitied on 02.07.2020.

[25]   https://www.nobelprize.org/prizes/chemistry/2005/chauvin/facts/, visitied on 02.07.2020.

[26]   D. Steinbron, *Grundlagen der metallorganischen Komplexkatalyse*, Vieweg+Teubner Verlag, Wiesbaden, **2010**.

[27]   R. H. Grubbs, *Handbook of Metathesis*, Wiley-VCH, Weinheim, **2003**.

[28]   A. J. Arduengo, R. Krafczyk, Auf der Suche nach Stabilen Carbenen, *Chem. unserer Zeit* **1998**, *32*, 6-14, 10.1002/ciuz.19980320103.

[29]   H.-W. Wanzlick, Helmuth Scheibler. 1882–1966, *Chem. Ber.* **1969**, *102*, 27-39, 10.1002/cber.19691020402.

[30]   M. N. Hopkinson, C. Richter, M. Schedler, F. Glorius, An overview of N-heterocyclic carbenes, *Nature* **2014**, *510*, 485-496, 10.1038/nature13384.

[31]   H. W. Wanzlick, E. Schikora, Ein neuer Zugang zur Carben-Chemie, *Angew. Chem.* **1960**, *72*, 494-494, 10.1002/ange.19600721409.

[32]   W. Kirmse, Die Anfänge der N-heterocyclischen Carbene, *Angew. Chem.* **2010**, *122*, 8980-8983, 10.1002/ange.201001658.

[33]   W. Kirmse, The beginnings of N-heterocyclic carbenes, *Angew. Chem. Int. Ed.* **2010**, *49*, 8798-8801, 10.1002/anie.201001658.

[34]   H.-W. Wanzlick, E. Schikora, Ein nucleophiles Carben, *Chem. Ber.* **1961**, *94*, 2389-2393, 10.1002/cber.19610940905.

[35]   K. Öfele, 1,3-Dimethyl-4-imidazolinyliden-(2)-pentacarbonylchrom ein neuer übergangsmetall-carben-komplex, *J. Organomet. Chem.* **1968**, *12*, P42-P43, 10.1016/s0022-328x(00)88691-x.

[36]   D. M. Lemal, R. A. Lovald, K. I. Kawano, Tetraaminoethylenes. The Question of Dissociation, *J. Am. Chem. Soc.* **1964**, *86*, 2518-2519, 10.1021/ja01066a044.

[37]   Y. Liu, D. M. Lemal, Concerning the 'Wanzlick equilibrium', *Tetrahedron Lett.* **2000**, *41*, 599-602, 10.1016/s0040-4039(99)02161-9.

[38]   F. E. Hahn, L. Wittenbecher, D. Le Van, R. Fröhlich, Evidence for an Equilibrium between an N-heterocyclic Carbene and Its Dimer in Solution, *Angew. Chem. Int. Ed.* **2000**, *39*, 541-544, 10.1002/(sici)1521-3773(20000204)39:3<541::aid-anie541>3.0.co;2-b.

[39]   R. W. Alder, M. E. Blake, L. Chaker, J. N. Harvey, F. Paolini, J. Schütz, Wann und wie dimerisieren Diaminocarbene?, *Angew. Chem.* **2004**, *116*, 6020-6036, 10.1002/ange.200400654.

[40] R. W. Alder, M. E. Blake, L. Chaker, J. N. Harvey, F. Paolini, J. Schutz, When and how do diaminocarbenes dimerize?, *Angew. Chem. Int. Ed.* **2004**, *43*, 5896-5911, 10.1002/anie.200400654.

[41] V. P. W. Böhm, W. A. Herrmann, Das „Wanzlick-Gleichgewicht", *Angew. Chem.* **2000**, *112*, 4200-4202, 10.1002/1521-3757(20001117)112:22<4200::aid-ange4200>3.0.co;2-m.

[42] M.-J. Cheng, C.-H. Hu, A computational study on the stability of diaminocarbenes, *Chem. Phys. Lett.* **2000**, *322*, 83-90, 10.1016/s0009-2614(00)00388-2.

[43] F. E. Hahn, L. Wittenbecher, D. Le Van, R. Fröhlich, Nachweis des Gleichgewichts zwischen einem N-heterocyclischen Carben und seinem Dimer in Lösung, *Angew. Chem.* **2000**, *112*, 551-554, 10.1002/(sici)1521-3757(20000204)112:3<551::aid-ange551>3.0.co;2-v.

[44] K. Öfele, Pentacarbonyl(2,3-diphenylcyclopropenyliden)-chrom(0), *Angew. Chem.* **1968**, *80*, 1032-1033, 10.1002/ange.19680802410.

[45] H.-J. Schönherr, H.-W. Wanzlick, Chemie nucleophiler Carbene, XX HX-Abspaltung aus 1.3-Diphenyl-imidazoliumsalzen. Quecksilbersalz-Carben-Komplexe, *Chem. Ber.* **1970**, *103*, 1037-1046, 10.1002/cber.19701030407.

[46] H.-J. Schönherr, H.-W. Wanzlick, Chemie nucleophiler Carbene, XVIII1) 1.3.4.5-Tetraphenyl-imidazoliumperchlorat, *Liebigs Ann. Chem.* **1970**, *731*, 176-179, 10.1002/jlac.19707310121.

[47] B. Lachmann, H.-W. Wanzlick, Chemie nucleophiler Carbene, XVII Zur Kenntnis der anomalen α-Eliminierung Aldehyde aus 1.3-Diphenyl-2-alkoxy-imidazolidinen und Grignard-Verbindungen, *Liebigs Ann. Chem.* **1969**, *729*, 27-32, 10.1002/jlac.19697290105.

[48] H. W. Wanzlick, Nucleophile Carben-Chemie, *Angew. Chem.* **1962**, *74*, 129-134, 10.1002/ange.19620740402.

[49] H. W. Wanzlick, Aspects of Nucleophilic Carbene Chemistry, *Angew. Chem. Int. Ed.* **1962**, *1*, 75-80, 10.1002/anie.196200751.

[50] A. J. Arduengo, R. L. Harlow, M. Kline, A stable crystalline carbene, *J. Am. Chem. Soc.* **1991**, *113*, 361-363, 10.1021/ja00001a054.

[51] A. J. Arduengo, H. V. R. Dias, R. L. Harlow, M. Kline, Electronic stabilization of nucleophilic carbenes, *J. Am. Chem. Soc.* **1992**, *114*, 5530-5534, 10.1021/ja00040a007.

[52] A. J. Arduengo, Looking for Stable Carbenes: The Difficulty in Starting Anew, *Accounts Chem. Res.* **1999**, *32*, 913-921, 10.1021/ar980126p.

[53] F. Wang, L.-j. Liu, W. Wang, S. Li, M. Shi, Chiral NHC–metal-based asymmetric catalysis, *Coord. Chem. Rev.* **2012**, *256*, 804-853, 10.1016/j.ccr.2011.11.013.

[54] A. J. Arduengo, F. Davidson, H. V. R. Dias, J. R. Goerlich, D. Khasnis, W. J. Marshall, T. K. Prakasha, An Air Stable Carbene and Mixed Carbene "Dimers", *J. Am. Chem. Soc.* **1997**, *119*, 12742-12749, 10.1021/ja973241o.

[55] T. Kato, H. Gornitzka, A. Baceiredo, A. Savin, G. Bertrand, On the Electronic Structure of (Phosphino)(silyl)carbenes: Single-Crystal X-ray Diffraction and ELF Analyses, *J. Am. Chem. Soc.* **2000**, *122*, 998-999, 10.1021/ja9939542.

[56] E. A. Carter, W. A. Goddard, Correlation-consistent singlet–triplet gaps in substituted carbenes, *J. Chem. Phys.* **1988**, *88*, 1752-1763, 10.1063/1.454099.

[57] M.-J. Cheng, C.-L. Lai, C.-H. Hu *, Theoretical study of the Wanzlick equilibrium, *Mol. Phys.* **2004**, *102*, 2617-2621, 10.1080/00268970412331292911.

[58]   T. A. Taton, P. Chen, A Stable Tetraazafulvalene, *Angew. Chem. Int. Ed.* **1996**, *35*, 1011-1013, 10.1002/anie.199610111.

[59]   A. J. Arduengo, J. R. Goerlich, W. J. Marshall, A stable diaminocarbene, *J. Am. Chem. Soc.* **1995**, *117*, 11027-11028, 10.1021/ja00149a034.

[60]   H. Jacobsen, A. Correa, A. Poater, C. Costabile, L. Cavallo, Understanding the M(NHC) (NHC=N-heterocyclic carbene) bond, *Coord. Chem. Rev.* **2009**, *253*, 687-703, 10.1016/j.ccr.2008.06.006.

[61]   C. Heinemann, W. Thiel, Ab initio study on the stability of diaminocarbenes, *Chem. Phys. Lett.* **1994**, *217*, 11-16, 10.1016/0009-2614(93)e1360-s.

[62]   A. Poater, F. Ragone, S. Giudice, C. Costabile, R. Dorta, S. P. Nolan, L. Cavallo, Thermodynamics of N-Heterocyclic Carbene Dimerization: The Balance of Sterics and Electronics, *Organometallics* **2008**, *27*, 2679-2681, 10.1021/om8001119.

[63]   T. Droge, F. Glorius, The measure of all rings--N-heterocyclic carbenes, *Angew. Chem. Int. Ed.* **2010**, *49*, 6940-6952, 10.1002/anie.201001865.

[64]   R. W. Alder, M. E. Blake, C. Bortolotti, S. Bufali, C. P. Butts, E. Linehan, J. M. Oliva, A. Guy Orpen, M. J. Quayle, Complexation of stable carbenes with alkali metals, *Chem. Commun.* **1999**, 241-242, 10.1039/a808951e.

[65]   F. Iwasaki, M. Yasui, S. Yoshida, H. Nishiyama, S. Shimamoto, N. Matsumura, Crystal and Molecular Structures of Novel Metal–Carbene Complexes III. Rh–Carbene Complexes and Cu Complex, *Bull. Chem. Soc. Jpn.* **1996**, *69*, 2759-2770, 10.1246/bcsj.69.2759.

[66]   P. Bazinet, G. P. Yap, D. S. Richeson, Constructing a stable carbene with a novel topology and electronic framework, *J. Am. Chem. Soc.* **2003**, *125*, 13314-13315, 10.1021/ja0372661.

[67]   P. Bazinet, T.-G. Ong, J. S. O'Brien, N. Lavoie, E. Bell, G. P. A. Yap, I. Korobkov, D. S. Richeson, Design of Sterically Demanding, Electron-Rich Carbene Ligands with the Perimidine Scaffold, *Organometallics* **2007**, *26*, 2885-2895, 10.1021/om0701827.

[68]   R. Jazzar, H. Liang, B. Donnadieu, G. Bertrand, A New Synthetic Method for the Preparation of Protonated-NHCs and Related Compounds, *J. Organomet. Chem.* **2006**, *691*, 3201-3205, 10.1016/j.jorganchem.2006.04.008.

[69]   W. A. Herrmann, S. K. Schneider, K. Öfele, M. Sakamoto, E. Herdtweck, First silver complexes of tetrahydropyrimid-2-ylidenes, *J. Organomet. Chem.* **2004**, *689*, 2441-2449, 10.1016/j.jorganchem.2004.04.032.

[70]   M. Otto, S. Conejero, Y. Canac, V. D. Romanenko, V. Rudzevitch, G. Bertrand, Mono- and diaminocarbenes from chloroiminium and -amidinium salts: synthesis of metal-free bis(dimethylamino)carbene, *J. Am. Chem. Soc.* **2004**, *126*, 1016-1017, 10.1021/ja0393325.

[71]   F. E. Hahn, M. C. Jahnke, Heterocyclische Carbene - Synthese und Koordinationschemie, *Angew. Chem.* **2008**, *120*, 3166-3216, 10.1002/ange.200703883.

[72]   F. E. Hahn, M. C. Jahnke, Heterocyclic carbenes: synthesis and coordination chemistry, *Angew. Chem. Int. Ed.* **2008**, *47*, 3122-3172, 10.1002/anie.200703883.

[73]   E. Despagnet-Ayoub, R. H. Grubbs, A stable four-membered N-heterocyclic carbene, *J. Am. Chem. Soc.* **2004**, *126*, 10198-10199, 10.1021/ja047892d.

[74]   D. Enders, K. Breuer, G. Raabe, J. Runsink, J. H. Teles, J.-P. Melder, K. Ebel, S. Brode, Darstellung, Struktur und Reaktivität von 1,3,4-Triphenyl-4,5-dihydro-1H-1,2,4-triazol-

5-yliden, einem neuen stabilen Carben, *Angew. Chem.* **1995**, *107*, 1119-1122, 10.1002/ange.19951070926.

[75] D. Enders, K. Breuer, G. Raabe, J. Runsink, J. H. Teles, J.-P. Melder, K. Ebel, S. Brode, Preparation, Structure, and Reactivity of 1,3,4-Triphenyl-4,5-dihydro-1H-1,2,4-triazol-5-ylidene, a New Stable Carbene, *Angew. Chem. Int. Ed.* **1995**, *34*, 1021-1023, 10.1002/anie.199510211.

[76] L. A. Schaper, X. Wei, P. J. Altmann, K. Ofele, A. Pothig, M. Drees, J. Mink, E. Herdtweck, B. Bechlars, W. A. Herrmann, F. E. Kuhn, Synthesis and comparison of transition metal complexes of abnormal and normal tetrazolylidenes: a neglected ligand species, *Inorg. Chem.* **2013**, *52*, 7031-7044, 10.1021/ic4005449.

[77] V. Lavallo, Y. Canac, C. Prasang, B. Donnadieu, G. Bertrand, Stable cyclic (alkyl)(amino)carbenes as rigid or flexible, bulky, electron-rich ligands for transition-metal catalysts: a quaternary carbon atom makes the difference, *Angew. Chem. Int. Ed.* **2005**, *44*, 5705-5709, 10.1002/anie.200501841.

[78] R. W. Alder, P. R. Allen, M. Murray, A. G. Orpen, Bis(diisopropylamino)carben, *Angew. Chem.* **1996**, *108*, 1211-1213, 10.1002/ange.19961081026.

[79] A. J. Arduengo, J. R. Goerlich, W. J. Marshall, A stable thiazol-2-ylidene and its dimer, *Liebigs Ann. Recl.* **1997**, *1997*, 365-374, 10.1002/jlac.199719970213.

[80] D. Martin, A. Baceiredo, H. Gornitzka, W. W. Schoeller, G. Bertrand, A stable P-heterocyclic carbene, *Angew. Chem. Int. Ed.* **2005**, *44*, 1700-1703, 10.1002/anie.200462239.

[81] S. Diez-Gonzalez, N. Marion, S. P. Nolan, N-heterocyclic carbenes in late transition metal catalysis, *Chem. Rev.* **2009**, *109*, 3612-3676, 10.1021/cr900074m.

[82] S. Bellemin-Laponnaz, S. Dagorne, Group 1 and 2 and early transition metal complexes bearing N-heterocyclic carbene ligands: coordination chemistry, reactivity, and applications, *Chem. Rev.* **2014**, *114*, 8747-8774, 10.1021/cr500227y.

[83] M. C. Jahnke, F. E. Hahn, Complexes with protic (NH,NH and NH,NR) N-heterocyclic carbene ligands, *Coord. Chem. Rev.* **2015**, *293-294*, 95-115, 10.1016/j.ccr.2015.01.014.

[84] E. Peris, Smart N-Heterocyclic Carbene Ligands in Catalysis, *Chem. Rev.* **2018**, *118*, 9988-10031, 10.1021/acs.chemrev.6b00695.

[85] M. Mayr, K. Wurst, K. H. Ongania, M. R. Buchmeiser, 1,3-dialkyl- and 1,3-diaryl-3,4,5,6-tetrahydropyrimidin-2-ylidene rhodium(i) and palladium(II) complexes: synthesis, structure, and reactivity, *Chem. Eur. J.* **2004**, *10*, 1256-1266, 10.1002/chem.200305437.

[86] G. C. Fortman, S. P. Nolan, N-Heterocyclic carbene (NHC) ligands and palladium in homogeneous cross-coupling catalysis: a perfect union, *Chem. Soc. Rev.* **2011**, *40*, 5151-5169, 10.1039/c1cs15088j.

[87] V. Ritleng, M. Henrion, M. J. Chetcuti, Nickel N-Heterocyclic Carbene-Catalyzed C–Heteroatom Bond Formation, Reduction, and Oxidation: Reactions and Mechanistic Aspects, *ACS Catal.* **2016**, *6*, 890-906, 10.1021/acscatal.5b02021.

[88] G. C. Vougioukalakis, R. H. Grubbs, Ruthenium-based heterocyclic carbene-coordinated olefin metathesis catalysts, *Chem. Rev.* **2010**, *110*, 1746-1787, 10.1021/cr9002424.

[89] J. Huang, E. D. Stevens, S. P. Nolan, J. L. Petersen, Olefin Metathesis-Active Ruthenium Complexes Bearing a Nucleophilic Carbene Ligand, *J. Am. Chem. Soc.* **1999**, *121*, 2674-2678, 10.1021/ja9831352.

[90]   M. Scholl, T. M. Trnka, J. P. Morgan, R. H. Grubbs, Increased ring closing metathesis activity of ruthenium-based olefin metathesis catalysts coordinated with imidazolin-2-ylidene ligands, *Tetrahedron Lett.* **1999**, *40*, 2247-2250, 10.1016/s0040-4039(99)00217-8.

[91]   L. Ackermann, A. Fürstner, T. Weskamp, F. J. Kohl, W. A. Herrmann, Ruthenium carbene complexes with imidazolin-2-ylidene ligands allow the formation of tetrasubstituted cycloalkenes by RCM, *Tetrahedron Lett.* **1999**, *40*, 4787-4790, 10.1016/s0040-4039(99)00919-3.

[92]   M. Scholl, S. Ding, C. W. Lee, R. H. Grubbs, Synthesis and activity of a new generation of ruthenium-based olefin metathesis catalysts coordinated with 1,3-dimesityl-4,5-dihydroimidazol-2-ylidene ligands, *Org. Lett.* **1999**, *1*, 953-956, 10.1021/ol990909q.

[93]   M. J. Benedikter, J. V. Musso, W. Frey, R. Schowner, M. R. Buchmeiser, Cationic Group VI Metal Imido Alkylidene N-Heterocyclic Carbene Nitrile Complexes: Bench-Stable, Functional-Group-Tolerant Olefin Metathesis Catalysts, *Angew. Chem. Int. Ed.* **2020**, 10.1002/anie.202011666.

[94]   M. J. Benedikter, J. V. Musso, W. Frey, R. Schowner, M. R. Buchmeiser, Cationic Group VI Metal Imido Alkylidene N-Heterocyclic Carbene Nitrile Complexes: Bench-Stable, Functional-Group-Tolerant Olefin Metathesis Catalysts, *Angew. Chem.* **2020**, 10.1002/ange.202011666.

[95]   M. R. Buchmeiser, S. Sen, J. Unold, W. Frey, N-heterocyclic carbene, high oxidation state molybdenum alkylidene complexes: functional-group-tolerant cationic metathesis catalysts, *Angew. Chem. Int. Ed.* **2014**, *53*, 9384-9388, 10.1002/anie.201404655.

[96]   D. A. Imbrich, I. Elser, W. Frey, M. R. Buchmeiser, First Neutral and Cationic Tungsten Imido Alkylidene N-Heterocyclic Carbene Complexes, *ChemCatChem* **2017**, *9*, 2996-3002, 10.1002/cctc.201700189.

[97]   I. Elser, M. J. Benedikter, R. Schowner, W. Frey, D. Wang, M. R. Buchmeiser, Molybdenum Imido Alkylidene N-Heterocyclic Carbene Complexes Containing Pyrrolide Ligands: Access to Catalysts with Sterically Demanding Alkoxides, *Organometallics* **2019**, *38*, 2461-2471, 10.1021/acs.organomet.9b00148.

[98]   https://www.nobelprize.org/prizes/chemistry/2005/summary/, visitied on 10.07.2020.

[99]   https://www.nobelprize.org/prizes/chemistry/2010/summary/, visitied on 10.07.2020.

[100]   C. E. Hartmann, S. P. Nolan, C. S. J. Cazin, Highly Active [Pd(μ-Cl)(Cl)(NHC)]$_2$(NHC = N-Heterocyclic Carbene) in the Cross-Coupling of Grignard Reagents with Aryl Chlorides, *Organometallics* **2009**, *28*, 2915-2919, 10.1021/om900072f.

[101]   S. B. Garber, J. S. Kingsbury, B. L. Gray, A. H. Hoveyda, Efficient and Recyclable Monomeric and Dendritic Ru-Based Metathesis Catalysts, *J. Am. Chem. Soc.* **2000**, *122*, 8168-8179, 10.1021/ja001179g.

[102]   M. Fevre, J. Pinaud, Y. Gnanou, J. Vignolle, D. Taton, N-Heterocyclic carbenes (NHCs) as organocatalysts and structural components in metal-free polymer synthesis, *Chem. Soc. Rev.* **2013**, *42*, 2142-2172, 10.1039/c2cs35383k.

[103]   A. M. Magill, B. F. Yates, An Assessment of Theoretical Protocols for Calculation of the pKa Values of the Prototype Imidazolium Cation, *Aust. J. Chem.* **2004**, *57*, 1205, 10.1071/ch04159.

[104]   T. L. Amyes, S. T. Diver, J. P. Richard, F. M. Rivas, K. Toth, Formation and stability of N-heterocyclic carbenes in water: the carbon acid pKa of imidazolium cations in aqueous solution, *J. Am. Chem. Soc.* **2004**, *126*, 4366-4374, 10.1021/ja039890j.

[105] A. M. Magill, K. J. Cavell, B. F. Yates, Basicity of nucleophilic carbenes in aqueous and nonaqueous solvents-theoretical predictions, *J. Am. Chem. Soc.* **2004**, *126*, 8717-8724, 10.1021/ja038973x.

[106] Y. Chu, H. Deng, J. P. Cheng, An acidity scale of 1,3-dialkylimidazolium salts in dimethyl sulfoxide solution, *J. Org. Chem.* **2007**, *72*, 7790-7793, 10.1021/jo070973i.

[107] E. M. Higgins, J. A. Sherwood, A. G. Lindsay, J. Armstrong, R. S. Massey, R. W. Alder, A. C. O'Donoghue, pKas of the conjugate acids of N-heterocyclic carbenes in water, *Chem. Commun.* **2011**, *47*, 1559-1561, 10.1039/c0cc03367g.

[108] Z. Wang, F. Wang, X. S. Xue, P. Ji, Acidity Scale of N-Heterocyclic Carbene Precursors: Can We Predict the Stability of NHC-CO_2 Adducts?, *Org. Lett.* **2018**, *20*, 6041-6045, 10.1021/acs.orglett.8b02290.

[109] Z. Wang, X. S. Xue, Y. Fu, P. Ji, Comprehensive Basicity Scales for N-Heterocyclic Carbenes in DMSO: Implications on the Stabilities of N-Heterocyclic Carbene and CO_2 Adducts, *Chem. Asian. J.* **2020**, *15*, 169-181, 10.1002/asia.201901418.

[110] M. H. Dunn, N. Konstandaras, M. L. Cole, J. B. Harper, Targeted and Systematic Approach to the Study of pKa Values of Imidazolium Salts in Dimethyl Sulfoxide, *J. Org. Chem.* **2017**, *82*, 7324-7331, 10.1021/acs.joc.7b00716.

[111] B. Bantu, G. Manohar Pawar, K. Wurst, U. Decker, A. M. Schmidt, M. R. Buchmeiser, CO_2, Magnesium, Aluminum, and Zinc Adducts of N-Heterocyclic Carbenes as (Latent) Catalysts for Polyurethane Synthesis, *Eur. J. Inorg. Chem.* **2009**, *2009*, 1970-1976, https://doi.org/10.1002/ejic.200801161.

[112] B. Bantu, G. M. Pawar, U. Decker, K. Wurst, A. M. Schmidt, M. R. Buchmeiser, CO_2 and Sn(II) adducts of N-heterocyclic carbenes as delayed-action catalysts for polyurethane synthesis, *Chem. Eur. J.* **2009**, *15*, 3103-3109, 10.1002/chem.200802670.

[113] O. Coutelier, M. El Ezzi, M. Destarac, F. Bonnette, T. Kato, A. Baceiredo, G. Sivasankarapillai, Y. Gnanou, D. Taton, N-Heterocyclic carbene-catalysed synthesis of polyurethanes, *Polym. Chem.* **2012**, *3*, 605, 10.1039/c2py00477a.

[114] H. A. Duong, T. N. Tekavec, A. M. Arif, J. Louie, Reversible carboxylation of N-heterocyclic carbenes, *Chem. Commun.* **2004**, 112-113, 10.1039/b311350g.

[115] S. J. Ryan, L. Candish, D. W. Lupton, Acyl anion free N-heterocyclic carbene organocatalysis, *Chem. Soc. Rev.* **2013**, *42*, 4906-4917, 10.1039/c3cs35522e.

[116] D. Enders, O. Niemeier, A. Henseler, Organocatalysis by N-heterocyclic carbenes, *Chem. Rev.* **2007**, *107*, 5606-5655, 10.1021/cr068372z.

[117] N. Marion, S. Diez-Gonzalez, S. P. Nolan, N-heterocyclic carbenes as organocatalysts, *Angew. Chem. Int. Ed.* **2007**, *46*, 2988-3000, 10.1002/anie.200603380.

[118] H. A. Duong, M. J. Cross, J. Louie, N-heterocyclic carbenes as highly efficient catalysts for the cyclotrimerization of isocyanates, *Org. Lett.* **2004**, *6*, 4679-4681, 10.1021/ol048211m.

[119] M. Movassaghi, M. A. Schmidt, N-heterocyclic carbene-catalyzed amidation of unactivated esters with amino alcohols, *Org. Lett.* **2005**, *7*, 2453-2456, 10.1021/ol050773y.

[120] S. Naumann, F. G. Schmidt, W. Frey, M. R. Buchmeiser, Protected N-heterocyclic carbenes as latent pre-catalysts for the polymerization of ε-caprolactone, *Polym. Chem.* **2013**, *4*, 4172-4181, 10.1039/c3py00548h.

[121] M. G. Dekamin, K. Varmira, M. Farahmand, S. Sagheb-Asl, Z. Karimi, Organocatalytic, rapid and facile cyclotrimerization of isocyanates using tetrabutylammonium

phthalimide-N-oxyl and tetraethylammonium 2-(carbamoyl)benzoate under solvent-free conditions, *Catal. Commun.* **2010**, *12*, 226-230, 10.1016/j.catcom.2010.08.018.

[122] J. J. Song, Z. Tan, J. T. Reeves, F. Gallou, N. K. Yee, C. H. Senanayake, N-heterocyclic carbene catalyzed trifluoromethylation of carbonyl compounds, *Org. Lett.* **2005**, *7*, 2193-2196, 10.1021/ol050568i.

[123] J. J. Song, F. Gallou, J. T. Reeves, Z. Tan, N. K. Yee, C. H. Senanayake, Activation of TMSCN by N-heterocyclic carbenes for facile cyanosilylation of carbonyl compounds, *J. Org. Chem.* **2006**, *71*, 1273-1276, 10.1021/jo052206u.

[124] Y. Suzuki, M. D. A. Bakar, K. Muramatsu, M. Sato, Cyanosilylation of aldehydes catalyzed by N-heterocyclic carbenes, *Tetrahedron* **2006**, *62*, 4227-4231, 10.1016/j.tet.2006.01.101.

[125] K. Zeitler, Extending mechanistic routes in heterazolium catalysis--promising concepts for versatile synthetic methods, *Angew. Chem. Int. Ed.* **2005**, *44*, 7506-7510, 10.1002/anie.200502617.

[126] C. Burstein, F. Glorius, Organokatalysierte konjugierte Umpolung von ?,?-ungesttigten Aldehyden zur Synthese von ?-Butyrolactonen, *Angew. Chem.* **2004**, *116*, 6331-6334, 10.1002/ange.200461572.

[127] C. Burstein, F. Glorius, Organocatalyzed conjugate umpolung of alpha,beta-unsaturated aldehydes for the synthesis of gamma-butyrolactones, *Angew. Chem. Int. Ed.* **2004**, *43*, 6205-6208, 10.1002/anie.200461572.

[128] D. Enders, T. Balensiefer, Nucleophilic carbenes in asymmetric organocatalysis, *Acc. Chem. Res.* **2004**, *37*, 534-541, 10.1021/ar030050j.

[129] L. R. Domingo, M. J. Aurell, M. Arnó, Understanding the mechanism of the N-heterocyclic carbene-catalyzed ring-expansion of 4-formyl-β-lactams to succinimide derivatives, *Tetrahedron* **2009**, *65*, 3432-3440, 10.1016/j.tet.2009.02.030.

[130] J. Pinaud, K. Vijayakrishna, D. Taton, Y. Gnanou, Step-Growth Polymerization of Terephthaldehyde Catalyzed by N-Heterocyclic Carbenes, *Macromolecules* **2009**, *42*, 4932-4936, 10.1021/ma900907f.

[131] A. T. Biju, N. Kuhl, F. Glorius, Extending NHC-catalysis: coupling aldehydes with unconventional reaction partners, *Acc. Chem. Res.* **2011**, *44*, 1182-1195, 10.1021/ar2000716.

[132] C. A. Tolman, Steric effects of phosphorus ligands in organometallic chemistry and homogeneous catalysis, *Chem. Rev.* **1977**, *77*, 313-348, 10.1021/cr60307a002.

[133] D. J. Nelson, S. P. Nolan, Quantifying and understanding the electronic properties of N-heterocyclic carbenes, *Chem. Soc. Rev.* **2013**, *42*, 6723-6753, 10.1039/c3cs60146c.

[134] A. R. Chianese, X. Li, M. C. Janzen, F. J. W., R. H. Carbtree, Rhodium and Iridium Complexes of N-Heterocyclic Carbenes via Transmetalation: Structure and Dynamics, *Organometallics* **2003**, *22*, 1663-1667, 10.1021/om021029+.

[135] R. A. Kelly Iii, H. Clavier, S. Giudice, N. M. Scott, E. D. Stevens, J. Bordner, I. Samardjiev, C. D. Hoff, L. Cavallo, S. P. Nolan, Determination of N-Heterocyclic Carbene (NHC) Steric and Electronic Parameters using the [(NHC)Ir(CO)$_2$Cl] System, *Organometallics* **2008**, *27*, 202-210, 10.1021/om701001g.

[136] S. Wolf, H. Plenio, Synthesis of (NHC)Rh(cod)Cl and (NHC)RhCl(CO)$_2$ complexes – Translation of the Rh- into the Ir-scale for the electronic properties of NHC ligands, *J. Organomet. Chem.* **2009**, *694*, 1487-1492, 10.1016/j.jorganchem.2008.12.047.

[137] T. Vorfalt, S. Leuthäußer, H. Plenio, An [(NHC)(NHC$_{EWG}$)RuCl$_2$(CHPh)] Complex for the Efficient Formation of Sterically Hindered Olefins by Ring-Closing Metathesis, *Angew. Chem.* **2009**, *121*, 5293-5296, 10.1002/ange.200900935.

[138] T. Vorfalt, S. Leuthausser, H. Plenio, An [(NHC)(NHC$_{EWG}$))RuCl$_2$(CHPh)] complex for the efficient formation of sterically hindered olefins by ring-closing metathesis, *Angew. Chem. Int. Ed.* **2009**, *48*, 5191-5194, 10.1002/anie.200900935.

[139] A. Furstner, M. Alcarazo, H. Krause, C. W. Lehmann, Effective modulation of the donor properties of N-heterocyclic carbene ligands by "through-space" communication within a planar chiral scaffold, *J. Am. Chem. Soc.* **2007**, *129*, 12676-12677, 10.1021/ja076028t.

[140] S. Naumann, A. P. Dove, N-Heterocyclic carbenes for metal-free polymerization catalysis: an update, *Polym. Int.* **2016**, *65*, 16-27, 10.1002/pi.5034.

[141] R. Breslow, On the Mechanism of Thiamine Action. IV.1Evidence from Studies on Model Systems, *J. Am. Chem. Soc.* **1958**, *80*, 3719-3726, 10.1021/ja01547a064.

[142] H. Zhao, F. W. Foss, Jr., R. Breslow, Artificial enzymes with thiazolium and imidazolium coenzyme mimics, *J. Am. Chem. Soc.* **2008**, *130*, 12590-12591, 10.1021/ja804577q.

[143] A. Berkessel, S. Elfert, V. R. Yatham, J. M. Neudorfl, N. E. Schlorer, J. H. Teles, Umpolung by N-heterocyclic carbenes: generation and reactivity of the elusive 2,2-diamino enols (Breslow intermediates), *Angew. Chem. Int. Ed.* **2012**, *51*, 12370-12374, 10.1002/anie.201205878.

[144] A. Berkessel, V. R. Yatham, S. Elfert, J. M. Neudorfl, Characterization of the key intermediates of carbene-catalyzed umpolung by NMR spectroscopy and X-ray diffraction: breslow intermediates, homoenolates, and azolium enolates, *Angew. Chem. Int. Ed.* **2013**, *52*, 11158-11162, 10.1002/anie.201303107.

[145] B. Maji, H. Mayr, Structures and ambient reactivities of azolium enolates, *Angew. Chem. Int. Ed.* **2013**, *52*, 11163-11167, 10.1002/anie.201303524.

[146] M. K. Denk, J. M. Rodezno, S. Gupta, A. J. Lough, Synthesis and reactivity of subvalent compounds, *J. Organomet. Chem.* **2001**, *617-618*, 242-253, 10.1016/s0022-328x(00)00551-9.

[147] W. A. Herrmann, N-Heterocyclische Carbene: ein neues Konzept in der metallorganischen Katalyse N-Heterocyclische Carbene, 31. Mitteilung. – 30. Mitteilung: Lit. [80], *Angew. Chem.* **2002**, *114*, 1342-1363, 10.1002/1521-3757(20020415)114:8<1342::aid-ange1342>3.0.co;2-a.

[148] W. A. Herrmann, N-Heterocyclic Carbenes: A New Concept in Organometallic Catalysis, *Angew. Chem. Int. Ed.* **2002**, *41*, 1290-1309, 10.1002/1521-3773(20020415)41:8<1290::aid-anie1290>3.0.co;2-y.

[149] E. Levin, E. Ivry, C. E. Diesendruck, N. G. Lemcoff, Water in N-heterocyclic carbene-assisted catalysis, *Chem. Rev.* **2015**, *115*, 4607-4692, 10.1021/cr400640e.

[150] C. Samojlowicz, M. Bieniek, K. Grela, Ruthenium-based olefin metathesis catalysts bearing N-heterocyclic carbene ligands, *Chem. Rev.* **2009**, *109*, 3708-3742, 10.1021/cr800524f.

[151] S. L. Balof, J. P'Pool S, N. J. Berger, E. J. Valente, A. M. Shiller, H. J. Schanz, Olefin metathesis catalysts bearing a pH-responsive NHC ligand: a feasible approach to catalyst separation from RCM products, *Dalton Trans.* **2008**, 5791-5799, 10.1039/b809793c.

[152] J. P. Gallivan, J. P. Jordan, R. H. Grubbs, A neutral, water-soluble olefin metathesis catalyst based on an N-heterocyclic carbene ligand, *Tetrahedron Lett.* **2005**, *46*, 2577-2580, 10.1016/j.tetlet.2005.02.096.

[153] S. H. Hong, R. H. Grubbs, Highly active water-soluble olefin metathesis catalyst, *J. Am. Chem. Soc.* **2006**, *128*, 3508-3509, 10.1021/ja058451c.

[154] S. H. Hong, R. H. Grubbs, Efficient removal of ruthenium byproducts from olefin metathesis products by simple aqueous extraction, *Org. Lett.* **2007**, *9*, 1955-1957, 10.1021/ol070512j.

[155] S. Naumann, M. R. Buchmeiser, Liberation of N-heterocyclic carbenes (NHCs) from thermally labile progenitors: protected NHCs as versatile tools in organo- and polymerization catalysis, *Catal. Sci. Technol.* **2014**, *4*, 2466-2479, 10.1039/c4cy00344f.

[156] A. Tudose, L. Delaude, B. André, A. Demonceau, Imidazol(in)ium carboxylates as N-heterocyclic carbene ligand precursors for Suzuki–Miyaura reactions, *Tetrahedron Lett.* **2006**, *47*, 8529-8533, 10.1016/j.tetlet.2006.09.139.

[157] A. M. Voutchkova, M. Feliz, E. Clot, O. Eisenstein, R. H. Crabtree, Imidazolium carboxylates as versatile and selective N-heterocyclic carbene transfer agents: synthesis, mechanism, and applications, *J. Am. Chem. Soc.* **2007**, *129*, 12834-12846, 10.1021/ja0742885.

[158] G. M. Pawar, M. R. Buchmeiser, Polymer-Supported, Carbon Dioxide-Protected N-Heterocyclic Carbenes: Synthesis and Application in Organo- and Organometallic Catalysis, *Adv. Synth. Catal.* **2010**, *352*, 917-928, 10.1002/adsc.200900658.

[159] S. Naumann, M. R. Buchmeiser, Latent and delayed action polymerization systems, *Macromol. Rapid. Commun.* **2014**, *35*, 682-701, 10.1002/marc.201300898.

[160] T. K. H. Trinh, J. P. Malval, F. Morlet-Savary, J. Pinaud, P. Lacroix-Desmazes, C. Reibel, V. Heroguez, A. Chemtob, Mixture of Azolium Tetraphenylborate with Isopropylthioxanthone: A New Class of N-Heterocyclic Carbene (NHC) Photogenerator for Polyurethane, Polyester, and ROMP Polymers Synthesis, *Chem. Eur. J.* **2019**, *25*, 9242-9252, 10.1002/chem.201901000.

[161] M. Fevre, J. Pinaud, A. Leteneur, Y. Gnanou, J. Vignolle, D. Taton, K. Miqueu, J. M. Sotiropoulos, Imidazol(in)ium hydrogen carbonates as a genuine source of N-heterocyclic carbenes (NHCs): applications to the facile preparation of NHC metal complexes and to NHC-organocatalyzed molecular and macromolecular syntheses, *J. Am. Chem. Soc.* **2012**, *134*, 6776-6784, 10.1021/ja3005804.

[162] M. Fevre, P. Coupillaud, K. Miqueu, J. M. Sotiropoulos, J. Vignolle, D. Taton, Imidazolium hydrogen carbonates versus imidazolium carboxylates as organic precatalysts for N-heterocyclic carbene catalyzed reactions, *J. Org. Chem.* **2012**, *77*, 10135-10144, 10.1021/jo301597h.

[163] D. M. Denning, M. D. Thum, D. E. Falvey, Photochemical Reduction of CO_2 Using 1,3-Dimethylimidazolylidene, *Org. Lett.* **2015**, *17*, 4152-4155, 10.1021/acs.orglett.5b01891.

[164] O. Coulembier, A. P. Dove, R. C. Pratt, A. C. Sentman, D. A. Culkin, L. Mespouille, P. Dubois, R. M. Waymouth, J. L. Hedrick, Latent, thermally activated organic catalysts for the on-demand living polymerization of lactide, *Angew. Chem. Int. Ed.* **2005**, *44*, 4964-4968, 10.1002/anie.200500723.

[165] S. Csihony, D. A. Culkin, A. C. Sentman, A. P. Dove, R. M. Waymouth, J. L. Hedrick, Single-component catalyst/initiators for the organocatalytic ring-opening polymerization of lactide, *J. Am. Chem. Soc.* **2005**, *127*, 9079-9084, 10.1021/ja050909n.

[166] G. W. Nyce, S. Csihony, R. M. Waymouth, J. L. Hedrick, A general and versatile approach to thermally generated N-heterocyclic carbenes, *Chem. Eur. J.* **2004**, *10*, 4073-4079, 10.1002/chem.200400196.

[167] O. Coulembier, B. G. G. Lohmeijer, A. P. Dove, R. C. Pratt, L. Mespouille, D. A. Culkin, S. J. Benight, P. Dubois, R. M. Waymouth, J. L. Hedrick, Alcohol Adducts of N-Heterocyclic Carbenes: Latent Catalysts for the Thermally-Controlled Living Polymerization of Cyclic Esters, *Macromolecules* **2006**, *39*, 5617-5628, 10.1021/ma0611366.

[168] M. H. Wang, K. A. Scheidt, Kooperative Katalyse mit N-heterocyclischen Carbenen, *Angew. Chem.* **2016**, *128*, 15134-15145, 10.1002/ange.201605319.

[169] M. H. Wang, K. A. Scheidt, Cooperative Catalysis and Activation with N-Heterocyclic Carbenes, *Angew. Chem. Int. Ed.* **2016**, *55*, 14912-14922, 10.1002/anie.201605319.

[170] R. Schowner, W. Frey, M. R. Buchmeiser, Understanding Synthetic Peculiarities of Cationic Molybdenum(VI) Imido Alkylidene N-Heterocyclic Carbene Complexes, *Eur. J. Inorg. Chem.* **2019**, *2019*, 1911-1922, 10.1002/ejic.201900021.

[171] M. Iglesias, D. J. Beetstra, J. C. Knight, L.-L. Ooi, A. Stasch, S. Coles, L. Male, M. B. Hursthouse, K. J. Cavell, A. Dervisi, I. A. Fallis, Novel Expanded Ring N-Heterocyclic Carbenes: Free Carbenes, Silver Complexes, And Structures, *Organometallics* **2008**, *27*, 3279-3289, 10.1021/om800179t.

[172] I. Elser, R. Schowner, W. Frey, M. R. Buchmeiser, Molybdenum and Tungsten Imido Alkylidene N-Heterocyclic Carbene Catalysts Bearing Cationic Ligands for Use in Biphasic Olefin Metathesis, *Chem. Eur. J.* **2017**, *23*, 6398-6405, 10.1002/chem.201700213.

[173] I. Elser, J. Groos, P. M. Hauser, M. Koy, M. van der Ende, D. Wang, W. Frey, K. Wurst, J. Meisner, F. Ziegler, J. Kästner, M. R. Buchmeiser, Molybdenum and Tungsten Alkylidyne Complexes Containing Mono-, Bi-, and Tridentate N-Heterocyclic Carbenes, *Organometallics* **2019**, *38*, 4133-4146, 10.1021/acs.organomet.9b00481.

[174] M. Koy, I. Elser, J. Meisner, W. Frey, K. Wurst, J. Kastner, M. R. Buchmeiser, High Oxidation State Molybdenum N-Heterocyclic Carbene Alkylidyne Complexes: Synthesis, Mechanistic Studies, and Reactivity, *Chem. Eur. J.* **2017**, *23*, 15484-15490, 10.1002/chem.201703313.

[175] H. M. J. Wang, I. J. B. Lin, Facile Synthesis of Silver(I)−Carbene Complexes. Useful Carbene Transfer Agents, *Organometallics* **1998**, *17*, 972-975, 10.1021/om9709704.

[176] J. C. Lin, R. T. Huang, C. S. Lee, A. Bhattacharyya, W. S. Hwang, I. J. Lin, Coinage metal-N-heterocyclic carbene complexes, *Chem. Rev.* **2009**, *109*, 3561-3598, 10.1021/cr8005153.

[177] V. H. Wong, S. V. Vummaleti, L. Cavallo, A. J. White, S. P. Nolan, K. K. Hii, Synthesis, Structure and Catalytic Activity of NHC-Ag(I) Carboxylate Complexes, *Chem. Eur. J.* **2016**, *22*, 13320-13327, 10.1002/chem.201601762.

[178] M. J. Ajitha, C. H. Suresh, Assessment of stereoelectronic factors that influence the CO_2 fixation ability of N-heterocyclic carbenes: a DFT study, *J. Org. Chem.* **2012**, *77*, 1087-1094, 10.1021/jo202382g.

[179] L. Delaude, A. Demonceau, J. Wouters, Assessing the Potential of Zwitterionic NHC·CS2Adducts for Probing the Stereoelectronic Parameters of N-Heterocyclic Carbenes, *Eur. J. Inorg. Chem.* **2009**, *2009*, 1882-1891, 10.1002/ejic.200801110.

[180] M. Hans, J. Wouters, A. Demonceau, L. Delaude, Synthesis and Organocatalytic Applications of Imidazol(in)ium-2-thiocarboxylates, *Eur. J. Org. Chem.* **2011**, *2011*, 7083-7091, 10.1002/ejoc.201101286.

[181] L. Delaude, Betaine Adducts of N-Heterocyclic Carbenes: Synthesis, Properties, and Reactivity, *Eur. J. Inorg. Chem.* **2009**, *2009*, 1681-1699, 10.1002/ejic.200801227.

[182] B. R. Van Ausdall, J. L. Glass, K. M. Wiggins, A. M. Aarif, J. Louie, A systematic investigation of factors influencing the decarboxylation of imidazolium carboxylates, *J. Org. Chem.* **2009**, *74*, 7935-7942, 10.1021/jo901791k.

[183] D. M. Denning, D. E. Falvey, Solvent-dependent decarboxylation of 1,3-dimethylimdazolium-2-carboxylate, *J. Org. Chem.* **2014**, *79*, 4293-4299, 10.1021/jo5007575.

[184] L. Benhamou, E. Chardon, G. Lavigne, S. Bellemin-Laponnaz, V. Cesar, Synthetic routes to N-heterocyclic carbene precursors, *Chem. Rev.* **2011**, *111*, 2705-2733, 10.1021/cr100328e.

[185] J. Li, J. Peng, Y. Bai, G. Lai, X. Li, Synthesis of rhodium N-heterocyclic carbene complexes and their catalytic activity in the hydrosilylation of alkenes in ionic liquid medium, *J. Organomet. Chem.* **2011**, *696*, 2116-2121, 10.1016/j.jorganchem.2010.11.017.

[186] C. Rijksen, R. D. Rogers, A solventless route to 1-ethyl-3-methylimidazolium fluoride hydrofluoride, [C2mim][F] x xHF, *J. Org. Chem.* **2008**, *73*, 5582-5584, 10.1021/jo800578b.

[187] I. Tommasi, F. Sorrentino, Utilisation of 1,3-dialkylimidazolium-2-carboxylates as CO_2-carriers in the presence of Na+ and K+: application in the synthesis of carboxylates, monomethylcarbonate anions and halogen-free ionic liquids, *Tetrahedron Lett.* **2005**, *46*, 2141-2145, 10.1016/j.tetlet.2005.01.106.

[188] S. Naumann, F. G. Schmidt, R. Schowner, W. Frey, M. R. Buchmeiser, Polymerization of methyl methacrylate by latent pre-catalysts based on CO_2-protected N-heterocyclic carbenes, *Polym. Chem.* **2013**, *4*, 2731-2740, 10.1039/c3py00073g.

[189] N. Kuhn, M. Steimann, G. Weyers, Synthese und Eigenschaften von 1,3-Diisopropyl-4,5-dimethylimidazolium- 2-carboxylat. Ein stabiles Carben-Addukt des Kohlendioxids [1] / Synthesis and Properties of 1,3-Diisopropyl-4,5-dimethylimidazolium -2-carboxylate. A Stable Carbene Adduct of Carbon Dioxide [1], *Z. Naturforsch., B: Chem. Sci.* **1999**, *54*, 427-433, 10.1515/znb-1999-0401.

[190] I. Tommasi, F. Sorrentino, Synthesis of 1,3-dialkylimidazolium-2-carboxylates by direct carboxylation of 1,3-dialkylimidazolium chlorides with CO_2, *Tetrahedron Lett.* **2006**, *47*, 6453-6456, 10.1016/j.tetlet.2006.06.106.

[191] N. Kuhn, M. Steimann, G. Weyers, G. Henkel, 1,3-Diisopropyl-4,5-dimethylimidazolium-2-N,N'-diisopropylamidinat, ein neuartiges Retain [1] / 1,3-Diisopropyl-4,5-dimethylimidazolium-2-N,N'-diisopropylamidinate, a Novel Betaine [1], *Z. Naturforsch., B: Chem. Sci.* **1999**, *54*, 434-440, 10.1515/znb-1999-0402.

[192] H. E. Winberg, D. D. Coffman, Chemistry of Peraminoethylenes, *J. Am. Chem. Soc.* **1965**, *87*, 2776-2777, 10.1021/ja01090a057.

[193] H. E. Winberg, J. E. Carnahan, D. D. Coffman, M. Brown, Tetraaminoethylenes, *J. Am. Chem. Soc.* **1965**, *87*, 2055-2056, 10.1021/ja01087a040.

[194] M. Regitz, J. Hocker, 1,3,6,9-Tetraaza-spiro[4.4]nonane aus Bi-[1,3-diphenyl-imidazolidinyliden-(2)] und lsocyanaten bzw. Isothiocyanaten, *Synthesis* **1970**, *1970*, 301-302, 10.1055/s-1970-21607.

[195] W. Schössler, M. Regitz, Stabile Dipole aus 1,1′,3,3′ -Tetraphenyl-2,2′-bimidazolidinyliden und Acyliso- bzw. Acylisothiocyanaten, *Chem. Ber.* **1974**, *107*, 1931-1948, 10.1002/cber.19741070617.

[196] J. Hocker, R. Merten, Parabansäure-Derivate Ein Beitrag zur Chemie der nucleophilen Carbene, *Liebigs Ann. Chem.* **1971**, *751*, 145-154, 10.1002/jlac.19717510117.

[197] M. Regitz, J. Hocker, W. Schössler, B. Weber, A. Liedhegener, Umsetzungen von Bis-[1.3-diaryl-imidazolidinylidenen-(2)] mit Iso-, Isothio- bzw. Isoselenocyanaten, *Liebigs Ann. Chem.* **1971**, *748*, 1-19, 10.1002/jlac.19717480102.

[198] R. W. Hoffmann, B. Hagenbruch, D. M. Smith, Carben-Reaktionen, VIII. Selektivität nucleophiler Carbene gegenüber Heterocumulenen, *Chem. Ber.* **1977**, *110*, 23-36, 10.1002/cber.19771100104.

[199] B. C. Norris, C. W. Bielawski, Structurally Dynamic Materials Based on Bis(N-heterocyclic carbene)s and Bis(isothiocyanate)s: Toward Reversible, Conjugated Polymers, *Macromolecules* **2010**, *43*, 3591-3593, 10.1021/ma100524g.

[200] B. C. Norris, D. G. Sheppard, G. Henkelman, C. W. Bielawski, Kinetic and thermodynamic evaluation of the reversible N-heterocyclic carbene-isothiocyanate coupling reaction: applications in latent catalysis, *J. Org. Chem.* **2011**, *76*, 301-304, 10.1021/jo101850g.

[201] A. R. Katritzky, D. Jishkariani, R. Sakhuja, C. D. Hall, P. J. Steel, Carbene-mediated transformations of 1-(benzylideneamino)benzimidazoles, *J. Org. Chem.* **2011**, *76*, 4082-4087, 10.1021/jo200088s.

[202] D. Jishkariani, C. D. Hall, A. Oliferenko, B. J. Tomlin, P. J. Steel, A. R. Katritzky, Thermal fragmentation of spirodithiohydantoins: A novel route to NHCs, *RCS Adv.* **2013**, *3*, 1669-1672, 10.1039/c2ra22487a.

[203] A. Takamizawa, K. Hirai, S. Matsumoto, T. Ishiba, Studies on Pyrimidine Derivatives and Related Compounds. LVI. Reaction of Thiamine with Isocyanates. (I), *Chem. Pharm. Bull.* **1968**, *16*, 2130-2136, 10.1248/cpb.16.2130.

[204] A. Takamizawa, K. Hirai, S. Matsumoto, T. Ishiba, Studies on pyrimidine derivatives and related compounds. LXI. Reaction of thiamine with isocyanates. 2, *Chem. Pharm. Bull.* **1969**, *17*, 462-466, 10.1248/cpb.17.462.

[205] D. Enders, K. Breuer, J. Runsink, J. Henrique Teles, Chemical Reactions of the Stable Carbene 1,3,4-Triphenyl-4,5-dihydro-1H-1,2,4-triazol-5-ylidene, *Liebigs Annalen* **1996**, *1996*, 2019-2028, 10.1002/jlac.199619961212.

[206] H. Küçükbay, R. Durmaz, E. Orhan, S. Günal, Synthesis, antibacterial and antifungal activities of electron-rich olefins derived benzimidazole compounds, *Il Farmaco* **2003**, *58*, 431-437, 10.1016/s0014-827x(03)00068-5.

[207] H. Küçükbay, E. Cetinkaya, R. Durmaz, Synthesis and anti-microbial activity of substituted benzimidazole, benzothiazole and imidazole derivatives, *Arzneim.-Forsch./Drug Res.* **1995**, *45*, 1331-1334,

[208] S.-i. Matsuoka, Y. Tochigi, K. Takagi, M. Suzuki, Sequential one-pot and three-component reactions of an N-heterocyclic carbene to form 4-(1,2,4-triazol-5-ylidene)pyrrolidine-2,5-diones: a tandem umpolung/annulation sequence via deoxy-Breslow intermediates, *Tetrahedron* **2012**, *68*, 9836-9841, 10.1016/j.tet.2012.08.076.

[209] F.-L. Jin, X. Li, S.-J. Park, Synthesis and application of epoxy resins: A review, *J. Ind. Eng. Chem.* **2015**, *29*, 1-11, 10.1016/j.jiec.2015.03.026.

[210] S.-J. Park, F.-L. Jin, Thermal stabilities and dynamic mechanical properties of sulfone-containing epoxy resin cured with anhydride, *Polym. Deg. Stab.* **2004**, *86*, 515-520, 10.1016/j.polymdegradstab.2004.06.003.

[211] K. Frank, C. Childers, D. Dutta, D. Gidley, M. Jackson, S. Ward, R. Maskell, J. Wiggins, Fluid uptake behavior of multifunctional epoxy blends, *Polymer* **2013**, *54*, 403-410, 10.1016/j.polymer.2012.11.065.

[212] S. Sprenger, Epoxy resin composites with surface-modified silicon dioxide nanoparticles: A review, *J. Appl. Polym. Sci.* **2013**, *130*, 1421-1428, 10.1002/app.39208.

[213] S. Sprenger, Fiber-reinforced composites based on epoxy resins modified with elastomers and surface-modified silica nanoparticles, *J. Mater. Sci.* **2013**, *49*, 2391-2402, 10.1007/s10853-013-7963-8.

[214] M. Fan, J. Liu, X. Li, J. Cheng, J. Zhang, Curing behaviors and properties of an extrinsic toughened epoxy/anhydride system and an intrinsic toughened epoxy/anhydride system, *Thermochim. Acta* **2013**, *554*, 39-47, 10.1016/j.tca.2012.12.007.

[215] A. C. Garg, Y.-W. Mai, Failure mechanisms in toughened epoxy resins—A review, *Compos. Sci. Technol.* **1988**, *31*, 179-223, 10.1016/0266-3538(88)90009-7.

[216] W. Dong, H.-C. Liu, S.-J. Park, F.-L. Jin, Fracture toughness improvement of epoxy resins with short carbon fibers, *J. Ind. Eng. Chem.* **2014**, *20*, 1220-1222, 10.1016/j.jiec.2013.06.053.

[217] S.-J. Park, H.-C. Kim, H.-I. Lee, D.-H. Suh, Thermal Stability of Imidized Epoxy Blends Initiated byN-Benzylpyrazinium Hexafluoroantimonate Salt, *Macromolecules* **2001**, *34*, 7573-7575, 10.1021/ma010792x.

[218] F.-L. Jin, S.-J. Park, Thermomechanical behavior of epoxy resins modified with epoxidized vegetable oils, *Polym. Int.* **2008**, *57*, 577-583, 10.1002/pi.2280.

[219] W. Jiang, F.-L. Jin, S.-J. Park, Synthesis of a novel phosphorus-nitrogen-containing intumescent flame retardant and its application to fabrics, *J. Ind. Eng. Chem.* **2015**, *27*, 40-43, 10.1016/j.jiec.2015.01.010.

[220] F.-L. Jin, S.-J. Park, Impact-strength improvement of epoxy resins reinforced with a biodegradable polymer, *Mater. Sci. Eng., B* **2008**, *478*, 402-405, 10.1016/j.msea.2007.05.053.

[221] J.-L. Chen, F.-L. Jin, S.-J. Park, Thermal stability and impact and flexural properties of epoxy resins/epoxidized castor oil/nano-CaCO$_3$ ternary systems, *Macromol. Res.* **2010**, *18*, 862-867, 10.1007/s13233-010-0911-4.

[222] L. Zhu, F.-L. Jin, S.-J. Park, Thermal Stability and Fracture Toughness of Epoxy Resins Modified with Epoxidized Castor Oil and Al$_2$O$_3$Nanoparticles, *Bull. Korean Chem. Soc.* **2012**, *33*, 2513-2516, 10.5012/bkcs.2012.33.8.2513.

[223] M. K. Gupta, R. P. Singh, Thermally induced cationic polymerization of glycidyl phenyl ether using novel xanthenyl phosphonium salts, *Macromol. Res.* **2009**, *17*, 221-226, 10.1007/bf03218683.

[224] R. A. Parıldar, A. A. B. Ibik, Characterization of tertiary amine and epoxy functional all-acrylic coating system, *Proc. Org. Coat.* **2013**, *76*, 955-958, 10.1016/j.porgcoat.2012.10.019.

[225] Y.-G. Hsu, K.-H. Lin, T.-Y. Lin, Y.-L. Fang, S.-C. Chen, Y.-C. Sung, Properties of epoxy-amine networks containing nanostructured ether-crosslinked domains, *Mater. Chem. Phys.* **2012**, *132*, 688-702, 10.1016/j.matchemphys.2011.11.087.

[226] Y. Tanaka, H. Kakiuchi, Study of epoxy compounds. Part I. Curing reactions of epoxy resin and acid anhydride with amine and alcohol as catalyst, *J. Appl. Polym. Sci.* **1963**, *7*, 1063-1081, 10.1002/app.1963.070070322.

[227] D. Foix, M. T. Rodríguez, F. Ferrando, X. Ramis, A. Serra, Combined use of sepiolite and a hyperbranched polyester in the modification of epoxy/anhydride coatings: A study of the curing process and the final properties, *Proc. Org. Coat.* **2012**, *75*, 364-372, 10.1016/j.porgcoat.2012.07.013.

[228] M. Flores, X. Fernández-Francos, F. Ferrando, X. Ramis, À. Serra, Efficient impact resistance improvement of epoxy/anhydride thermosets by adding hyperbranched polyesters partially modified with undecenoyl chains, *Polymer* **2012**, *53*, 5232-5241, 10.1016/j.polymer.2012.09.031.

[229] B. Steinmann, Investigations on the curing of epoxy resins with hexahydrophthalic anhydride, *J. Appl. Polym. Sci.* **1989**, *37*, 1753-1776, 10.1002/app.1989.070370702.

[230] D. Foix, Y. Yu, A. Serra, X. Ramis, J. M. Salla, Study on the chemical modification of epoxy/anhydride thermosets using a hydroxyl terminated hyperbranched polymer, *Eur. Polym. J.* **2009**, *45*, 1454-1466, 10.1016/j.eurpolymj.2009.02.003.

[231] C. Li, J. Cheng, Y. Jian, W. Chang, J. Nie, Photopolymerization kinetics and thermal properties of dimethacrylate based on bisphenol-S, *J. Appl. Polym. Sci.* **2013**, *127*, 3418-3423, 10.1002/app.37511.

[232] W. N. Olmstead, Z. Margolin, F. G. Bordwell, Acidities of water and simple alcohols in dimethyl sulfoxide solution, *J. Org. Chem.* **2002**, *45*, 3295-3299, 10.1021/jo01304a032.

[233] F. G. Bordwell, R. J. McCallum, W. N. Olmstead, Acidities and hydrogen bonding of phenols in dimethyl sulfoxide, *J. Org. Chem.* **2002**, *49*, 1424-1427, 10.1021/jo00182a020.

[234] W. Fisch, W. Hofmann, J. Koskikallio, The curing mechanism of epoxy resins, *J. Appl. Chem.* **1956**, *6*, 429-441, 10.1002/jctb.5010061005.

[235] F.-L. Jin, S.-J. Park, Thermal properties and toughness performance of hyperbranched-polyimide-modified epoxy resins, *J. Polym. Sci., Part B: Polym Phys.* **2006**, *44*, 3348-3356, 10.1002/polb.20990.

[236] Y. Zhu, C. Romain, C. K. Williams, Sustainable polymers from renewable resources, *Nature* **2016**, *540*, 354-362, 10.1038/nature21001.

[237] R. Auvergne, S. Caillol, G. David, B. Boutevin, J. P. Pascault, Biobased thermosetting epoxy: present and future, *Chem. Rev.* **2014**, *114*, 1082-1115, 10.1021/cr3001274.

[238] J. Leukel, W. Burchard, R.-P. Krüger, H. Much, G. Schulz, Mechanism of the anionic copolymerization of anhydride-cured epoxies – analyzed by matrix-assisted laser desorption ionization time-of-flight mass spectrometry (MALDI-TOF-MS), *Macromol. Rapid Commun.* **1996**, *17*, 359-366, 10.1002/marc.1996.030170512.

[239] L. Matějka, J. Lövy, S. Pokorný, K. Bouchal, K. Dušek, Curing epoxy resins with anhydrides. Model reactions and reaction mechanism, *J. Polym. Sci: Polym. Chem. Ed.* **1983**, *21*, 2873-2885, 10.1002/pol.1983.170211003.

[240] R. F. Fischer, Polyesters from expoxides and anhydrides, *J. Polym. Sci.* **1960**, *44*, 155-172, 10.1002/pol.1960.1204414314.

[241] G. Couture, L. Granado, F. Fanget, B. Boutevin, S. Caillol, Limonene-Based Epoxy: Anhydride Thermoset Reaction Study, *Molecules* **2018**, *23*, 10.3390/molecules23112739.

[242] M. R. Buchmeiser, J. A. Kammerer, S. Naumann, J. Unold, R. Ghomeshi, S. K. Selvarayan, P. Weichand, R. Gadow, Latent CO_2-Protected N-Heterocyclic Carbene-Based Single-Component System-Derived Epoxy/Glass Fiber Composites, *Macromol. Mater. Eng.* **2015**, *300*, 937-943, 10.1002/mame.201500090.

[243] J. Raynaud, W. N. Ottou, Y. Gnanou, D. Taton, Metal-free and solvent-free access to alpha,omega-heterodifunctionalized poly(propylene oxide)s by N-heterocyclic carbene-induced ring opening polymerization, *Chem. Commun.* **2010**, *46*, 3203-3205, 10.1039/b925415c.

[244] R. Lindner, M. L. Lejkowski, S. Lavy, P. Deglmann, K. T. Wiss, S. Zarbakhsh, L. Meyer, M. Limbach, Ring-Opening Polymerization and Copolymerization of Propylene Oxide Catalyzed by N-Heterocyclic Carbenes, *ChemCatChem* **2014**, *6*, 618-625, 10.1002/cctc.201300802.

[245] B. Guo, D. Jia, W. Fu, Q. Qiu, Hygrothermal stability of dicyanate-novolac epoxy resin blends, *Polym. Deg. Stab.* **2003**, *79*, 521-528, 10.1016/s0141-3910(02)00368-3.

[246] S.-J. Park, M.-K. Seo, J.-R. Lee, Isothermal cure kinetics of epoxy/phenol-novolac resin blend system initiated by cationic latent thermal catalyst, *J. Polym. Sci., Part A: Polym. Chem.* **2000**, *38*, 2945-2956, 10.1002/1099-0518(20000815)38:16<2945::aid-pola120>3.0.co;2-6.

[247] M. J. Yoo, S. H. Kim, S. D. Park, W. S. Lee, J.-W. Sun, J.-H. Choi, S. Nahm, Investigation of curing kinetics of various cycloaliphatic epoxy resins using dynamic thermal analysis, *Eur. Polym. J.* **2010**, *46*, 1158-1162, 10.1016/j.eurpolymj.2010.02.001.

[248] W. Liu, Z. Wang, Silicon-Containing Cycloaliphatic Epoxy Resins with Systematically Varied Functionalities: Synthesis and Structure/Property Relationships, *Macromol. Chem. Phys.* **2011**, *212*, 926-936, 10.1002/macp.201000779.

[249] S. G. Tan, W. S. Chow, Biobased Epoxidized Vegetable Oils and Its Greener Epoxy Blends: A Review, *Polym.-Plast. Technol.* **2010**, *49*, 1581-1590, 10.1080/03602559.2010.512338.

[250] S. J. Park, F. L. Jin, J. R. Lee, Thermal and mechanical properties of tetrafunctional epoxy resin toughened with epoxidized soybean oil, *Mater. Sci. Eng., A* **2004**, *374*, 109-114, 10.1016/j.msea.2004.01.002.

[251] M.-C. Lee, T.-H. Ho, C.-S. Wang, Synthesis of tetrafunctional epoxy resins and their modification with polydimethylsiloxane for electronic application, *J. Appl. Polym. Sci.* **1996**, *62*, 217-225, 10.1002/(sici)1097-4628(19961003)62:1<217::aid-app25>3.0.co;2-0.

[252] W. Jiang, F.-L. Jin, S.-J. Park, Thermo-mechanical behaviors of epoxy resins reinforced with nano-Al_2O_3 particles, *J. Ind. Eng. Chem.* **2012**, *18*, 594-596, 10.1016/j.jiec.2011.11.140.

[253] F.-L. Jin, C.-J. Ma, S.-J. Park, Thermal and mechanical interfacial properties of epoxy composites based on functionalized carbon nanotubes, *Mater. Sci. Eng., B* **2011**, *528*, 8517-8522, 10.1016/j.msea.2011.08.054.

[254] T. Habets, F. Siragusa, B. Grignard, C. Detrembleur, Advancing the Synthesis of Isocyanate-Free Poly(oxazolidones)s: Scope and Limitations, *Macromolecules* **2020**, *53*, 6396-6408, 10.1021/acs.macromol.0c01231.

[255] V. A. Pankratov, T. M. Frenkel, A. M. Fainleib, 2-Oxazolidinones, *Russ. Chem. Rev.* **1983**, *52*, 576-593, 10.1070/RC1983v052n06ABEH002864.

[256] V. Sendijarevic, A. Sendijarevic, H. Lekovic, H. Lekovic, K. C. Frisch, Polyoxazolidones for High Temperature Applications, *J. Elastomers Plast.* **1996**, *28*, 63-83, 10.1177/009524439602800104.

[257] P. I. Kordomenos, J. E. Kresta, K. C. Frisch, Thermal stability of isocyanate-based polymers. 2. Kinetics of the thermal dissociation of model urethane, oxazolidone, and isocyanurate block copolymers, *Macromolecules* **2002**, *20*, 2077-2083, 10.1021/ma00175a006.

[258] J. i. E. Kresta, K. H. Hsieh, The Co-Catalytic Effect of Carbamate Groups in Cyclotrimerization of Isocyanates, *Macromol. Chem. Phys.* **1978**, *179*, 2779-2782, 10.1002/macp.1978.021791120.

[259] P. I. Kordomenos, K. C. Frisch, J. E. Kresta, Oxazolidone coatings. Part II: Structure-properties relationships and thermal stability, *J. Coat. Technol.* **1983**, *55*, 59-61,

[260] S. R. Sandler, Poly-2-oxazolidones as cryogenic adhesives, *J. Appl. Polym. Sci.* **1969**, *13*, 2699-2703, 10.1002/app.1969.070131217.

[261] N. Kinjo, S.-I. Numata, T. Koyama, T. Narahara, Synthesis and viscoelastic properties of new thermosetting resins having isocyanurate and oxazolidone rings in their molecular structures, *J. Appl. Polym. Sci.* **1983**, *28*, 1729-1741, 10.1002/app.1983.070280516.

[262] K. Irako, S. Anzai, F. Odaka, Y. Isda, M. Kitayama, Synthesis and Properties of Polyoxazolidone Elastomers from Diepoxides and Diisocyanates, *Rubber Chem. Technol.* **1980**, *53*, 1-13, 10.5254/1.3535029.

[263] V. Sendijarevic, A. Sendijarevic, K. C. Frisch, P. Reulen, Novel isocyanate-based matrix resins for high temperature composite applications, *Polym. Compos.* **1996**, *17*, 180-186, 10.1002/pc.10603.

[264] T. Pelzer, B. Eling, H.-J. Thomas, G. A. Luinstra, Toward polymers with oxazolidin-2-one building blocks through tetra-n-butyl-ammonium halides (Cl, Br, I) catalyzed coupling of epoxides with isocyanates, *Eur. Polym. J.* **2018**, *107*, 1-8, 10.1016/j.eurpolymj.2018.07.039.

[265] D. A. Evans, Studies in Asymmetric Synthesis. The Development of Practical Chiral Enolate Synthons., *Aldrichim. Acta* **1982**, *15*, 23-32,

[266] D. A. Evans, K. T. Chapman, J. Bisaha, Asymmetric Diels-Alder cycloaddition reactions with chiral .alpha.,.beta.-unsaturated N-acyloxazolidinones, *J. Am. Chem. Soc.* **1988**, *110*, 1238-1256, 10.1021/ja00212a037.

[267] D. A. Evans, W. C. Black, Total synthesis of (+)-A83543A [(+)-lepicidin A], *J. Am. Chem. Soc.* **1993**, *115*, 4497-4513, 10.1021/ja00064a011.

[268] S. Gennen, B. Grignard, T. Tassaing, C. Jérôme, C. Detrembleur, CO_2-Sourced α-Alkylidene Cyclic Carbonates: A Step Forward in the Quest for Functional Regioregular Poly(urethane)s and Poly(carbonate)s, *Angew. Chem.* **2017**, *129*, 10530-10534, 10.1002/ange.201704467.

[269] S. Gennen, B. Grignard, T. Tassaing, C. Jerome, C. Detrembleur, CO_2-Sourced alpha-Alkylidene Cyclic Carbonates: A Step Forward in the Quest for Functional Regioregular Poly(urethane)s and Poly(carbonate)s, *Angew. Chem. Int. Ed.* **2017**, *56*, 10394-10398, 10.1002/anie.201704467.

[270] B. Grignard, S. Gennen, C. Jerome, A. W. Kleij, C. Detrembleur, Advances in the use of CO_2 as a renewable feedstock for the synthesis of polymers, *Chem. Soc. Rev.* **2019**, *48*, 4466-4514, 10.1039/c9cs00047j.

[271] W. J. Yoo, C. J. Li, Copper-Catalyzed Four-Component Coupling between Aldehydes, Amines, Alkynes, and Carbon Dioxide, *Adv. Synth. Catal.* **2008**, *350*, 1503-1506, 10.1002/adsc.200800232.

[272] D. Teffahi, S. Hocine, C.-J. Li, Synthesis of Oxazolidinones, Dioxazolidinone and Polyoxazolidinone (A New Polyurethane) Via A Multi Component-Coupling of Aldehyde, Diamine Dihydrochloride, Terminal Alkyne and CO_2, *Lett. Org. Chem.* **2012**, *9*, 585-593, 10.2174/157017812802850221.

[273] Q. Wu, J. Chen, X. Guo, Y. Xu, Copper(I)-Catalyzed Four-Component Coupling Using Renewable Building Blocks of CO_2 and Biomass-Based Aldehydes, *Eur. J. Org. Chem.* **2018**, *2018*, 3105-3113, 10.1002/ejoc.201800461.

[274] Y. Iwakura, S.-I. Izawa, F. Hayano, Polyoxazolidones prepared from bisurethans and bisepoxides, *J. Polym. Sci., Part A: Polym. Chem.* **1966**, *4*, 751-760, 10.1002/pol.1966.150040402.

[275] Y. Iwakura, S.-i. Izawa, Glycidyl Ether Reactions with Urethanes and Ureas. A New Synthetic Method for 2-Oxazolidones, *J. Org. Chem.* **1963**, *29*, 379-382, 10.1021/jo01025a031.

[276] R. R. Dileone, Synthesis of poly-2-oxazolidones from diisocyanates and diepoxides, *J. Polym. Sci., Part A: Polym. Chem.* **1970**, *8*, 609-615, 10.1002/pol.1970.150080304.

[277] A. Sendijarević, V. Sendijarević, K. C. Frisch, Studies in the formation of poly(oxazolidones) I. Kinetics and mechanism of the model oxazolidone formation from phenyl isocyanate and phenylglycidyl ether. Selectivity of catalysts, *J. Polym. Sci., Part A: Polym. Chem.* **1987**, *25*, 151-170, 10.1002/pola.1987.080250113.

[278] S. R. Sandler, F. Berg, G. Kitazawa, Poly-2-oxazolidones, *J. Appl. Polym. Sci.* **1965**, *9*, 1994-1996, 10.1002/app.1965.070090531.

[279] D. Braun, J. Weinert, Poly-2-oxazolidinone aus isocyanaten und epoxiden, *Macromol. Mater. Eng.* **1979**, *78*, 1-19, 10.1002/apmc.1979.050780101.

[280] G. P. Speranza, W. J. Peppel, Preparation of Substituted 2-Oxazolidones from 1,2-Epoxides and Isocyanates, *J. Org. Chem.* **1958**, *23*, 1922-1924, 10.1021/jo01106a027.

[281] K. Ashida, K. C. Frisch, Modified Isocyanurate Foams. II, *J. Cell. Plast.* **1972**, *8*, 194-200, 10.1177/0021955x7200800405.

[282] K. Ashida, K. C. Frisch, Epoxy-Modified Isocyanurate Foams, *J. Cell. Plast.* **1972**, *8*, 160-167, 10.1177/0021955x7200800307.

[283] A. Prokofyeva, H. Laurenzen, D. J. Dijkstra, E. Frick, A. M. Schmidt, C. Guertler, C. Koopmans, A. Wolf, Poly-2-oxazolidones with tailored physical properties synthesized by catalyzed polyaddition of 2,4-toluene diisocyanate and different bisphenol-based diepoxides, *Polym. Int.* **2017**, *66*, 399-404, 10.1002/pi.5279.

[284] G. Bald, K. Kretzschmar, H. Markert, M. Wimmer, Thermisches Verhalten von Mono-, Bis- und Poly-2-oxazolidinonen, *Macromol. Mater. Eng.* **1975**, *44*, 151-163, 10.1002/apmc.1975.050440113.

[285] J. E. Herweh, W. Y. Whitmore, Poly-2-oxazolidones: Preparation and characterization, *J. Polym. Sci., Part A: Polym. Chem.* **1970**, *8*, 2759-2773, 10.1002/pol.1970.150081004.

[286] X. Zhang, W. Chen, C. Zhao, C. Li, X. Wu, W. Z. Chen, A Facile and Efficient Synthesis of 3-Aryloxazolidin-2-ones from Isocyanates and Epoxides Promoted by MgI2Etherate, *Synth. Commun.* **2010**, *40*, 3654-3659, 10.1080/00397910903470525.

[287] S. H. Eldin, A. Renner, Cyanoacetamide accelerators for the epoxide/isocyanate reaction, *J. Appl. Polym. Sci.* **1990**, *41*, 1505-1516, 10.1002/app.1990.070410713.

[288] S. Okumoto, S. Yamabe, A computational study of base-catalyzed reactions between isocyanates and epoxides affording 2-oxazolidones and isocyanurates, *J. Comput. Chem.* **2001**, *22*, 316-326, 10.1002/1096-987x(200102)22:3<316::aid-jcc1004>3.0.co;2-5.

[289] H. Ulrich, Synthesis of polymers from isocyanates in polar solvents, *J. Polym. Sci. Macromol. Rev.* **1976**, *11*, 93-133, 10.1002/pol.1976.230110103.

[290] M. Azechi, T. Endo, Synthesis and property of polyoxazolidone having fluorene moiety by polyaddition of diisocyanate and diepoxide, *J. Polym. Sci., Part A: Polym. Chem.* **2014**, *52*, 1755-1760, 10.1002/pola.27181.

[291] H. K. Reimschuessel, Nylon 6. Chemistry and mechanisms, *J. Polym. Sci. Macromol. Rev.* **1977**, *12*, 65-139, 10.1002/pol.1977.230120102.

[292] K. Marchildon, Polyamides - Still Strong After Seventy Years, *Marcomol. React. Eng.* **2011**, *5*, 22-54, 10.1002/mren.201000017.

[293] J. A. N. Šebenda, Lactam Polymerization, *J. Macromol. Sci. A* **1972**, *6*, 1145-1199, 10.1080/10601327208056889.

[294] S. Russo, E. Casazza, *Polymer Science: A Comprehensive Reference; chapter 4.14 Ring-Opening Polymerization of Cyclic Amides (Lactams), Vol. 4*, Elsevier, **2012**.

[295] P. Kubisa, S. Penczek, Cationic activated monomer polymerization of heterocyclic monomers, *Prog. Polym. Sci.* **1999**, *24*, 1409-1437, 10.1016/s0079-6700(99)00028-3.

[296] F. N. Tüzün, Effect of the Activator Type and Catalyst/Activator Ratio on Physical and Mechanical Properties of Cast PA-6, *Polym.-Plast. Technol.* **2008**, *47*, 532-541, 10.1080/03602550801978008.

[297] M. Mohammadi, S. Ahmadi, I. Ghasemi, M. Rahnama, Anionic copolymerization of nylon 6/12: A comprehensive review, *Polym. Eng. Sci.* **2019**, *59*, 1529-1543, 10.1002/pen.25171.

[298] S. A. Iobst, Polymerization and Crystallization Behavior of Anionic Nylon-6, *Polym. Eng. Sci.* **1985**, *25*, 425-430, DOI 10.1002/pen.760250708.

[299] Y. Pae, Structure and properties of polyimide-g-nylon 6 and nylon 6-b-polyimide-b-nylon 6 copolymers, *J. Appl. Polym. Sci.* **2006**, *99*, 300-308, 10.1002/app.22480.

[300] S. Russo, S. Maniscalco, L. Ricco, Some new perspectives of anionic polyamide 6 (APA 6) synthesis, *Polym. Adv. Technol.* **2015**, *26*, 851-854, 10.1002/pat.3505.

[301] P. Dubois, O. Coulembier, J. M. Raquez, *Handbook of Ring-Opening Polymerization*, Wiley-VCH, **2009**.

[302] L. Ricco, S. Russo, G. Orefice, F. Riva, Anionic Poly(ε-caprolactam): Relationships among Conditions of Synthesis, Chain Regularity, Reticular Order, and Polymorphism, *Macromolecules* **1999**, *32*, 7726-7731, 10.1021/ma9909004.

[303] K. Hashimoto, Ring-opening polymerization of lactams. Living anionic polymerization and its applications, *Prog. Polym. Sci.* **2000**, *25*, 1411-1462, 10.1016/s0079-6700(00)00018-6.

[304] F. G. Bordwell, G. E. Drucker, H. E. Fried, Acidities of carbon and nitrogen acids: the aromaticity of the cyclopentadienyl anion, *J. Org. Chem.* **1981**, *46*, 632-635, 10.1021/jo00316a032.

[305] F. G. Bordwell, H. E. Fried, Heterocyclic aromatic anions with 4n + 2 .pi.-electrons, *J. Org. Chem.* **1991**, *56*, 4218-4223, 10.1021/jo00013a027.

[306] K. Udipi, R. S. Davé, R. L. Kruse, L. R. Stebbins, Polyamides from lactams via anionic ring-opening polymerization: 1. Chemistry and some recent findings, *Polymer* **1997**, *38*, 927-938, 10.1016/s0032-3861(96)00566-6.

[307] K. J. Kim, Y. Y. Kim, B. S. Yoon, K. J. Yoon, Mechanism and kinetics of adiabatic anionic polymerization of ε-caprolactam in the presence of various activators, *J. Appl. Polym. Sci.* **1995**, *57*, 1347-1358, 10.1002/app.1995.070571111.

[308] L. Ricco, O. Monticelli, S. Russo, A. Paglianti, A. Mariani, Fast-activated anionic polymerization of ε-caprolactam in suspension, 1, *Macromol. Chem. Phys.* **2002**, *203*, 1436-1444, 10.1002/1521-3935(200207)203:10/11<1436::aid-macp1436>3.0.co;2-v.

[309] J. Stehlíček, K. Gehrke, J. Šebenda, Alkaline polymerization of 6-caprolactam. XXIV. N-Carbamoylcaprolactams as activators of the alkaline polymerization of caprolactam, *Collect. Czech. Chem. Commun.* **1967**, *32*, 370-381, 10.1135/cccc19670370.

[310] J. Stehlíček, J. Labský, J. Šebenda, Alkaline polymerization of 6-caprolactam. XXV. The effect of structure of the acyl on polymerization activated by acylcaprolactams or diacylamines, *Collect. Czech. Chem. Commun.* **1967**, *32*, 545-557, 10.1135/cccc19670545.

[311] S. Barzakay, M. Levy, D. Vofsi, Studies on anionic polymerization of lactams. Part II. Effect of cocatalysts on the polymerization of pyrrolidone, *J. Polym. Sci., Part A: Polym. Chem.* **1966**, *4*, 2211-2218, 10.1002/pol.1966.150040915.

[312] G. Champetier, H. Sekiguchi, Mecanisme Reactionnel de la Polymerisation Anionique des Lactames, *J. Polym. Sci.* **1960**, *48*, 309-319, 10.1002/pol.1960.1204815029.

[313] H. Sekiguchi, Mécanisme réactionnel de la polymérisation alcaline des lactames, *Journal of Polymer Science Part A: General Papers* **1963**, *1*, 1627-1633, 10.1002/pol.1963.100010515.

[314] T. M. Frunze, V. A. Kotel'nikov, T. V. Volkova, V. V. Kurashov, Ions and ion pairs in anionic activated polymerization of ε-caprolactam, *Eur. Polym. J.* **1981**, *17*, 1079-1084, 10.1016/0014-3057(81)90031-8.

[315] T. M. Frunze, V. A. Kotel'nikov, T. V. Volkova, V. V. Kurašev, S. P. Davtjan, I. V. Stankevič, The active centres in the anionically activated polymerization of ε-caprolactam, *Acta Polym.* **1981**, *32*, 31-35, 10.1002/actp.1981.010320108.

[316] O. Wichterle, On Caprolactam Polymerization, *Macromol. Chem. Phys.* **1960**, *35*, 174-182, 10.1002/macp.1960.020350108.

[317] J. Šebenda, Alkaline polymerization of 6-caprolactam. XIX. The Claisen condensation of N-ethyldiacetamide in a system of sodium salt of N-ethylacetamide and N-ethylacetamide, *Collect. Czech. Chem. Commun.* **1966**, *31*, 1501-1512, 10.1135/cccc19661501.

[318] K. Ueda, K. Yamada, M. Nakai, T. Matsuda, M. Hosoda, K. Tai, Synthesis of High Molecular Weight Nylon 6 by Anionic Polymerization of ε-Caprolactam, *Polym. J.* **1996**, *28*, 446-451, 10.1295/polymj.28.446.

[319] W. Tam, D. T. Williamson, Ring Opening Polymerization of Cyclic Amides using N-Heterocyclic Carbene Catalysts, **2006**, WO2006053071.

[320] M. Wilhelm, R. Wendel, M. Aust, P. Rosenberg, F. Henning, Compensation of Water Influence on Anionic Polymerization of ε-Caprolactam: 1. Chemistry and Experiments, *J. Compos. Sci.* **2020**, *4*, 7, 10.3390/jcs4010007.

[321] R. Wendel, P. Rosenberg, M. Wilhelm, F. Henning, Anionic Polymerization of ε-Caprolactam under the Influence of Water: 2. Kinetic Model, *J. Compos. Sci.* **2020**, *4*, 8, 10.3390/jcs4010008.

[322] H.-M. Müller, D. Seebach, Poly(hydroxyalkanoates): A Fifth Class of Physiologically Important Organic Biopolymers?, *Angew. Chem. Int. Ed.* **1993**, *32*, 477-502, 10.1002/anie.199304771.

[323] Y. Hori, T. Hagiwara, Ring-opening polymerisation of β-butyrolactone catalysed by distannoxane complexes: study of the mechanism, *Int. J. Biol. Macromol.* **1999**, *25*, 237-245, 10.1016/s0141-8130(99)00038-0.

[324] R. N. Reusch, Physiological importance of poly-(R)-3-hydroxybutyrates, *Chem. Biodivers.* **2012**, *9*, 2343-2366, 10.1002/cbdv.201200278.

[325] R. N. Reusch, Poly-beta-hydroxybutyrate/calcium polyphosphate complexes in eukaryotic membranes, *Proc. Soc. Exp. Biol. Med.* **1989**, *191*, 377-381, 10.3181/00379727-191-42936.

[326] R. N. Reusch, H. L. Sadoff, Putative structure and functions of a poly-beta-hydroxybutyrate/calcium polyphosphate channel in bacterial plasma membranes, *Proc. Natl. Acad. Sci. U.S.A.* **1988**, *85*, 4176-4180, 10.1073/pnas.85.12.4176.

[327] M. Doudoroff, R. Y. Stanier, Role of poly-beta-hydroxybutyric acid in the assimilation of organic carbon by bacteria, *Nature* **1959**, *183*, 1440-1442, 10.1038/1831440a0.

[328] L. P. Lin, S. Pankratz, H. L. Sadoff, Ultrastructural and physiological changes occurring upon germination and outgrowth of Azotobacter vinelandii cysts, *J. Bacteriol.* **1978**, *135*, 641-646, 10.1128/JB.135.2.641-646.1978.

[329] A. J. Anderson, E. A. Dawes, Occurrence, metabolism, metabolic role, and industrial uses of bacterial polyhydroxyalkanoates, *Microbiol. Rev.* **1990**, *54*, 450-472,

[330] R. Griebel, Z. Smith, J. M. Merrick, Metabolism of poly-beta-hydroxybutyrate. I. Purification, composition, and properties of native poly-beta-hydroxybutyrate granules from Bacillus megaterium, *Biochemistry* **1968**, *7*, 3676-3681, 10.1021/bi00850a047.

[331] F. M. García-Valle, V. Tabernero, T. Cuenca, M. E. G. Mosquera, J. Cano, S. Milione, Biodegradable PHB from rac-β-Butyrolactone: Highly Controlled ROP Mediated by a Pentacoordinated Aluminum Complex, *Organometallics* **2018**, *37*, 837-840, 10.1021/acs.organomet.7b00843.

[332] M. Arcana, O. Giani-Beaune, R. Schue, F. Schue, W. Amass, A. Amass, Ring-opening copolymerization of racemic ?-butyrolactone with ?-caprolactone and ?-valerolactone by distannoxane derivative catalysts: study of the enzymatic degradation in aerobic media of obtained copolymers, *Polym. Int.* **2002**, *51*, 859-866, 10.1002/pi.1036.

[333] P. J. Hocking, R. H. Marchessault, M. R. Timmins, R. W. Lenz, R. C. Fuller, Enzymatic Degradation of Single Crystals of Bacterial and Synthetic Poly(β-hydroxybutyrate), *Macromolecules* **1996**, *29*, 2472-2478, 10.1021/ma951361f.

[334] Y. Kumagai, Y. Doi, Physical properties and biodegradability of blends of isotactic and atactic poly(3-hydroxybutyrate), *Macromol. Rapid Commun.* **1992**, *13*, 179-183, 10.1002/marc.1992.030130308.

[335] X. Dong, J. R. Robinson, The role of neutral donor ligands in the isoselective ring-opening polymerization of rac-β-butyrolactone, *Chemical Science* **2020**, *11*, 8184-8195, 10.1039/d0sc03507f.

[336] H. Sardon, A. P. Dove, Plastics recycling with a difference, *Science* **2018**, *360*, 380-381, 10.1126/science.aat4997.

[337] R. J. Samuels, Quantitative structural characterization of the melting behavior of isotactic polypropylene, *J. Polym. Sci., Part B: Polym Phys.* **1975**, *13*, 1417-1446, 10.1002/pol.1975.180130713.

[338] K. Ishikawa, Y. Kawaguchi, Y. Doi, Plasticization of bacterial polyester by the addition of acylglycerols and its enzymatic degradability, *Kobunshi Ronbunshu* **1991**, *48*, 221-226, 10.1295/koron.48.221.

[339] Y. Wang, R. Chen, J. Cai, Z. Liu, Y. Zheng, H. Wang, Q. Li, N. He, Biosynthesis and thermal properties of PHBV produced from levulinic acid by Ralstonia eutropha, *PLoS One* **2013**, *8*, e60318, 10.1371/journal.pone.0060318.

[340] L. R. Rieth, D. R. Moore, E. B. Lobkovsky, G. W. Coates, Single-site beta-diiminate zinc catalysts for the ring-opening polymerization of beta-butyrolactone and beta-valerolactone to poly(3-hydroxyalkanoates), *J. Am. Chem. Soc.* **2002**, *124*, 15239-15248, 10.1021/ja020978r.

[341] V. Purohit, R. A. Orzel, Polypropylene: A Literature Review of the Thermal Decomposition Products and Toxicity, *J. Am. Coll. Toxicol.* **2016**, *7*, 221-242, 10.3109/10915818809014521.

[342] Y. Tsuchiya, K. Sumi, Thermal decomposition products of polypropylene, *J. Polym. Sci., Part A: Polym. Chem.* **1969**, *7*, 1599-1607, 10.1002/pol.1969.150070704.

[343] E. Jakab, G. Várhegyi, O. Faix, Thermal decomposition of polypropylene in the presence of wood-derived materials, *J. Anal. Appl. Pyrolysis* **2000**, *56*, 273-285, 10.1016/s0165-2370(00)00101-7.

[344] J. H. Hong, H. J. Jeon, J. H. Yoo, W.-R. Yu, J. H. Youk, Synthesis and characterization of biodegradable poly(ε-caprolactone-co-β-butyrolactone)-based polyurethane, *Polym. Deg. Stab.* **2007**, *92*, 1186-1192, 10.1016/j.polymdegradstab.2007.04.007.

[345] Y. D. Getzler, V. Mahadevan, E. B. Lobkovsky, G. W. Coates, Synthesis of beta-lactones: a highly active and selective catalyst for epoxide carbonylation, *J. Am. Chem. Soc.* **2002**, *124*, 1174-1175, 10.1021/ja017434u.

[346] A. K. Hubbell, G. W. Coates, Nucleophilic Transformations of Lewis Acid-Activated Disubstituted Epoxides with Catalyst-Controlled Regioselectivity, *J. Org. Chem.* **2020**, *85*, 13391-13414, 10.1021/acs.joc.0c01691.

[347] M. Okada, Chemical syntheses of biodegradable polymers, *Prog. Polym. Sci.* **2002**, *27*, 87-133, 10.1016/s0079-6700(01)00039-9.

[348] T. L. Gresham, J. E. Jansen, F. W. Shaver, J. T. Gregory, W. L. Beears, β-Propiolactone. V. Reaction with Alcohols, *J. Am. Chem. Soc.* **1948**, *70*, 1004-1006, 10.1021/ja01183a034.

[349] Y. Okamoto, Cationic ring-opening polymerization of lactones in the presence of alcohol, *Macromol. Symp.* **1991**, *42-43*, 117-133, 10.1002/masy.19910420109.

[350] M. Basko, A. Duda, S. Kazmierski, P. Kubisa, Cationic copolymerization of racemic-β-butyrolactone with L,L-lactide: One-pot synthesis of block copolymers, *J. Polym. Sci., Part A: Polym. Chem.* **2013**, *51*, 4873-4884, 10.1002/pola.26916.

[351] G. Schnee, C. Fliedel, T. Avilés, S. Dagorne, Neutral and Cationic N-Heterocyclic Carbene Zinc Adducts and the BnOH/Zn(C$_6$F$_5$)$_2$ Binary Mixture - Characterization and Use in the Ring-Opening Polymerization of β-Butyrolactone, Lactide, and Trimethylene Carbonate, *Eur. J. Inorg. Chem.* **2013**, *2013*, 3699-3709, 10.1002/ejic.201300292.

[352] C. W. Lee, R. Urakawa, Y. Kimura, Copolymerization of γ-butyrolactone and β-butyrolactone, *Macromol. Chem. Phys.* **1997**, *198*, 1109-1120, 10.1002/macp.1997.021980414.

[353] D. J. Walsh, M. G. Hyatt, S. A. Miller, D. Guironnet, Recent Trends in Catalytic Polymerizations, *ACS Catal.* **2019**, *9*, 11153-11188, 10.1021/acscatal.9b03226.

[354] A. Couffin, B. Martín-Vaca, D. Bourissou, C. Navarro, Selective O-acyl ring-opening of β-butyrolactone catalyzed by trifluoromethane sulfonic acid: application to the preparation of well-defined block copolymers, *Polym. Chem.* **2014**, *5*, 161-168, 10.1039/c3py00935a.

[355] F. A. Jaipuri, B. D. Bower, N. L. Pohl, Protic acid-catalyzed polymerization of β-lactones for the synthesis of chiral polyesters, *Tetrahedron: Asymmetry* **2003**, *14*, 3249-3252, 10.1016/j.tetasy.2003.08.025.

[356] H. R. Kricheldorf, N. Scharnagl, Polyactones. 17. Anionic Polymerization of β-D,L-Butyrolactone, *J. Macromol. Sci. A* **1989**, *26*, 951-968, 10.1080/00222338908052023.

[357] H. R. Kricheldorf, M. Berl, N. Scharnagl, Poly(lactones). 9. Polymerization mechanism of metal alkoxide initiated polymerizations of lactide and various lactones, *Macromolecules* **1988**, *21*, 286-293, 10.1021/ma00180a002.

[358] Z. Jedlinski, M. Kowalczuk, Nature of the active centers and the propagation mechanism of the polymerization of .beta.-propiolactones initiated by potassium anions, *Macromolecules* **1989**, *22*, 3242-3244, 10.1021/ma00198a008.

[359] P. Kurcok, M. Kowalczuk, K. Hennek, Z. Jedlinski, Anionic polymerization of .beta.-lactones initiated with alkali-metal alkoxides: reinvestigation of the polymerization mechanism, *Macromolecules* **1992**, *25*, 2017-2020, 10.1021/ma00033a027.

[360] O. Coulembier, X. Delva, J. L. Hedrick, R. M. Waymouth, P. Dubois, Synthesis of Biomimetic Poly(hydroxybutyrate): Alkoxy- and Carboxytriazolines as Latent Ionic Initiator, *Macromolecules* **2007**, *40*, 8560-8567, 10.1021/ma071575k.

[361] S. Slomkowski, S. Penczek, Influence of Dibenzo-18-crown-6 Ether on the Kinetics of Anionic Polymerization of β-Propiolactone, *Macromolecules* **1976**, *9*, 367-369, 10.1021/ma60050a040.

[362] A. Deffieux, S. Boileau, Use of Cryptates in Anionic Polymerization of Lactones, *Macromolecules* **1976**, *9*, 369-371, 10.1021/ma60050a041.

[363] S. Slomkowski, S. Penczek, Macroions and Macroion Pairs in the Anionic Polymerization of β-Propiolactone (β-PL), *Macromolecules* **1980**, *13*, 229-233, 10.1021/ma60074a005.

[364] Z. Jedlinski, M. Kowalczuk, W. Glowkowski, J. Grobelny, M. Szwarc, Novel polymerization of β-butyrolactone initiated by potassium naphthalenide in the presence of a crown ether or a cryptand, *Macromolecules* **1991**, *24*, 349-352, 10.1021/ma00002a002.

[365] Z. Jedlinski, M. Kowalczuk, P. Kurcok, What is the real mechanism of anionic polymerization of β-lactones by potassium alkoxides? A critical approach, *Macromolecules* **1991**, *24*, 1218-1219, 10.1021/ma00005a042.

[366] A. C. Albertsson, I. K. Varma, Recent developments in ring opening polymerization of lactones for biomedical applications, *Biomacromolecules* **2003**, *4*, 1466-1486, 10.1021/bm034247a.

[367] A. Duda, Anionic polymerization of 4-methyl-2-oxetanone (β-butyrolactone), *J. Polym. Sci., Part A: Polym. Chem.* **1992**, *30*, 21-29, 10.1002/pola.1992.080300103.

[368] A. Hofman, S. Słomkowski, S. Penczek, Structure of active centers and mechanism of the anionic polymerization of lactones, *Macromol. Chem. Phys.* **1984**, *185*, 91-101, 10.1002/macp.1984.021850110.

[369] W. Kuran, *Principles of Coordination Polymerisation*, Wiley-VCH, **2001**.

[370] J. E. Kemnitzer, S. P. McCarthy, R. A. Gross, Syndiospecific ring-opening polymerization of .beta.-butyrolactone to form predominantly syndiotactic poly(.beta.-

hydroxybutyrate) using tin(IV) catalysts, *Macromolecules* **1993**, *26*, 6143-6150, 10.1021/ma00075a001.

[371] R. Ligny, M. M. Hanninen, S. M. Guillaume, J. F. Carpentier, Highly Syndiotactic or Isotactic Polyhydroxyalkanoates by Ligand-Controlled Yttrium-Catalyzed Stereoselective Ring-Opening Polymerization of Functional Racemic beta-Lactones, *Angew. Chem. Int. Ed.* **2017**, *56*, 10388-10393, 10.1002/anie.201704283.

[372] R. Ligny, M. M. Hänninen, S. M. Guillaume, J.-F. Carpentier, Highly Syndiotactic or Isotactic Polyhydroxyalkanoates by Ligand-Controlled Yttrium-Catalyzed Stereoselective Ring-Opening Polymerization of Functional Racemic β-Lactones, *Angew. Chem.* **2017**, *129*, 10524-10529, 10.1002/ange.201704283.

[373] P. T. Altenbuchner, A. Kronast, S. Kissling, S. I. Vagin, E. Herdtweck, A. Pothig, P. Deglmann, R. Loos, B. Rieger, Mechanistic Investigations of the Stereoselective Rare Earth Metal-Mediated Ring-Opening Polymerization of beta-Butyrolactone, *Chem. Eur. J.* **2015**, *21*, 13609-13617, 10.1002/chem.201501156.

[374] M. Bouyahyi, N. Ajellal, E. Kirillov, C. M. Thomas, J. F. Carpentier, Exploring electronic versus steric effects in stereoselective ring-opening polymerization of lactide and beta-butyrolactone with amino-alkoxy-bis(phenolate)-yttrium complexes, *Chem. Eur. J.* **2011**, *17*, 1872-1883, 10.1002/chem.201002779.

[375] S. A. Cotton, Titanium, zirconium and hafnium, *Annu. Rep. Prog. Chem., Sect. A: Inorg. Chem.* **2007**, *103*, 137-146, 10.1039/b612679k.

[376] Y. Kim, G. K. Jnaneshwara, J. G. Verkade, Titanium alkoxides as initiators for the controlled polymerization of lactide, *Inorg. Chem.* **2003**, *42*, 1437-1447, 10.1021/ic026139n.

[377] J. Cayuela, V. Bounor-Legaré, P. Cassagnau, A. Michel, Ring-Opening Polymerization of ε-Caprolactone Initiated with Titaniumn-Propoxide or Titanium Phenoxide, *Macromolecules* **2006**, *39*, 1338-1346, 10.1021/ma051272v.

[378] Y. Takashima, Y. Nakayama, T. Hirao, H. Yasuda, A. Harada, Bis(amido)titanium complexes having chelating diaryloxo ligands bridged by sulfur or methylene and their catalytic behaviors for ring-opening polymerization of cyclic esters, *J. Organomet. Chem.* **2004**, *689*, 612-619, 10.1016/j.jorganchem.2003.10.042.

[379] Y. Pérez, I. del Hierro, I. Sierra, P. Gómez-Sal, M. Fajardo, A. Otero, Polymerization of ε-caprolactone using bulky alkoxo-titanium complexes and structural analysis of [Ti(OBorneoxo)$_2$Cl$_2$(thf)$_2$], *J. Organomet. Chem.* **2006**, *691*, 3053-3059, 10.1016/j.jorganchem.2006.03.019.

[380] F. Gornshtein, M. Kapon, M. Botoshansky, M. S. Eisen, Titanium and Zirconium Complexes for Polymerization of Propylene and Cyclic Esters, *Organometallics* **2007**, *26*, 497-507, 10.1021/om060723c.

[381] C. J. Chuck, M. G. Davidson, M. D. Jones, G. Kociok-Kohn, M. D. Lunn, S. Wu, Air-stable titanium alkoxide based metal-organic framework as an initiator for ring-opening polymerization of cyclic esters, *Inorg. Chem.* **2006**, *45*, 6595-6597, 10.1021/ic060969+.

[382] H. R. Kricheldorf, S.-R. Lee, Polylactones. 35. Macrocyclic and Stereoselective Polymerization of .beta.-D,L-Butyrolactone with Cyclic Dibutyltin Initiators, *Macromolecules* **1995**, *28*, 6718-6725, 10.1021/ma00124a004.

[383] H. R. Kricheldorf, S.-R. Lee, S. Bush, Polylactones 36. Macrocyclic Polymerization of Lactides with Cyclic Bu2Sn Initiators Derived from 1,2-Ethanediol, 2-Mercaptoethanol, and 1,2-Dimercaptoethane, *Macromolecules* **1996**, *29*, 1375-1381, 10.1021/ma9509826.

[384] H. R. Kricheldorf, S. Eggerstedt, Polylactones. 41. Polymerizations of β-d,l-Butyrolactone with Dialkyltinoxides as Initiators, *Macromolecules* **1997**, *30*, 5693-5697, 10.1021/ma970244c.

[385] H. R. Kricheldorf, K. Hauser, Macrocycles. 3. Telechelic Polylactones via Macrocylic Polymerization, *Macromolecules* **1998**, *31*, 614-620, 10.1021/ma971055x.

[386] H. R. Kricheldorf, H. Hachmann-Thießen, Telechelic and Star-Shaped Poly(ε-caprolactone) Functionalized with Triethoxysilyl Groups - New Biodegradable Coatings and Adhesives, *Macromol. Chem. Phys.* **2005**, *206*, 758-766, 10.1002/macp.200400494.

[387] J. Brzeska, A. M. Elert, M. Morawska, W. Sikorska, M. Kowalczuk, M. Rutkowska, Branched Polyurethanes Based on Synthetic Polyhydroxybutyrate with Tunable Structure and Properties, *Polymers* **2018**, *10*, 10.3390/polym10080826.

[388] J. Brzeska, A. Tercjak, W. Sikorska, M. Kowalczuk, M. Rutkowska, Morphology and Physicochemical Properties of Branched Polyurethane/Biopolymer Blends, *Polymers* **2019**, *12*, 10.3390/polym12010016.

[389] J. Brzeska, A. Tercjak, W. Sikorska, M. Kowalczuk, M. Rutkowska, Predicted Studies of Branched and Cross-Linked Polyurethanes Based on Polyhydroxybutyrate with Polycaprolactone Triol in Soft Segments, *Polymers* **2020**, *12*, 10.3390/polym12051068.

[390] B. Maji, M. Breugst, H. Mayr, N-heterocyclic carbenes: organocatalysts with moderate nucleophilicity but extraordinarily high Lewis basicity, *Angew. Chem. Int. Ed.* **2011**, *50*, 6915-6919, 10.1002/anie.201102435.

[391] S. Naumann, P. B. Scholten, J. A. Wilson, A. P. Dove, Dual Catalysis for Selective Ring-Opening Polymerization of Lactones: Evolution toward Simplicity, *J. Am. Chem. Soc.* **2015**, *137*, 14439-14445, 10.1021/jacs.5b09502.

[392] J. Meisner, J. Karwounopoulos, P. Walther, J. Kastner, S. Naumann, The Lewis Pair Polymerization of Lactones Using Metal Halides and N-Heterocyclic Olefins: Theoretical Insights, *Molecules* **2018**, *23*, 10.3390/molecules23020432.

[393] A. L. Borgne, N. Spassky, C. L. Jun, A. Momtaz, ^{13}C NMR study of the tacticity of poly(propylene oxide)s prepared by polymerization with α,β,γ,δ-tetraphenylporphyrin/AlEt2Cl as initiator system: An example of first-order markovian statistics in ring-opening polymerization, *Macromol. Chem. Phys.* **1988**, *189*, 637-650, 10.1002/macp.1988.021890316.

[394] F. C. Schilling, A. E. Tonelli, Carbon-13 NMR determination of poly(propylene oxide) microstructure, *Macromolecules* **2002**, *19*, 1337-1343, 10.1021/ma00159a010.

[395] M. I. Childers, J. M. Longo, N. J. Van Zee, A. M. LaPointe, G. W. Coates, Stereoselective epoxide polymerization and copolymerization, *Chem. Rev.* **2014**, *114*, 8129-8152, 10.1021/cr400725x.

[396] J. Raynaud, C. Absalon, Y. Gnanou, D. Taton, N-heterocyclic carbene-induced zwitterionic ring-opening polymerization of ethylene oxide and direct synthesis of alpha,omega-difunctionalized poly(ethylene oxide)s and poly(ethylene oxide)-b-poly(epsilon-caprolactone) block copolymers, *J. Am. Chem. Soc.* **2009**, *131*, 3201-3209, 10.1021/ja809246f.

[397] J. Tang, T. Mohan, J. G. Verkade, Selective and Efficient Syntheses of Perhydro-1,3,5-triazine-2,4,6-triones and Carbodiimides from Isocyanates Using ZP(MeNCH2CH2)3N Catalysts, *J. Org. Chem.* **2002**, *59*, 4931-4938, 10.1021/jo00096a041.

[398] T. Ageyeva, I. Sibikin, J. Karger-Kocsis, Polymers and Related Composites via Anionic Ring-Opening Polymerization of Lactams: Recent Developments and Future Trends, *Polymers* **2018**, *10*, 10.3390/polym10040357.

[399] I. Sibikin, J. Karger-Kocsis, Toward industrial use of anionically activated lactam polymers: Past, present and future, *Adv. Ind. Eng. Polym. Res.* **2018**, *1*, 48-60, 10.1016/j.aiepr.2018.06.003.

[400] J. Troitzsch, Flame retardant polymers current status and future trends, *Macromol. Symp.* **1993**, *74*, 125-135, 10.1002/masy.19930740115.

[401] I. van der Veen, J. de Boer, Phosphorus flame retardants: properties, production, environmental occurrence, toxicity and analysis, *Chemosphere* **2012**, *88*, 1119-1153, 10.1016/j.chemosphere.2012.03.067.

[402] A. Viale, D. Santelia, R. Napolitano, R. Gobetto, W. Dastrù, S. Aime, The Detection of PHIP Effects Allows New Insights into the Mechanism of Olefin Isomerisation during Catalytic Hydrogenation, *Eur. J. Inorg. Chem.* **2008**, *2008*, 4348-4351, 10.1002/ejic.200800356.

[403] H. E. Gottlieb, V. Kotlyar, A. Nudelman, NMR Chemical Shifts of Common Laboratory Solvents as Trace Impurities, *J. Org. Chem.* **1997**, *62*, 7512-7515, 10.1021/jo971176v.

[404] G. R. Fulmer, A. J. M. Miller, N. H. Sherden, H. E. Gottlieb, A. Nudelman, B. M. Stoltz, J. E. Bercaw, K. I. Goldberg, NMR Chemical Shifts of Trace Impurities: Common Laboratory Solvents, Organics, and Gases in Deuterated Solvents Relevant to the Organometallic Chemist, *Organometallics* **2010**, *29*, 2176-2179, 10.1021/om100106e.